



UNIVERSITÀ  
DEGLI STUDI  
FIRENZE

PhD in  
Biomedical Science

CICLO XXXIII

COORDINATOR Prof. Stefani Massimo

*Biochemical investigation on the bioactive properties of the Posidonia oceanica (L.) Delile  
marine plant*

Academic Discipline (SSD) BIO/10

**Doctoral Candidate**

Dr. Vasarri Marzia

**Supervisor**

Prof. Degl'Innocenti Donatella

**Coordinator**

Prof. Stefani Massimo

Years 2017/2020

---

# INDEX

<b>1. INTRODUCTION</b>	<b>3</b>
1.1. THE SEAGRASS <i>POSIDONIA OCEANICA</i> (L.) DELILE	3
1.2. MORPHOLOGY, STRUCTURE AND REPRODUCTION	6
1.3. <i>P. OCEANICA</i> ECOSYSTEM	9
1.4. <i>P. OCEANICA</i> ECOLOGICAL SIGNIFICANCE	10
1.5. <i>P. OCEANICA</i> AND HUMANS: A MILLENNIAL HISTORY	11
1.5.1. Pre-project pharmacological studies on <i>P. oceanica</i> extract bioactivities	13
1.6. MARINE NATURAL PRODUCTS: FROM THE SEA TO HUMAN HEALTH	13
1.7. SECONDARY METABOLITES OF <i>P. OCEANICA</i> LEAVES	16
<b>2. AIM OF THE THESIS</b>	<b>19</b>
<b>3. RESULTS AND DISCUSSION</b>	<b>20</b>
3.1. HYDROALCOHOLIC EXTRACTION FROM <i>P. OCEANICA</i> LEAVES	20
3.2. <i>P. OCEANICA</i> IN THE FIGHT AGAINST CANCER	21
3.2.1. <i>P. oceanica</i> inhibits cancer cell migration through autophagy modulation	21
3.2.1.1. <i>P. oceanica</i> anti-migratory role on human fibrosarcoma HT1080 cells	21
3.2.1.2. <i>P. oceanica</i> anti-migratory role on human neuroblastoma SH-SY5Y cells	27
3.2.2. Bio-enhancement of <i>P. oceanica</i> anti-migratory role by nanotechnology	31
3.3. <i>P. OCEANICA</i> AGAINST OXIDATIVE STRESS-RELATED DAMAGE	36
3.3.1. The antioxidant power of <i>P. oceanica</i>	36
3.3.2. The anti-inflammatory role of <i>P. oceanica</i>	38
3.3.2.1. Efficacy of <i>P. oceanica</i> extract against inflammatory pain in vivo	42
3.4. FROM TRADITION TO SCIENCE: THE ANTIDIABETIC ROLE OF <i>P. OCEANICA</i>	44
<b>4. MATERIALS AND METHODS</b>	<b>48</b>
4.1. MATERIALS AND REAGENTS	48
4.2. PREPARATION OF <i>P. OCEANICA</i> LEAVES EXTRACT	49
4.3. DETERMINATION OF TOTAL POLYPHENOLS AND CARBOHYDRATES CONTENT IN POE	50
4.4. EVALUATION OF ANTIOXIDANT AND RADICAL SCAVENGING ACTIVITIES OF POE	50
4.5. CELL LINES AND CULTURE CONDITIONS	50
4.6. CELL VIABILITY ASSAY	51
4.7. WOUND HEALING ASSAY	52
4.8. GELATIN ZYMOGRAPHY	52

4.9. ANALYSIS OF AUTOPHAGIC VACUOLES	53
4.10. SDS-PAGE AND WESTERN BLOT ASSAY	53
4.11. IMMUNOFLUORESCENCE ASSAY	54
4.12. DETECTION OF INTRACELLULAR ROS AND NITRIC OXIDE NITRIC OXIDE PRODUCTION	55
4.12.1. Measurement of intracellular ROS levels	55
4.12.2. Griess reaction assay	55
4.13. ADVANCED GLYCATION END PRODUCTS OF ALBUMIN (AAGES)	56
4.13.1. The <i>in vitro</i> formation of aAGEs	56
4.13.2. Detection of aAGEs by means of fluorescent measurements and polyacrylamide gel electrophoresis under native conditions (N-PAGE)	56
4.13.3. Inhibition of aAGEs formation	56
<b>5. CONCLUSIONS AND FUTURE PERSPECTIVES</b>	<b>58</b>
<b>REFERENCES</b>	<b>62</b>

# 1. INTRODUCTION

## 1.1. The seagrass *Posidonia oceanica* (L.) Delile

Seagrasses, although commonly confused with marine macroalgae, are flowering and rhizomatous plants belonging to the monocotyledonous order Alismatales exclusively living in marine habitats. They are vascular plants deriving from higher terrestrial plants which, 70 to 100 million years ago, secondarily recolonized marine habitats. While sharing many of the primary and secondary metabolic features with their relatives of Alismatales order living in terrestrial and freshwater habitats [1], marine phanerogams are well adapted to life in the marine environment in shallow water at a depth of fewer than 50 meters [2].

About 60 species of monocotyledons are known with over 300,000 species of angiosperms, but this small number compared to terrestrial species is by no means proportional to the importance of their ecological and economic aspect [3,4]. The 60 seagrasses described in the world belong to four different families, namely Cymodoceaceae, Hydrocharitaceae, Posidoniaceae and Zosteraceae. The Mediterranean Sea is populated by five seagrass species, i.e. *Posidonia oceanica* (L.) Delile, *Cymodocea nodosa* (Ucria), *Zostera marina* L., *Z. noltii* Hornemann and *Halophila stipulacea* (Forsskål) Ascherson (non-native species) (Table 1) [5].

Species	Distribution	Habitat	Max. depth (m)
<i>Posidonia oceanica</i>	Mediterranean Sea, stops at the borderline where Mediterranean and Atlantic waters mix	Common on sandy bottoms, is often found on rock and coralline	50
<i>Cymodocea nodosa</i>	Widely distributed throughout the Mediterranean, around the Canary Islands and down the North African coast	Common on sandy bottoms, it prefers calm hydrodynamic environments	40
<i>Zostera marina</i>	Limited and point form; reported in Italy	Common on sandy and muddy bottoms, it suits low-salt waters, low tolerance to desiccation	7
<i>Zostera noltii</i>	Widely distributed throughout the Mediterranean	Common on sandy and muddy bottoms, it suits low-salt waters	6
<i>Halophila stipulacea</i>	Present in the eastern Mediterranean, reported in Italy	Common on sandy bottoms	30

**Table 1.** Summary of the distribution, habitat and maximum depth of the Mediterranean seagrasses species (modified from Buia et al., 2003 [6]).



As for *P. oceanica*, it belongs to the Posidoniaceae family (see the taxonomic classification in Table 2) which has only one genus, Posidonia, comprising a total of 9 species with bipolar distribution: 8 of these are widespread on the Australian coasts, while *Posidonia oceanica* (L.) Delile is the only endemic species of the Mediterranean Sea.

<i>Posidonia oceanica</i> (L.) Delile	
Empire	Eukaryota
Kingdom	Plantae
Phylum	Tracheophyta
Subphylum	Euphyllophytina
Infraphylum	Spermatophytae
Superclass	Angiospermae
Class	Monocots
Order	Alismatales
Family	Posidoniaceae
Genus	Posidonia
Species	oceanica

**Table 2.** Taxonomic classification of *P. oceanica* (www.algaebase.org)

*P. oceanica*, the most abundant and widely distributed seagrass in the Mediterranean Sea, forms vast underwater grasslands (Figure 1) extending from 25,000 to 50,000 square kilometres from the surface up to 40 meters deep, representing the most important seagrass species for the coastal ecological balance of the Mediterranean Sea [5,7].



**Figure 1.** *Posidonia oceanica* (L.) Delile seagrass meadows. The photo was taken by authorized personnel of the Interuniversity Center for Marine Biology and Applied Ecology “G. Bacci” in the protected area of Meloria (Livorno, Tuscany, Italy).

It is present almost throughout the Mediterranean, although less abundant in the Levantine Sea. Its distribution on the western border is located about 250 kilometres east of the Strait of Gibraltar, where a complex mixture of waters of varying density between the Atlantic Ocean and the Mediterranean Sea (known as the Almeria-Oran front) creates the appropriate conditions for its survival (Figure 2) [8].



**Figure 2.** Geographical distribution of *P. oceanica* (red line) along the coast of the Mediterranean Sea. The picture was taken from Vacchi et al., 2017 [8].

*P. oceanica* can grow on different types of substrate, including sand easily penetrated by the roots, but also on detrital and rocky bottoms, where very robust roots can penetrate through the cracks [9,10].

The strong lighting, transparency and depth of water are determining factors for its growth. Withstands relatively significant temperature changes between 10 °C and 28 °C, however, the absence of *P. oceanica* from the Levantine coast and its scarcity in the northern Adriatic could be due to summer and winter temperatures respectively. Therefore, the temperature is considered an essential parameter for this species geographical distribution. It also needs a constant salinity level, it appears to resist high salinity levels more successfully, so it is not common in estuaries or lagoons. Moreover, *P. oceanica* dislikes too intense hydrodynamics, currents and wave action prevents seagrass growth and distribution by causing sediment resuspension and transport [11].

Although *P. oceanica* can grow in extraordinarily different environmental conditions, thanks to its physiological and morphological adaptations, it is particularly affected by changes in the quality of the marine environment and the meadows tend to regress when pollution is too accentuated.

In recent years the strong anthropogenic impact with anchoring and trawling activities and pollution has caused numbness of marine waters, contributing to the rather dramatic regression of *P. oceanica* meadows. Also the coastal development (such as the coast

hardening, urban and port infrastructures), the excessive grazing of hedgehogs and herbivorous fish and the competition with macroalgae accidentally introduced the Mediterranean Sea strongly contribute to this phenomenon [9,12]. This overall decrease has been measured around 34% in the last 50 years [13].

For all these reasons, greater efforts have been made for the legal protection of *P. oceanica* in many Mediterranean countries [14], becoming one of the main goals for the protection and management of the Mediterranean environment.

*P. oceanica* meadows are identified by the European Union's Habitat Directive (92/43/CEE) among the habitats of priority interest [9,15,16], and they are protected by the Berne and Barcelona Conventions and other national legislation. Furthermore, in 2008 the MFSD (2008/56/EC) also selected *P. oceanica* as a representative species of the quality elements of angiosperms for the Mediterranean environment due to its sensitivity to disturbances, its wide distribution along the coast, and the good knowledge of the specific response of the plant and its ecosystem associated with the specific impact [17,18].

## **1.2. Morphology, structure and reproduction**

*P. oceanica* is a slow-growing marine phanerogam organized in roots, rhizomes and leaves (Figure 3) [7,8]. Its thin, soft and very often branched roots allow the anchoring and absorption of nutrients and act as an oxygen reserve.

The rhizomes can be distinguished by the type of growth, horizontal (plagiotropic rhizome) or vertical (orthotropic rhizome).

The plagiotropic rhizomes ensure the plant anchor to the substrate through the roots and favour the substrate colonization. The orthotropic rhizomes, growing in height, contrast the progressive silting up due to the continuous sedimentation, allowing to make the most of the available space and light.

The growth orientation of the rhizome is dynamic and varies according to the available substrate and environmental conditions. However, in both cases the growth rate of rhizomes is rather slow and heavily dependent on seasonality.

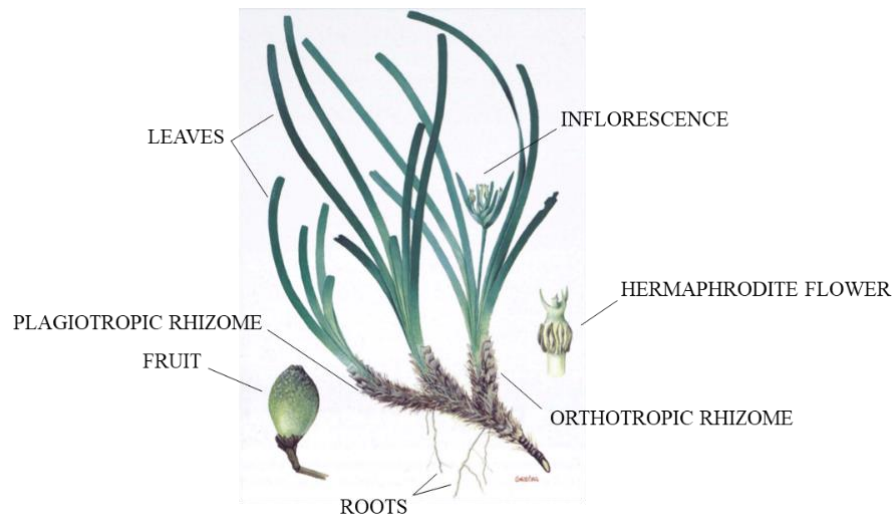


**Figure 3.** *P. oceanica* anatomical details. Picture taken from the book «Praderas y Bosques Marinos de Andalucía» [19].

A unique characteristic of *P. oceanica* meadows is the formation of the so-called "matte" (Figure 4), consisting of the intertwining of several layers of trapped and compacted rhizomes, roots and sediments; the vegetative apex is only at the top of this formation. The substratum features play a key role in the distribution and colonization of *P. oceanica*, and highly influence its morphology and growth dynamics [20-23].

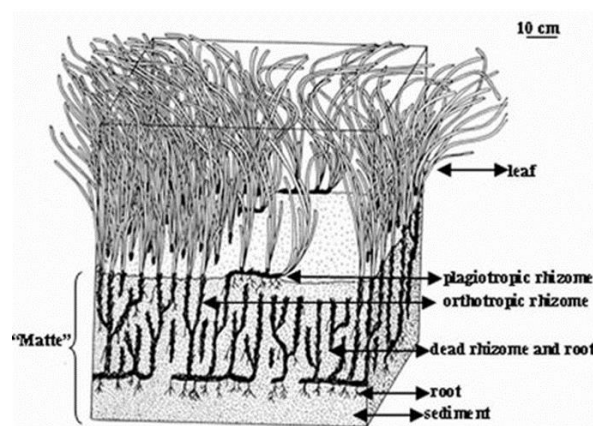


**Figure 4.** Schematic representation of the "matte" structure of *P. oceanica* (modified from Gobert et al., 2006 [7]).

The matte growth speed depends on plant growth and hydrodynamics. In very sheltered areas the matte can create real natural barriers, while in very exposed areas the matte is continuously eroded resulting in the meadows death. Considering that 1 m of matte takes more than 100 years to form, the loss of every cm of meadow lost is serious.

The leaves of *P. oceanica* are ribbon-like, with rounded tips and intense green colour. They can vary in length, from 1 cm up to 1 m. They are generally arranged in bundles

(about 6-7 leaves each) typically fan-shaped: the oldest is distributed outside the bundle, while the younger ones are inside. The leaves are produced continuously, but their growth rate is strongly influenced by season. In summer, *P. oceanica* meadows are full of very long leaves densely covered with epiphytes. With the arrival of autumn and climatic changes, there is a massive fall of adult leaves and a subsequent production of juvenile leaves during the winter period. Autumn storms tend to drag the fallen leaves to the coast, forming the typical accumulations on the beaches, called "banquets" of recognized ecological importance (Figure 5).



**Figure 5.** A relatively thin banquet of *P. oceanica* leaves. The picture was taken from Boudouresque et al., 2017 [24].

As for the reproductive aspects, *P. oceanica* reproduces both asexually (or vegetative way) and sexually [25].

However, *P. oceanica* reproduces mainly through vegetative mode by stolonization, or by multiplication and growth of plagiotropic and orthotropic rhizomes. It is a slow process that involves a 2 cm/year rhizomes elongation, a process generally faster for plagiotropic rhizomes than for the orthotropic ones.

*P. oceanica* is also able to multiply through sexual reproduction by flower fertilization, fruit ripening and seed production [26]. It produces inflorescences which in early autumn carry an average of 3-5 hermaphroditic flowers. Fruiting takes place in spring, through the production of the so-called "sea olives" (Figure 6) which, detached from the plant, float until the seed is released from which a new plant will develop.

However, flowering and fruiting of *P. oceanica* are rare events and little information is available on them.



**Figure 6.** *P. oceanica* fruits called “sea olives”. The picture was taken from Ruiz et al., 2015 [27].

### **1.3. *P. oceanica* ecosystem**

*P. oceanica* meadows are among the most important habitats in the Mediterranean Sea [9,28]. They constitute a complex and well-structured ecosystem playing an important and effective role as a pole of biodiversity, hosting approximately 20-25% of all living species in the Mediterranean Sea. The *P. oceanica* habitat structure makes available numerous vital resources for other organisms' survival [29].

In this habitat, both residents and migrant species use *P. oceanica* as a source of food, refuge from predators or as a suitable place for reproduction and laying of eggs. Indeed, *P. oceanica* ecosystem also constitutes nursery areas for juvenile fish growth thanks to the abundant organic matter and the possibility of shelter among the leaves.

The rich and diverse animal and plant communities populating *P. oceanica* meadows contribute to creating a complex, highly efficient and productive food network, capable of exporting energy to other systems. In this food chain, the epiphytic community growing on *P. oceanica* leaves and rhizomes contributes up to 30% to the overall system production [10,30].

In terms of species, there are few direct herbivores due to the inherent characteristics of *P. oceanica* leaves; only 10% of primary production is used by herbivores, especially *Sarpa salpa* [31]. Indirect herbivores and depositivores, grazers of the epiphytic flora of leaves, on the other hand, are the most represented categories among the animal communities of the leaves. Most of the biomass produced (24-85%) is instead exported as dead leaves [32].

However, the consumption of living *P. oceanica* is limited to a few non-selective animal species capable of taking relatively high quantities of food in which the different nutritional resources are present. In fact, in many seagrass systems, algal epiphytes prove to be a more pleasant food source for herbivores than seagrass tissue, constituting up to 40% of the total biomass of *P. oceanica* leaves [33].



Overall, the high energy content of *P. oceanica* and its sizeable biomass is only minimally available for direct trophic interaction. Hence, *P. oceanica* is defined as a complex structure that plays a primary role as a refuge, a direct and indirect source of food, as well as a producer of energy that is exported to adjacent systems. It is a very varied image in which highly dynamic interactions take place between the different components of the *P. oceanica* system.

#### **1.4. *P. oceanica* ecological significance**

*P. oceanica* meadows are defined as "climax communities" of the Mediterranean Sea. This definition indicates the maximum level of development and complexity that an ecosystem can reach. *P. oceanica* is the essential component for the balance and richness of the Mediterranean coastal environment, and it is important from an ecological, geological and economic point of view, providing benefits to humans [34-38]. Below are the essential biological functions that *P. oceanica* meadows perform in the natural ecosystem of the Mediterranean coastal areas:

- ✓ *P. oceanica* meadows play a crucial role in the balance and health of the Mediterranean coastal environment given the richness of associated flora and fauna, but also for their high primary production. *P. oceanica* seagrass produces a large amount of plant biomass in nearby and deep systems which also implies a high rate of oxygen production. *P. oceanica* is called "the lung of the Mediterranean" producing 14 to 20 litres of oxygen per day per square meter, a photosynthetic by-product which, when released, becomes available for other marine organisms [38].
- ✓ *P. oceanica* meadows are characterized by high biomass production, about 20 g C/m<sup>2</sup>/day, and therefore are recognized among the most productive marine environments. About 50% of organic substances produced by the meadows and by the foliar epiphytes is consumed within the biocenosis, but a considerable part of this primary production (from 25% to 85%) [38] is exported in the form of dead leaves both to the neighbouring ecosystems and in-depth. Therefore, *P. oceanica* meadows play a fundamental role in the circulation of organic substances between the coastal and pelagic systems. The pelagic domain, almost a biological desert when compared to the fertile coastal waters, is thus supplied by a constant flow of food and energy in the form of organic debris, eggs, gametes, larvae, and other forms of organic particles. Furthermore, precisely this characteristic of high primary production makes the

ecosystem of *P. oceanica* grasslands able to sequester large quantities of carbon called "blue carbon" and therefore large quantities of carbon dioxide from the atmosphere [39] with an average rate of 83 g C/m<sup>2</sup>/year, thus managing to significantly oxygenate the coastal waters and helping to alleviate the effects of climate change.

- ✓ The *P. oceanica* ecosystem plays an essential role in coastal dynamics given its role in the seabed consolidation and in sedimentological processes [38,40]. *P. oceanica* stabilizes the seabed with its roots, consolidating and compacting inconsistent substrates. This role makes it possible to counteract the excessive transport of thin sediments from coastal currents. This phenomenon is due to the double action of *P. oceanica* leaves both on the fine particles that are captured and harnessed between rhizomes, and on the waves and currents whose intensity is considerably reduced.
- ✓ *P. oceanica* is a real natural system of defence and protection of the shoreline which slows down and effectively absorbs the hydrodynamics at the seabed. Dead leaves carried by the currents to the shore, especially during winter storms, tend to accumulate forming masses mixed with sand that can even exceed one meter in height, i.e. banquettes [9,41,42]. These structures represent real protection for the beaches, mitigating the damage caused by storm surges and the consequent erosive action of the waves. About 1 m<sup>2</sup> of retreating meadows can cause the erosion of about 15 meters of sandy shoreline.

### **1.5. *P. oceanica* and humans: a millennial history**

Even before discovering its enormous ecological value, archaeological and historical evidence tells of a millennial relationship between *P. oceanica* seagrass and humans. Curiously, in the cave du Lazaret, in the French Maritime Alps, remains of leaves dating back to the end of the Riss glaciation (over 100,000 years ago) were found, presumably used as a bed by the occupants. *P. oceanica* claims numerous traditional uses in human history in various commercial and industrial sectors thanks to its innumerable properties. The first details on *P. oceanica* use in human civilization date back to ancient Egypt, where the *P. oceanica* egagropylys (agglomerates of fairly spherical fibres from dead leaves formed by hydrodynamics in shallow waters and then thrown back onto the beaches, see Figure 7) were used for the production of footwear [43,44].





**Figure 7.** *P. oceanica* egagropylys.

Moreover, for decades *P. oceanica* leaves were used by Venetians to wrap and transport their renowned fragile glass, in fact they were known as "Venetian straw" [45].

Among other practices, *P. oceanica* leaves were also used for the packaging of ceramics and even fresh fish sold in the markets. In the early 20<sup>th</sup> century, the biological characteristics of the seagrass were also exploited in the construction sector, especially by the coastal populations of northern Africa (Egypt, Libya, and Tunisia) who used dry leaves as roofing [46] and thermal insulation for habitations [45].

*P. oceanica* also claims use in agriculture, thanks to the high mineral content of the leaves. In particular, *P. oceanica* leaves were used as an agricultural fertilizer to improve the properties of the soil, a practice long used by farmers on the Mediterranean coast [47-49]. In Tunisia, *P. oceanica* leaves were used as livestock bedding, still in use today thanks to their antifungal and insect repellent properties. Considering the nutritional value of *P. oceanica* leaves similar to that of forage plants, they were also used as food supplements for poultry and livestock [9]. Among other uses, *P. oceanica* was employed in paper production in the late 19<sup>th</sup> century [50,51].

Beyond varied applications in human activities, *P. oceanica* seagrass has traditionally been used also as a medical plant in the treatment of various human disorders.

The first information on the *P. oceanica* healing properties comes from ancient Egypt, where it was supposedly used for sore throat and skin problems [52]. An old botanical handbook of Cazzuola also mentions *P. oceanica* as a popular pharmacopoeia product [53]. It has also been documented that *P. oceanica* leaves were used to treat inflammation and irritation, but also as a remedy for acne, lower limb pain and colitis [54].

On the other hand, the curious use of *P. oceanica* as padding for cushions and mattresses dates back to the 16<sup>th</sup> century. It is believed that this practice served to prevent respiratory infections and to alleviate the conditions of people with tuberculosis.

The use of the decoction of *P. oceanica* leaves as a natural remedy for diabetes and hypertension belongs to a more recent tradition by the inhabitants of the coastal areas of western Anatolia [55].

Therefore, the queen of the seas for 120 million years, *P. oceanica* has also proved to be a precious ally for the care of human health.

### **1.5.1. Pre-project pharmacological studies on *P. oceanica* extract bioactivities**

Before the beginning of my research project, the literature reported very little pharmacological studies on the bioactive properties of *P. oceanica* extracts or derived compounds with potential therapeutic applicability to human health.

In 1989, a study by Pesando et al. [56] had shown antibacterial and antifungal activities in a rhizome extract of *P. oceanica*.

Then in 2008 Goecke et al. conducted a study on the potential therapeutic benefits of a hydroethanolic extract of *P. oceanica* leaves against diabetes-related endothelial dysfunction and oxidative damage. It was observed that continuous oral administration of *P. oceanica* leaves extract in alloxan-induced diabetic rats was able to reduce blood glucose, strongly recover the activity of antioxidant enzymes, and reduce the process of lipid peroxidation [55].

Subsequently, the antioxidant power of an ethanolic extract of *P. oceanica* leaves was further highlighted by a study by Cornara et al. (2018) [57]. In this study, the possible applications of this extract for the treatment of skin and associated diseases were evaluated. These experiments showed that *P. oceanica* was able to stimulate fibroblast proliferation and collagen production, lipolysis in adipocytes and have anti-melanogenic activity, suggesting that *P. oceanica* extract could find applications in skin anti-aging, anti-cellulite and depigmenting products.

Based on these data reported in the literature, my scientific research investigated from a biochemical point of view the bioactive properties of this marine plant that had potential therapeutic applicability for human health.

## **1.6. Marine natural products: from the sea to human health**

Comprehending the potential of the natural world to produce secondary metabolites is noticeable in a broad range of fields, including the discovery of new drugs.

Many pharmacological treatments owe their existence to natural products that currently provide or inspire the production of 50-70% among all agents in clinical use [58].

Interest in the discovery of drugs based on natural marine products emerged in the late 19<sup>th</sup> century, thanks to advances in new technologies and skin-diver equipment.

With more than 70% of the earth's surface area, the marine environment is the biggest terrestrial habitat and prolific supply of biologically active compounds because of its extraordinary biodiversity, which is relatively unexplored in comparison to terrestrial environments.

Therefore, marine natural products with a wide range of biological activities have increasingly attracted the attention of many researchers as a useful resource for developing drugs for the treatment of human diseases [59]. In 2019, the medical and scientific community honoured the 50<sup>th</sup> anniversary of the introduction of cytarabine, the first marine-derived drug, into clinics. Cytarabine (Cytosar-U<sup>®</sup>) was first isolated from a sea sponge [60], and was approved in 1969 by the Food and Drug Administration (FDA, MD, USA) as a drug for leukemia treatment. Shortly thereafter, in 1976, the FDA approved Vidarabine (Vira-A<sup>®</sup>), another drug of marine origin, for the treatment of Herpes simplex virus infection [61]. After a nearly 40-year setback, marine drug development at the beginning of the 21<sup>st</sup> century has entered a period of renaissance.

Nowadays, while many terrestrial natural products are well-documented, marine organisms have become the main source of reliable and varied chemicals. Given the specific environmental conditions, marine organisms are characterized by particular biochemistry which mostly outcomes in unique secondary metabolites. Approximately 28,000 natural marine products have been isolated today, of which 1490 in 2017 alone [62], and hundreds of new compounds are identified daily.

Over the past 20 years, enormous progress has been made in marine drug design, and by the end of 2020 the following drugs were already in use in cancer therapy, and not only:

- *Cytarabine* (Ara-C, Cytosar-U<sup>®</sup> [Pfizer]), deriving from marine sponge, mentioned above;
- *Vidarabine* (Ara-A, Vira-A<sup>®</sup> [Mochida Pharmaceutical Co.]), deriving from marine sponge, mentioned above;
- *Ziconotide* (Prialt<sup>®</sup> [Jazz Pharmaceuticals]), deriving from cone snail, is an N-type calcium channel antagonist. First approved in 2004 for the management of severe chronic pain in patients;
- *Omega-3-acid ethyl esters* (Lovaza<sup>®</sup> [Glaxo Smith Kline]), deriving from fish, is a combination of ethyl esters of omega 3 fatty acids, principally EPA and DHA.

First approved in 2004 for reducing triglyceride levels in adult patients with severe hypertriglyceridemia;

- *Eribulin mesylate* (E7389, Halaven<sup>®</sup> [Eisai Inc.]), deriving from marine sponge, is a microtubule inhibitor. First approved in 2010 for metastatic breast cancer treatment;
- *Brentuximab vedotin* (SGN-35, Adcetris<sup>®</sup> [Seattle Genetics]), deriving from mollusk/cyanobacterium, is a CD30-directed antibody-drug conjugate. First approved in 2011 for the treatment of systemic malignant anaplastic large T-cell lymphomas and Hodgkin's lymphomas.
- *Icosapent ethyl* (Vascepa<sup>®</sup> [Amarin]), deriving from fish, is an ethyl ester of eicosapentaenoic acid (EPA). First approved in 2012 for reducing triglyceride levels in adult patients with severe hypertriglyceridemia;
- *Omega-3-carboxylic acid* (Epanova<sup>®</sup> [AstraZeneca]) is a fish-oil deriving mixture of free fatty acids primarily of EPA and DHA. First approved in 2014 for reducing triglyceride levels in adult patients with severe hypertriglyceridemia;
- *Trabectedin* (ET-743, Yondelis<sup>®</sup> [PharmaMar]), deriving from tunicate, is an ascidian alkaloid. First approved in 2015 for the treatment of soft tissue sarcoma and ovarian cancer;
- *Plitidepsin* (dehydrodidemnin B, Aplidin<sup>®</sup> [PharmaMar]), deriving from tunicate, is a cyclic depsipeptide. First approved in 2018 for leukemia, lymphoma and multiple myeloma treatment;
- *Polatuzumab vedotin* (DCDS-4501A, Polivy<sup>™</sup> [Genetech, Roche]), deriving from mollusk/cyanobacterium, is a CD79b-directed antibody–drug conjugate. First approved in 2019 for the treatment of chronic lymphocytic leukemia, B-cell lymphomas, non-Hodgkin's lymphomas;
- *Enfortumab vedotin* (PADCEV<sup>®</sup> [Astellas Pharma & Seattle Genetics]), deriving from mollusk/cyanobacterium, is a Nectin-4-directed antibody and microtubule inhibitor conjugate. First approved in 2019 for the treatment of adult patients with locally advanced or metastatic urothelial cancer;
- *Belantamab Mafodotin* (Blenrep<sup>™</sup> [Glaxo Smith Kline]) deriving from mollusk/cyanobacterium, is a B-cell maturation antigen (BCMA)-directed antibody and microtubule inhibitor conjugate. First approved in 2020 for the treatment of adult patients with relapsed or refractory multiple myeloma.

- *Lurbinectedin* (ZEPZELCA™ [Pharmamar]), deriving from tunicate, is an alkylating drug. First approved in 2020 for the treatment of adult patients with metastatic small cell lung cancer (SCLC) with disease progression on or after platinum-based chemotherapy.

As of October 2020, other marine-derived compounds are in Phase III, II, or I drug development and are part of the global marine pharmaceutical clinical pipeline (<https://www.midwestern.edu/departments/marinepharmacology/clinical-pipeline.xml>).

In 2015, an analysis found that more than half of the new marine natural products discovered between 1985 and 2012 were used in cancer therapy [59,63]. In addition, marine drugs with antibacterial [64], anti-inflammatory [65], antifungal, antiviral, analgesic [66] and other activities [67] have been discovered.

Pharmaceutical companies are always looking for new resources to develop effective and safe drugs for the growing needs of world population. Given the latest advances in the development, approval and therapeutic use of marine-derived drugs, the marine environment represents enormous potential in the pharmacological field to fight various human diseases [68].

## 1.7. Secondary metabolites of *P. oceanica* leaves

For years *P. oceanica* has been the focus of numerous ecological studies aimed at investigating its role within the entire marine ecosystem.

The strong interest of scientific research for this seagrass has encouraged studies for the metabolic characterization of *P. oceanica* in order to deepen the knowledge on a marine plant of inestimable value.

From these studies it appears that *P. oceanica* is a rich source of secondary metabolites, mainly represented by phenolic compounds [69,70], which physiologically seem to play a key role in the self-protection from photosynthetic stress, reactive oxygen, anthropogenic pressures and inter-specific competition, predators and pathogens [71,72]. Among the phenolic compounds, chicoric acid is recognized as the major secondary metabolite in *P. oceanica* leaves extracts [57,73-75], which, however, also abound in *p*-coumaric, ferulic, gallic, chlorogenic, caffeic, caftaric, cinnamic and gentisic acids [57,69,73,75] (Figure 7).

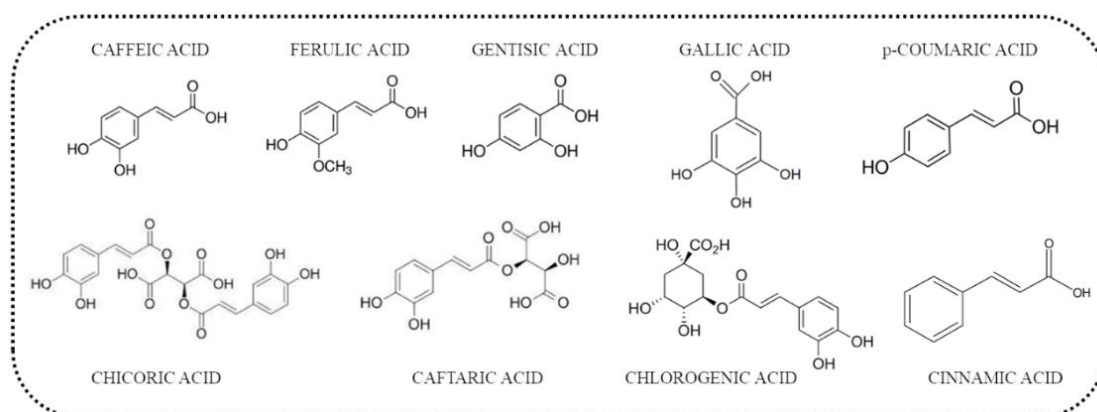


**Figure 7.** Structures of the main secondary metabolites in *P. oceanica* leaves.

Furthermore, myricetin, quercetin, isorhamnetin and kaempferol, found in the diethyl layer of a hydrochloric acid solution used for extraction from *P. oceanica* leaves, have been recognized as the most represented secondary metabolites belonging to the class of flavonoids [76,77] (Figure 8).

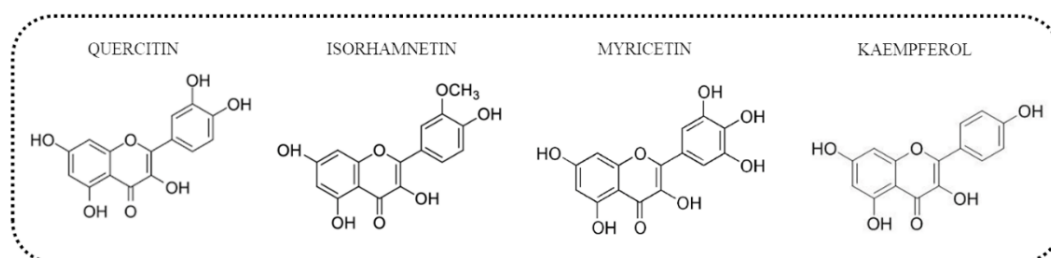


**Figure 8.** Structures of the most represented flavonoids in *P. oceanica* leaves.

Other phenolic derivatives were identified and quantified in *P. oceanica* leaves extracts, including phloroglucinol, pyrocatechol, pyrogallol, vanillin aldehyde, 4-hydroxybenzaldehyde, 3,4-dihydroxybenzaldehyde, benzoic acid, *p*-hydroxybenzoic acid, *p*-anisic acid, vanillic acid, syringic acid, proanthocyanidins and calchones (as phloretin and phloridzin) [73,76].

*P. oceanica* seagrass is also characterized by the presence of long-chain fatty acids. The lipid fraction of *P. oceanica* leaves extracts was found to consist mainly of palmitic, palmitoleic, oleic and linoleic acids, as well as phytosteroids campesterol, stigmasterol and  $\beta$ -sitosterol [78].

In 2013, a new sesquiterpene alcohol called posidozinol was also isolated from a chloroform extract of *P. oceanica* leaves [79].

However, a comparison of results from different extraction methods reported in literature is hardly feasible because of the different strategies used and because *P. oceanica* leaves were not harvested from the same seasonal periods and ecological conditions.

## 2. AIM OF THE THESIS

Although a fair amount of literature discloses the millennial close relationship between *P. oceanica* seagrass and humans, very little attention has been given through the years to the potential benefits of *P. oceanica* for human health.

In 2015 the research group of Prof. Degl'Innocenti of the Department of Experimental and Clinical Biomedical Sciences "Mario Serio" (University of Florence, Italy) launched a scientific investigation aimed at exploring the bioactive properties of *P. oceanica*, testing on biological assays secondary hydrophilic metabolites recovered from leaves by a hydroalcoholic extraction method. Although each individual characterized metabolite was independently tested, none by themselves showed as strong bioactivity as that of the total crude extract. Furthermore, cell-based bioactivity experiments clearly showed that *P. oceanica* extract was effective without leaving obvious signs of cytotoxicity.

The use of phytocomplexes has always been considered, in phytotherapeutic field, an advantage over the use of single molecules (natural or synthetic). A phytocomplex can have greater biological effects than single compounds, in fact their components could act synergistically and exert an overall activity greater than that of the its individual constituents. Furthermore, it very often happens that the mechanism of action of drugs (natural or synthetic), as in the case of anticancer drugs, is based on cellular cytotoxicity, therefore sometimes with toxic side effects and inevitable repercussions on the patient's quality of life.

Therefore, the possibility of using a phytocomplex free from cellular toxicity aroused my interest in continuing the investigation of *P. oceanica* leaves extract as an attractive reservoir of potent and cell-safe molecules. In this regard, the main objective of my PhD research project was to explore the mechanisms and molecular interactions and targeted signalling pathways underlying various bioactivities of the *P. oceanica* phytocomplex, with the future prospective of exploring its, hitherto unknown, potential benefits for human health. Overall, this research sheds light for the first time on *P. oceanica* seagrass as an innovative and promising source of secondary metabolites of possible pharmaceutical interest for the development of new health promoting products for the treatment and/or prevention of numerous diseases.



### 3. RESULTS AND DISCUSSION

My PhD research project focused on studying the bioactive properties of the secondary metabolites of *P. oceanica* leaves. In the following paragraphs, the results achieved during my research activity, and already mostly published in peer-reviewed international scientific journals, will be reported and discussed. For the realization of this PhD project a collaboration has been established with the Interuniversity Center of Marine Biology and Applied Ecology "G. Bacci" (CIBM) of Livorno (Tuscany, Italy), whose expert and authorized personnel collected and supplied fresh leaves of *P. oceanica*.

#### 3.1. Hydroalcoholic extraction from *P. oceanica* leaves

All the bioactive properties of *P. oceanica*, described in the following paragraphs, were investigated by testing the hydrophilic fraction of a *P. oceanica* leaves extract, named POE, in different experimental models. POE was obtained according to the hydroalcoholic extraction method described by Barletta et al., (2015) [80], which consisted of an initial phase of extraction in water/ethanol (30:70 v/v) and a subsequent degumming step with *n*-hexane. This method allowed to remove hydrophobic compounds and recover water-soluble secondary metabolites compatible with biological buffers for *in vitro* and *in vivo* studies. A first UPLC characterization analysis showed that POE consisted of 88% phenolic compounds. Of these, about 85% was represented by (+) catechins, while the remaining 5% by a mixture of gallic acid, ferulic acid, (-) catechin, epicatechin and chlorogenic acid. The small remaining fraction (12%) was represented by minor peaks, indicating the presence of additional compounds which, although detectable as phenols, are unknown/uncharacterized (Figure 8) [80].

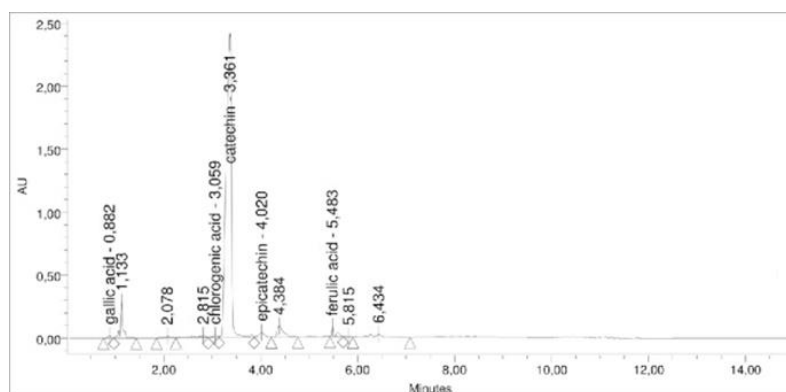


**Figure 8.** UPLC chromatogram of the hydroalcoholic extract of *P. oceanica* leaves. The picture was taken from Barletta et al., 2015 [80].

However, this extraction method proved to be extremely reproducible, as shown by both the quantity of dry extract obtained from each different extraction and the values of the biochemical composition, in terms of total polyphenol and carbohydrate content and antioxidant activities, which are comparable to each other (Table 3).

	Extraction 1	Extraction 2	Extraction 3
Dry extract	20	18	14
Total polyphenols (TP)	5.7 ± 0.3	3.6 ± 0.3	2.0 ± 0.002
Total carbohydrates (TC)	13 ± 2	7 ± 2	16 ± 0.77
Antioxidant activity	1.5 ± 0.3	0.9 ± 0.1	0.6 ± 0.01
Radical scavenging activity	12.8 ± 0.7	11 ± 0.7	3.6 ± 0.3

**Table 3.** The first line indicates the dry extract values (mg) obtained from three different extractions from *P. oceanica* leaves. All other values concern the biochemical characterization of the three extracts and are reported as means ± standard deviations from at least three independent measurements, and expressed in mg/mL of extract after resuspension.

Since natural products have a limited stability over time, POE was tested after one week from solubilization stored at 4 °C. Its composition and activity were very similar to those of fresh prepared batches, demonstrating its stability. However, all experiments were performed with freshly resuspended POE.

Although the extract appears to be mostly composed of catechins it was already curiously observed in Barletta et al., (2015) [80] that its bioactivity was higher than that of pure catechin. Probably all the constituents of the extract, from catechins to less represented components, contribute synergistically to the bioactivity of the extract. Therefore, in my PhD project, I tested the various bioactivities of *P. oceanica* as a phytocomplex and not as individual fractions.

## 3.2. *P. oceanica* in the fight against cancer

### 3.2.1. *P. oceanica* inhibits cancer cell migration through autophagy modulation

#### 3.2.1.1. *P. oceanica* anti-migratory role on human fibrosarcoma HT1080 cells

Cancer is arguably among the most life-threatening diseases in the world. The International Agency for Research on Cancer has estimated that around 18 million new cases of cancer occurred worldwide in 2018 [81].

Although care and long-term survival have already been achieved for some human cancers, current therapies are not without serious side effects that often dramatically

worsen patients' quality of life. These problems place incredible value on the search for new and more effective therapeutic options with less harmful effects [82].

Substantial improvements in the discovery and development of modern drugs make such research feasible. Over 60% of the anticancer drugs approved from 2000 to 2018 were derived from or structurally similar to natural products [83].

Since the 19<sup>th</sup> century attention to the marine environment has grown considerably as an invaluable resource of new phytochemicals with different and unique chemical structures, potentially useful for new drug discovery [84-86], as mentioned in §1.6.

Cancer is commonly characterized by abnormal cell proliferation and the possibility of invading and metastasizing other parts of the body. In solid tumors, invasion and metastasis are determining factors for the clinical stages and prognosis of patients and generally cause over 90% of deaths among cancer patients.

In general, the invasiveness of tumor cells into surrounding tissue and the vascular system is a first step in tumor metastasis. During this process, cells attach to specific extracellular matrix (ECM) receptors and express and release matrix metalloproteinases (MMPs), a family of zinc-dependent endopeptidases, into the surrounding environment. MMPs, and in particular MMP-2 and MMP-9, strongly contribute to the ECM degradation. Then, cells migrate to the degraded area of ECM and the repetition of these events results in cellular invasiveness (Figure 9) [87].

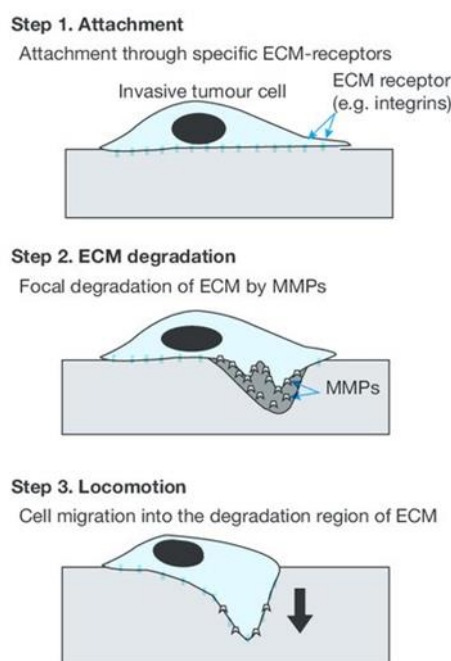


**Figure 9.** Molecular events that take place during cell invasion: the three-step theory. This picture was taken from Nigel et al., 2002 [87].

Unsurprisingly, targeting the ability of cancer cells to migration and consequently invade ECM and establish secondary tumors is crucial in fighting cancer progression. Therefore, the exploration of effective compounds capable of disrupting or normalizing metastatic processes is a key goal of cancer research.

The research of Prof. Degl'Innocenti concerning the *P. oceanica* seagrass as a source of potentially useful bioactive molecules in various phytotherapeutic fields fits into this scenario. In fact, in 2015 Barletta et al. have shown the unprecedented ability of a hydroalcoholic extract from *P. oceanica* leaves (POE) to inhibit the migration of cancer cells [80]. POE was found to significantly inhibit the highly migratory behaviour of human fibrosarcoma HT1080 cells by reducing the expression and activity of MMP-2/9 with no detectable signs of cytotoxicity. For the first time, these findings shed light on POE as an adequate source of secondary metabolites capable of hindering the migration of cancer cells.

The potential of a phytocomplex to effectively exert its bioactivity without affecting cell viability has sparked my interest in studying the mechanism by which POE controlled the motile phenotype of cancer cells.

The literature documents an intricate interplay between autophagy and many other cellular processes, including cell migration. Autophagy is a preserved evolutionary intracellular degradation system that delivers cytoplasmic material to the lysosome (Figure 10).

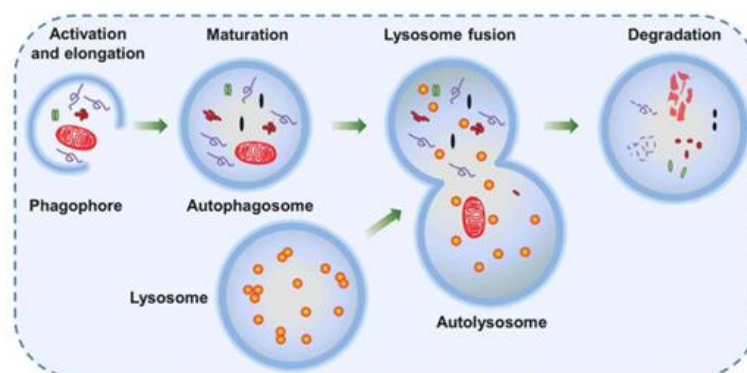


**Figure 10.** Autophagy is activated in response to various stimuli. The phagophore, a double-membrane vesicle, begins to elongate into an autophagosome to engulf cytosolic material for elimination, i.e. damaged, old and long-lived proteins or organelles. Reached complete maturation, the autophagosome merges with the lysosome forming an autolysosome, which provides hydrolytic enzymes with an acidic environment to hydrolyse the material inside. The picture was taken from Li et al., 2019 [88].

In relation to cell migration, some works report that autophagy could counteract the initial stages of the epithelium-mesenchymal transition (EMT) process in which cancer cells lose the typical properties of epithelial phenotype and acquire motile characteristics [89]. Based on these considerations, my research focused on verifying whether POE inhibited the migration of HT1080 cells by triggering the autophagic process.

Initially my research confirmed the ability of POE to inhibit human fibrosarcoma HT1080 cell migration with direct control of MMP-2/9 gelatinolytic activity, through wound healing (§4.7) and gelatin zymography assays (§4.8). Then, several features and markers of autophagy were examined over time in POE-treated cells.

A Cyto-ID<sup>®</sup> staining immunofluorescence assay (§4.9) revealed a clear increase in the number of selectively labelled autophagic vacuoles in the cytosol of POE-treated cells, suggesting that the presence of POE promoted the autophagosome formation.

Therefore, the most common signalling pathways that control autophagy have been explored with the Western blot technique (§4.10), focusing the analysis on the upstream and downstream pathways of the mammalian target of rapamycin (mTOR), the best known suppressive regulator of autophagy (Figure 11).

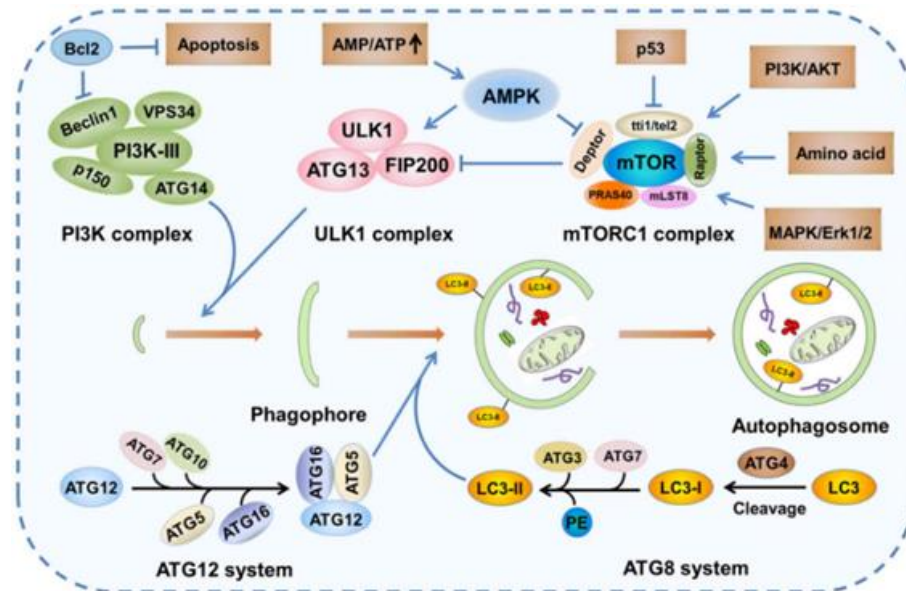


**Figure 11.** The foremost signalling pathways of autophagy. The picture was taken from Li et al., 2019 [88].

In particular, both a reduction in AKT phosphorylation levels, at least up to 7h of treatment, and an early increase in ERK1/2 phosphorylation, were observed in POE-treated cells, compared to untreated control cells. This concomitant and inverse

correlation of the AKT and ERK1/2 phosphorylation state led to the activation of an autophagic flux, as demonstrated by the reduced phosphorylation of S6, a major target used for monitoring mTOR activity, in POE-treated cells.

In addition, the expression levels of Beclin-1, a crucial target for the initial phase of autophagosome formation (upstream event in the autophagic signalling cascade) and therefore a marker of activation of autophagy, was monitored over time.

The levels of Beclin-1 progressively increased until reaching a maximum expression peak at 7h of POE treatment. At this time point, the detection of a slight increase in the conversion of LC3-I to LC3-II (the lipid form), a well-accepted marker of autophagosome elongation, strengthened the evidence for early traces of autophagosome maturation.

While the unchanged level of p62 protein, a marker of autophagy degradation phase, at 7h of POE treatment suggested that autophagolysosome formation was in its early stage. However, the net reduction of Beclin-1 and p62 levels and the marked increase in the lipidation levels of LC3-II at longer times were clear signs of full autophagolysosome formation in POE-treated cells.

The kinetics of autophagy activation upon POE treatment in all the above markers was therefore in agreement with the results obtained with the Cyto-ID<sup>®</sup>.

Furthermore, some studies report that AKT phosphorylation and subsequent signalling are positively correlated with cell motility and gelatinase activation. Thus, the POE-induced reduction in cell motility and MMP-2/9 activity, concurrent with the reduction in AKT phosphorylation, suggests that POE-induced autophagy may have a control over HT1080 cell migration. Furthermore, the literature reports that the insulin-like growth factor receptor 1 (IGF-1R), which translocates to cell nuclei in response to PI3K/AKT signalling, controls MMP-2 expression and thus cell migration [90]. In this regard, through an immunofluorescence analysis (§4.11) my study showed a complete accumulation of IGF-1R in the nuclei of untreated cells, confirming the close association between the nuclear localization of IGF-1R and the motile phenotype of HT1080 cells. An early redistribution of IGF-1R on the cell surface was observed after POE treatment, which progressively decreased after 7h of treatment. Therefore, these kinetic data were perfectly consistent with autophagic signalling and also with the phenotype of POE-treated cells.

Finally, to further confirm the interaction between POE-induced autophagy and its effect on cell migration, POE-treated cells were added with chloroquine, which blocks the

acidification of lysosomes in the last step of autophagy, at 7h - i.e. the most relevant time point for autophagy activation -.

By recording cell migration in a time-lapse wound healing assay, POE was found to block wound closure kinetics after 7h-treatment, but the addition of chloroquine at this time point resulted in the recovery of the motile phenotype.

In conclusion, taken together these results demonstrated for the first time that POE effects on cell migration occurred through the activation of an autophagic flux with no detectable effect on cell viability (Figure 12). The detailed analysis of the achieved results can be found in the published paper [91] attached below.

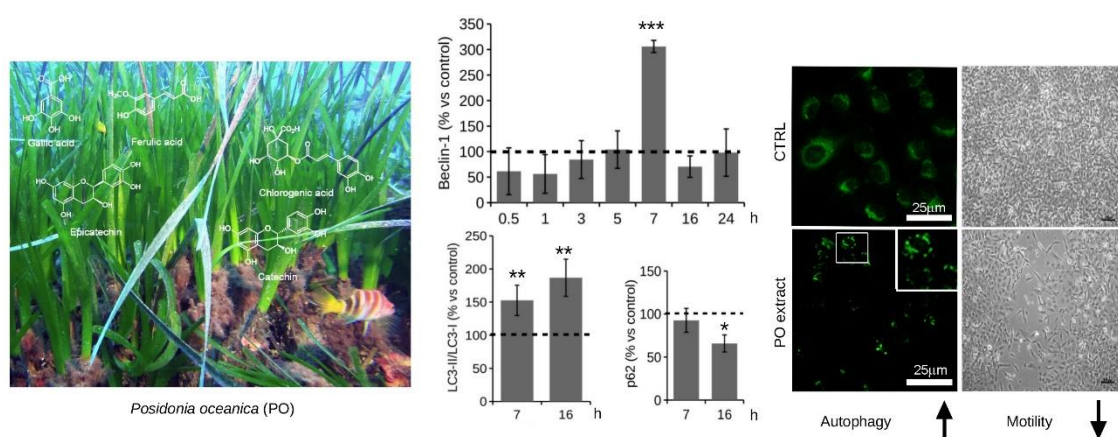



**Figure 12.** Graphical abstract summarizing the results obtained from my research activity on *P. oceanica* anti-migratory activity through autophagy modulation. These results have already been published in 2018 in the international peer-reviewed scientific journal *Marine Drugs* [91].



Article

# Bioactive Compounds from *Posidonia oceanica* (L.) Delile Impair Malignant Cell Migration through Autophagy Modulation

Manuela Leri <sup>1,2,†</sup>, Matteo Ramazzotti <sup>1,†</sup> , Marzia Vasarri <sup>1</sup>, Sara Peri <sup>1</sup>, Emanuela Barletta <sup>1</sup>, Carlo Pretti <sup>3,4</sup> and Donatella Degl'Innocenti <sup>1,4,\*</sup>

<sup>1</sup> Dipartimento di Scienze Biomediche, Sperimentali e Cliniche “Mario Serio”, Università degli Studi di Firenze, viale Morgagni 50, 50134 Firenze, Italy; manuela.leri@unifi.it (M.L.); matteo.ramazzotti@unifi.it (M.R.); marzia.vasarri@unifi.it (M.V.); sara.peri@student.unifi.it (S.P.); emanuela.barletta@unifi.it (E.B.)

<sup>2</sup> Dipartimento di Neuroscienze, Psicologia, Area del Farmaco e Salute del Bambino (NEUROFARBA), Università degli Studi di Firenze, viale Pieraccini 6, 50139 Firenze, Italy

<sup>3</sup> Dipartimento di Scienze Veterinarie, Università degli Studi di Pisa, viale delle Piagge 2, 56124 Pisa, Italy; carlo.pretti@unipi.it

<sup>4</sup> Centro Interuniversitario di Biologia Marina ed Ecologia Applicata “G. Bacci”, Viale N. Sauro, 4, 57128 Livorno, Italy

\* Correspondence: donatella.deglinnocenti@unifi.it; Tel.: +39-055-275-1280

† These authors contributed equally to this work.

Received: 9 April 2018; Accepted: 19 April 2018; Published: 21 April 2018



**Abstract:** *Posidonia oceanica* (L.) Delile is a marine plant with interesting biological properties potentially ascribed to the synergistic combination of bioactive compounds. Our previously described extract, obtained from the leaves of *P. oceanica*, showed the ability to impair HT1080 cell migration by targeting both expression and activity of gelatinases. Commonly, the lack of knowledge about the mechanism of action of phytocomplexes may be an obstacle regarding their therapeutic use and development. The aim of this study was to gain insight into the molecular signaling through which such bioactive compounds impact on malignant cell migration and gelatinolytic activity. The increase in autophagic vacuoles detected by confocal microscopy suggested an enhancement of autophagy in a time and dose dependent manner. This autophagy activation was further confirmed by monitoring pivotal markers of autophagy signaling as well as by evidencing an increase in IGF-1R accumulation on cell membranes. Taken together, our results confirm that the *P. oceanica* phytocomplex is a promising reservoir of potent and cell safe molecules able to defend against malignancies and other diseases in which gelatinases play a major role in progression. In conclusion, the attractive properties of this phytocomplex may be of industrial interest in regard to the development of novel health-promoting and pharmacological products for the treatment or prevention of several diseases.

**Keywords:** *Posidonia oceanica*; autophagy; cell migration; gelatinase; HT1080 cell line

## 1. Introduction

The angiosperm *Posidonia* (*P.*) *oceanica* (L.) Delile is a sea-grass widely distributed in the Mediterranean Sea forming dense underwater meadows that cover tens to thousands of square kilometres. In the sea coast of Western Anatolia, the decoction of *P. oceanica* leaves became an herbal preparation used for diabetes mellitus and hypertension remedies. In fact, the antidiabetic and vasoprotective properties of a *P. oceanica* extract have been confirmed in treated alloxan diabetic rats [1].



Further data on the bioactivity of *P. oceanica* have been described, such as antibacterial and antifungal properties as well as antimelanogenic and lypolitic activities [2] of a crude extract of leaves.

Hence, the interest in *P. oceanica* as a potential source of novel natural products that are useful for the treatment or prevention of different pathological processes has greatly increased. Consequently, the molecular mechanisms through which the bioactive compounds of *P. oceanica* exert their activities need to be clarified.

In our previous work, we used UPLC analysis to characterize the polyphenolic profile of a hydrophilic fraction of *P. oceanica* extract (POE), evidencing a large amount of catechins and minor amounts of polyphenols [3] (Figure 1). Very low doses of POE showed the ability to drastically reduce the motility of the highly invasive HT1080 fibrosarcoma cell line. This effect was due to the concomitant presence of phenolic compounds in the total extract that synergistically decreased the expression of gelatinases and directly inhibited gelatinolytic activity [3].

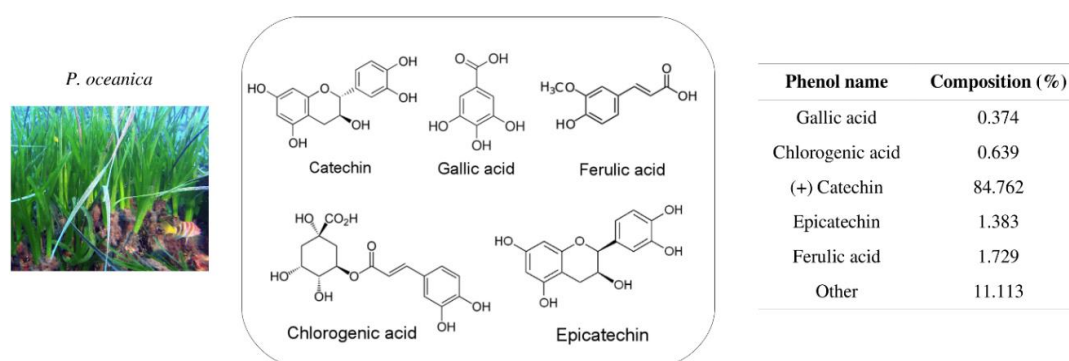


**Figure 1.** Polyphenolic profile characterization of *P. oceanica* extract (POE) by UPLC analysis [3].

Gelatinases, as members of the matrix metalloproteinase MMP family, are fundamental players in maintaining the cellular environments needed by several physiological processes. However, they could participate in the development of important physio-pathological chronic processes, such as neurodegeneration, inflammation and cancer development. Specifically, in cancers, MMPs take part in extracellular matrix degradation and cancer cell invasion and metastasis making cancer cells able to migrate and propagate [4].

Recent studies have correlated cancer cell migration with autophagy (i.e., macroautophagy), the major cellular digestion process conserved from yeast to mammals [5]. Autophagy process leads cells to digest parts and components of their own cytoplasm to overcome intracellular or environmental stress conditions, as nutrient deprivation or hypoxia [6,7].

Generally, motile and invasive cancer cells require autophagy augmentation to survive in stressful conditions during invasive and metastatic processes, but recently it has been proven that autophagy could contrast with early stages of the epithelial to mesenchymal transition (EMT) in which cancer cells lose typical epithelial phenotype properties and acquire motility features [8]. The literature reports that nutrient deprivation in glioblastoma cells impairs both migration and invasion and reverts EMT [9]. On the contrary, the knockdown of key autophagy inhibitors has been proven to stimulate cell migration and  $\beta$ -integrin recycling in HeLa cells [10].

Many different signaling pathways have been described to modulate autophagy, specifically by influencing the activity of the mammalian target of rapamycin (mTOR), its key master regulator [11].

Phosphatidylinositol-3-kinases (PI3K) /Protein Kinase B (AKT)/mTOR and Ras/Raf/Mitogen-activated protein kinase/ERK kinase (MEK)/extracellular-signal-regulated kinase (ERK) (Ras/MEK/ERK) signal transduction pathways are well-established upstream regulators of mTOR, the master autophagy suppressor. They are the main cellular mechanisms for controlling cell proliferation, survival, differentiation, metabolism and motility and both are well-known mediators of autophagy in response to extracellular stimuli [12]. AKT positively modulates mTOR activity and, accordingly, inhibition of

AKT could stimulate the autophagy process by lowering mTOR activity [13] and consequently enhancing Beclin-1 levels, one of the mTOR downstream targets. Beclin-1 is a well-established marker of the early stages of autophagy [14] that promotes nucleation of the autophagic vesicle named the autophagosome. During autophagosome maturation, the phosphatidylethanolamine lipidation of the protein LC3-I to LC3-II occurs. Unlike Beclin-1, LC3-II is a marker of autophagosome full maturation that, in turn, forms the autophagolysosome upon fusion with a lysosome. Lysosomal hydrolases then act to break down the cargo mainly through p62 (i.e., sequestosome 1, SQSTM1), a ubiquitin-binding scaffold protein that drives attached protein targets to autophagosomes for selective degradation (the so-called selective autophagy) and is specifically considered a marker of the degradation phase of autophagy [15].

Beyond its known role in cell survival, the PI3K/AKT axis promotes cell migration in several cancer cell lines, including the HT1080 cell line [16] by increasing cell motility and expression and/or the activity of gelatinases [17]. Specifically, cell-surface insulin-like growth factor-1 receptor (IGF-1R), which senses IGF-1 levels, is an upstream regulator of PI3K/AKT through which it enhances cell proliferation and migration [18]. Pieces of evidence have indicated that the activated IGF-1R translocates to the nuclei of several human cancer cells and regulates, by acting as a transcription regulator, cancer cell migration through the modulation of MMP-2 expression [19,20]. Thus, suppression of the IGF-1R/PI3K/AKT/mTOR signaling pathway could interfere with IGF-1R or AKT activity and could impair cell migration by affecting the expression of gelatinases [21]. Furthermore, it has been demonstrated that the dietary flavonoid, luteolin, reduces the migration of HT1080 cells and attenuates the EMT process via suppression of the IGF-1R/PI3K/AKT/mTOR pathway [22].

As expected from a very basic cell process with a fundamental role in cell homeostasis, an intricate interplay between autophagy and many other processes has been described. It is therefore useful to refer to updated guidelines for the use and interpretation of assays for monitoring autophagy [5].

In order to better clarify our previous findings on POE effects, in this study we aimed to investigate the role of autophagy in the inhibition of the motility of HT1080 cells. In this framework, we used wound-healing assay, zymography, Western blotting as well as confocal microscopy to investigate whether POE could exert, in the absence of other stimuli, its inhibitory effects on migration by modulating autophagy without affecting cell viability.

## 2. Results and Discussion

### 2.1. Biochemical Characterization of POE

Our previous results reported that the water–ethanol extraction method is able to efficiently recover polyphenols and carbohydrates from minced *P. oceanica* dried leaves [3]. In the present study, POE was shown to contain  $13 \pm 2$  mg/mL glucose equivalents of carbohydrates and  $5.7 \pm 0.3$  mg/mL gallic acid equivalents of polyphenols. Their bioactive antioxidant properties were further investigated, evidencing radical scavenging and antioxidant activity of  $12.8 \pm 0.7$  mg/mL and to  $1.5 \pm 0.3$  mg/mL ascorbic acid equivalents, respectively. These values, reported in Table 1, although slightly lower, are in agreement with our previous report, confirming the robustness of our extraction procedure [3]. All treatments hereafter described were done with 1:500 or 1:1000 dilutions of freshly prepared POE corresponding to polyphenol concentrations of 11.4 and 5.7  $\mu$ g/mL gallic acid equivalents. (corresponding to 67  $\mu$ M and 33.5  $\mu$ M), respectively.

**Table 1.** *P. oceanica* extract biochemical composition. All values are reported as means  $\pm$  standard deviations from at least three independent extractions and are expressed in mg/mL of extract after resuspension, as described in the text.

	Polyphenols	Antioxidant Activity	Radical Scavenging	Carbohydrates
Method	Folin–Ciocalteu	Ferrozine®	DPPH	Phenol/Sulfuric acid
Reference control	Gallic acid	Ascorbic acid	Ascorbic acid	Glucose
POE	$5.7 \pm 0.3$	$1.5 \pm 0.3$	$12.8 \pm 0.7$	$13 \pm 2$

## 2.2. HT1080 Cell Migration in Heat-Inactivated Fetal Bovine Serum (FBS) Medium

Classically, starvation medium condition is used to induce EMT and activate the motility features of cells [23]. Abundant literature reports that heat inactivation of FBS (HI-FBS) markedly decreases the levels of several plasma factors, such as MMPs, chemokines and cytokines, compared to the condition with FBS [24]. Hence the use of HI-FBS medium decreases unwanted and unpredictable serum factors that could interfere with various cellular processes. In our experimental set-up, the incubation of cells in conditions such as starvation, FBS medium or HI-FBS medium allowed us to verify the innate motility phenotype of HT1080 cells in correlation with growth conditions. By means of a wound-healing assay, we found that the motility of HT1080 cells decreased but was not abolished in both serum-containing conditions with respect to the starvation medium (Figure 2). In addition, the invasive potential of cells was found to be very similar between HI-FBS and FBS media, clearly showing that the innate motility features of HT1080 cells are maintained in non-stressful, serum-containing conditions. Accordingly, all further experiments were based on cells grown in HI-FBS medium, so that unwanted side effects on cellular processes were minimized while the typical motility phenotype of HT1080 cells was maintained.

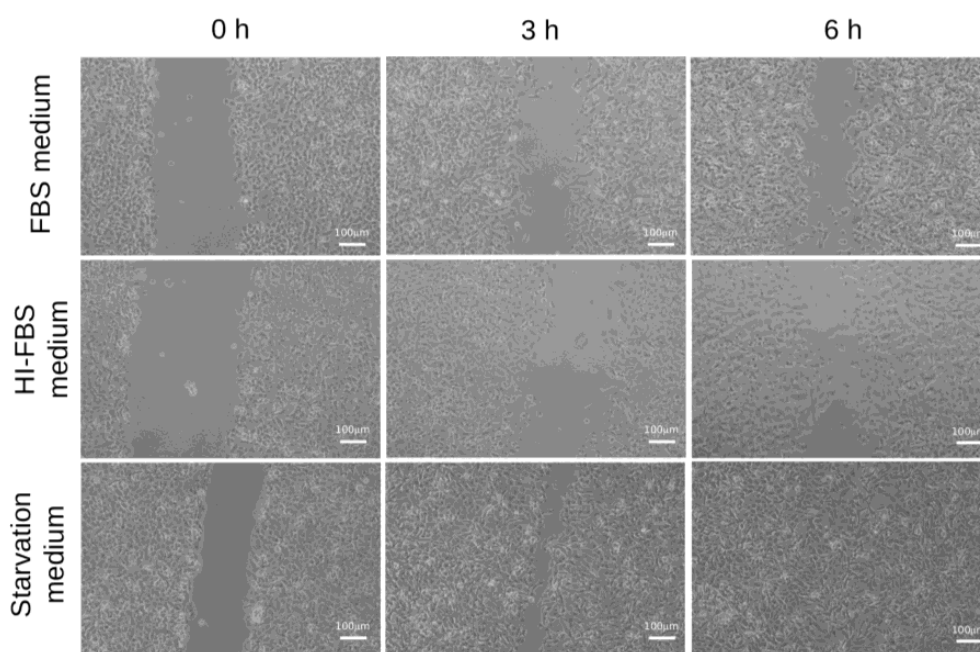


**Figure 2.** Wound-healing assays of HT1080 cells growing in FBS medium (**top**), HI-FBS (**middle**) or starvation medium (**bottom**). Three time points are shown. HT1080 cells maintained their motility phenotype in HI-FBS medium, a favourable condition that is not associated with a basal increase in autophagy.

## 2.3. HT1080 Cell Migration Impairment Following POE Treatment

Having established that the motility phenotype of HT1080 cells was maintained in HI-FBS medium, we performed the wound-healing assays in the presence of 1:500 and 1:1000 POE dilutions. Both treatments did not affect cell viability (Figure 3B) and reduced cell motility in the first seven hours after treatment, an effect that was not present after 16 h (Figure 3A). Such results were further supported by gelatin zymography aimed at monitoring the activity of MMP-2 and MMP-9, well-known markers of cell migration, in conditioned media collected at different time points. The zymography analysis showed a total gelatinase activity reduction after 1:500 and 1:1000 POE treatments. In particular, the 1:500 and 1:1000 treatments led to an observed MMP-2 activity decrease of about 22% during the first 7 h. A more pronounced behaviour during the same time range was found for MMP-9

activity, with a reduction of about 35% for the first 7 h. Such trends were not observed in non-treated control cells at the same times. Gelatinase activities were clearly recovered after 16 h POE treatments, at any tested dose (Figure 3C). These results confirmed that the anti-invasive properties of bioactive compounds from POE on the highly motile HT1080 cell line were, at least in part, due to a transient reduction of gelatinase production or secretion.

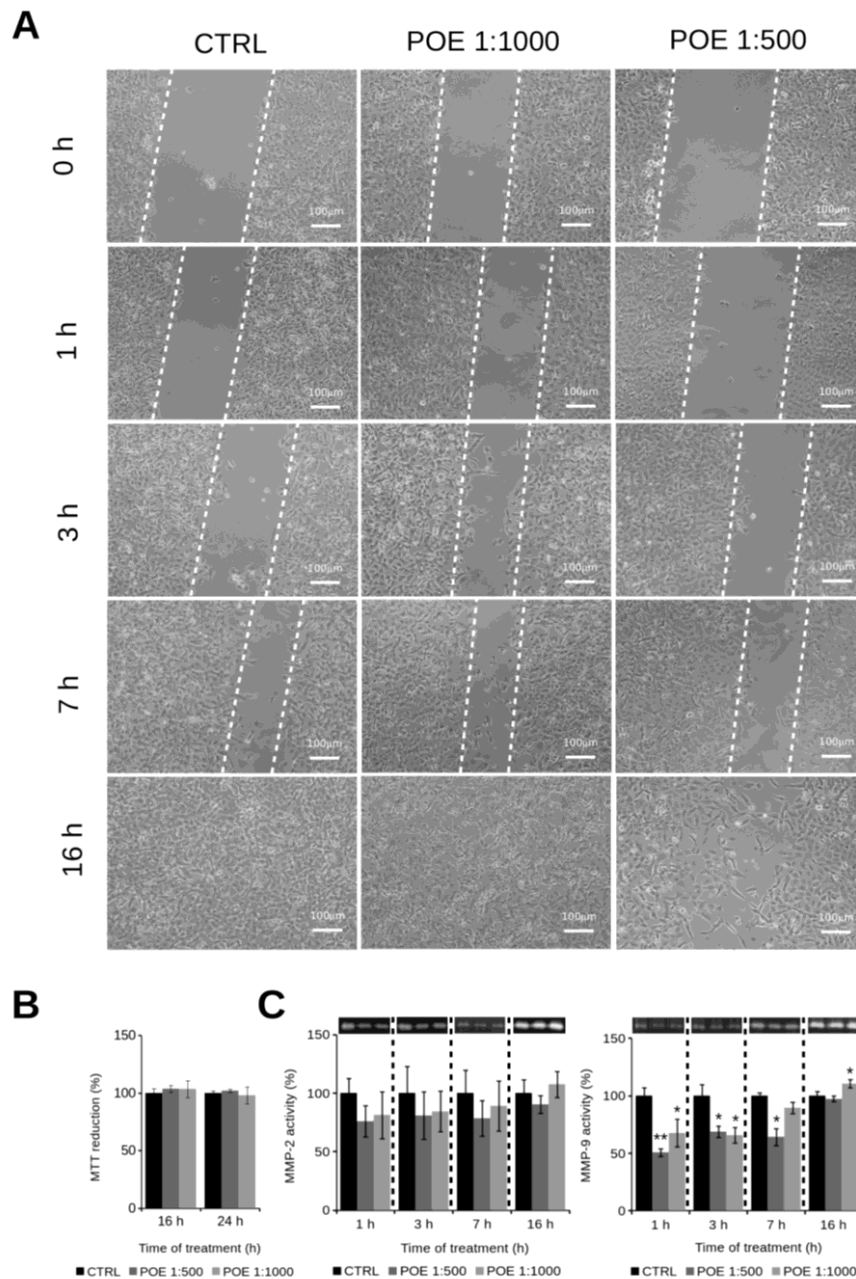


**Figure 3.** (A) Wound-healing assays of HT1080 cells growing in HI-FBS medium, treated or not treated with 1:1000 and 1:500 POE dilutions. The dashed lines mark the boundaries of the wound area; (B) MTT assay showing a substantial absence of cell toxicity by POE; (C) Gelatin zymography of HT1080 conditioned medium collected at 1, 3, 7 and 16 h time points of HT1080 cells cultured in the presence or absence of 1:500 and 1:1000 POE dilutions. The ability of HT1080 cells to migrate to the cell-free space is drastically reduced by the addition of POE in the absence of cell toxicity, in a dose- and time-dependent manner influencing the production or the release of both MMP-2 and MMP-9. \*:  $p$ -value < 0.05; \*\*:  $p$ -value < 0.01; Student  $t$ -test,  $n = 3$ .



#### 2.4. POE Treatment Induces Autophagy in HT1080 Cells

In order to examine the molecular mechanism(s) through which compounds of POE exert the reduction of cell motility demonstrated above, we initially investigated several features and markers of the autophagy process. In fact, recent studies have reported that cell migration could be modulated by autophagy [8]. Firstly, we analysed HT1080 cells treated with POE using Cyto-ID<sup>®</sup> staining, a selective fluorescent marker for autophagic vacuoles [25]. Immunofluorescence results showed a clear increase in autophagy in HT1080 treated cells compared to untreated control cells (Figure 4). The increase of fluorescence intensity and the number of labelled particles in treated cells suggested that POE treatment promotes the formation of autophagosomes in the cytosol. Specifically, we observed a significant increase in Cyto-ID<sup>®</sup> intensity of about 80% and 130% at 1:1000 and 1:500 POE dilutions after 16 h treatment, respectively, compared to untreated cells (Figure 4B). The autophagy modulation was confirmed by using chloroquine and rapamycin as controls. In particular, cells treated with chloroquine did not show an increase in Cyto-ID<sup>®</sup> signal intensity, confirming its autophagy inhibitory role [26]. On the contrary, the autophagy inducer, rapamycin [27], significantly increased the Cyto-ID<sup>®</sup> signal after 16 h of treatment (Figure 4B).

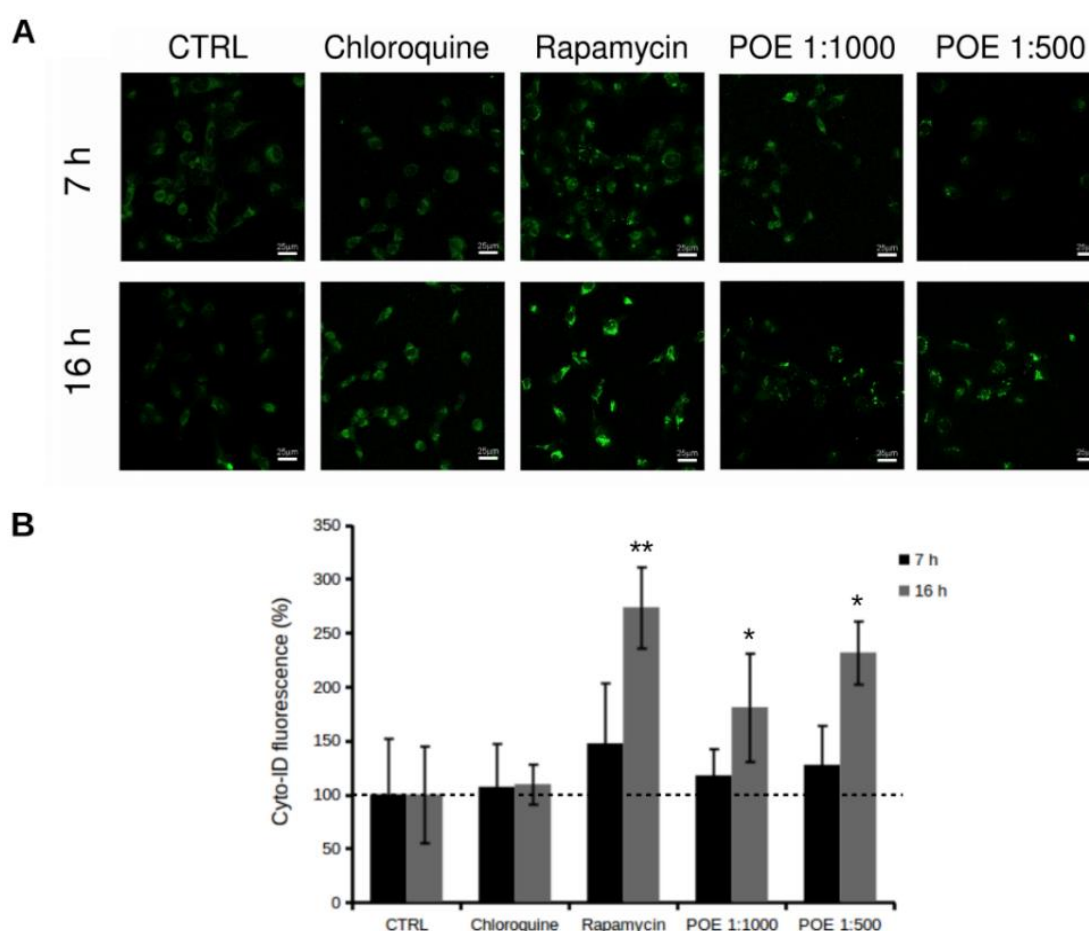


**Figure 4.** Increase of autophagy in HT1080 cells following POE addition. (A) Autophagy specific dye Cyto-ID<sup>®</sup> was analysed by confocal microscopy in HT1080 cells after 7 h and 16 h of treatment with 1:500 and 1:1000 POE dilutions. Rapamycin and chloroquine were used as positive and negative controls, respectively. Autophagy vacuoles increased upon addition of POE in a dose- and time-dependent manner compared to untreated control cells (CTRL); (B) Quantification of Cyto-ID<sup>®</sup> fluorescence. Autophagy significantly increased upon POE treatment in a dose- and time-dependent manner. \*:  $p$ -value < 0.05; \*\*:  $p$ -value < 0.01; Student  $t$ -test,  $n = 3$ .

Given this enabling evidence, we investigated the most common signaling pathways controlling autophagy by Western blotting, focusing our analysis on the upstream and downstream pathways of mTOR, the most well-known suppressive regulator of autophagy. As shown in Figure 5, we assayed signaling pathways in HT1080 cell lysates at different times during 1:500 POE treatment, from 0.5 h to 24 h (considering the ability of the chosen dose to consistently activate autophagy in the absence of toxicity, as shown in Figures 4 and 3B). We showed a reduction in the phosphorylation levels of AKT at 1 h ( $20 \pm 16\%$ ), 3 h ( $15 \pm 12\%$ ) and 5 h ( $24 \pm 18\%$ ) during POE treatments. Since AKT activation by phosphorylation is considered a pro-survival stimulus related to the PI3K/AKT/mTOR survival pathway, the reduction we observed could be potentially ascribed to a pro-apoptotic stimulus. We further monitored the phosphorylation status of ERK, showing an increase in the phosphorylation levels of ERK at 1 h and 3 h, of  $54 \pm 10\%$  and  $66 \pm 11\%$ , respectively. The concomitant and inverse correlations between the phosphorylation status' of AKT and ERK is common in drug-induced stimulation of autophagy [28–30], and it is probably one of the several feedback mechanisms involving pathways fundamental for cellular homeostasis. After 7 h of treatment, the effect of the AKT activity reduction led to a decrease in S6 phosphorylation ( $14 \pm 11\%$ ), one of the main targets used to monitor mTOR activity as a mainstream inhibitor of autophagy. At this time point, AKT maintained a low level of phosphorylation ( $26 \pm 38\%$ ) while ERK phosphorylation returned to control levels. At the 16 h time point, AKT recovered its baseline phosphorylation status while both ERK and S6 phosphorylation continued to decline, as evidenced after 24 h of treatment. We further investigated the dynamics of Beclin-1 levels, since this alteration is considered a crucial event for the initial step of autophagosome formation (so, a downstream event in the autophagic signaling cascade) and therefore, a marker of effective activation of the autophagy process. We observed a progressive increase from 0.5 h up to a peak of activation after 7 h of treatment ( $206 \pm 12\%$ ) with Beclin-1, supporting the observed autophagy enhancement. At the 7 h time point, we further showed initial traces of autophagosome maturation, as supported by a slight increase in the conversion of LC3-I to LC3-II (the lipidated form) ( $86 \pm 8\%$ ), a well-accepted marker of lengthening of the autophagosome. The level of p62 protein, a marker of the degradation phase of autophagy, proved to be substantially unchanged with respect to the untreated control at this 7 h time point, suggesting that the autophagolysosome formation was in its early stage. At the 16 h time point, we detected clear signs of full autophagolysosome formation, with a net reduction in Beclin-1 (that remained unchanged until 24 h, the latest time point we measured), a marked rise in the levels of LC3-II lipidation and a net reduction in p62 protein levels ( $35 \pm 3\%$ ). It is important to underline that the kinetics of the autophagy process activation upon POE treatment in all of the above-mentioned markers is in agreement with the results obtained with the Cyto-ID<sup>®</sup> analysis. In fact, the highest level of Beclin-1 was established at 7 h and correlated well with the initial autophagosome formation that was already evident at 7 h in the Cyto-ID<sup>®</sup> results. The concomitant decrease in Beclin-1, the marked presence of the LC3-II lipidated form and the fall in the p62 protein level after 16 h of POE treatment suggested that the autophagy process was fully mature. This further supports the evidence for the effective maturation of autophagolysosomes, reinforcing the results obtained with Cyto-ID<sup>®</sup> (Figure 4), which in fact is reported to co-localize with LC3 [31].

### 2.5. Autophagy Modulation by POE Decreases Cell Migration

Observed autophagy modulation by POE treatment could contribute to the HT1080 cell migration reduction that we described above. Recent studies have reported the existence of a correlation between autophagy and cell migration. In particular, AKT phosphorylation and the consequent signaling is described as being positively correlated with cell motility and gelatinase activation. Our results show that POE treatment causes a reduction in motility and a reduction in MMP-2/9 activity, concomitant with the reduction in AKT phosphorylation. The literature further reports that MMP-2 expression, and thus, cell migration, can be regulated by IGF-1R which translocates into the cell nucleus in response to PI3K/AKT signaling [17]. We therefore investigated, by confocal microscopy, the relationships between the cell membrane and nuclear accumulation of IGF-1R in untreated cells or cells treated with POE

1:500. It is important to re-emphasize here that HT1080 cells are widely used as a model of cancer cell migration due to their extremely motile phenotype. Our analysis showed complete accumulation of IGF-1R in the nuclei of untreated cells, confirming its association with motility in this cell line (Figure 6). After 0.5 h of POE treatment, cells showed a marked IGF-1R nuclear localization and consequently, a redistribution on the cell membrane, in particular after 3 h of treatment. The documented early increase in IGF-1R redistribution on the cell surface was found to be reduced at 7 h and fully abolished after 16 h of treatment, confirming that the POE effect was transient and lasted for a few hours only. Our kinetic data regarding IGF-1R accumulation was found to be perfectly coherent with the autophagy signaling data shown above and, more importantly, with the overall change in cell phenotype and behaviour upon POE treatment.

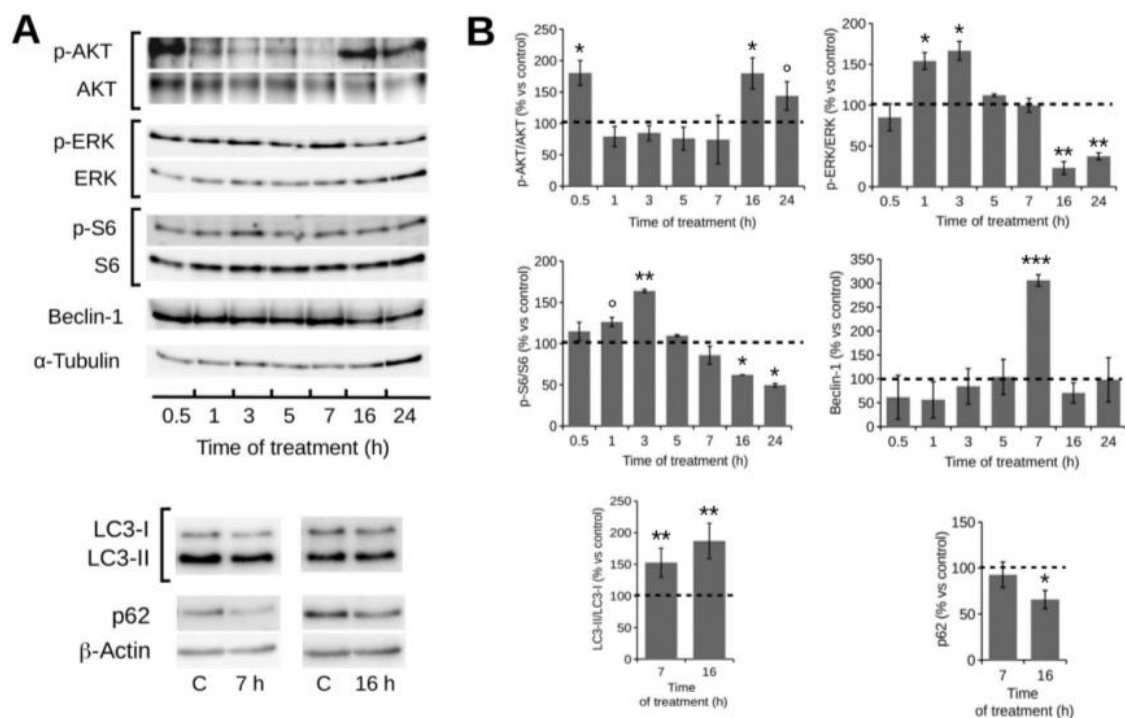


**Figure 5.** Western blotting analysis of the status of autophagy markers in HT1080 cells following 1:500 POE treatment. (A) Representative Western blots of all of the assayed markers; (B) Quantification of signals from a densitometry analysis of at least three independent experiments. Error bars represent standard errors. POE treatment reduces AKT and S6 phosphorylation and increases ERK phosphorylation at the early stages of the HT1080 cell response, while, at late stages, an inverse trend can be observed for AKT and ERK. Beclin-1 progressively increases, reaching the highest peak at 7 h. The LC3-II form increases only at the late stages of the response with a concomitant decrease in p62. <sup>o</sup>: *p*-value < 0.1; \*: *p*-value < 0.05; \*\*: *p*-value < 0.01; \*\*\*: *p*-value < 0.001; Wilcoxon test, *n* = 3.

We further investigated the relationship between POE-induced autophagy and its effect on cell migration by adding chloroquine, which blocks lysosome acidification, i.e., the last step of the autophagy process. We recorded cell migration in a time-lapse wound-healing assay, and we found that, as depicted in Figure 7, the presence of POE determined a stall in wound area closure kinetics after 7 h, in contrast to what was observed in untreated controls (in agreement with the zymographic data shown in Figure 3). The addition of chloroquine at 7 h in POE treated cells, the most relevant time point for autophagy activation, showed a recovery of the motility phenotype. Taken together, such results demonstrate that the effects of POE on cell migration impairment occur through the modulation of the autophagy process.

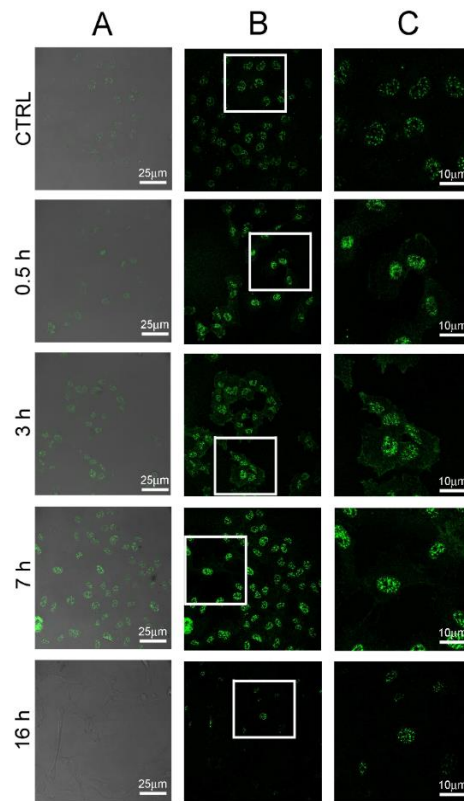


**Figure 6.** Immunofluorescence analysis of cell-surface insulin-like growth factor-1 receptor (IGF-1R) localization. HT1080 cells untreated (CTRL) or treated with 1:500 POE for 0.5 h, 3 h, 7 h and 16 h. (A) Merging of differential interference contrast (DIC) and IGF-1R staining with Alexa 488 (green) channels; (B) Alexa 488 (green) channel; (C) Magnification of selected areas of panel B, showing details of IGF-1R localization within cells.

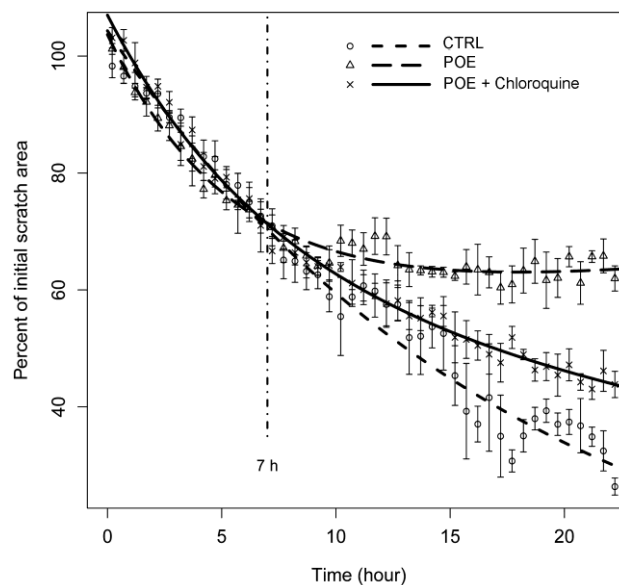


**Figure 7.** Time-lapse experiment of HT1080 migration following treatment with POE and chloroquine. CTRL: untreated HT1080 cells; POE: HT1080 cells treated with 1:500 POE; POE + Chloroquine: HT1080 cells treated with 10  $\mu$ M chloroquine after 7 h treatment with 1:500 POE. A clear recovery of motility was induced by the addition of the autophagy inhibitor, chloroquine, indicating the major involvement of autophagy in the migration arrest induced by POE.



### 3. Materials and Methods

#### 3.1. Materials

3-(2-Pyridyl)-5,6-diphenyl-1,2,4-triazine-4',4''-disulfonic acid sodium salt (Ferrozine<sup>®</sup>),  $\alpha,\alpha$ -diphenyl- $\beta$ -picrylhydrazyl (DPPH), Folin–Ciocalteu's phenol reagent, gallic acid, ascorbic acid, D-glucose, gelatin, Coomassie Brilliant Blue R-250, 1-(4,5-dimethylthiazol-2-yl)-3,5-diphenylformazan (MTT), Dulbecco's Modified Eagle's Medium (DMEM), Fetal Bovine Serum (FBS) and Bovine Serum Albumin (BSA) were all purchased from Sigma Aldrich-Merck (St. Louis, MO, USA). 30% Acrylamide/Bis 37.5:1 solution, ammonium persulfate (APS), 1,2-Bis (dimethylamino) ethane (TEMED), Tris/Glycine buffers, nitrocellulose membranes (0.45  $\mu$ M) blotting membranes and Clarity Western ECL solution were purchased from Bio-Rad. Disposable plastics were from Corning. Photometric measurements from multi-well plates were recorded on an iMARK microplate reader (Bio-Rad, Hercules, CA, USA). When not otherwise specified, all chemicals and solvents, such as ethanol, methanol and n-hexane, were of the highest analytical grade and were purchased from Sigma Aldrich-Merck.

#### 3.2. Preparation of *P. oceanica* Extract

The collection of *P. oceanica* (L.) Delile and the extraction of its hydrophilic components were performed using a previously-described protocol [3]. Briefly, dried *P. oceanica* leaves (collected in July 2016) were minced and suspended overnight in 10 mL of ethanol (70% per gram of leaves) under stirring conditions at 65 °C for 3 h. *P. oceanica* ethanol extract was separated from debris by centrifugation, and the supernatant was mixed in a 1:1 ratio. Hydrophobic compounds were removed by repeatedly shaking, while hydrophilic compounds were mainly contained in the cleaned and recovered phase of the extract and subsequently, were dispensed in aliquots of 1 mL. Batches of the extract were dried by a Univapo<sup>™</sup> vacuum-spin concentrator, and then single batches were dissolved in 0.5 mL 70% ethanol in sterile water before use.

#### 3.3. Determination of Total Polyphenol Content

The total polyphenol content of POE was determined according to the colorimetric Folin–Ciocalteu method [32]. Scalar volumes of POE were dispensed in a 96-well microplate and diluted with H<sub>2</sub>O (final volume 20  $\mu$ L). Then, 100  $\mu$ L of the Folin–Ciocalteu's phenol reagent (diluted 1:10 in H<sub>2</sub>O) was added to each well. After 5 min of incubation at room temperature (RT), 80  $\mu$ L of 7.5% sodium carbonate solution was added per well and incubated for further 2 h. The absorbance at 595 nm was recorded with a microplate reader. Polyphenol content was determined by linear regression using gallic acid as a reference in the range of 0–10  $\mu$ g.

#### 3.4. Determination of Total Carbohydrate Content

The total carbohydrate content of POE was determined according to the phenol–sulfuric acid method [33]. Briefly, scalar aliquots of POE were added to a 96-well microplate and diluted with H<sub>2</sub>O (final volume 50  $\mu$ L), and then 150  $\mu$ L of concentrated sulfuric acid was added to each well. After 5 min of incubation at RT under continuous shaking, 30  $\mu$ L of 5% phenol solution was added to each well and heated for 10 min at 90 °C. After cooling to room temperature for 20 min, the absorbance at 490 nm was recorded with a microplate reader. The carbohydrate content was determined by linear regression using D-glucose as a reference in the range of 0–50  $\mu$ g.

#### 3.5. Determination of Radical Scavenging Activity

The radical scavenging activity of POE was determined by adapting the method from Fukumoto and Mazza [34]. Briefly, scalar aliquots of POE were diluted with 95% methanol (final volume 100  $\mu$ L) and then mixed with 100  $\mu$ L of freshly prepared DPPH solution (0.15 mg/mL in 95% methanol) in

a 96-well microplate. After 30 min of incubation at RT in the dark, the absorbance was recorded at 490 nm with a microplate reader. Radical scavenging activity was determined by linear regression using ascorbic acid as a reference in the range of 0–4  $\mu\text{g}$ .

### 3.6. Determination of Total Antioxidant Activity

The total antioxidant activity of POE was estimated using the FRAP (ferric-reducing/antioxidant power) method [35]. Briefly, scalar aliquots of POE were diluted with water (final volume 50  $\mu\text{L}$ ) and 200  $\mu\text{L}$  of Ferrozine™ reagent (10 mM Ferrozine™ in 40 mM HCl:20 mM ferric chloride:0.3 M acetate buffer pH 3.6, ratio 1:1:10) was added to each aliquot in a 96-well microplate. After 5 min of incubation at RT in the dark, the absorbance was measured at 595 nm with a microplate reader. Antioxidant activity was determined by linear regression using 0.1 mg/mL ascorbic acid as a reference in the range of 0–4  $\mu\text{g}$ .

### 3.7. Cell Line and Culture Conditions

The HT1080 human fibrosarcoma cell line was grown in DMEM (Dulbecco's Modified Eagles Medium) supplemented with 2 mM L-glutamine, 100  $\mu\text{g}/\text{mL}$  streptomycin, 100 U/mL penicillin and 10% fetal bovine serum (FBS medium), at 37 °C in a 5% CO<sub>2</sub>-humidified atmosphere. At 90% confluence, cells were detached by trypsinization (trypsin 0.025%-EDTA 0.5 mM) and propagated after appropriate dilution. Medium supplemented with FBS was inactivated at 56 °C for 30 min (HI-FBS medium), and serum-free medium (starvation medium) was used for some of the following experiments. HT1080 cells were grown in the presence or absence of freshly-dissolved POE and appropriate controls.

### 3.8. Cell Viability Assay

Cell viability was assessed using the colorimetric 3-(4,5-dimethylthiazol-2-yl)-2,5-diphenyltetrazolium bromide (MTT) metabolic activity assay after different cell treatment conditions [36]. In brief, cells were grown in a 24-well plate ( $5 \times 10^5$  cells/well) in HI-FBS medium for 24 h. Then, cells were treated with two different POE dilutions, 1:500 and 1:1000, for 16 h and 24 h, while untreated cells were used as a control. After removing the incubation medium and washing with PBS, 200  $\mu\text{L}/\text{well}$  of 0.5 mg/mL MTT solution was added and incubated in the dark at 37 °C for 1 h. Next, after PBS washing, cells were lysed in 200  $\mu\text{L}$  dimethyl sulfoxide (DMSO) and absorbance values were measured at 595 nm with a microplate reader. Data were expressed in terms of percentage with respect to untreated controls.

### 3.9. Cell Migration Assay

Cell migration was assayed using the scratch wound healing assay. HT1080 cells were seeded in 12-well plates at a high density ( $5 \times 10^5$  cells/well) and grown to confluence overnight in three different culture media, namely FBS medium, HI-FBS medium and starvation medium, with or without POE treatment. Next, we made a vertical wound through the cell monolayers using a sterile plastic tip, and plates were washed several times with PBS to remove cell debris and medium. Fresh culture media was added again, and then the cell-free area was observed under phase contrast microscopy, and images were captured at time points ranging from 0 h to 16 h using a Nikon TS-100 microscope equipped with a digital acquisition system (Nikon Digital Sight DS Fi-1, Nikon, Minato-ku, Tokyo). Time-lapse experiments were performed by seeding  $1 \times 10^6$  cells on 10 cm<sup>2</sup> culture plates and culturing them in HI-FBS medium supplemented with 20 mM HEPES in order to maintain the desired pH without requiring CO<sub>2</sub>. Cells were treated with and without POE (1:500). After 7 h of incubation with POE, the medium was supplemented with chloroquine (10  $\mu\text{M}$ ). The wounded cell-free area was observed under phase contrast microscopy for 24 h at 37 °C. Three frames from the same optical field were captured every 5 min by time-lapse recording, and wound size was analyzed with TScratch software (ETH CSElab, Zurich, Switzerland) and further processed with R statistical software.

### 3.10. Gelatin Zymography

Gelatinase activity was assayed by gelatin zymography using conditioned medium from HT1080 cell cultures previously seeded at a density of  $2 \times 10^5$  cells/well in 24-well culture plates and incubated in FBS medium for 18 h. Subsequently, culture medium was removed, and cells were incubated in HI-FBS medium following addition of 1:500 and 1:1000 POE dilutions for up to 16 h, while untreated cells were used as a control. After these incubation time points, culture supernatants were collected and centrifuged at  $9700 \times g$  for 1 min at  $4^\circ\text{C}$  in order to pellet cell debris. Then,  $2.5 \mu\text{L}$  aliquots of conditioned medium from control or POE treated HT1080 cells were electrophoresed under non-reducing conditions in 8% polyacrylamide gels containing 1 mg/mL gelatin. After the electrophoretic separation, gels were washed twice in 2.5% Triton X-100 for 1 h to remove SDS and then incubated at  $37^\circ\text{C}$  for 24 h in reaction buffer (50 mM Tris-HCl pH 7.4, 0.2 M NaCl, 5 mM  $\text{CaCl}_2$ , 1  $\mu\text{M}$  ZnCl). Gels were stained with 0.05% Colloidal Coomassie Brilliant Blue G-250 dissolved in 1.6% phosphoric acid, 8% ammonium sulfate and 20% methanol and destained in 1% acetic acid. Gelatinase activities appeared as clear bands against a blue background. Zymography images were acquired with a digital scanner.

### 3.11. Analysis of Autophagic Vacuoles

The Cyto-ID<sup>®</sup> Autophagy Detection Kit (Enzo Life Sciences, Shanghai, China) was used to monitor the induction of autophagy using fluorescence microscopy, in accordance with the manufacturer's instructions. Cyto-ID<sup>®</sup> dye selectively labelled the autophagic vacuoles in living cells, so HT1080 cells ( $5 \times 10^4$  cells/well) were seeded for 24 h in a 24-well culture plate containing sterilized glass coverslips. Following treatments for 7 and 16 h with 1:500 and 1:1000 POE dilutions, as well as 0.5  $\mu\text{M}$  of rapamycin and 10  $\mu\text{M}$  of chloroquine as positive and negative controls, respectively, cells were washed twice with PBS and then with 100  $\mu\text{L}$  of  $1 \times$  Assay Buffer provided with the detection kit.

Then, cells were incubated for 30 min at  $37^\circ\text{C}$  with 100  $\mu\text{L}$  of dual detection reagent (prepared by diluting Cyto-ID<sup>®</sup> Green Detection Reagent 330 times in a mixture of  $1 \times$  Assay Buffer), protected from light. Finally, cells were fixed with 2% paraformaldehyde for 20 min and washed three times with the  $1 \times$  Assay Buffer. Then coverslips were placed on microscope slides using a Fluoromount<sup>™</sup> Aqueous Mounting Medium (Sigma Aldrich-Merck). Fluorescent signals were visualized using a Leica TCS SP5 confocal scanning microscope (Leica, Mannheim, Germany) equipped with a HeNe/Ar laser source to allow fluorescence measurements at 488 nm. The cell observations were performed using a Leica Plan 7 Apo X63 oil immersion objective, suited with optics for DIC acquisition. Cells from three independent experiments and three different fields (about 20 cells/field) per experiment were analysed. The fluorescence intensity was analysed with the ImageJ software (Image 1.51j8 version, National Institutes of Health Bethesda, Bethesda, MD, USA), and expressed as percentage increase respect to untreated cells.

### 3.12. Analysis of IGF-1R Localization

HT1080 cells were plated at a density of  $5 \times 10^4$  cells per well in a 24-well culture plate containing sterilized glass coverslips and grown for 24 h. Next, cells were treated with 1:500 POE dilution for 0.5, 3, 7 and 16 h, fixed with 2% paraformaldehyde for 5 min and permeabilized with ice cold 50% acetone/50% ethanol solution for 4 min at RT. After PBS washing, cells were blocked in saturated solution (0.5% BSA and 2% gelatin) for 30 min at  $37^\circ\text{C}$ . After 1 h of incubation at  $37^\circ\text{C}$  with a mouse anti-IGF-1R monoclonal antibody (Cell Signaling) diluted to 1:100 in saturated solution, cells were washed with PBS for 30 min under stirring conditions and then incubated with Alexa 488-conjugated anti-mouse secondary antibody (Invitrogen Molecular Probes) diluted to 1:200 in PBS for 1 h at  $37^\circ\text{C}$  in the dark. Finally, cells were washed twice with PBS, and coverslips were placed onto microscope slides using a Fluoromount<sup>™</sup> Aqueous Mounting Medium. Fluorescent signals were visualized using a Leica TCS SP5 confocal scanning microscope (Leica, Mannheim, Germany) equipped with a HeNe/Ar

laser source for fluorescence measurements. The observations were performed using a Leica Plan 7 Apo X63 oil immersion objective, suited with optics for DIC acquisition.

### 3.13. Detection of Autophagy Markers

HT1080 cells ( $2 \times 10^5$  cells) were seeded in 60 mm dishes in HI-FBS medium condition and were incubated for 24 h. Subsequently, cells were treated with 1:500 POE dilution and after PBS washing they were lysed at different time points, ranging from 0.5 h to 24 h, in 150  $\mu$ L of Laemmli buffer (62.5 mM Tris-HCl pH 6.8, 10% (*w/v*) SDS, 25% (*w/v*) glycerol) without bromophenol blue. The protein concentration of lysates was measured by a BCA protein assay. Equal amounts of cellular lysates (15  $\mu$ g), added with  $\beta$ -mercaptoethanol and bromophenol blue, were resolved by 12% PAGE and transferred onto nitrocellulose membranes. After blocking with 5% (*w/v*) BSA in 0.1% (*v/v*) PBS-Tween-20 for 1 h, membranes were incubated overnight at 4 °C with the primary antibodies of specific protein markers involved in autophagy signaling listed in Table 2. Then, nitrocellulose membranes were washed three times in 0.1% (*v/v*) PBS-Tween-20 and were incubated for 1 h with specific goat anti-rabbit (Invitrogen Molecular Probes) and goat anti-mouse secondary antibodies (Invitrogen Molecular Probes) at a dilution of 1:10,000 in blocking buffer. After washing in 0.5% (*v/v*) PBS-Tween-20, specific protein bands were detected using Clarity Western ECL solution, and chemiluminescent signals were acquired by using Amersham TM 600 Imager (GE Healthcare Life Science, Pittsburgh, PA, USA) imaging system. Immunoreactive bands were quantified by Quantity One software (4.6.6 version, Bio-Rad).

**Table 2.** Primary antibodies used in Western blotting experiments.

Antibody	Target	Dilution	Host	Source
SQTSM1/p62	SQTSM1/p62 protein	1:1000	Rabbit	Abcam
LC3A/B	Microtubule-associated protein light chain 3 (A/B)	1:1000	Rabbit	Cell Signaling
P-AKT1	P-AKT1 serine/threonine kinase (Ser473)	1:5000	Rabbit	Abcam
AKT1/2	AKT1/2 serine/threonine kinase	1:5000	Rabbit	Abcam
p44/42 MAPK(ERK1/2)	Mitogen-activated protein kinases p44/42 (ERK 1/2)	1:2000	Mouse	Cell Signaling
P-p44/42 MAPK(ERK 1/2)	Mitogen-activated protein kinases p44/42 (ERK 1/2) (Thr202/Thr204)	1:1000	Rabbit	Cell Signaling
Beclin-1	Beclin-1 protein	1:1000	Rabbit	Cell Signaling
S6	Ribosomal protein S6	1:1000	Rabbit	Cell Signaling
P-S6	Ribosomal protein S6 (Ser235/236)	1:2000	Rabbit	Cell Signaling
Alpha-Tubulin	Alpha-Tubulin protein	1:1000	Mouse	Cell Signaling
Actin	Actin protein	1:1000	Mouse	Santa Cruz

### 3.14. Data Analysis and Figure Preparation

Where not otherwise specified, data are reported as the mean  $\pm$  standard error of values from three independent experiments, after mean centering as a normalizing strategy across experiments. Plots were drawn with LibreOffice Calc, and panels were assembled with LibreOffice Impress and further adapted with Gimp 2.8.

## 4. Conclusions

In this work, we evaluated the contribution of autophagy to the previously demonstrated reduction of cell migration after POE treatment [3]. After verifying that the HT1080 cell line, a well-known model of cell migration, exhibits a motility phenotype in the absence of starvation (it was important in order to avoid a basal increase in autophagy), we demonstrated that the effects of POE compounds on motility reduction are highly correlated with a transient autophagy increase that has no detectable effect on cell viability.

Usually, the mechanisms of action of anti-cancer drugs are based essentially on the differential cell toxicity and sensibility of actively growing cancer cells with respect to normal cells. Our results demonstrate the potential of POE bioactive compounds to work against cell invasion (e.g., metastasis) with a completely non-toxic mechanism. *P. oceanica* decoction has been historically used as a vitalizer

and traditional remedy for diabetes in Anatolia villages, and the administration of *P. oceanica* extract to rats showed no signs of toxicity [1]. Further studies will be needed to confirm the absence of POE toxicity in humans under experimentally controlled conditions and, more importantly, to establish its anti-metastatic effects in vivo. Nevertheless, this work documents important potential therapeutic properties of *P. oceanica* compounds regarding the prevention of malignancies and other physio-pathological chronic processes, such as neurodegeneration, inflammation and skin aging, in whose progression gelatinolytic activity is the hallmark.

**Acknowledgments:** This work was supported by grant of Fondazione Livorno (N° 2015.0188) and by grant of University of Florence (Fondi di Ateneo 2015 to D.D.).

**Author Contributions:** M.L., M.V., S.P. and M.R. performed the experiments and drafted the manuscript; E.B. and C.P. revised the manuscript; D.D. conceived and supervised the work and revised the manuscript. All authors have read and approved the manuscript.

**Conflicts of Interest:** The authors declare no conflicts of interest.

## References

1. Gokce, G.; Haznedaroglu, M.Z. Evaluation of antidiabetic, antioxidant and vasoprotective effects of *Posidonia oceanica* extract. *J. Ethnopharmacol.* **2007**, *115*, 122–130. [[CrossRef](#)] [[PubMed](#)]
2. Cornara, L.; Pastorino, G.; Borghesi, B.; Salis, A.; Clericuzion, M.; Marchetti, C.; Damonte, G.; Burlando, B. *Posidonia oceanica* (L.) Delile Ethanolic Extract Modulates Cell Activities with Skin Health Applications. *Mar. Drugs* **2018**, *16*, 21. [[CrossRef](#)] [[PubMed](#)]
3. Barletta, E.; Ramazzotti, M.; Fratianni, F.; Pessani, D.; Degl'Innocenti, D. Hydrophilic extract from *Posidonia oceanica* inhibits activity and expression of gelatinases and prevents HT1080 human fibrosarcoma cell line invasion. *Cell Adhes. Migr.* **2015**, *9*, 422–431. [[CrossRef](#)] [[PubMed](#)]
4. Kessenbrock, K.; Plaks, V.; Werb, Z. Matrix metalloproteinases: Regulators of the tumor microenvironment. *Cell* **2010**, *141*, 52–67. [[CrossRef](#)] [[PubMed](#)]
5. Klionsky, D.J.; Abdelmohsen, K.; Abe, A.; Abedin, M.J.; Abeliovich, H.; Acevedo Arozena, A.; Adachi, H.; Adams, C.M.; Adams, P.D.; Adeli, K.; et al. Guidelines for the use and interpretation of assays for monitoring autophagy (3rd edition). *Autophagy* **2016**, *12*, 1–222. [[CrossRef](#)] [[PubMed](#)]
6. Klionsky, D.J.; Emr, S.D. Autophagy as a regulated pathway of cellular degradation. *Science* **2000**, *290*, 1717–1721. [[CrossRef](#)] [[PubMed](#)]
7. DeBerardinis, R.J.; Chandel, N.S. Fundamentals of cancer metabolism. *Sci. Adv.* **2016**, *2*, e1600200. [[CrossRef](#)] [[PubMed](#)]
8. Gugnoni, M.; Sancisi, V.; Manzotti, G.; Gandolfi, G.; Ciarrocchi, A. Autophagy and epithelial-mesenchymal transition: An intricate interplay in cancer. *Cell Death Dis.* **2016**, *7*, e2520. [[CrossRef](#)] [[PubMed](#)]
9. Catalano, M.; D'Alessandro, G.; Lepore, F.; Corazzari, M.; Caldarola, S.; Valacca, C.; Faienza, F.; Esposito, V.; Limatola, C.; Cecconi, F.; et al. Autophagy induction impairs migration and invasion by reversing EMT in glioblastoma cells. *Mol. Oncol.* **2015**, *9*, 1612–1625. [[CrossRef](#)] [[PubMed](#)]
10. Tuloup-Minguez, V.; Hamai, A.; Greffard, A.; Nicolas, V.; Codogno, P.; Botti, J. Autophagy modulates cell migration and  $\beta$ 1 integrin membrane recycling. *Cell Cycle* **2013**, *12*, 3317–3328. [[CrossRef](#)] [[PubMed](#)]
11. Shimobayashi, M.; Hall, M.N. Making new contacts: The mTOR network in metabolism and signalling crosstalk. *Nat. Rev. Mol. Cell Biol.* **2014**, *15*, 155–1719. [[CrossRef](#)] [[PubMed](#)]
12. Mendoza, M.C.; Er, E.E.; Blenis, J. The Ras-ERK and PI3K-mTOR pathways: Cross-talk and compensation. *Trends Biochem. Sci.* **2011**, *36*, 320–328. [[CrossRef](#)] [[PubMed](#)]
13. Jung, C.H.; Ro, S.H.; Cao, J.; Otto, N.M.; Kim, D.H. mTOR regulation of autophagy. *FEBS Lett.* **2010**, *584*, 1287–1295. [[CrossRef](#)] [[PubMed](#)]
14. Kang, R.; Zeh, H.J.; Lotze, M.T.; Tang, D. The Beclin 1 network regulates autophagy and apoptosis. *Cell Death Differ.* **2011**, *18*, 571–580. [[CrossRef](#)] [[PubMed](#)]
15. Tanida, I.; Waguri, S. Measurement of autophagy in cells and tissues. *Methods Mol. Biol.* **2010**, *648*, 193–214. [[PubMed](#)]
16. Kim, D.; Kim, S.; Koh, H.; Yoon, S.O.; Chung, A.S.; Cho, K.S.; Chung, J. Akt/PKB promotes cancer cell invasion via increased motility and metalloproteinase production. *FASEB J.* **2001**, *15*, 1953–1962. [[CrossRef](#)] [[PubMed](#)]



17. Mutschelknaus, L.; Azimzadeh, O.; Heider, T.; Winkler, K.; Vetter, M.; Kell, R.; Tapio, S.; Merl-Pham, J.; Huber, S.M.; Edalat, L.; et al. Radiation alters the cargo of exosomes released from squamous head and neck cancer cells to promote migration of recipient cells. *Sci. Rep.* **2017**, *7*, 12423. [[CrossRef](#)] [[PubMed](#)]
18. Ma, J.; Sawai, H.; Matsuo, Y.; Ochi, N.; Yasuda, A.; Takahashi, H.; Wakasugu, T.; Funahashi, H.; Sato, M.; Takeyanna, H. IGF-1 mediates PTEN suppression and enhances cell invasion and proliferation via activation of the IGF-1/PI3K/Akt signaling pathway in pancreatic cancer cells. *J. Surg. Res.* **2010**, *160*, 90–101. [[CrossRef](#)] [[PubMed](#)]
19. Aleksic, T.; Chitnis, M.M.; Perestenko, O.V.; Gao, S.; Thomas, P.H.; Turner, G.D.; Protheroe, A.S.; Howarth, M.; Macaulay, V.M. Type 1 IGF receptor translocates to the nucleus of human tumor cells. *Cancer Res.* **2011**, *70*, 6412–6419. [[CrossRef](#)] [[PubMed](#)]
20. Donglei, Z.; Pnina, B. Type 1 insulin-like growth factor regulates MT1-MMP synthesis and tumor invasion via PI 3-kinase/Akt signaling. *Oncogene* **2003**, *22*, 974–982.
21. Karam, A.K.; Santiskulvong, C.; Fekete, M.; Zabih, S.; Eng, C.; Dorigo, O. Cisplatin and PI3kinase Inhibition Decrease Invasion and Migration of Human Ovarian Carcinoma Cells and Regulate Matrix-Metalloproteinase Expression. *Cytoskeleton* **2010**, *67*, 535–544. [[CrossRef](#)] [[PubMed](#)]
22. Wang, Q.; Wang, H.; Jia, Y.; Ding, H.; Zhang, L.; Pan, H. Luteolin reduces migration of human cell line via inhibition of the p-IGF-IR/PI3K/AKT/mTOR signaling pathway. *Oncol. Lett.* **2017**, *14*, 3545–3551. [[CrossRef](#)] [[PubMed](#)]
23. Davis, F.M.; Azimi, I.; Faville, R.A.; Peters, A.A.; Jalink, K.; Putney, J.W.; Goodhill, G.J.; Thompson, E.W.; Roberts-Thomson, S.J.; Monteith, G.R. Induction of epithelial-mesenchymal transition (EMT) in breast cancer cells is calcium signal dependent. *Oncogene* **2013**, *33*, 2307–2316. [[CrossRef](#)] [[PubMed](#)]
24. Hernández-Castellano, L.E.; Almeida, A.M.; Renaut, J.; Argüello, A.; Castro, N. A proteomics study of colostrum and milk from the two major small ruminant dairy breeds from the Canary Islands: A bovine milk comparison perspective. *J. Dairy Res.* **2016**, *83*, 366–374. [[CrossRef](#)] [[PubMed](#)]
25. Marx, V. Autophagy: Eat thyself, sustain thyself. *Nat. Methods* **2015**, *12*, 1121–1125. [[CrossRef](#)] [[PubMed](#)]
26. Pasquier, B. Autophagy inhibitors. *Cell. Mol. Life Sci.* **2015**, *73*, 985–1001. [[CrossRef](#)] [[PubMed](#)]
27. Heitman, J. On the Discovery of TOR as the Target of Rapamycin. *PLoS Pathog.* **2015**, *11*, e1005245. [[CrossRef](#)] [[PubMed](#)]
28. Butler, D.E.; Marlein, C.; Walker, H.F.; Frame, F.M.; Mann, V.M.; Simms, M.S.; Davies, B.R.; Collins, A.T.; Maitland, N.J. Inhibition of the PI3K/AKT/mTOR pathway activates autophagy and compensatory Ras/Raf/MEK/ERK signalling in prostate cancer. *Oncotarget* **2017**, *8*, 56698–56713. [[CrossRef](#)] [[PubMed](#)]
29. Shinjima, N.; Yokoyama, T.; Kondo, Y.; Kondo, S. Roles of the Akt/mTOR/p70S6K and ERK1/2 signaling pathways in curcumin-induced autophagy. *Autophagy* **2007**, *3*, 635–637. [[CrossRef](#)] [[PubMed](#)]
30. Ellington, A.A.; Berhow, M.A.; Singletary, K.W. Inhibition of Akt signaling and enhanced ERK1/2 activity are involved in induction of macroautophagy by triterpenoid B-group soyasaponins in colon cancer cells. *Carcinogenesis* **2006**, *27*, 298–306. [[CrossRef](#)] [[PubMed](#)]
31. Prior, R.L.; Wu, X.; Schaich, K. Standardized methods for the determination of antioxidant capacity and phenolics in foods and dietary supplements. *J. Agric. Food Chem.* **2005**, *53*, 4290–4302. [[CrossRef](#)] [[PubMed](#)]
32. Oeste, C.L.; Seco, E.; Patton, W.F.; Boya, P.; Pérez-Sala, D. Interactions between autophagic and endo-lysosomal markers in endothelial cells. *Histochem. Cell Biol.* **2012**, *139*, 659–670. [[CrossRef](#)] [[PubMed](#)]
33. Masuko, T.; Minami, A.; Iwasaki, N.; Majima, T.; Nishimura, S.; Lee, Y.C. Carbohydrate analysis by a phenol-sulfuric acid method in microplate format. *Anal. Biochem.* **2005**, *339*, 69–72. [[CrossRef](#)] [[PubMed](#)]
34. Fukumoto, L.R.; Mazza, G. Assessing antioxidant and prooxidant activities of phenolic compounds. *J. Agric. Food Chem.* **2000**, *48*, 3597–3604. [[CrossRef](#)] [[PubMed](#)]
35. Pulido, R.; Bravo, L.; Saura-Calixto, F. Antioxidant activity of dietary polyphenols as determined by a modified ferric reducing/antioxidant power assay. *J. Agric. Food Chem.* **2000**, *48*, 3396–3402. [[CrossRef](#)] [[PubMed](#)]
36. Berridge, M.V.; Herst, P.M.; Tan, A.S. Tetrazolium dyes as tools in cell biology: New insights into their cellular reduction. *Biotechnol. Annu. Rev.* **2005**, *11*, 127–152. [[PubMed](#)]



### 3.2.1.2. *P. oceanica* anti-migratory role on human neuroblastoma SH-SY5Y cells

Nearly 90% of cancer-associated deaths are due to metastasis and secondary tumor burden in cancer patients. As described in the previous paragraph, a key aspect of metastasis is the invasive ability of tumor cells to reach other sites driven mainly by their migratory capacity [92]. Targeting cancer cell migration, and thus preventing the formation of metastasis, is the rationale for a more effective anticancer therapy. Furthermore, classical cancer therapeutics hardly work by discriminating cancer cells from normal cells, and this often leads to a high therapy-related toxicity, and consequently to serious patient's health problems. Agents capable of negatively influencing the cell migration process according to a non-toxic mechanism for cells could provide a new tool to manage malignant tumors by reducing the high toxicity associated with anticancer drugs.

In light of these considerations, the results obtained regarding the ability of *P. oceanica* phytocomplex to inhibit HT1080 cell migration with a cell-safe profile (§3.2.1.1.) convinced me to test this ability on another cell line with highly motile and invasive phenotype, i.e. human neuroblastoma cells.

Neuroblastoma (NB) is a solid childhood cancer with high mortality. Although many cases of low-risk NB regress spontaneously or with conventional treatment options, more than half of children with aggressive high-risk NB suffer from refractory or relapsing disease that develop widespread metastases to other organs [93]. Although the risk of many cancers in adults can be reduced with some lifestyle changes, there is currently no way to prevent most cancers in children, as there are no lifestyle or environmental causes related to NB, and known risk factors (age and heredity) cannot be changed. Therefore, preventing metastasis by targeting cell migration and invasiveness could be a good therapeutic strategy against tumor progression.

In my as yet unpublished study, the inhibitory control of *P. oceanica* phytocomplex on cancer cell motility was confirmed by monitoring the migration of POE-treated SH-SY5Y cells over time through the wound healing assay (§4.7). It was observed that the untreated control cells migrated rapidly until the complete wound closure after 24h, while POE-treated cells migrated more slowly, in fact at 24h the wound width was about 25% greater than that of the initial scratch (Figure 13).

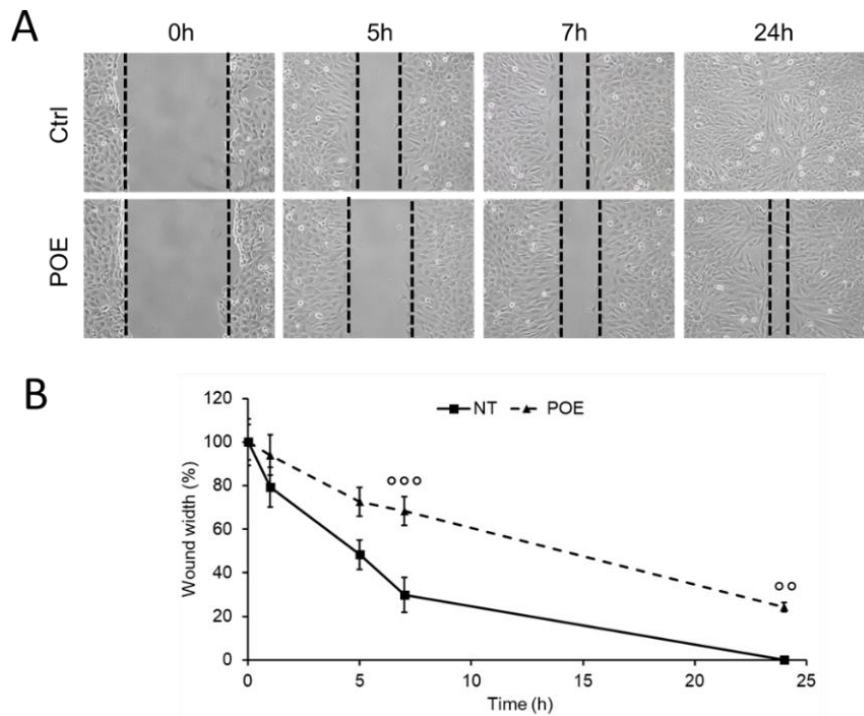


**Figure 13.** POE effect on SH-SY5Y cell migration. (A) Representative image of SH-SY5Y cells, untreated (Ctrl) or treated with POE for 24h. Scratch closure was tracked over time in the cells. The dotted lines mark the edges of the wound area. (B) Time-course analysis of scratch closure of untreated or POE-treated cells. Wound width values were reported as a percentage ratio with respect to the 0h time point. Data are expressed as the mean standard deviation of at least three independent experiments. The error bars represent the standard deviation. °°  $p$ -value <0.01, °°°  $p$ -value <0.001 vs. untreated control cells; Kruskal-Wallis test.

These findings agree with those already obtained on HT1080 cells, further supporting the role of the phytocomplex as an effective inhibitor of cancer cell migration.

Hence, the effect of POE on gelatinolytic activity was verified through a gelatin zymography assay (§4.8). Since MMP-9 is generally secreted in negligible quantities by NB cells [94], it was possible to observe and quantify the effect of POE only on the activity of MMP-2 secreted in the culture medium. POE proved to have a direct role on MMP-2 activity, which was reduced by about 25% after 5h of POE treatment compared to untreated control cells (Figure 14). These data were comparable with those obtained on HT1080 cells.



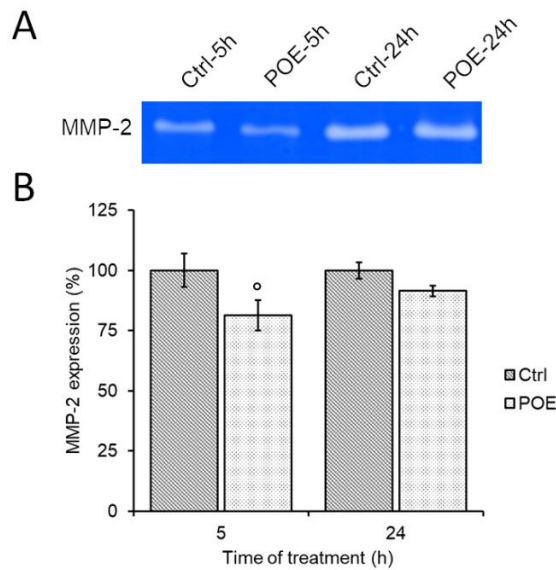


**Figure 14.** POE effect on MMP-2 gelatinolytic activity. (A) Representative image of gelatin zymography on 5h- and 24-hours conditioned medium from untreated control cells (Ctrl) and cells treated with POE.

(B) Quantification of signals from bands in A was determined by densitometry analysis of three independent experiments. Error bars represent standard deviations. °:  $p$ -value < 0.05 vs. the untreated control cells; Kruskal-Wallis test.

Furthermore, the lack of cytotoxicity in POE activity, observed with the MTT assay (§4.6) (Figure 15), confirmed the totally cell-safe profile of *P. oceanica* phytocomplex.

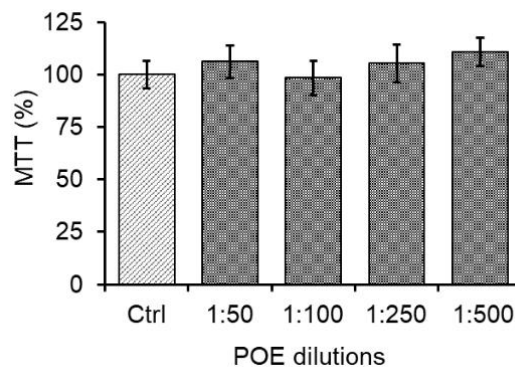


**Figure 15.** POE effect on SH-SY5Y cell viability. MTT assay was performed on cells treated with POE for 24h. Untreated cells were used as control (Ctrl). Data are reported as percentage values compared to untreated control cells and expressed as the mean  $\pm$  standard deviation of at three independent experiments.

This prompted me to verify whether *P. oceanica* phytocomplex was able to act on SH-SY5Y cell migration by activating an autophagic transient not related to cell death as well as already observed in HT1080 cells. Thus, the expression level of the main autophagic markers in POE-treated cells was investigated through the Western blot technique (§4.10) (Figure 16). In particular, the levels of S6 phosphorylation, an mTOR activation marker

(suppressive regulator of autophagy), of LC3-II, a marker of autophagosome elongation, and of p62, a marker of the degradation phase of autophagy, were monitored over time. After 5h of POE treatment, SH-SY5Y cells showed a 50% reduced level of S6 phosphorylation ( $46 \pm 0.5\%$ ) compared to that of untreated control cells. This proved that the phytochemical had inhibitory control over the activation of the mTOR signalling cascade, already at an early stage, leading to the activation of an autophagic transient. The LC3-II expression peak at 5h of POE treatment ( $182.2 \pm 17\%$ ), which coincided with the utmost inhibition of mTOR, indicated that POE-induced autophagy was in the autophagosome elongation phase.

The concomitant and inverse relationship between the expression levels of LC3-II and p62, and in particular the expression of p62 below baseline levels at 5h of treatment, suggested that degradation of the cytosolic material occurred at this time. In fact, when p62 interacts with autophagic substrates and transports them to the autophagosomes for degradation, it is itself degraded, justifying the reduction of about 25% ( $76.8 \pm 5\%$ ) of p62 levels, already at 1h and 5h, in POE-treated cells compared to baseline levels of untreated control cells.

The progressive accumulation of p62 in POE-treated cells starting from 7h, concomitant with the progressive reduction of LC3-II and S6 phosphorylation levels suggested that the POE-activated autophagic transient was moving towards its final step.

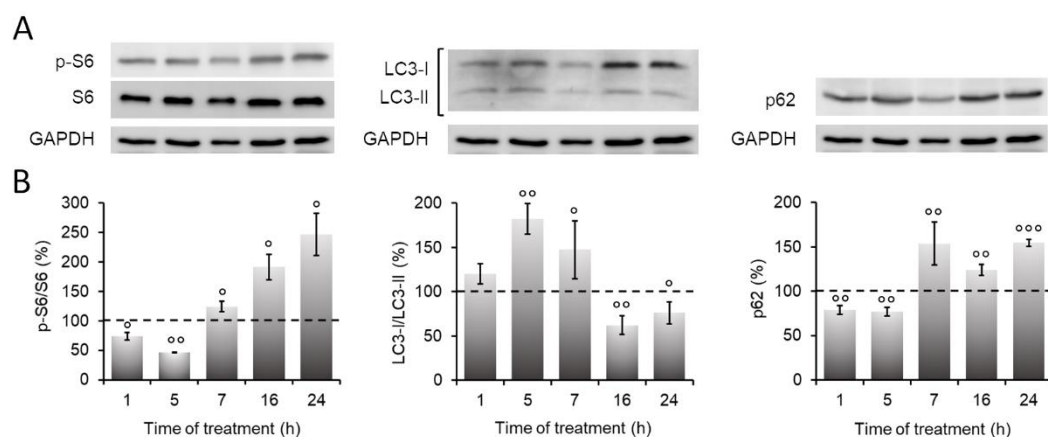


**Figure 16.** POE effect on the autophagic flux activation. **(A)** Representative images of the main autophagic markers obtained with the Western blot. **(B)** Quantification of signals from bands in A through a densitometric analysis of at least three independent experiments. Error bars represent standard errors: °:  $p$ -value  $< 0.05$ ; °°:  $p$ -value  $< 0.01$ ; °°°:  $p$ -value  $< 0.001$  vs. the untreated control cells; Kruskal-Wallis test.

Overall, these results strengthened that POE is able to drastically inhibit cell migration by reducing gelatinolytic activity through the modulation of an autophagic process unrelated to cell death.

One of the approaches used to treat high-risk NB is the differentiation therapy. Inducing cell differentiation has the advantage of reducing the nonspecific toxicity compared to conventional therapies, since the differentiating agents would, theoretically, not affect mature functional cells [95]. The 13-cis-retinoic acid is the most effective differentiation agent available for the treatment of neuroblastoma and is currently used as standard care for post-remission maintenance therapy in patients with high-risk NB. However, the resistance of some neuroblastomas to retinoic acid makes it necessary to identify new differentiating agents to treat retinoic acid-resistant neuroblastomas [96].

In this regard, other experimental investigations are currently underway to evaluate whether POE is able to control the differentiation of SH-SY5Y cells. The possibility of POE both to inhibit cell migration and to trigger a first phase of cell differentiation would mean slowing down the high proliferative rate of cancer cells, and therefore blocking one of the main characteristics underlying the progression of cancer.

To date my research can propose POE as an adequate source of secondary metabolites effective against cancer cell migration. Study on the role of POE on SH-SY5Y cell differentiation could reinforce these findings in support of the POE efficacy against tumor progression.

### **3.2.2. Bio-enhancement of *P. oceanica* anti-migratory role by nanotechnology**

Advances in cancer prevention, detection and treatment date back to recent years thanks to a better understanding of the biological mechanisms of cancer.

However, conventional anti-cancer treatments - i.e. surgery, chemotherapy, radiotherapy, immunotherapy, and hormone therapy - often show high toxicity related to severe adverse effects due to their low specificity. Furthermore, almost all cancer therapeutics can induce a drug resistance response in cancer cells. For these reasons, cancer therapy research is continually seeking new and more effective therapeutic approaches [97].

In this regard, nanotechnologies have obtained excellent results in improving anticancer therapies by reducing side effects and overcoming the problems of drug resistance [98,99]. Numerous nanosystems are designed to deliver drugs in different types of formulations - i.e. liposomes, polymer nanocapsules and dendrimers -, and are made up

of materials capable of masking the unfavourable biopharmaceutical properties of the encapsulated molecule [98].

Nanoparticles (NPs) (Figure 17) are increasingly seen as potential candidates for safely transporting therapeutic agents in targeted compartments, and a wide variety of NPs classes are being studied for cancer treatment, including lipid-based, polymer-based, inorganic nanoparticles and drug-conjugated nanoparticles [98,100].

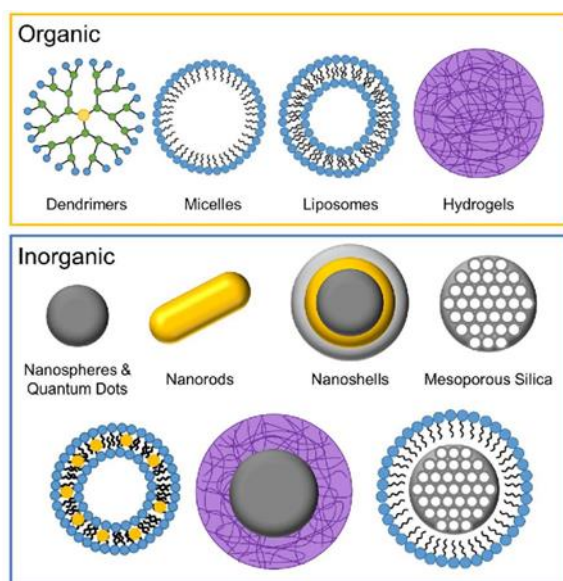


**Figure 17.** Schematic examples of some common types of organic and inorganic NPs explored in cancer therapeutics and diagnostics. This picture was taken from Falagan-Lotsch et al., 2017 [100].

For years natural products have shown effective anticancer activities, proving to be a good source of chemotherapy and cancer prevention agents [83]. Unfortunately, the reduced bioavailability of natural products, often related to their hydrophilic or lipophilic nature, and their possible cytotoxicity limits the use of natural products in anti-cancer therapy, but also in the treatment of other pathologies [98].

The use of different nano-delivery systems for the administration of natural products can increase their stability and bioavailability *in vivo*, but also reduce the adverse effects by improving their selective activity against cancer cells. The use of nanotechnologies is thus an exceptional tool to improve the bioactive efficacy of many natural products [101,102]. In this perspective, in collaboration with the research group of Prof. Maria Camilla Bergonzi (Department of Chemistry, University of Florence, Italy), my research intended to verify whether the use of nanoformulations could increase the aqueous solubility of *P. oceanica* phytocomplex and improve its bioactivity, in particular its ability to inhibit SH-SY5Y human neuroblastoma cell migration. Hence, this research aimed to explore

possible alternative and innovative approaches to the management of cancer progression, such as high-risk neuroblastoma.

This study envisaged the development of nanosystems capable of transporting no single molecules but a phytocomplex containing molecules with different polarity.

In this regard, Prof. Bergonzi's laboratory supplied both chitosan nanoparticles and Soluplus polymeric micelles, both loaded with POE and named respectively NP-POE and PM-POE. These nanoformulations were chemically and physically characterized in terms of size, homogeneity,  $\zeta$ -potential, morphology, encapsulation efficiency and storage stability. *In vitro* release studies were also performed.

In terms of size, it was found that POE loading into the chitosan nanoparticles induced an increase in size, while this did not occur for POE loading into the polymeric micelles. This phenomenon, as reported in the literature, could be due to the interference of the extract on the cohesive force between chitosan and tripolyphosphate [103]. The different sizes and morphological characterization of NP-POE and PM-POE are shown in Figure 18.

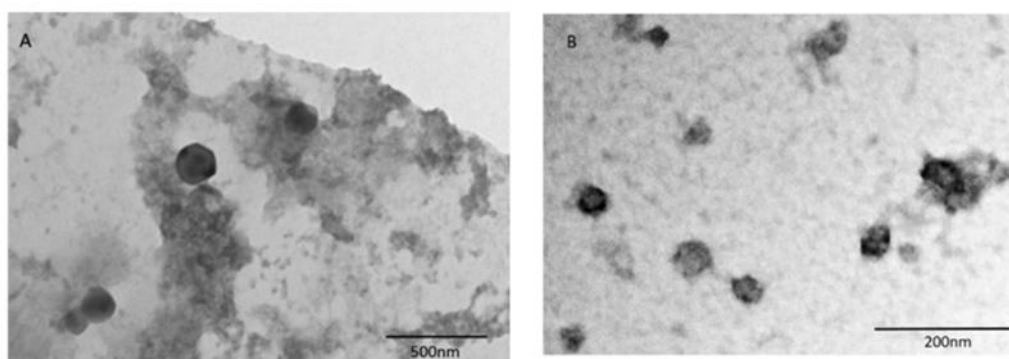


**Figure 18.** TEM images of (A) POE-loaded nanoparticles (NP-POE) and (B) POE-loaded Soluplus polymeric nanomicelles (PM-POE).

Furthermore, the encapsulation efficiency (EE%) studies showed that both nanoformulations increased the aqueous solubility of the extract, but with a higher EE% for PM-POE rather than NP-POE. This was in line with the literature which already describes a good ability of nanomicelles to improve the solubility of extracts [104].

However, for the first time this work used Soluplus nanomicelles to increase the solubility of a phytocomplex of marine origin.

According to the *in vitro* release studies, Prof. Bergonzi obtained that NP-POE released the extract in a sustained manner probably due to the diffusion of adsorbed extract and its

diffusion through the polymeric matrix, mechanisms that regulate the release of drugs from chitosan nanoparticles.

On the other hand, for PM-POE the release profile was slower and more prolonged over time than both NP-POE and POE solution. The results obtained are in agreement with the literature that refers to a delayed release of nanoformulations of polymeric micelles.

Once the nanoformulations were chemically and physically characterized, my task was to test NP-POE, PM-POE and their respective controls on human neuroblastoma SH-SY5Y cells.

First, cell viability was assessed by the MTT assay (§4.6). It was observed that NP-POE had no effect on cell viability, as well as POE. In the case of cells treated with PM-POE, however, the cell viability was about 80% due to the low toxicity attributable to polymeric micelles, as already described in the literature.

The effect of *P. oceanica* phytocomplex, alone or loaded in nanoformulations, on the migration of SH-SY5Y cells through wound healing assays (§4.7) was then monitored over time. Untreated cells, POE-treated cells and cells treated with empty nanoformulations were used as controls.

The ability of POE to inhibit SH-SY5Y cell migration, described in §3.2.1.2, was confirmed, as the wound was not completely closed after 24h of treatment compared to that of untreated control cells.

Furthermore, it was observed that empty nanoparticles and NP-POE did not have a significant inhibitory effect on cell migration, in fact after 24h of treatment the wound was completely closed as in untreated control cells.

On the other hand, PM-POE was found to enhance the inhibitory effect of POE on cell migration. After 24h of treatment, PM-POE prevented the complete closure of the wound; also the empty polymeric micelles prevented a total wound closure at 24h keeping it open by about 10%, compared to the initial scratch. This delay in wound closure compared to untreated control cells could be attributed to the reduced cell viability observed after 24h of vehicle treatment. However, despite the slight inhibition of empty polymeric micelles on cell migration, PM-POE inhibited migration of SH-SY5Y cells by 30% more than 24-hour POE.

Overall, these results showed that polymeric micelles were able to enhance the inhibitory efficacy of POE on cell migration. This phenomenon could be attributed to the physical and chemical characteristics of PM-POE, that is, an amphiphilic vector capable of increasing the solubility of both lipophilic and hydrophilic constituents of the *P. oceanica*

extract. Prolonged release of POE from nanomicelles could also be a factor responsible for the proven bio-enhancement of POE (Figure 19).

The detailed analysis of the achieved results can be found in the published paper [105] attached below.

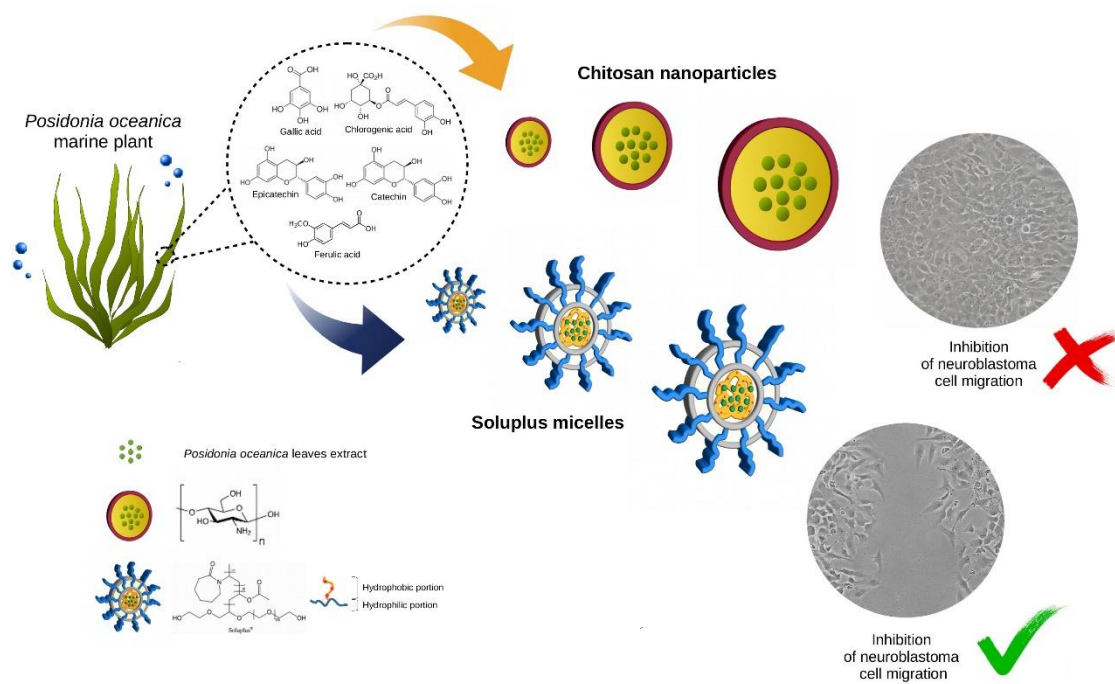







**Figure 9.** Graphic abstract summarizing the results obtained from my research activity on the bio-enhancement of *P. oceanica* anti-migratory activity by Soluplus nanoformulations. These results have already been published in 2019 in the international peer-reviewed scientific journal *Pharmaceutics* [105].



Article

# Comparison of Chitosan Nanoparticles and Soluplus Micelles to Optimize the Bioactivity of *Posidonia oceanica* Extract on Human Neuroblastoma Cell Migration

Vieri Piazzini <sup>1,†</sup> , Marzia Vasarri <sup>2,†</sup> , Donatella Degl'Innocenti <sup>2</sup> , Asia Guastini <sup>1</sup>,  
Emanuela Barletta <sup>2</sup> , Maria Cristina Salvatici <sup>3</sup> and Maria Camilla Bergonzi <sup>1,\*</sup> 

<sup>1</sup> Department of Chemistry, University of Florence, Via Ugo Schiff 6, 50019 Sesto Fiorentino, Italy; vieri.piazzini@unifi.it (V.P.); asia.guastini@stud.unifi.it (A.G.)

<sup>2</sup> Department of Experimental and Clinical Biomedical Sciences “Mario Serio”, University of Florence, Viale Morgagni 50, 50134 Florence, Italy; marzia.vasarri@unifi.it (M.V.); donatella.deglinnocenti@unifi.it (D.D.); emanuela.barletta@unifi.it (E.B.)

<sup>3</sup> ICCOM—Centro di Microscopie Elettroniche “Laura Bonzi”, CNR, 50019 Sesto Fiorentino, Italy; salvatici@ceme.fi.cnr.it

\* Correspondence: mc.bergonzi@unifi.it; Tel.: +39-055-457-3678

† These authors contributed equally to this work.

Received: 8 October 2019; Accepted: 3 December 2019; Published: 6 December 2019



**Abstract:** *Posidonia oceanica* (L.) Delile is a marine plant endemic of Mediterranean Sea endowed with interesting bioactivities. The hydroalcoholic extract of *P. oceanica* leaves (POE), rich in polyphenols and carbohydrates, has been shown to inhibit human cancer cell migration. Neuroblastoma is a common childhood extracranial solid tumor with high rate of invasiveness. Novel therapeutics loaded into nanocarriers may be used to target the migratory and metastatic ability of neuroblastoma. Our goal was to improve both the aqueous solubility of POE and its inhibitory effect on cancer cell migration. Methods: Chitosan nanoparticles (NP) and Soluplus polymeric micelles (PM) loaded with POE have been developed. Nanoformulations were chemically and physically defined and characterized. In vitro release studies were also performed. Finally, the inhibitory effect of both nanoformulations was tested on SH-SY5Y cell migration by wound healing assay and compared to that of unformulated POE. Results: Both nanoformulations showed excellent physical and chemical stability during storage, and enhanced the solubility of POE. PM-POE improved the inhibitory effect of POE on cell migration probably due to the high encapsulation efficiency and the prolonged release of the extract. Conclusions: For the first time, a phytocomplex of marine origin, i.e., *P. oceanica* extract, has enhanced in terms of aqueous solubility and bioactivity once encapsulated inside nanomicelles.

**Keywords:** *Posidonia oceanica*; nanoparticles; polymeric micelles; SH-SY5Y cell migration; wound healing assay

## 1. Introduction

*Posidonia oceanica* (L.) Delile is a marine angiosperm belonging to Posidoniaceae family endemic of the Mediterranean Sea forming expanse underwater meadows of considerable importance for marine ecosystems [1]. The decoction of *P. oceanica* leaves has been dated to ancient Egypt; but more recently, it has been documented to be used by villagers of the sea coast of Western Anatolia as a traditional natural remedy for diabetes, hypertension, and for its antiprotozoal activity [2,3]. In addition, *P. oceanica* has proved to be a promising reservoir of bioactive compounds with antibacterial and antimycotic

properties [4]. Over the years, *P. oceanica* has gained a growing interest for its potential benefits on healthcare, mostly related to the antioxidant and antiradical action of its phenolic component. Recently, a study on *P. oceanica* extract highlighted its biological activity even in the dermatological field. In fact, *P. oceanica* has proved to be an efficient anti-aging agent by improving fibroblast activity and collagen production [5]. Moreover, the hydroalcoholic extract of *P. oceanica* (POE) was found to prevent human cancer cell migration with non-toxic mechanism of action. Specifically, the *P. oceanica* phytocomplex has been proven to reduce the motility of human fibrosarcoma cells and the activity of metalloproteases (MMP-2/9) through the activation of a transient autophagic process without any detectable effect on cell viability [6,7]. The anti-inflammatory mechanism of *P. oceanica* phytocomplex was recently elucidated [8].

Neuroblastoma is a common childhood extracranial solid tumor with high mortality originating from the sympathetic nervous system. It represents about 10% of solid tumors and occurs in very young children with an average age of 17 months at diagnosis. The clinical picture of neuroblastoma is very variable and depends on the stage and location of the tumor [9]. In the clinical field, various anti-cancer drugs and therapies are used to prevent the high proliferation of neuroblastoma, including surgery, chemotherapy, immunotherapy, radiotherapy, myeloablative treatment, and retinoids therapy [10]. Despite this, high-stage neuroblastoma presents a poor prognosis with extremely low overall survival. Therefore, the search for novel therapeutics is important in the case of pediatric malignancies to improve patient survival by reducing high toxicity associated with anticancer drugs. Over decades, crude extracts derived from medicinal plants are of great interest for scientific research due to their natural origin and their interesting bioactive compounds which can act synergistically in the prevention or treatment of various human diseases. Furthermore, innovative strategies, like nanotechnology, have achieved great results toward ameliorating cancer therapeutics. The use of new therapeutics delivery system, as nanocarriers, may improve efficacy and decrease systemic toxicity during treatment of malignancies compared to the use of “free” drugs [11–13]. Among the varieties of nanoformulations known in the literature, nanoparticles and polymeric micelles are of great interest for pharmacological applications.

In particular, chitosan is one of the polymeric constituents most used in the formulation of nanoparticles, due to its advantageous characteristics and interesting biological activities. It is biocompatible, biodegradable, and free of toxicity. It is a versatile compound, suitable for various routes of administration and multifunctional due to the possibility of functionalizing the molecule to obtain specific targeting. Thanks to its qualities, chitosan is used as nanocarrier of various types of active ingredients: proteins, antibodies, genes, hormones, drugs, but also natural molecules [14]. Chitosan nanoparticles for plant extracts have also been described, such as the *Nigella sativa* L. aqueous extract or the cherry extract from *Prunus avium* L. [15,16].

Regarding polymeric micelles, they are colloidal association systems consisting of blocks of amphiphilic co-polymers, formed by a hydrophilic (e.g., PEG, PVP) and a lipophilic portion (e.g., polyesters, polyanhydrides, and polyamino acids) [17].

Soluplus is a tri-block copolymer consisting of polyvinylcaprolactam-polyvinylacetate-polyethylene glycol. PEG is the hydrophilic portion and polyvinylcaprolactam-polyvinylacetate moieties are arranged in the hydrophobic core. The polymeric micelles have the possibility of incorporating functionality in both core and shell regions: the hydrophobic molecules in the core, less hydrophobic molecules in the core, but near the hydrophilic moiety [18].

Soluplus is biodegradable, and it has a low CMC (7.6 mg/L), which gives its micelles high stability even after dilution [19,20]. Soluplus micelles have been applied to delivery natural and chemical compounds. For example, it has been seen that the use of Soluplus micelles significantly improves the solubility of silymarin, extracted from the fruits of *Silybum marianum* (L.) Gaertn. (Asteraceae), increasing its solubility and its intestinal permeability [21]. Other applications described the use of Soluplus for doxorubicin delivery in the treatment of resistant tumors [20] or to increase acyclovir permeability across the cornea and sclera [22] or even to enhance oral bioavailability and hypouricemic activity of scopoletin [23]. Numerous other applications are described in the literature [24–27].

Considering the high migratory and metastatic capacity of neuroblastoma, it is possible to exploit new therapies loaded in nanocarriers to improve the drug efficacy in order to counteract these specific neuroblastoma abilities. Nanoformulations can also be used for the delivery of molecules of natural origin or phytocomplexes to optimize the effectiveness of herbal medicines [13,20,27]. In this perspective, the possibility of using the whole crude extract carried by nanocarriers leads to having better biological efficacy due to the synergistic action of the bioactive compounds of the phytocomplex with respect to the activity of the single compounds.

In this work, we therefore studied—for the first time—the anti-migratory ability of POE loaded in nanoformulations on the human neuroblastoma cell line SH-SY5Y. Our goal was to improve both the aqueous solubility of the POE and its inhibitory effect on cancer cell migration, providing a sustained and prolonged release. For this purpose, we developed and compared two types of POE-loaded nanocarriers, such as chitosan nanoparticles (NP-POE) and Soluplus polymeric micelles (PM-POE), usually applied to the delivery of single compounds. This study aims to develop biocompatible, biodegradable and easy to prepare carriers and to extend their application to carry a phytocomplex, containing molecules with different polarity. Given the chitosan characteristics, this polymer has already been applied to the formulation of nanoparticles for the delivery of polar extracts [15,16]. Polymeric micelles are easy to prepare, stable, biocompatible, and suitable for compounds with different polarity. The authors developed mixed polymeric micelles of Soluplus/TPGS-Vit. E for the formulation of silymarin [21].

The nanoformulations were chemically and physically characterized in terms of size, homogeneity,  $\zeta$ -potential, morphology, encapsulation efficiency, and storage stability. In vitro release studies were also performed. Finally, the inhibitory effect of both NP-POE and PM-POE on SH-SY5Y cell migration was evaluated by the wound healing assay and compared to that of unformulated POE.

## 2. Materials and Methods

### 2.1. Materials

Sigma-Aldrich (Milan, Italy) provided all chemicals, and analytical grade and HPLC grade solvents. Chitosan low molecular weight (Sigma-Aldrich, Milan, Italy; cat no. 448869, mol wt. 50,000–190,000 Da, viscosity 20–300 cP, 1 wt % in 1% acetic acid, 25 °C, Brookfield). Soluplus was a gift of BASF (Ludwigshafen, Germany) with the support of BASF Italia, BTC Chemical Distribution Unit (Cesano Maderno, Monza e Brianza, Italy). Distilled water was obtained from a Simplicity<sup>®</sup> UV Water Purification System, Merck Millipore (Darmstadt, Germany). Phosphotungstic acid (PTA) was from Electron Microscopy Sciences (Hatfield, PA, USA). Dialysis kit was from Spectrum Laboratories, Inc. (Breda, The Netherlands). Dulbecco's modified Eagle's medium (DMEM), Ham's F-12 nutrient mixture, fetal bovine serum (FBS), L-glutamine, penicillin and streptomycin, 1-(4,5-dimethylthiazol-2-yl)-3,5-diphenyl formazan (MTT) were purchased from Sigma Aldrich-Merck (Saint Louis, MO, USA). Disposable plastics were from Sarstedt (Nümbrecht, Germany).

### 2.2. *P. oceanica* Extract (POE) Preparation

The leaves of *P. oceanica* were extracted as previously described [6]. Briefly, 10 mL of EtOH/H<sub>2</sub>O (70:30 *v/v*) per gram of dried and minced *P. oceanica* leaves were left to shake overnight at 37 °C. Hydrophobic compounds were removed from the water-ethanol extraction by repeated shaking in *n*-hexane (1:1), whereas the hydrophilic fraction, recovered in the lower phase, was dispensed in 1 mL aliquots and then dried. Single batch of *P. oceanica* extract was dissolved in 0.5 mL of EtOH/H<sub>2</sub>O (70:30 *v/v*) before to use and hereafter referred to as POE. Freshly-dissolved POE was characterized for total polyphenols and carbohydrates content and antioxidant and radical scavenging activities, according to previously described methods [6,7]. Drug: extract ratio (D.E.R) was 8:1.

### 2.3. HPLC-DAD Analytical Method

POE analyses were performed with an HP 1100 HPLC (Agilent Technologies, Santa Clara, CA, USA) equipped with DAD detector and a Luna Omega Polar (150 × 3 mm, 5 μm) (all from Agilent Technologies) RP-C18 analytical column. The software was HP 9000 (Agilent Technologies). The mobile phase consisted of (A) formic acid/water pH 3.2 and (B) acetonitrile. The following gradient profile was applied: 0–2 min 95% A and 5% B; 2–8 min 75% A and 25% B; 8–10 min 70% A and 30% B; 10–12 min 70% A and 30% B; 12–16 min 60% A and 40% B; 16–18 min 40% A and 60% B; 18–22 min 5% A and 95% B; 22–23 min 5% A and 95% B; 23–25 min 95% A and 5% B. The flow rate was 0.5 mL/min, injection volume 10 μL, and the temperature 25 °C. The calibration curve was prepared using a standard solution of catechin (0.435 mg/mL) diluted 10, 20, 50, 100, 200, and 500 times. The concentration absorption relationship was above than 0.9996. The chromatographic profile of POE polyphenols was acquired at 260 nm and the total polyphenol content was expressed as catechin, using the external standard method.

### 2.4. Preparation of Chitosan Nanoparticles (NP and NP-POE)

NP-POE were prepared using the ionotropic gelation method reported in literature [28,29], modified for the optimization of our formulation. A solution (2 mg/mL) of chitosan (CS) in 1% acetic acid was prepared and kept under magnetic stirring for 24 h, then filtered with a 0.45 μm filter membrane. Tripolyphosphate (TPP) water solution (2 mg/mL) was also prepared and 2 mL of this solution was added to 4 mL of CS solution to prepare empty nanoparticles. The resultant mixture was kept under magnetic stirring for 30 min.

To prepare NP-POE, 4 mL of POE hydroalcoholic solution (5 mg/mL in EtOH/H<sub>2</sub>O 70:30 *v/v*) were added to 4 mL of CS solution (2 mg/mL), then 1.5 mL of TPP solution (2 mg/mL) were added dropwise. The mixture was stirred (500 rpm) at room temperature for 30 min, followed by 15 min of sonication in the ultrasonic bath. The final concentrations of POE, CS, and TPP were 2.11 mg/mL, 0.84 mg/mL, and 0.32 mg/mL, respectively.

### 2.5. Preparation of Soluplus Polymeric Micelles (PM and PM-POE)

PM-POE were prepared by the thin film method [17,30,31]. In brief, 250 mg of Soluplus, and 10.55 mg of POE were dissolved in 20 mL of a mixture EtOH/H<sub>2</sub>O (70:30 *v/v*). Then, the solvents were evaporated under vacuum at 30 °C until the formation of a thin film. Finally, the film was hydrated with 5 mL of distilled water under sonication for 5 min followed by 20 min of magnetic stirring at 200 rpm. The final concentration of POE was 2.11 mg/mL. Empty micelles were prepared with the same method.

### 2.6. Physical Characterization by Dinamic Light Scattering (DLS)

Hydrodynamic diameter, size distribution and ζ-potential were measured by Dinamic Light Scattering (DLS), using a Zsizer Nanoseries ZS90 (Malvern Instruments, Worcestershire, UK) outfitted with a JDS Uniphase 22 mW He-Ne laser operating at 632.8 nm, an optical fiber-based detector, a digital LV/LSE-5003 correlator and a temperature controller (Julabo water-bath) set at 25 °C. Time correlation functions were analysed by the Cumulant method, to obtain the hydrodynamic diameter of the vesicles (Z-average) and the particle size distribution (polydispersity index, PDI) using the ALV-600 software V.3.X provided by Malvern. ζ-potential, instead, was calculated from the electrophoretic mobility, applying the Helmholtz–Smoluchowski equation using the same instrument. The samples were opportunely diluted in distilled water and an average of three measurements at stationary level was taken. A Haake temperature controller kept the temperature constant at 25 °C. The analyses were performed in triplicate.

### 2.7. Morphological Characterization by Transmission Electron Microscopy (TEM)

The morphological characterization of nanoformulations was performed by TEM CM12 (Philips, The Netherlands) equipped with an OLYMPUS Megaview G2 camera at accelerating voltage of 80 keV. Before the analyses, the samples were diluted in distilled water and placed onto a 200-mesh copper grid coated with carbon. Most of the sample was blotted from the grid with filter paper to form a thin film. After the adhesion of formulation, 5  $\mu$ L of phosphotungstic acid solution (1% *w/v* in sterile water, Electron Microscopy Sciences, Hatfield, PA, USA) were dropped onto the grid as a staining medium and the excess solution was removed with filter paper. Samples were dried for 3 min, after which they were examined with the electron microscope [32].

### 2.8. Encapsulation Efficiency (EE%)

The encapsulation efficiency of the NP-POE was calculated employing the indirect method, as reported in the literature [33]. In brief, the NP-POE were centrifuged at 18000 rpm (Ultracentrifuge Mikro 22, Hettick, Kirchlengern, Germany) for 30 min at 4 °C. The supernatant, containing the non-encapsulated extract, was analyzed by HPLC analysis. POE encapsulation efficiency was calculated according to Equation (1)

$$EE = \frac{\text{TotalPOE} - \text{FreePOE}}{\text{TotalPOE}} \times 100 \quad (1)$$

In the case of PM-POE, the dialysis bag method was applied to remove non-encapsulated POE. The bag (cellulose membranes, MWCO 3.5–5 kD, Spectrum Laboratories, Inc., Breda, The Netherlands) was kept in 1 L of distilled water for 30 min at room temperature with continuing stirring at 150 rpm. Then, POE retained in the PM was quantified after dilution with ethanol and sonication for 30 min in an ultrasonic bath. The resulted mixture was analysed by HPLC after centrifugation for 10 min at 14000 rpm [34–36]. The Equation (2) was applied to EE% determination.

$$EE = \frac{\text{mgPOEencapsulated}}{\text{TotalPOE}} \times 100 \quad (2)$$

### 2.9. Stability Studies

Stability studies were conducted over 3 months. NP-POE and PM-POE were stored at 4 °C, in the test tubes coated with aluminium foils. The particle size, PdI,  $\zeta$ -potential and encapsulation efficiency were investigated at regular intervals to assess the chemical and physical stability of the samples.

### 2.10. In Vitro POE Release from NP-POE and PM-POE

The release of POE from NP-POE and PM-POE were studied using the dialysis bag method (cellulose membranes, MWCO 3.5–5 kD, Spectrum Laboratories, Inc., Breda, The Netherlands). In order to mimic the sink condition, as release medium a PBS solution at pH 7.4 was used. Each formulation (2 mL) was introduced into the dialysis membrane and placed in the release medium (200 mL) at 37 °C, under magnetic stirring. The dissolution medium was 0.01 M PBS (pH 7.4, NaCl 0.138 M, KCl 0.0027 M). At different time points, 1 mL of the release medium was taken and replaced with the same volume of PBS to maintain the sink condition [21,37]. The experiment was conducted for 24 h and 72 h for NP-POE and MP-POE, respectively. The amount of released extract was quantified by HPLC. A hydroalcoholic solution of POE (2 mg/mL) was used as a control. All samples were in a sink condition with the same amount of POE. The released extract in the dissolution media was quantified by HPLC [33].

### 2.11. Cell Culture and Culture Conditions

The SH-SY5Y human neuroblastoma cell line, purchased from American Type Culture Collection (ATCC<sup>®</sup>, Manassas, VA, USA), were grown in a 1:1 mixture of Ham's F12 and DMEM supplemented



with 2 mM L-glutamine, 100 µg/mL streptomycin, 100 U/mL penicillin and 10% FBS, at 37 °C in a humidified atmosphere of 5% CO<sub>2</sub>. Once cells reached 70% to 80% confluence, they were detached by trypsinization (0.25% trypsin, 0.5 mM EDTA solution) and propagated after appropriate dilutions. SH-SY5Y experiments were performed in serum-free medium (starvation medium) after exposure to unformulated POE and POE-loaded nanocarriers, as NP-POE and PM-POE, opportunely diluted in culture medium to obtain 3 µg/mL final concentration of POE. Untreated cells were used as control.

### 2.12. Cell Viability Assay

Cell viability was assessed using the colorimetric MTT activity assay. SH-SY5Y cells were seeded in a 96-well plate ( $5 \times 10^3$  cells/well) in complete medium overnight. Then, cells were treated with POE, NP-POE, and PM-POE in starvation medium for 24 h. Culture medium was removed and adherent cells were washed with PBS. Subsequently, 100 µL/well of 0.5 mg/mL MTT solution were added and incubated in the dark at 37 °C for 1 h. Next, cells were washed with PBS and lysed in 80 µL/well of lysis buffer (20% (*w/v*) sodium dodecyl sulfate (SDS) in 50% (*v/v*) *N,N*-dimethylformamide). Absorbance values were measured at 595 nm using iMARK microplate reader (Bio-Rad, Philadelphia, PA, USA). Data on relative cell viability were expressed in terms of percentage of the untreated cells.

### 2.13. Wound Healing Assay

The wound healing assay [6,7] was used to test SH-SY5Y cell migration. Cells were plated in 6-well plate at  $5 \times 10^5$  cells/well density in complete medium. Once cells reached confluence, a longitudinal scratch was performed through the cell monolayer using a 200 µL sterile plastic tip. Plates were then washed three times with PBS to remove non-adherent cells. Fresh starvation medium containing POE, NP-POE, PM-POE, or empty nanoformulations at appropriate dilutions was added. Cell-free area was observed under phase contrast microscopy and images were captured at 0, 5, 7, and 24 h after wounding using a Nikon TS-100 microscope equipped with a digital acquisition system (Nikon Digital Sight DS Fi-1, Nikon, Minato-ku, Tokyo, Japan). Marked edges along each wound were used to measure cell migration considering the horizontal distance between the initial scratch and the scratch following migration.

### 2.14. Statistical Analysis and Graphics Preparation

The experiments were repeated three times and results were expressed as a mean ± standard deviation, after centralizing mean as a normalization strategy between replicated experiments. The statistical analysis of cell assay was performed with Tukey's test. Furthermore, the graphs were drawn using LibreOffice Calc. Panels were assembled with LibreOffice Impress and adapted with Gimp 2.8.

## 3. Results and Discussion

### 3.1. Preparation and Characterization of POE-Nanoformulations

#### 3.1.1. NP and NP-POE Preparation

POE has been characterized for the total content of polyphenols and carbohydrates and for its antioxidant and radical scavenging activities as described in previous works [6–8] and reported in Table S1 of Supplementary material.

The presence of polyphenols was also confirmed by the HPLC analysis of extract [6]. The percentage of polyphenols was 10% of dried extract of *P. oceanica*, the main peak at 11.83 min is catechin, other compounds identified by UV-vis spectrum and by comparison with the standards are reported in the Figure 1, and they are in agreement with previous findings [6].

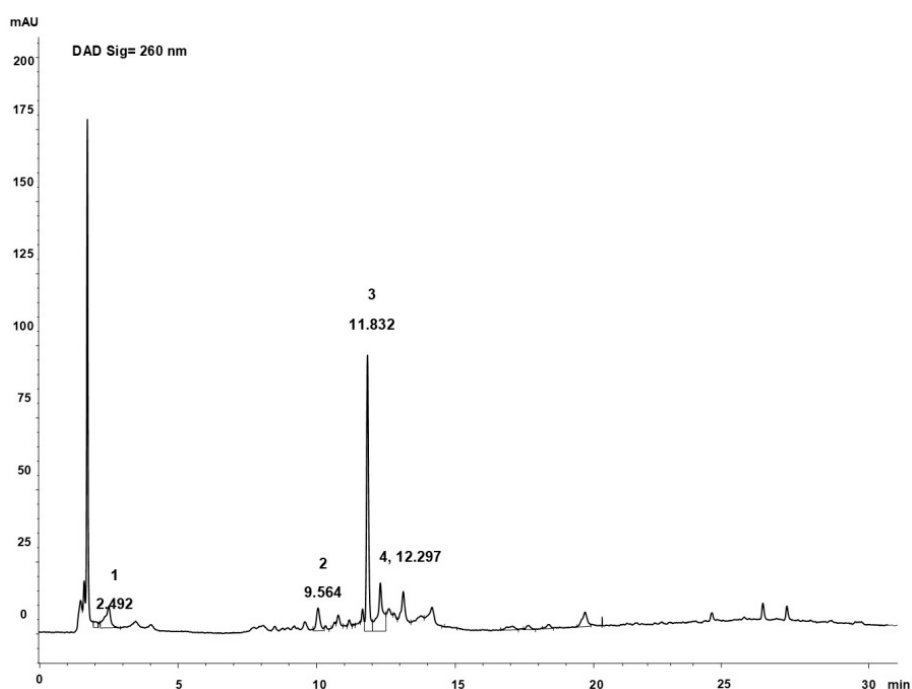


**Figure 1.** Chromatographic profile of POE (260 nm). 1: gallic acid; 2: chlorogenic acid; 3: catechin; 4: ferulic acid.

For the preparation of the empty NP various concentrations and ratio of CS and TPP solutions have been considered. The best system in terms of size PDI and  $\zeta$ -potential (Table 1) was obtained by reacting 4 mL of the CS solution (2 mg/mL) with 2 mL of the TPP solution (2 mg/mL). Our results are in agreement with previous studies performed with similar conditions [28,29,38].

**Table 1.** Physical and chemical characterization of both empty and POE loaded NP and MP nanoformulations (Mean  $\pm$  SD,  $n = 3$ )

Sample	Average Diameter (nm)	PdI	$\zeta$ -Potential (mV)	EE%
NP <sup>1</sup>	153.70 $\pm$ 1.74	0.29 $\pm$ 0.02	22.00 $\pm$ 0.46	-
PM <sup>1</sup>	58.25 $\pm$ 0.03	0.05 $\pm$ 0.01	-5.21 $\pm$ 1.10	-
NP-POE <sup>1</sup>	252.40 $\pm$ 5.02	0.24 $\pm$ 0.02	19.70 $\pm$ 0.76	10.63% $\pm$ 0.71
PM-POE <sup>1</sup>	55.74 $\pm$ 0.39	0.08 $\pm$ 0.02	-8.47 $\pm$ 2.31	85.55 $\pm$ 2.54

<sup>1</sup> NP: chitosan nanoparticles; PM: polymeric micelles of Soluplus; NP-POE: POE-loaded chitosan nanoparticles; PM-POE: POE-loaded polymeric micelles.

The incorporation of the extract into the NP was carried out by adding 4 mL of POE hydroalcoholic solution (5 mg/mL) to the CS solution, before adding the TPP solution. In the presence of the extract the amount of the TPP solution was decreased to 1.5 mL respect to the preparation of empty NP, to optimize size and PDI of the sample.

Thus, the final concentrations of POE, CS, and TPP were 2.11 mg/mL, 0.84 mg/mL, and 0.32 mg/mL, respectively. The NP are homogeneous, with a positive  $\zeta$ -potential, due to the presence of chitosan. The loading of the extract inside the NP induces an increase in the size, but the system still remains useful for pharmaceutical administration. As reported in the literature, after drug loading into chitosan nanoparticles, the particle size becomes bigger [39,40]. A possible reason for this phenomenon is that the loaded drug (or extract in this case) reduces the cohesive force between chitosan and tripolyphosphate [41]. TEM analysis shows spherical and not aggregated particles (Figure 2A).



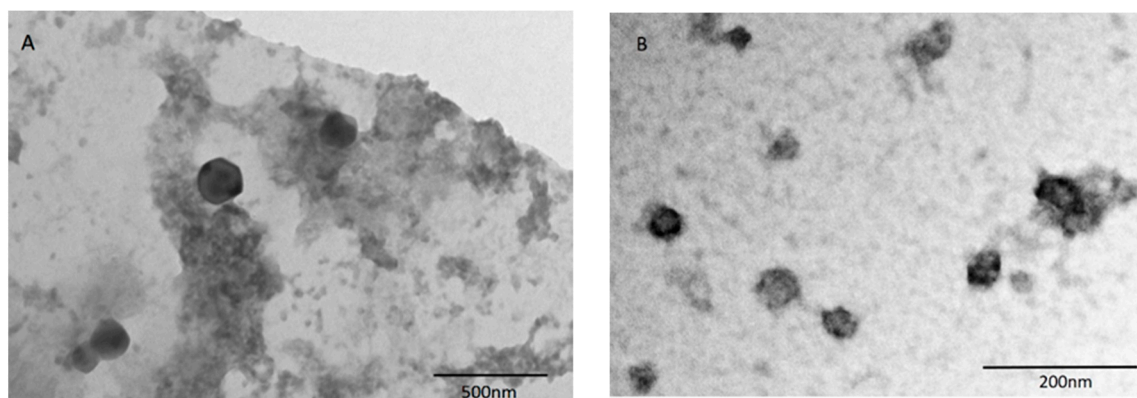


**Figure 2.** (A) TEM image of POE-loaded nanoparticles (NP-POE); (B) TEM image of POE-loaded Soluplus polymeric nanomicelles (PM-POE).

In the case of NP-POE, the encapsulation efficiency was calculated by the indirect method [33], as reported in the experimental section, because the direct method employs drastic conditions [38] which can alter the stability of the extract. The EE% value is  $10.63\% \pm 0.71$ . This value is not high, but it corresponds to a final POE concentration of 2.11 mg/mL, with 0.22 mg/mL encapsulated into the NP. This represents a remarkable improvement of the aqueous solubility of the extract, that is completely insoluble. This aspect was also confirmed by the change of the color of the mixture, that from colorless becomes light yellow in the presence of nanoparticles. Similar values of EE% were reported in literature for analogous nanoparticles of chitosan carrying natural substances such as eugenol and carvacrol. In the case of eugenol, the EE value ranges from 2% to 29% increasing the initial eugenol content respect to chitosan from 1:0.25 to 1:1.25 *w/w*. In the case of carvacrol, the EE% ranges from 13% to 31% with increasing initial carvacrol content [28,38].

Our research represents one of the few studies in which an attempt was made to formulate an extract rather than a single compound. In the literature, there are few examples of nanoformulations of extracts using nanoparticles, such as gelatin NP of *Centella asiatica* and Cardamono extracts [42,43] and chitosan NP of *Nigella sativa* and cherry extracts [15,16]. The nanoparticles are not easy to prepare for extract delivery, due to the presence of various compounds with different polarity, but the application of nanotechnology to extract is of great interest in the phytotherapy field given the remarkable benefits that traditional medicine attributes to the synergistic action of the bioactive compounds present in phytocomplexes.

### 3.1.2. PM and PM-POE

Soluplus micelles were prepared using the “thin film hydration” technique [17,23,31]. Soluplus is a tri-block copolymer consisting of polyvinylcaprolactam–polyvinylacetate–polyethylene glycol. PEG is the hydrophilic portion and polyvinylcaprolactam–polyvinylacetate moiety are arranged in the hydrophobic core. PM have the possibility of incorporating functionality in both core and shell regions: the hydrophobic molecules of POE in the core, less hydrophobic molecules in the core, but near the hydrophilic moiety [18].

During the optimization process, the hydroalcoholic solution (EtOH/H<sub>2</sub>O 70:30 *v/v*) was selected as the best solvent mixture to solubilize both the extract and the polymer. Micelles of Soluplus (5% *w/v*), containing 2.11 mg/mL of extract, have the physical parameters showed in Table 2. In the case of PM-POE, the increase of sizes was not observed, probably for the high extract solubilisation in the PM core–shell structure. Indeed, Soluplus exhibits the capability of solubilizing both hydrophobic and hydrophilic drugs into the core and shell of the micelles. This ability might be attributed to the interactions between the drug and the polymer. For example, the phenolic groups might interact with the terminal –OH and ether oxygen groups in Soluplus and form hydrogen bonds [44].

**Table 2.** Storage stability test of NP-POE at 4 °C for 3 months (Mean  $\pm$  SD,  $n = 3$ )

Days	Average Diameter (nm)	PdI	$\zeta$ -Potential (mV)
0	252.40 $\pm$ 5.02	0.24 $\pm$ 0.02	19.70 $\pm$ 0.76
30	276.80 $\pm$ 6.34	0.22 $\pm$ 0.01	17.80 $\pm$ 0.78
60	278.40 $\pm$ 5.42	0.22 $\pm$ 0.01	18.50 $\pm$ 0.64
90	277.50 $\pm$ 2.91	0.20 $\pm$ 0.01	17.10 $\pm$ 0.70

The morphological characterization of PM-POE is reported in Figure 2B. The micelles appear as spherical with the dimensions consistent with those detected by DLS. The dialysis purification method is usually employed for the determination of the encapsulation efficiency in the case of micelles [45,46] and it has been employed as direct process to determine the EE% of PM-POE. The EE% value is 85.55%  $\pm$  2.54, corresponding to 1.81 mg/mL of POE effectively encapsulated.

As evidenced for NP-POE, also PM-POE increased the solubility of the extract but with a higher EE% compared to NP-POE. Furthermore, while in an aqueous solution the extract remains completely undissolved, the micellar solution is able to solubilize about 2 mg/mL of POE and it becomes colored in yellow, proof of a change in solubility of the extract. As reported in literature, the nanomicelles have achieved good results in improving the solubility of extracts, such as the silymarin phytocomplex [21]. For the first time in this work Soluplus nanomicelles have been used to increase the solubility of a phytocomplex of marine origin.

### 3.2. Stability Study

Tables 2 and 3 reported the physical stability of both POE nanoformulations over 3 months at 4 °C. All physical parameters, named size, PdI and  $\zeta$ -potential, resulted unchanged for both NP-POE and PM-POE.

**Table 3.** Storage stability test of PM-POE at 4 °C for 3 months (Mean  $\pm$  SD,  $n = 3$ )

Days	Average Diameter (nm)	PdI	$\zeta$ -Potential (mV)
0	55.74 $\pm$ 0.39	0.08 $\pm$ 0.02	−8.47 $\pm$ 2.31
30	56.43 $\pm$ 6.34	0.09 $\pm$ 0.01	−8.52 $\pm$ 0.78
60	56.81 $\pm$ 0.04	0.12 $\pm$ 0.02	−8.65 $\pm$ 1.70
90	56.22 $\pm$ 0.33	0.10 $\pm$ 0.01	−6.53 $\pm$ 0.56

Also the chemical stability of the formulated extract before and after the storage was substantially comparable, as confirmed by EE% values. The EE% ranges from 10.63  $\pm$  0.71% to 8.83  $\pm$  0.43% after 90 days, and from 85.55  $\pm$  2.54% to 75.80  $\pm$  2.55% after 90 days, are referred to NP-POE and PM-POE respectively.

The PM-POE stability study well correlate with its in vitro activity, that was maintained until 3 months, as proved by its inhibitory effect on SH-SY5Y cell migration.

### 3.3. In Vitro Release Studies

The release profile of POE solution and POE nanoformulations is shown in Figure 3. In particular, NP-POE released 30% of POE after 3 h, 45% after 4 h and 90% within 24 h of dialysis at 37 °C. The release of the extract by NP-POE is not rapid and immediate as POE solution; the latter in fact already after 3 h reached 60% of release and after 4 h exceeded 90%. NP-POE released the extract in a sustained fashion probably due to the diffusion of the adsorbed extract and its diffusion through the polymeric matrix, mechanisms which govern drug release from chitosan nanoparticles.

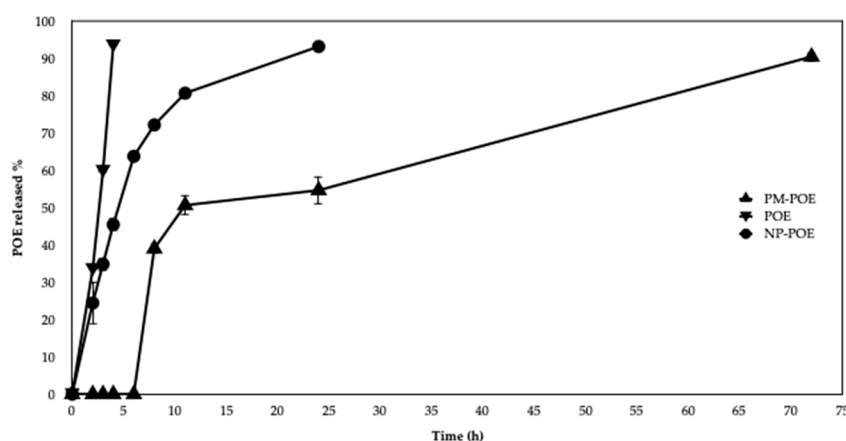


**Figure 3.** In vitro release profiles of POE from POE solution and POE loaded into nanoformulations (NP-POE and PM-POE).

As for PM-POE, the release profile was slower and prolonged over time compared to both POE solution and NP-POE, as evidenced in Figure 3. The release of the extract from PM-POE is not immediate but rather delayed, it begins to increase after 5 h, reaching 40% after 8 h, 50% after 12 h, and 90% after 72 h. The obtained results are in agreement with the literature, which refers to a time-delayed release by PM formulations. In fact, it was recently observed that polymeric micelles of Soluplus/P407 release a 6.8% of quercetin in the first 8 h and a 28.75% after 24 h [44]. Evidence of a prolonged lag time in POE release encourages the use of polymeric micelles to optimize POE release.

#### 3.4. NP-POE and PM-POE Effect on SHSY5Y Cell Migration

POE and POE-loaded into nanoformulations (NP-POE and PM-POE) were tested on human neuroblastoma SH-SY5Y cell line, at the final concentration of 3  $\mu\text{g}/\text{mL}$  according to data previously obtained on POE bioactivities [6–8].

The effect of POE, NP-POE, and PM-POE on SH-SY5Y cell viability was determined after 24 h treatment by MTT assay, also the effect of empty NP and PM nanocarriers was investigated. In particular, POE had no cytotoxic effects on cell viability as well as cells showed no signs of toxicity in the presence of NP-POE. As for PM-POE, cell viability value was about 80% due to the very low cytotoxicity ascribed to PM as just reported [21] (Figure S1, in Supplementary Material). Therefore, considering that SH-SY5Y cell viability was maintained over 80% up to 24 h of POE, NP-POE, and PM-POE treatments, cell migration was evaluated by the wound healing assay and compared to their vehicles. After wounding cell monolayers, scratched area images were captured at different time points and the distance from the edges was measured. In particular, Figures 4 and 5 show that POE treatment determined a clear reduction of SH-SY5Y cell migration so that as early as 5 h from the initial scratch the wound width was about  $70\% \pm 4\%$ , while the untreated control cells migrated up to about  $45 \pm 6\%$  of the wound width. The inhibitory effect of POE on cell migration was maintained over time determining a  $57 \pm 7\%$  of wound width after 7 h of treatment and preventing complete closure at 24 h ( $22 \pm 1\%$  of wound width). Conversely, scratch closure rapidly progressed in untreated control cells after 7 h ( $29 \pm 7\%$ ) until complete closure at 24 h.

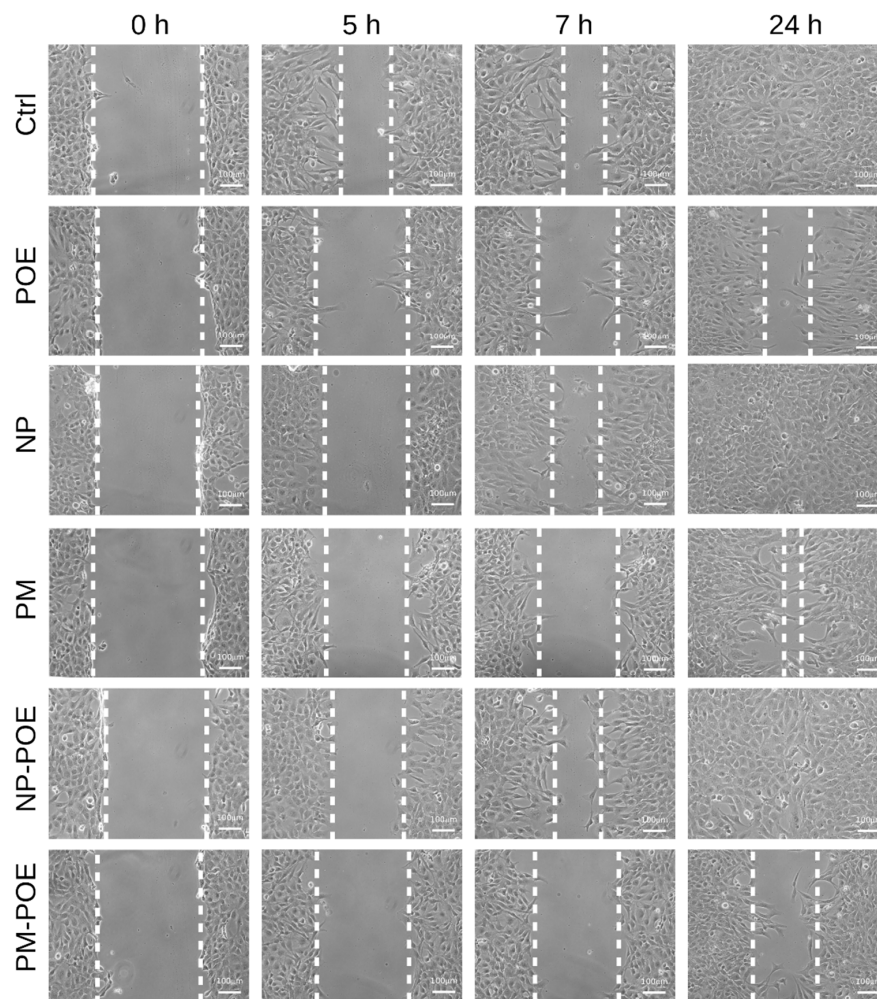


**Figure 4.** Evaluation of SH-SY5Y cell migration by wound healing assay. Representative image of SH-SY5Y cells, untreated or treated with POE, NP, PM, NP-POE, or PM-POE for 24 h. Scratch closure was monitored over time in cells. The dashed lines mark the edges of the wound area.

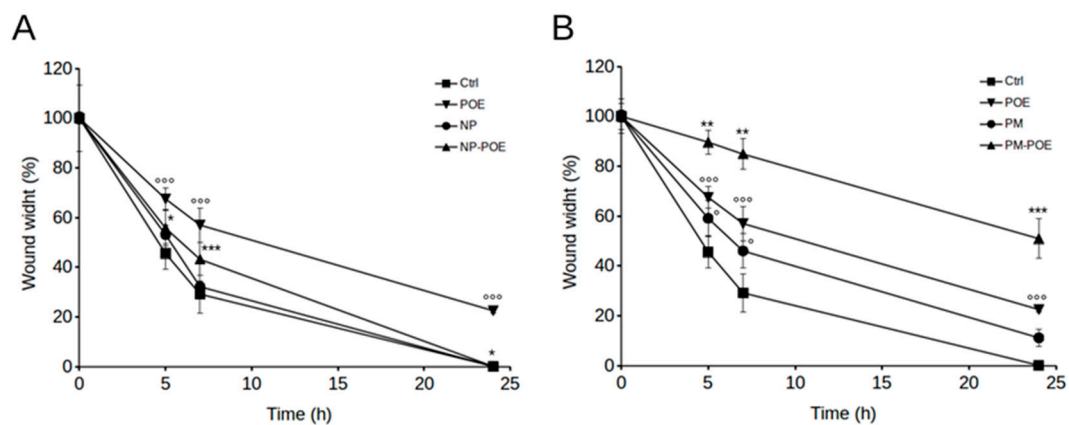


**Figure 5.** Time course analysis of the scratch closure of SH-SY5Y cells (A) treated with NP-POE and (B) treated with PM-POE and both with the respective controls. Wound width values were measured considering the horizontal distance between the initial scratch and the scratch following migration at different time points. Data are representative of at least three different experiments. Error bars represent standard deviation. °:  $p$ -value < 0.05, °°°:  $p$ -value < 0.001 vs. untreated control cells; \*:  $p$ -value < 0.05, \*\*:  $p$ -value < 0.01, \*\*\*:  $p$ -value < 0.001 vs. POE treated cells. Tukey's test.



These results are perfectly in agreement with previously results obtained on the ability of POE to inhibit human fibrosarcoma cancer cell migration [6,7]. Therefore, POE confirmed to be a good candidate for the design of novel therapeutic approaches in phytotherapy. Given the ability of POE to prevent the complete closure of the scratch, we investigated SH-SY5Y cell migration in the presence of NP-POE and PM-POE. The effect of empty NP and PM nanocarriers on cell migration was also monitored over time (Figure 4). As reported in Figure 5A, empty NP and NP-POE showed no effect on SH-SY5Y cell migration leading to a complete closure of the wound at 24 h as the untreated control cells. Differently, PM-POE was able to enhance the inhibitory effect of POE on cell migration (Figure 5B). As early as 5 h PM-POE showed the ability to impair SH-SY5Y cell migration ( $90 \pm 5\%$  of wound width) reducing the wound closure of about 20% compared to 5 h POE treatment.

Comparing the results with those of the in vitro release (Figure 3), the release percentage of POE starts after 5 h and becomes 40% at 8 h, whereas the PM-POE enhanced the inhibitory effect of POE on cell migration as early as after just 5 h. This apparent different behavior of PM in the two in vitro tests can be explained first with the different media and conditions of tests. The in vitro release of POE from PM was done in PBS and using dialysis bag while the wound healing experiment was performed in starvation medium and in direct contact of PM-POE with cells. Furthermore, in the in vitro release assay, POE is released from PM also significantly at shorter times than 8 h. Between 0 h and 8 h there is no release ranging from 0% to 40%, but there are intermediate time points where the release of the extract has already begun. For this reason, it is explained why PM have improved the inhibitory effect of POE on cell migration already after 5 h.

The inhibitory effect of PM-POE on SH-SY5Y cell migration results were clear at 24 h of treatment as PM-POE prevented the complete closure of the wound ( $50 \pm 8\%$  of wound width). The empty PM prevented a total closure of the wound at 24 h maintaining the wound width of approximately  $11 \pm 4\%$  compared to the initial scratch. This delay in the wound closure with respect to untreated control cells could be ascribed to the reduced cell viability observed after 24 h PM treatment. Considering these results, we obtained that PM-POE are able to improve the inhibitory effect of POE on cell migration. Despite the slight inhibitory effect of the empty PM, at 24 h PM-POE inhibited SH-SY5Y cell migration by 30% more than POE.

The activity of PM-POE was maintained until 3 months confirming the results of the stability study previously reported. PM-POE are amphiphilic carriers able to increase the solubility of both lipophilic and hydrophilic constituents of *P. oceanica* extract, as demonstrated by the high EE% with respect to NP-POE. Moreover, the inhibitory activity of *P. oceanica* on cell migration could be ascribed to the prolonged release of POE from nanomicelles. Therefore, the development of nanoformulations, particularly nanomicelles, could be exploited to improve the traditional application of *P. oceanica* in others chronic diseases, such as diabetes [2] and inflammatory-related diseases [8].

#### 4. Conclusions

In this work, we have developed two different POE nanoformulations. Both NP-POE and PM-POE were good candidates for increasing the solubility of *P. oceanica* hydroalcoholic extract, showing good physical and chemical characteristics for parenteral administration and excellent physical and chemical stability during storage at 4 °C for three months. However, only the PM-POE nanoformulation was able to improve the POE inhibitory activity against neuroblastoma cell migration. To date, herbal medicine represents an interesting source for the realization of new drugs. Therefore, the development of adequate systems for the administration of natural compounds, such as nanoformulations, offers an advanced approach to improve the bioavailability and/or optimize the solubility and stability of individual natural compounds or extracts. In this work, for the first time, a phytocomplex of marine origin, i.e., *P. oceanica* extract, has shown an increase in terms of aqueous solubility and bioactivity once encapsulated inside nanomicelles. Therefore, we can assert that Soluplus polymeric nanomicelles are a suitable nanoformulation for the release and the improvement of bioactive properties of phytocomplexes.

**Supplementary Materials:** The following are available online at <http://www.mdpi.com/1999-4923/11/12/655/s1>, Figure S1: SH-SY5Y cell viability. MTT test on cells untreated (control), treated with POE, PM-POE and NP-POE or with vehicles only (PM and NP) for 24 h, Table S1: Total polyphenols and carbohydrates content in POE and its antioxidant and radical scavenging activities.

**Author Contributions:** V.P., M.V., D.D.I., E.B., and M.C.B. conceived and designed the experiments; V.P., A.G., M.V., and M.C.S. performed the experiments; V.P., M.V., D.D.I., and M.C.B. analyzed the data; M.C.B., D.D.I., and M.V. wrote the paper; M.C.B. and D.D.I., provided materials and equipment for the experiments; M.C.B., D.D.I., M.V., V.P., and M.C.S. reviewed and revised the paper.

**Funding:** This work was fully supported by grant of University of Florence (Fondi di Ateneo 2018 to DD and MCB).

**Acknowledgments:** We thank MIUR-Italy (“Progetto Dipartimenti di Eccellenza 2018–2022” allocated to Department of Chemistry “Ugo Schiff”).

**Conflicts of Interest:** The authors declare no conflict of interest.

## References

1. Fella-Naouel, A.; Mamerid, N.; Guibal, E. Pb(II) biosorption on *Posidonia oceanica* biomass. *Chem. Eng. J.* **2011**, *168*, 1174–1184. [[CrossRef](#)]
2. Gokce, G.; Haznedaroglu, M.Z. Evaluation of antidiabetic, antioxidant and vasoprotective effects of *Posidonia oceanica* extract. *J. Ethnopharmacol.* **2008**, *115*, 122–130. [[CrossRef](#)] [[PubMed](#)]
3. Orhan, I.; Sener, B.; Atici, T.; Brun, R.; Perozzo, R.; Tasdemir, D. Turkish freshwater and marine macrophyte extracts show in vitro antiprotozoal activity and inhibit FabI, a key enzyme of *Plasmodium falciparum* fatty acid biosynthesis. *Phytomedicine* **2006**, *13*, 735–739. [[CrossRef](#)] [[PubMed](#)]
4. Bernard, P.; Pesando, D. Antibacterial and antifungal activity of extracts from the rhizomes of the mediterranean seagrass *Posidonia oceanica* (L.) Delile. *Bot. Mar.* **1989**, *32*, 85–88. [[CrossRef](#)]
5. Cornara, L.; Pastorino, G.; Borghesi, B.; Salis, A.; Clericuzio, M.; Marchetti, C.; Damonte, G.; Burlando, B. *Posidonia oceanica* (L.) Delile Ethanol Extract Modulates Cell Activities with Skin Health Applications. *Mar. Drugs* **2018**, *16*, 21. [[CrossRef](#)]
6. Barletta, E.; Ramazzotti, M.; Fratianni, F.; Pessani, D.; Degl’Innocenti, D. Hydrophilic extract from *Posidonia oceanica* inhibits activity and expression of gelatinases and prevents HT1080 human fibrosarcoma cell line invasion. *Cell Adhes. Migr.* **2015**, *5*, 422–431. [[CrossRef](#)]
7. Leri, M.; Ramazzotti, M.; Vasarri, M.; Peri, S.; Barletta, E.; Pretti, C.; Degl’Innocenti, D. Bioactive Compounds from *Posidonia oceanica* (L.) Delile Impair Malignant Cell Migration through Autophagy Modulation. *Mar. Drugs* **2018**, *16*, 137. [[CrossRef](#)]
8. Vasarri, M.; Leria, M.; Barletta, E.; Ramazzotti, M.; Marzocchia, R.; Degl’Innocenti, D. Anti-inflammatory properties of the marine plant *Posidonia oceanica* (L.) Delile. *J. Ethnopharmacol.* **2020**, *247*, 112252. [[CrossRef](#)]
9. Maris, J.M. Recent advances in neuroblastoma. *N. Engl. J. Med.* **2010**, *362*, 2202–2211. [[CrossRef](#)]
10. Castel, V.; Cañete, A. A comparison of current neuroblastoma chemotherapeutics. *Expert Opin. Pharmacother.* **2004**, *5*, 71–80. [[CrossRef](#)]
11. Kumari, P.; Ghosh, B.; Biswas, S. Nanocarriers for cancer-targeted drug delivery. *J. Drug Target.* **2016**, *24*, 179–191. [[CrossRef](#)] [[PubMed](#)]
12. Rodríguez-Nogales, C.; González-Fernández, Y.; Aldaz, A.; Couvreur, P.; Blanco-Prieto, M.J. Nanomedicines for Pediatric Cancers. *ACS Nano* **2018**, *12*, 7482–7496. [[CrossRef](#)] [[PubMed](#)]
13. Bilia, A.R.; Piazzini, V.; Risaliti, L.; Vanti, G.; Casamonti, M.; Wang, M.; Bergonzi, M.C. Nanocarriers: A Successful Tool to Increase Solubility, Stability and Optimise Bioefficacy of Natural Constituents. *Curr. Med. Chem.* **2018**, *25*, 1–24. [[CrossRef](#)] [[PubMed](#)]
14. Akbar, A.; Shakeel, A. A review on chitosan and its nanocomposites in drug delivery. *Int. J. Biol. Macromol.* **2018**, *109*, 273–286. [[CrossRef](#)]
15. Elkadery, A.A.S.; Elsherif, E.A.; Ezz Eldin, H.M.; Fattah Fahmy, I.A.; Mohammad, O.S. Efficient therapeutic effect of *Nigella sativa* aqueous extract and chitosan nanoparticles against experimentally induced *Acanthamoeba keratitis*. *Parasitol. Res.* **2019**, *118*, 2443–2454. [[CrossRef](#)]
16. Beconcini, D.; Fabiano, A.; Zambito, Y.; Berni, R.; Santoni, T.; Piras, A.M.; Di Stefano, R. Chitosan-Based Nanoparticles Containing Cherry Extract from *Prunus avium* L. to Improve the Resistance of Endothelial Cells to Oxidative Stress. *Nutrients* **2018**, *10*, 1598. [[CrossRef](#)]

17. Kesharwania, S.S.; Shamandeep, K.; Hemachand, T.; Abhay, T.S. Multifunctional approaches utilizing polymeric micelles to circumvent multidrug resistant tumors. *Colloids Surf. B Biointerfaces* **2019**, *173*, 581–590. [[CrossRef](#)]
18. Deshmukh, A.S.; Chauhan, P.N.; Noolvi, M.N.; Chaturvedi, K.; Ganguly, K.; Shukla, S.S.; Nadagouda, M.N.; Aminabhavi, T.M. Polymeric micelles: Basic research to clinical practice. *Int. J. Pharm.* **2017**, *532*, 249–268. [[CrossRef](#)]
19. Dian, L.; Yu, E.; Chen, X.; Wen, X.; Zhang, Z.; Qin, L. Enhancing oral bioavailability of quercetin using novel Soluplus polymeric micelles. *Nanoscale Res. Lett.* **2014**, *9*, 2406. [[CrossRef](#)]
20. Jin, X.; Zhou, B.; Xue, L.; San, W. Soluplus micelles as a potential drug delivery system for reversal of resistant tumor. *Biomed. Pharmacother.* **2015**, *69*, 388–395. [[CrossRef](#)]
21. Piazzini, V.; D'Ambrosio, M.; Luceri, C.; Cinci, L.; Landucci, E.; Bilia, A.R.; Bergonzi, M.C. Formulation of Nanomicelles to Improve the Solubility and the Oral Absorption of Silymarin. *Molecules* **2019**, *24*, 1688. [[CrossRef](#)] [[PubMed](#)]
22. Varela-Garcia, A.; Concheiro, A.; Alvarez-Lorenzo, C. Soluplus micelles for acyclovir ocular delivery: Formulation and cornea and sclera permeability. *Int. J. Pharm.* **2018**, *552*, 39–47. [[CrossRef](#)] [[PubMed](#)]
23. Zeng, Y.C.; Sha, L.; Chang, L.; Tao, G.; Xun, S.; Yao, F.; Zhang, Z.R. Soluplus micelles for improving the oral bioavailability of scopoletin and their hypouricemic effect in vivo. *Acta Pharmacol. Sin.* **2017**, *38*, 424–433. [[CrossRef](#)] [[PubMed](#)]
24. Manolya, S.; Cheng, W.P.; Palmer, N.; Tierney, R.; Francis, R.; MacLellan-Gibson, K.; Khan, A.; Mawas, F. Nano-sized Soluplus polymeric micelles enhance the induction of tetanus toxin neutralising antibody response following transcutaneous immunisation with tetanus toxoid. *Vaccine* **2017**, *35*, 2489–2495. [[CrossRef](#)]
25. Alopaeus, J.F.; Hagesæther, E.; Tho, I. Micellisation Mechanism and Behaviour of Soluplus-Furosemide Micelles: Preformulation Studies of an Oral Nanocarrier-Based System. *Pharmaceutics* **2019**, *12*, 15. [[CrossRef](#)]
26. Alvarez-Rivera, F.; Fernandez-Villanueva, D.; Concheiro, A.; Alvarez-Lorenzo, C. Alpha-Lipoic acid in Soluplus(R) polymeric nanomicelles for ocular treatment of diabetes-associated corneal diseases. *J. Pharm. Sci.* **2016**, *105*, 2855–2863. [[CrossRef](#)]
27. Wu, H.; Wang, K.; Wang, H.; Chen, F.; Huang, W.; Chen, Y.; Chen, J.; Tao, J.; Wen, X.; Xiong, S. Novel self-assembled tacrolimus nanoparticles cross-linking thermosensitive hydrogels for local rheumatoid arthritis therapy. *Colloids Surf. B Biointerfaces* **2017**, *149*, 97–104. [[CrossRef](#)]
28. Woranuch, S.; Yoksan, R. Eugenol-loaded chitosan nanoparticles: I. Thermal stability improvement of eugenol through encapsulation. *Carbohydr. Polym.* **2013**, *96*, 578–585. [[CrossRef](#)]
29. Ameenuzzafar, A.J.; Bhatnagar, A.; Kumar, N.; Ali, A. Formulation and optimization of levofloxacin loaded chitosan nanoparticle for ocular delivery: In-vitro characterization, ocular tolerance and antibacterial activity. *Int. J. Biol. Macromol.* **2018**, *108*, 650–659. [[CrossRef](#)]
30. Zhang, J.; Li, Y.; Fang, X.; Zhou, D.; Wang, Y.; Chen, M. TPGS-g-PLGA/Pluronic F68 mixed micelles for tanshinone IIA delivery in cancer therapy. *Int. J. Pharm.* **2014**, *476*, 185–198. [[CrossRef](#)]
31. Cagel, M.; Tesan, F.C.; Bernabeu, E.; Salgueiro, M.J.; Zubillaga, M.B.; Moretton, M.A.; Chiappetta, D.A. Polymeric mixed micelles as nanomedicines: Achievements and perspectives. *Eur. J. Pharm. Biopharm.* **2017**, *113*, 211–228. [[CrossRef](#)]
32. Graverini, G.; Piazzini, V.; Landucci, E.; Casamenti, F.; Pantano, D.; Pellegrini-Giampietro, D.; Bilia, A.R.; Bergonzi, M.C. Solid lipid nanoparticles for delivery of andrographolide across the blood-brain barrier: In vitro and in vivo evaluation. *Colloids Surf. B Biointerfaces* **2018**, *161*, 302–313. [[CrossRef](#)]
33. Baltzley, S.; Atiquzzaman, M.; Ahmad, H.M.; Abeer, M.A.-G. Intranasal Drug Delivery of Olanzapine-Loaded Chitosan Nanoparticles. *AAPS PharmSciTech* **2014**, *15*, 1598–1602. [[CrossRef](#)] [[PubMed](#)]
34. Piazzini, V.; Lemmi, B.; D'Ambrosio, M.; Cinci, L.; Luceri, C.; Bilia, A.R.; Bergonzi, M.C. Nanostructured Lipid Carriers as Promising Delivery Systems for Plant Extracts: The Case of Silymarin. *Appl. Sci.* **2018**, *8*, 1163. [[CrossRef](#)]
35. Righeschi, C.; Bergonzi, M.C.; Isacchi, B.; Bazzicalupi, C.; Gratteri, P.; Bilia, A.B. Enhanced curcumin permeability by SLN formulation: The PAMPA approach. *LWT Food Sci. Technol.* **2016**, *66*, 475–483. [[CrossRef](#)]



36. Huang, J.; Wang, Q.; Li, T.; Xia, N.; Xia, Q. Nanostructured lipid carrier (NLC) as a strategy for encapsulation of quercetin and linseed oil: Preparation and in vitro characterization studies. *J. Food Eng.* **2017**, *215*, 1–12. [[CrossRef](#)]
37. Piazzini, V.; Landucci, E.; Graverini, G.; Pellegrini-Giampietro, D.E.; Bilia, A.R.; Bergonzi, M.C. Stealth and Cationic Nanoliposomes as Drug Delivery Systems to Increase Andrographolide BBB Permeability. *Pharmaceutics* **2018**, *10*, 128. [[CrossRef](#)]
38. Keawchaoon, L.; Yoksan, R. Preparation, characterization and in vitro release study of carvacrol-loaded chitosan nanoparticles. *Colloids Surf. B Biointerfaces* **2011**, *84*, 163–171. [[CrossRef](#)]
39. Hosseini, S.F.; Zandi, M.; Rezaei, M.; Farahmandghavi, F. Two-step method for encapsulation of oregano essential oil in chitosan nanoparticles: Preparation, characterization and in vitro release study. *Carbohydr. Polym.* **2013**, *95*, 50–56. [[CrossRef](#)]
40. Ahmadi, Z.; Saber, M.; Akbari, A.; Mahdavinia, G.R. Encapsulation of *Satureja hortensis* L. (Lamiaceae) in chitosan/TPP nanoparticles with enhanced acaricide activity against *Tetranychus urticae* Koch (Acari: Tetranychidae). *Ecotoxicol. Environ. Saf.* **2018**, *161*, 111–119. [[CrossRef](#)]
41. Yuan, H.; Lu, L.-J.; Du, Y.-Z.; Hu, F.-Q. Stearic Acid-g-chitosan Polymeric Micelle for Oral Drug Delivery: In Vitro Transport and in Vivo Absorption. *Mol. Pharm.* **2010**, *8*, 225–238. [[CrossRef](#)]
42. Yongsirasawad, K.; Patchanee, Y.; Suvaluk, A.; Suksun, A.; Malinee, S. The Drug Delivery System of *Centella asiatica* extractloaded Gelatin Nanoparticles using of One-step desolvation Method, ICBBB 2018. In Proceedings of the 2018 8th International Conference, Tokyo, Japan, 18–20 January 2018; ACM: New York, NY, USA, 2018; pp. 91–98. [[CrossRef](#)]
43. Nejat, H.; Rabiee, M.; Varshochian, R.; Tahriri, M.; Jazayeri, H.E.; Rajadas, J.; Ye, H.; Cui, Z.; Tayebi, L. Preparation and characterization of cardamom extract-loaded gelatin nanoparticles as effective targeted drug delivery system to treat glioblastoma. *React. Funct. Polym.* **2017**, *120*, 46–56. [[CrossRef](#)]
44. Singh, J.; Mittal, P.; Bonde, G.V.; Ajmal, G.; Mishra, B. Design, optimization, characterization and in-vivo evaluation of Quercetin enveloped Soluplus®/P407 micelles in diabetes treatment. *Artif. Cells Nanomed. Biotechnol.* **2018**, *46*, S546–S555. [[CrossRef](#)]
45. Kohori, F.; Yokoyama, M.; Sakai, K.; Okano, T. Process design for efficient and controlled drug incorporation into polymeric micelle carrier systems. *J. Control. Release* **2002**, *78*, 155–163. [[CrossRef](#)]
46. Yoo, H.S.; Park, T.G. Biodegradable polymeric micelles composed of doxorubicin conjugated PLGA-PEG block copolymer. *J. Control. Release* **2001**, *70*, 63–70. [[CrossRef](#)]



© 2019 by the authors. Licensee MDPI, Basel, Switzerland. This article is an open access article distributed under the terms and conditions of the Creative Commons Attribution (CC BY) license (<http://creativecommons.org/licenses/by/4.0/>).

### **3.3. *P. oceanica* against oxidative stress-related damage**

#### **3.3.1. The antioxidant power of *P. oceanica***

The high content of phenolic compounds and their derivatives has directed scientific attention to *P. oceanica* seagrass as a source of antioxidant molecules for applications in various research fields [106-110].

Physiologically, *P. oceanica* uses antioxidant power as a real self-protection mechanism against various environmental pressures [111], or other stressful conditions such as competition from invasive macroalgae [112,113], which strongly contribute to the phanerogams regression phenomenon in the Mediterranean Sea.

In recent years, bioactive compounds with antioxidant activity have found applications in a wide range of sectors, such as biomedicine or food science, and therefore the exploration of new extracts with these functional properties is a topic of great current interest for human well-being as the main focus.

In 2008 Gokce et al. demonstrated that the crosstalk between the antioxidant and vasoprotective properties of a *P. oceanica* leaves extract could provide therapeutic benefits in diabetes-related endothelial dysfunction and oxidative damage. The oral administration of *P. oceanica* extract in alloxan-induced diabetic rats was able to strongly restore the activity of antioxidant enzymes and decrease the lipid peroxidation process [55]. However, the antioxidant and the radical scavenging activity of *P. oceanica* extract was unlikely to be the only mechanism associated with its antidiabetic and vasoprotective effects.

In 2015 the research team of Prof. Degl'Innocenti studied a hydroalcoholic extract from *P. oceanica* leaves (POE). Through a UPLC analysis it emerged that polyphenolic compounds, including catechins, epicatechins and gallic, ferulic and chlorogenic acids, were the most representative components of the extract [80]. The data relating to the antioxidant and radical scavenging activity of POE were in agreement with those already reported in the literature and attributable to the phenolic composition of the extract.

The antioxidant power of a *P. oceanica* leaves extract was further highlighted by a study of Cornara et al. (2018) [57]. Here, it seemed that chicoric acid, the main constituent of this extract, was responsible for the effects observed on the proliferation of fibroblasts and on the production of collagen, and for its anti-melanogenic and lipolytic activities, suggesting its possible use against the formation of wrinkles, skin aging, unwanted hyperpigmentation and cellulite, in which oxidative stress plays a crucial role [57].

It is well known that the imbalance between the production of reactive oxygen species (ROS) and their elimination by protective mechanisms generates oxidative stress and triggers signalling cascades that can lead to the onset and progression of inflammatory diseases. As a result, increased ROS generation by immune cells at the site of inflammation causes oxidative stress and tissue damage (Figure 20).

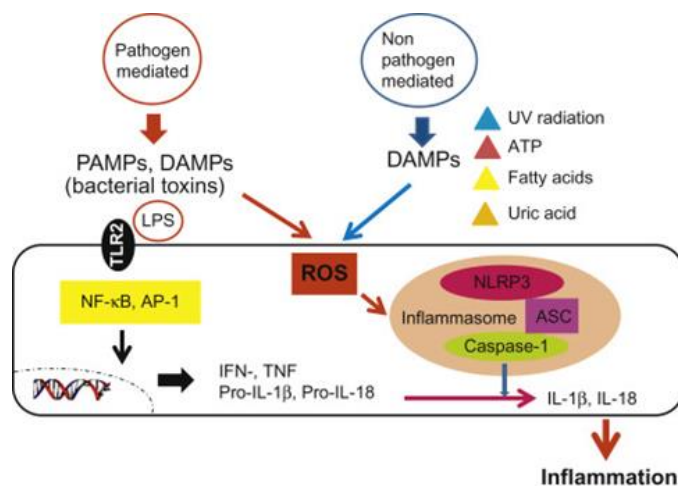


**Figure 20.** Schematic representation of the interrelation between oxidative stress and inflammation. This picture was taken from Hsieh et al., 2013 [114].

In light of the interrelation between oxidative stress and inflammation and considering the consistent data on the *P. oceanica* antioxidant power, my research verified whether POE was able to reduce the high ROS formation in murine RAW264.7 macrophages activated by lipopolysaccharide (LPS) and thus to inhibit the resulting inflammatory process.

Specifically, this study clearly showed that the intracellular ROS levels, detected by using a fluorescent probe (§4.12.1), were drastically reduced in cells exposed to LPS and treated with POE compared to the positive control. Likewise, production of the pro-inflammatory mediator nitric oxide (NO), examined by the Griess reaction (§4.12.2), also decreased in POE-treated cells.

The inhibitory effect of POE on NO production was supported by the evident inhibition of the inducible nitric oxide synthase (iNOS) enzyme expression observed in LPS-activated and POE-treated cells compared to the positive control.

Since the overproduction of NO under abnormal conditions, together with the production of ROS, strongly contributes to an inflammatory state mediated by oxidative stress, the

results obtained in this study strongly suggest the dual antioxidant and anti-inflammatory potential of POE (detailed in the next paragraph) [115].

Curiously, thanks to its antioxidant and antimicrobial power, described by other authors [107], the *P. oceanica* seagrass has captured the interest of the scientific community for its potential benefits in food science. Some microorganisms can adversely affect the quality, safety and shelf life of food products and oxidative processes can have an impact on the quality of food, with repercussions on human well-being.

In this regard, the current trend in food processing is focusing on the use of natural compounds, which are considered safe alternatives to chemical additives [116,117]. Some studies have examined the potential applications of *P. oceanica* in the field of food preservation, considering that the protective effects of antioxidants with reference to human health derive from their ability to reduce or eliminate pathogens and deteriorating microorganisms in food.

### 3.3.2. The anti-inflammatory role of *P. oceanica*

Inflammation is a finely regulated physiological response against harmful stimuli that leads to the recruitment and activation of immune cells. Among these, macrophages play an essential role in the immune response, from activating and resolving inflammation to orchestrating the healing of the damaged tissue structure. However, when the response is not controlled, inflammation becomes a pathological condition characterizing many of the most difficult chronic diseases of our time [118] (Figure 21).

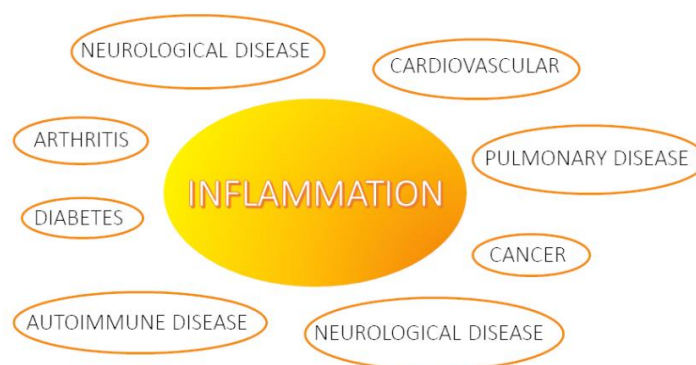


**Figure 21.** Some of the chronic inflammation associated diseases/disorders due to long-term course of inflammation.

Conventional non-steroidal anti-inflammatory drugs (NSAIDs) are commonly prescribed to relieve pain and reduce inflammation. However, their use is often associated with several side effects that could cause serious complications in patients. The use of

beneficial natural anti-inflammatory compounds with antioxidant properties could be useful as an adjuvant therapy for many chronic diseases overcoming the problems associated with conventional drugs.

In this regard, the consistency of data on *P. oceanica* antioxidant properties and the close relationship between oxidative stress and inflammation, described in the literature, directed my research to investigate the potential antioxidant and anti-inflammatory role of the hydroalcoholic extract of *P. oceanica* leaves (POE) in murine RAW264.7 macrophages activated by lipopolysaccharide (LPS), a recognized pro-inflammatory stimulus.

First, it was observed that LPS-stimulated cells treated with POE showed no signs of cellular toxicity, as POE was able to totally prevent LPS-induced reduction in cell viability, as revealed the results from the MTT assay (§4.6).

In conditions of inflammation, the uncontrolled production of reactive oxygen species (ROS) during the so-called "oxidative burst" is closely linked to the histolesivity of inflammation which represents the "dark" side of the inflammatory process associated with suffering cells and tissues [119].

In my study, Western blot analysis (§4.10) showed that POE was able to decisively suppress the expression level of the main enzymes associated with inflammation, i.e. the inducible nitric oxide synthase (iNOS) and cyclooxygenase-2 (COX-2), compromising the production of metabolites harmful to cells and tissues, such as nitric oxide (NO), and in general the production of ROS (as described in §3.3.1).

Since the expression and activity of iNOS and COX-2 and many other inflammatory mediators depend on the activation of the nuclear transcription factor NF- $\kappa$ B, a key regulator of inflammation, the influence of POE on the NF- $\kappa$ B signalling was examined. In the NF- $\kappa$ B signalling cascade, upon arrival of specific stimuli, I $\kappa$ B $\alpha$  (NF- $\kappa$ B inhibitor) undergoes degradation allowing phosphorylated NF- $\kappa$ B (p-NF- $\kappa$ B) to move into the cell nucleus, where it in turn regulates the expression of numerous pro-inflammatory genes pathway (Figure 22).

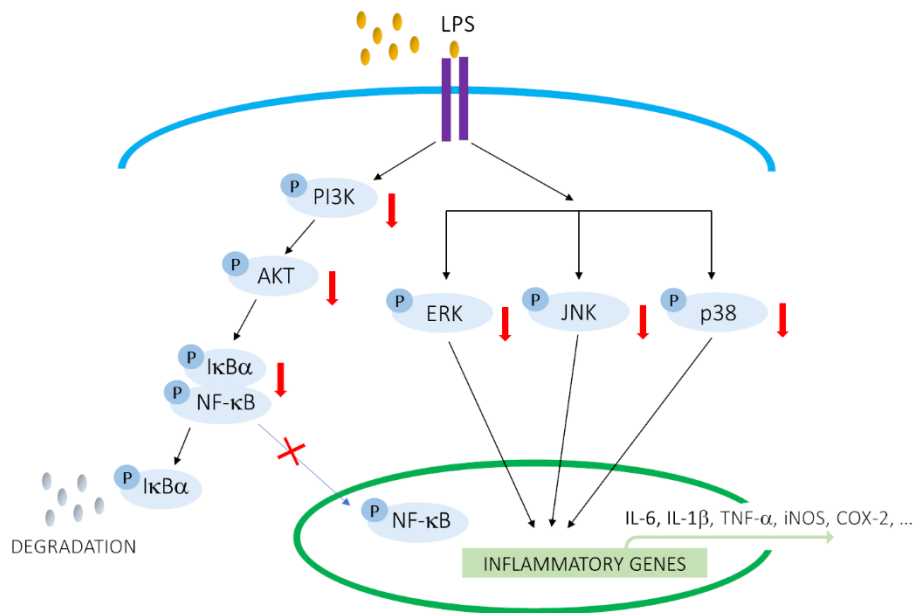


**Figure 22.** Schematic representation of the NF- $\kappa$ B pathway. The red markings indicate the potential inhibition mechanism by anti-inflammatory agents in LPS-induced inflammation.

Through Western blot technique, it was observed that cells stimulated by LPS and treated with POE exhibited an increased levels of p-NF- $\kappa$ B and a reduced levels of I $\kappa$ B $\alpha$  compared to the positive control. These results highlighted that POE was able to inhibit the LPS-induced degradation of I $\kappa$ B $\alpha$  and consequently prevent the NF- $\kappa$ B activation.

The nuclear translocation of p-NF- $\kappa$ B from the cytoplasm to the cell nucleus was then observed by means of an immunofluorescence assay. While untreated control cells maintained low basal levels of p-NF- $\kappa$ B in the cytoplasm, LPS stimulation was observed to significantly increase p-NF- $\kappa$ B levels in the nucleus. When LPS-activated cells were treated with POE, the levels of p-NF- $\kappa$ B in the nucleus were significantly reduced and comparable to those of untreated control cells.

Therefore, the ability of POE to target the NF- $\kappa$ B signalling pathway further supported its anti-inflammatory role.

In order to investigate the POE effect on the activation state of upstream signalling pathways involved in the progression of inflammation in LPS-activated cells, the phosphorylation of ERK1/2 (p-ERK1/2) and AKT (p-AKT), both involved in the release of pro-inflammatory mediators through the regulation of NF- $\kappa$ B pathway (Figure 22), was explored. In particular, the results revealed a marked decrease in p-ERK1/2 and p-AKT levels in LPS-activated and POE-treated cells compared to the positive control.

These findings revealed POE ability to regulate the inflammatory process through the modulation of ERK1/2 signalling and AKT pathways.

Overall, the new awareness of *P. oceanica* molecular mechanism of action on the inflammatory process suggested the potential use of POE as a safe and effective phytocomplex capable of working upstream in inflammation to influence the expression of pro-inflammatory genes (Figure 23).

The detailed analysis of the achieved results can be found in the published paper [115] attached below.

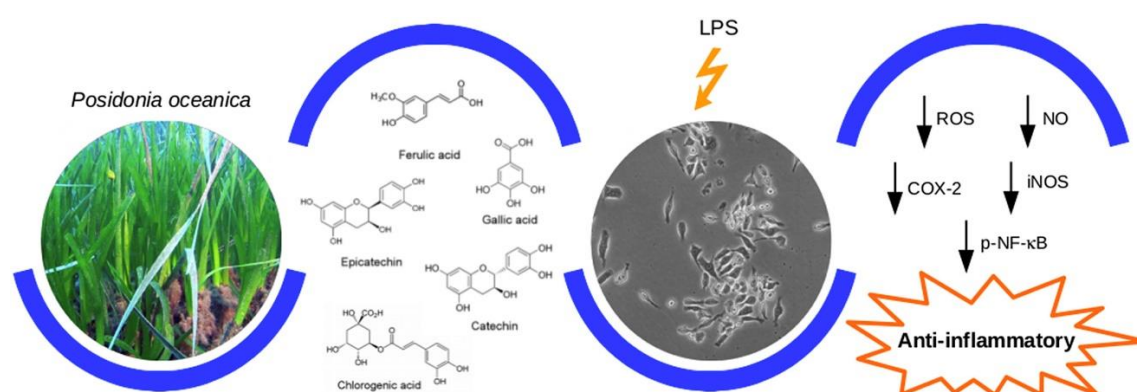


**Figure 23.** Graphic abstract summarizing the results obtained from my research activity on the *P. oceanica* anti-inflammatory role. These results have already been published in 2020 in the international peer-reviewed scientific *Journal of Ethnopharmacology* [115].





## Anti-inflammatory properties of the marine plant *Posidonia oceanica* (L.) Delile



Marzia Vasarri<sup>a</sup>, Manuela Leri<sup>a</sup>, Emanuela Barletta<sup>a</sup>, Matteo Ramazzotti<sup>a</sup>, Riccardo Marzocchini<sup>a</sup>, Donatella Degl'Innocenti<sup>a,b,\*</sup>

<sup>a</sup> Dipartimento di Scienze Biomediche, Sperimentali e Cliniche "Mario Serio", Università degli Studi di Firenze, viale Morgagni 50, 50134, Firenze, Italy

<sup>b</sup> Centro Interuniversitario di Biologia Marina ed Ecologia Applicata "G. Bacci", Viale N. Sauro, 4, 57128, Livorno, Italy

### ARTICLE INFO

#### Keywords:

*Posidonia oceanica*  
Plant extract  
Bioactive compounds  
Macrophages  
Anti-Inflammatory

### ABSTRACT

**Ethnopharmacological relevance:** *Posidonia oceanica* (L.) Delile is an endemic seagrass of the Mediterranean Sea whose use has been documented as a traditional herbal remedy for diabetes and hypertension. Our recently described *Posidonia oceanica* leaves extract is a phytocomplex endowed with interesting bioactivities, including the inhibitory property on human cancer cell migration.

**Aim of the study:** The aim of this study was to investigate the anti-inflammatory effects of *P. oceanica* extract underlying its mechanism of action.

**Materials and methods:** We explored the anti-inflammatory effects of *P. oceanica* extract on RAW264.7 murine macrophages activated by LPS. We investigated the reactive oxygen species (ROS) and nitric oxide (NO) production and the expression of inducible nitric oxide synthase (iNOS) and cyclooxygenase-2 (COX-2). Then, we examined *P. oceanica* extract role on the regulation of NF- $\kappa$ B signaling pathway.

**Results:** *P. oceanica* phytocomplex exhibited a strong ability to inhibit oxidative stress by affecting the production of both ROS and NO and to reduce iNOS and COX-2 levels. In addition, it was evidenced its anti-inflammatory role via inhibiting NF- $\kappa$ B signaling pathway through modulation of ERK1/2 and Akt intracellular cascades.

**Conclusions:** Our results recognize an anti-inflammatory role of *P. oceanica* phytocomplex particularly emphasizing its cell safe mechanism of action. In conclusion, the marine plant *P. oceanica* may be of great interest for scientific research as a source of promising molecules for designing alternative strategies to the conventional treatment of inflammatory diseases.

### 1. Introduction

Inflammation is a finely regulated physiological response against harmful stimuli, such as pathogens and tissue injury, characterized by the recruitment and activation of immune cells, which quickly orchestrate resolution and healing of injured tissue structure. However, when the response goes unchecked, inflammation sometimes develops in pathology (Chen et al., 2018). Macrophage cells play a significant role in immune responses and inflammatory process covering a broad variety of functions, from activation to resolution of inflammation and in the regulation of tissue repair. Lipopolysaccharide (LPS) is one of the most widely used pro-inflammatory stimulus able to activate macrophages and trigger the inflammatory response. Under inflammation conditions, macrophages synthesize and release reactive oxygen species

(ROS) during the so-called "oxidative burst". High concentrations of ROS promote oxidative stress causing cellular damage associated with the histolesivity of inflammation (Mittal et al., 2014). In addition, activated macrophages release a considerable amount of nitric oxide (NO) as pro-inflammatory mediator largely produced by inducible nitric oxide synthase (iNOS) (Sharma et al., 2007). The interaction between NO and other oxygen-derived free radicals may lead to the formation of highly reactive species with damaging effects on the host tissues. Similarly, the activity of cyclooxygenase-2 (COX-2), a well-known inflammation-associated enzyme, contributes to the progression of inflammation (Ricciotti and FitzGerald, 2011).

Inflammatory responses are regulated at transcriptional level by nuclear factor-kappa B (NF- $\kappa$ B) (Dorrington and Fraser, 2019). At first, inflammatory stimulus triggers many upstream signaling cascades,

\* Corresponding author. Dipartimento di Scienze Biomediche, Sperimentali e Cliniche "Mario Serio", Università degli Studi di Firenze, viale Morgagni 50, 50134, Firenze, Italy.

E-mail address: [donatella.deglinnocenti@unifi.it](mailto:donatella.deglinnocenti@unifi.it) (D. Degl'Innocenti).

<https://doi.org/10.1016/j.jep.2019.112252>

Received 8 July 2019; Received in revised form 24 September 2019; Accepted 24 September 2019

Available online 25 September 2019

0378-8741/ © 2019 Elsevier B.V. All rights reserved.

including ERK1/2 and Akt pathways, that in turn lead to activation of NF- $\kappa$ B pathway (Ngabire et al., 2018). Indeed, ERK1/2 and Akt kinases contribute to degradation of the inhibitory proteins (I $\kappa$ Bs) allowing NF- $\kappa$ B dimers to translocate from cytoplasm to nucleus of cells, and thus to promote the expression of pro-inflammatory genes.

Conventional non-steroidal anti-inflammatory drugs (NSAIDs) are commonly prescribed for relieving pain and reducing inflammation. However, their usage is associated with several side effects that could cause serious complications in patients (Wongrakpanich et al., 2018). Therefore, the employment of beneficial natural anti-inflammatory compounds with antioxidant properties might be helpful as adjuvant therapy for many chronic diseases by overcoming problems related to conventional drugs. Many plants have been described as important sources of antioxidant and anti-inflammatory compounds capable of modulating the functional phenotype of macrophages and thus of mitigating inflammatory disorders. Since the beginning of the last century, traditional herbal medicine products, from terrestrial and marine environments, have been used in health care and in the prevention and/or treatment of many disorders, including inflammatory diseases. Plant extract benefits on health are ascribed to phytochemical compounds able to evoke, individually or synergically, various physiological responses (Wink, 2015). Therefore, research on plant bioactive compounds has a long history of success at global level and offers great opportunities for development of novel therapeutic plant-based molecules. Although medicinal plants are gaining, over the years, a greater interest in herbal medicine because they are considered as “safe”, natural products sometimes contain therapeutic as well as toxic compounds.

*P. oceanica* (L.) Delile is a marine angiosperm and the only species of the Posidoniaceae family endemic of Mediterranean Sea forming underwater meadows of remarkable ecological importance (Vacchi et al., 2017). *P. oceanica* leaves have been described in terms of bioactivity. Particularly, Gokce and Haznedaroglu have reported in 2008 that the decoction of *P. oceanica* leaves has been used as a traditional natural remedy for diabetes and hypertension by villagers living by the sea coast of Western Anatolia. Based on these notions, the antidiabetic and vasoprotective effects of *P. oceanica* have been demonstrated in a pre-clinical study by administering *P. oceanica* extract orally to alloxan-induced diabetic rats.

Considering the effectiveness of *P. oceanica* extract in pre-clinical studies, we recently have investigated our ethanolic extract of *P. oceanica* leaves regarding to its potential use in human health, notably disclosing that *P. oceanica* inhibits human cancer cell migration (Barletta et al., 2015; Leri et al., 2018). We have characterized by UPLC analysis the hydrophilic fraction of *P. oceanica* leaves extract, evidencing a large amount of catechins and minor amounts of other polyphenols (Barletta et al., 2015) (Fig. 1).

It is well known that oxidative stress and inflammation are pivotal factors associated with chronic disease such as hypertension and diabetes (Pouvreau et al., 2018). As this regard, a potential anti-inflammatory effect of *P. oceanica* could be exploited in the management not only of hypertension and diabetes, but also of many other inflammation related pathologies.

Therefore, in this work we investigated the anti-inflammation

properties of *P. oceanica* by testing our extract on RAW264.7 murine macrophages activated by LPS. Firstly, we explored the effect of *P. oceanica* on the NO and ROS production and then on the expression of iNOS and COX-2. Finally, we examined the *P. oceanica* role on the regulation of NF- $\kappa$ B signaling pathway.

## 2. Materials and Methods

### 2.1. Materials

Dulbecco's modified Eagle's medium (DMEM), fetal bovine serum (FBS), L-glutamine, penicillin and streptomycin, lipopolysaccharide (LPS), 1-(4,5-dimethylthiazol-2-yl)-3,5-diphenyl formazan (MTT), 2',7'-dichlorofluorescein diacetate (DCFH-DA), Griess reagent and all chemicals and solvents were purchased from Sigma Aldrich-Merck. Electrophoresis reagents were purchased from Bio-Rad (Hercules, CA, USA). Primary antibodies for iNOS (1:1000), COX-2 (1:1000), p-NF- $\kappa$ B p65 (1:1000), NF- $\kappa$ B p65 (1:1000), I $\kappa$ B $\alpha$  (1:1000), p-ERK1/2 (p44/42 MAPK) (1:1000), ERK1/2 (p44/42 MAPK) (1:1000) and  $\alpha$ -Tubulin (1:1000) were purchased from Cell Signaling Technology (Beverly, MA, USA), p-Akt (1:5000) and Akt (1:5000) were purchased from Abcam (Cambridge, UK). Secondary antibodies as goat anti-rabbit IgG HRP-linked, goat anti-mouse IgG HRP-linked and Alexa 488-conjugated anti-rabbit IgG were purchased from Molecular Probes™ (Invitrogen, USA). Disposable plastics were from Sarstedt (Nümbrecht, Germany). The leaves of *P. oceanica* were collected in the protected marine area of Meloria, specifically in the partial reserve zone C (bounded by the conjunction of the following points: point A 43° 36' 45" N and 010° 07' 00" E; point B 43° 36' 45" N and 010° 12' 20" E; point C 43° 35' 05" N and 010° 14' 20" E; point D 43° 32' 06" N and 010° 14' 20" E; point E 43° 30' 58" N and 010° 07' 00" E). In particular, the *P. oceanica* leaves were collected by the authorized personnel of the Interuniversity Center of Marine Biology and Applied Ecology “G. Bacci” at a depth of about 15 m at the following geographical coordinates: 43° 35' 13" N and 010° 10' 21" E.

### 2.2. Preparation of *P. oceanica* extract

The extraction of the hydrophilic components of *P. oceanica* was performed as previously described (Barletta et al., 2015). Briefly, dried *P. oceanica* leaves (collected in July) were minced and suspended overnight in 10 mL per gram of leaves of 70% (v/v) ethanol at room temperature under stirring conditions and at 65 °C for further 3h. The water-ethanol extract was separated from debris by centrifugation at 2000 $\times$ g, and supernatant was mixed with n-hexane in a 1:1 ratio. Hydrophobic compounds were removed by repeated shaking, while hydrophilic compounds were recovered in the lower phase. Subsequently, the hydrophilic phase was dispensed in aliquots of 1 mL and dried by a Univapo™ vacuum-spin concentrator. Before each experiment, a single batch of *P. oceanica* extract was dissolved in 0.5 mL of DMSO, and hereafter named POE.

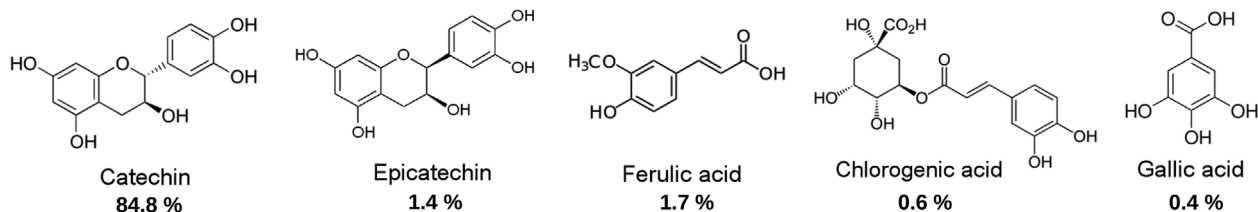


Fig. 1. Phenolic profile of *P. oceanica* extract. The phenolic composition of POE was obtained from UPLC analysis (Barletta et al., 2015). The percentage of each individual phenolic compound is reported below each chemical structure. An additional 11% of the extract composition remained unknown and/or uncharacterized.

### 2.3. Determination of total polyphenols and carbohydrates

Total polyphenol and carbohydrate content in POE was determined according to the colorimetric Folin-Ciocalteu method and the phenol-sulfuric acid method, respectively (Barletta et al., 2015). Polyphenol and carbohydrate content was determined by linear regression with gallic acid and D-glucose, respectively, as references in the range 0–10 µg. Total polyphenols and carbohydrates were expressed as mg of gallic acid and D-glucose equivalents, respectively, per mL of extract after resuspension.

### 2.4. Antioxidant assays

The antioxidant and radical scavenging activities of POE were investigated using the FRAP (ferric-reducing/antioxidant power) assay and DPPH ( $\alpha,\alpha$ -Diphenyl- $\beta$ -picrylhydrazyl) assay, respectively (Barletta et al., 2015). Both antioxidant and radical scavenging activities were determined by linear regression with ascorbic acid as reference in the range 0–4 µg. The antioxidant activities of POE were expressed as mg of ascorbic acid equivalents per mL of extract after resuspension.

### 2.5. Cell line and culture conditions

Murine RAW264.7 macrophage cell line, purchased from American Type Culture Collection (ATCC®) were grown in DMEM supplemented with 2 mM L-glutamine, 100 µg/mL streptomycin, 100 U/mL penicillin and 10% FBS, at 37 °C in an atmosphere of 5% CO<sub>2</sub>. At 90% confluence, cells were collected by scraping and seeded at appropriate cell density. All the following experiments were performed in serum-free medium (starvation medium). When not otherwise specified, after 6h incubation in starvation condition, cells were treated with or without 1:500 dilution of freshly-dissolved POE (corresponding to 2.88 µg/mL dried weight of extract) in the presence or absence of LPS (1 µg/mL) or untreated (control) for further 18h (Xu et al., 2017).

### 2.6. Cell viability assay

Cell viability was determined by MTT assay. Cells were grown in 96-well plates (10<sup>4</sup> cells/well) for 24h. Firstly, cells were treated with 1:100, 1:250 and 1:500 dilutions of POE (corresponding to 14.4, 5.76 and 2.88 µg/mL dried weight of extract, respectively) or with DMSO vehicle solutions for 18h. Subsequently, we tested 1:500 POE dilution on RAW264.7 cells in the presence of LPS stimulus (1 µg/mL) for 18h. After cell treatments, 100 µL of MTT solution (0.5 mg/mL) were added on each well and cells were incubated in the dark at 37 °C for a further 1h. After washing out supernatant, insoluble formazan product was dissolved in 80 µL/well of lysis buffer [20% (w/v) sodium dodecyl sulfate (SDS) in 50% (v/v) N,N-dimethylformamide]. Absorbance values were measured using iMARK microplate reader (Bio-Rad, USA) at 595 nm. Data were expressed in terms of percentage with respect to untreated control cells.

### 2.7. Determination of intracellular ROS

RAW264.7 cells were seeded in 24-well plate at 5 × 10<sup>5</sup> cells/well density for 24h. After the appropriate cell treatments, ROS-sensitive fluorescence probe DCFH-DA (10 µM) was added to each well and incubated in the dark for 1.5 h at 37 °C to detect the intracellular ROS levels. Then, culture medium was removed and cells were lysed with 200 µL/well of RIPA lysis buffer (50 mM Tris-HCl, 150 mM NaCl, 100 mM NaF, 2 mM EGTA, 1% Triton™ X-100; pH 7.5) and 100 µL of each cell lysate were transferred into 96-well black plate. The DCF fluorescence intensity was detected at an excitation and emission wavelengths of 485/538 nm, respectively, using a fluorescence microplate reader (Fluoroskan Ascent™ FL Microplate Fluorometer, Thermo Fisher Scientific, USA). Data were normalized to total cellular proteins and

expressed in terms of percentage with respect to untreated control cells.

### 2.8. Nitric oxide assay

RAW264.7 cells were seeded at a density of 4 × 10<sup>4</sup> cells/well in 96-well plate for 24h. The NO production was determined by measuring nitrite levels in culture media according to the Griess reaction. Briefly, 50 µL of cell culture medium from each treatment were collected and mixed with equal volume of Griess reagent and then incubated at room temperature for 15 min. The 540 nm absorbance was recorded with iMARK microplate reader. The concentration of nitrite in the sample was determined using sodium nitrite as a reference in the range of 0–50 µM. Data were normalized to cell viability and expressed in terms of percentage with respect to untreated control cells.

### 2.9. Western blot analysis

RAW264.7 cells (5 × 10<sup>5</sup> cells/well) were grown in 24-well plate for 24h and then treated for different time points. Cells were then washed with cold PBS and then lysed in 80 µL of Laemmli buffer [62.5 mM Tris-HCl pH 6.8, 10% (w/v) SDS, 25% (w/v) glycerol] without bromophenol blue. Whole cell lysates were collected and boiled at 95 °C for 5 min and then centrifuged at 12,000 × g for 5 min at 4 °C. The total protein concentration of lysates was measured by the BCA protein assay kit. An equal amount of protein (25 µg) from each sample, added with  $\beta$ -mercaptoethanol and bromophenol blue, was separated on 12% SDS-polyacrylamide gels by electrophoresis and transferred onto PVDF membranes (0.45 µm). Next, membranes were saturated using blocking solution [5% (w/v) BSA in 0.1% (v/v) PBS-Tween®-20] and then incubated overnight at 4 °C with primary antibodies appropriately diluted in blocking buffer. After washing three times in 0.1% (v/v) PBS-Tween®-20 solution, membranes were incubated for 1h at room temperature with specific goat anti-rabbit IgG or goat anti-mouse IgG secondary antibodies (Invitrogen, USA) at a dilution of 1:10,000 in blocking buffer. Finally, membranes were washed three times in 0.5% (v/v) PBS-Tween®-20 and protein bands were detected using Clarity Western ECL solution and chemiluminescent signals were acquired by using Amersham™ 600 Imager imaging system (GE Healthcare Life Science, Pittsburgh, PA, USA). Densitometric analysis was conducted using Quantity One software (4.6.6 version, Bio-Rad).

### 2.10. Immunofluorescence staining

RAW264.7 cells were seeded (2 × 10<sup>5</sup> cell/well) in a 24-well plate containing sterilized glass coverslips for 24h. To label the nuclei, cells were successively incubated with 33342 Hoescht for 30 min at room temperature. Next, cells were fixed with 2% paraformaldehyde for 5 min and permeabilized with cold 50% acetone/50% ethanol solution for 4 min at room temperature. Cells were then washed in PBS and blocked in 0.5% BSA and 2% gelatin solution for 30 min at 37 °C. After 1h incubation at room temperature with rabbit anti-p-NF- $\kappa$ B p65 antibody (1:100 dilution in blocking solution), cells were washed with PBS for 30 min under stirring conditions. Subsequently, cells were incubated with Alexa 488-conjugated anti-rabbit secondary antibody (1:200 dilution in PBS). Non-specific antibodies were removed by washing twice in PBS and once in distilled water. Fluorescent signals were visualized using a Leica TCS SP8 AOBs confocal scanning microscope (Leica, Mannheim, Germany). The observations were performed from at least two experiments using a Leica HC PL Apo CS2 × 63 oil immersion objective.

### 2.11. Data analysis and figure preparation

Where not otherwise specified, data are expressed as mean ± standard error from at least three independent experiments, after mean centering as a normalizing strategy across experiments. Plots were

**Table 1**

Polyphenols and carbohydrates content in POE and its antioxidant properties. All values are reported as means  $\pm$  standard deviations from at least three independent extractions and are expressed in mg/mL of extract after resuspension.

	Polyphenols	Carbohydrates	Antioxidant	Radical Scavenging
Method	Folin-Ciocalteu	Phenol/Sulfuric acid	Ferrozine®	DPPH
Reference control	Gallic acid	Glucose	Ascorbic acid	Ascorbic acid
POE	3.6 $\pm$ 0.3	7.0 $\pm$ 2	0.9 $\pm$ 0.2	11.0 $\pm$ 0.7

drawn with LibreOffice Calc, and panels were assembled with LibreOffice Impress and further adapted with Gimp 2.8.

### 3. Results

#### 3.1. Biochemical characterization and antioxidant activity of POE

The water-ethanol extraction method is able to recover polyphenols and carbohydrates from minced *P. oceanica* dried leaves. In the present study, POE was found to contain 3.6  $\pm$  0.3 mg/mL gallic acid equivalents of polyphenols and 7.0  $\pm$  2 mg/mL glucose equivalents of carbohydrates. Polyphenols and carbohydrates antioxidant activity was further evaluated by DPPH and FRAP assays. Particularly POE exhibited radical scavenging and antioxidant activities of 11.0  $\pm$  0.7 mg/mL and 0.9  $\pm$  0.2 mg/mL ascorbic acid equivalents, respectively (Table 1). DMSO vehicle showed no effect on antioxidant assays nor on evaluation of polyphenolic and carbohydrate content (data not showed).

#### 3.2. Effect of POE on macrophage viability

The effect of POE on RAW264.7 cell viability was assessed using MTT assay. As shown in Fig. 2, POE maintains high cell viability at 1:100, 1:250 and 1:500 dilutions in culture medium. Given such results and considering that DMSO vehicle had no effects on cell viability at 1:500 dilution (data not showed), all experiments hereafter were performed using 1:500 POE dilution (2.88  $\mu$ g/mL dried weight of extract), previously proved to be safe to cells and effective (Leri et al., 2018). In order to investigate the anti-inflammatory property of POE, RAW264.7 cells were co-treated for 18h with POE and LPS (1  $\mu$ g/mL), a widely used pro-inflammatory stimulus which is known to significantly reduce cell viability (Zhuang and Wogan, 1997). Our results showed that POE was able to totally prevent the decrease in cell viability induced by LPS (Fig. 2). Moreover, a little increase in RAW264.7 cell viability was observed in POE-treated cells.

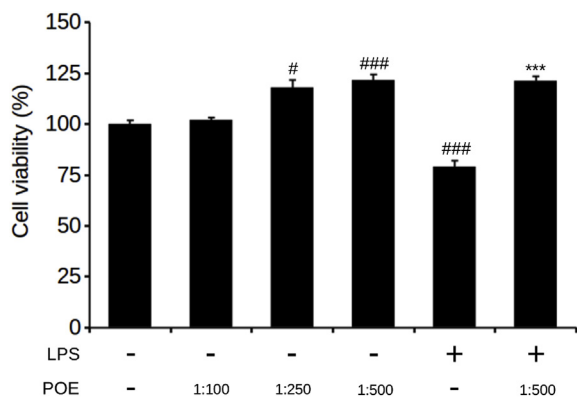


**Fig. 2.** The effect of POE on RAW264.7 cell viability. MTT assay on cells untreated (-) or exposed to different POE dilutions in the absence (-) or in the presence (+) of LPS (1  $\mu$ g/mL) for 18 h. Data were reported as mean  $\pm$  standard error. #: p-value < 0.05, ###: p-value < 0.001 vs. the untreated cells; \*\*\*: p-value < 0.001 vs. the LPS-stimulated cells. Tukey's test, (n = 3).

#### 3.3. POE inhibits oxidative stress induced by LPS

Oxidative stress and inflammation are processes closely linked by an excessive production of oxygen-derived free radicals – i.e. ROS – and NO, which in state of inflammation is highly produced by iNOS contributing to the oxidative stress in cells and tissues (Mittal et al., 2014; Sharma et al., 2007). In this study, we investigated whether POE was able to modulate the inflammatory-related oxidative stress by reducing both intracellular ROS levels and NO production in RAW264.7 macrophages. We observed that POE alone had no effect on ROS and NO generation, which were almost undetectable in both untreated and POE-treated cells (Fig. 3). Differently, LPS stimulation induced an increase up to 10 times of ROS intracellular levels (Fig. 3A) and, similarly, an increase of 9 times of NO release in culture medium (Fig. 3B) compared to untreated cells. In addition, POE treatment was found to significantly reduce both the intracellular ROS levels and the amount of NO released during LPS stimulation of about 2 times compared to LPS-stimulated cells.

These results suggest that POE inhibits oxidative stress in RAW264.7 macrophages activated by LPS evidencing an anti-inflammatory role associated with antioxidant properties.

#### 3.4. POE reduces iNOS and COX-2 expression in LPS-stimulated macrophages

In order to confirm the anti-inflammatory role of POE, we examined the expression of iNOS and COX-2, both enzymes responsible for the production of pro-inflammatory mediators (Sharma et al., 2007; Ricciotti and FitzGerald, 2011).

Fig. 4 shows the expression levels of iNOS and COX-2 following 18h treatments (Xu et al., 2017). Particularly, LPS induced a considerable increase of both iNOS and COX-2 levels (approximately 20 and 90 times, respectively, compared to untreated cells), whereas POE had no effect on the expression of both enzymes. POE treatment drastically inhibited (approximately 4 times) iNOS levels in activated cells (Fig. 4A), thus reinforcing previous results on the reduced production of NO under the same condition (Fig. 3B). In addition, we observed that POE was able to attenuate COX-2 expression levels by almost 2 times during LPS stimulation (Fig. 4B).

Taken together, such results confirm that POE mitigates the inflammatory process by affecting the expression of both iNOS and COX-2 enzymes.

#### 3.5. POE prevents the activation of NF- $\kappa$ B signaling pathway induced by LPS

Given the well-recognized function of NF- $\kappa$ B in the regulation of inflammatory process, we further investigated whether POE exerts its anti-inflammatory role by regulating NF- $\kappa$ B signaling pathway in LPS-activated macrophages. Particularly, we focused on the NF- $\kappa$ B p65 phosphorylated (p-NF- $\kappa$ B) and I $\kappa$ B $\alpha$ , as members of NF- $\kappa$ B pathway. In unstimulated cells, I $\kappa$ B $\alpha$  binds to NF- $\kappa$ B and maintain it in the cytoplasm. Upon arrival of specific stimuli, I $\kappa$ B $\alpha$  undergoes to degradation allowing p-NF- $\kappa$ B to move to the nucleus, where it in turn regulates the expression of pro-inflammatory genes (Dorrington and Fraser, 2019).

Firstly, we analysed the levels of p-NF- $\kappa$ B and I $\kappa$ B $\alpha$  after 45 min of



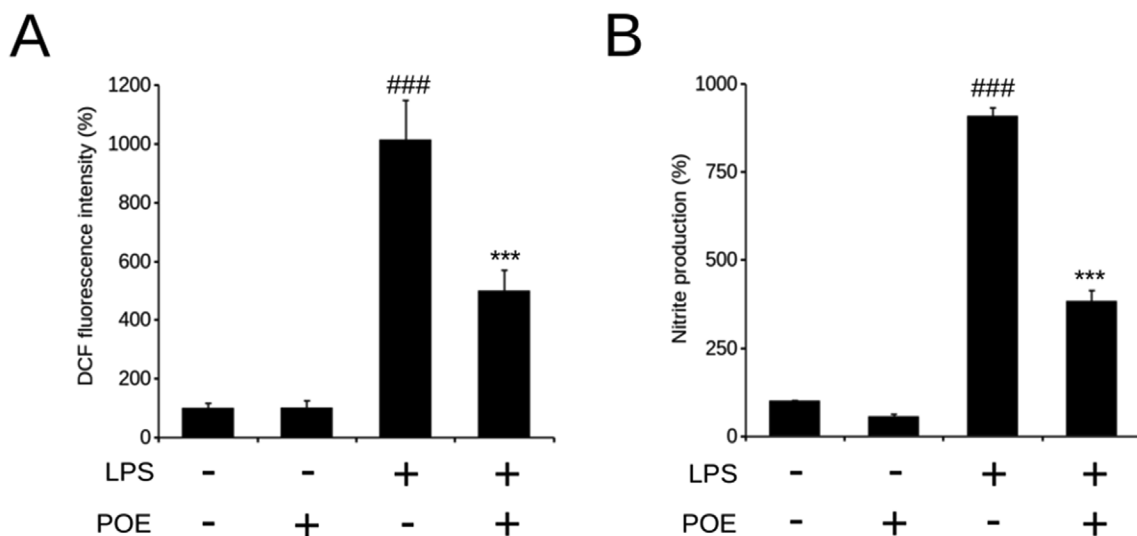


**Fig. 3.** Effect of POE on LPS-induced oxidative stress in RAW264.7 macrophages. Cells were untreated (-) or treated (+) with POE (1:500 dilution) or with LPS (1 µg/mL) for 18 h. (A) DCF fluorescence intensity of cells was measured as indicator of intracellular ROS amount. (B) The nitrite production, as indicator of NO generation, was determined in cell supernatants using Griess reagent. Data are presented as mean ± standard error. ###: p-value < 0.001 vs. the untreated cells; \*\*\*: p-value < 0.001 vs. the LPS-stimulated cells. Tukey's test, (n = 3).

treatment, considering that LPS stimulation always leads to a rapid NF-κB response (Hobbs et al., 2018). Our results showed that POE maintained low basal levels of p-NF-κB and high basal levels of IκBα as in unstimulated cells (Fig. 5A and B). This baseline inverse correlation between p-NF-κB and IκBα levels was completely reversed in LPS-activated cells, resulting in an almost 5 times increase of p-NF-κB (Fig. 5A) and in a reduction of 4 times of IκBα (Fig. 5B), compared to untreated cells. When cells were concomitantly exposed to POE and LPS, POE counteracts the LPS effect on the expression of both p-NF-κB and IκBα. Particularly, data represented in Fig. 5A and B evidence a 2 fold decrease in p-NF-κB and a 2 fold increase in IκBα compared to LPS-stimulated cells.

Such results highlight the ability of POE to inhibit the degradation of IκBα-induced by LPS and consequently to prevent NF-κB activation.

Furthermore, we verified the role of POE on LPS-induced NF-κB activation by using confocal microscopy. Particularly, we focused our analysis on p-NF-κB nuclear translocation from cytoplasm to cell nucleus. As represented in Fig. 5C, p-NF-κB was not detected in the nuclei of untreated cells since NF-κB was distributed in the cytoplasm. Following LPS stimulation, we observed that p-NF-κB rapidly translocated into nuclei, as shown by the strong NF-κB nuclear staining (Fig. 5C). POE treatment almost completely inhibited the accumulation of p-NF-κB in the nuclei on LPS-activated cells. Since deregulated NF-κB activation is a hallmark of the inflammatory process, the ability of POE to

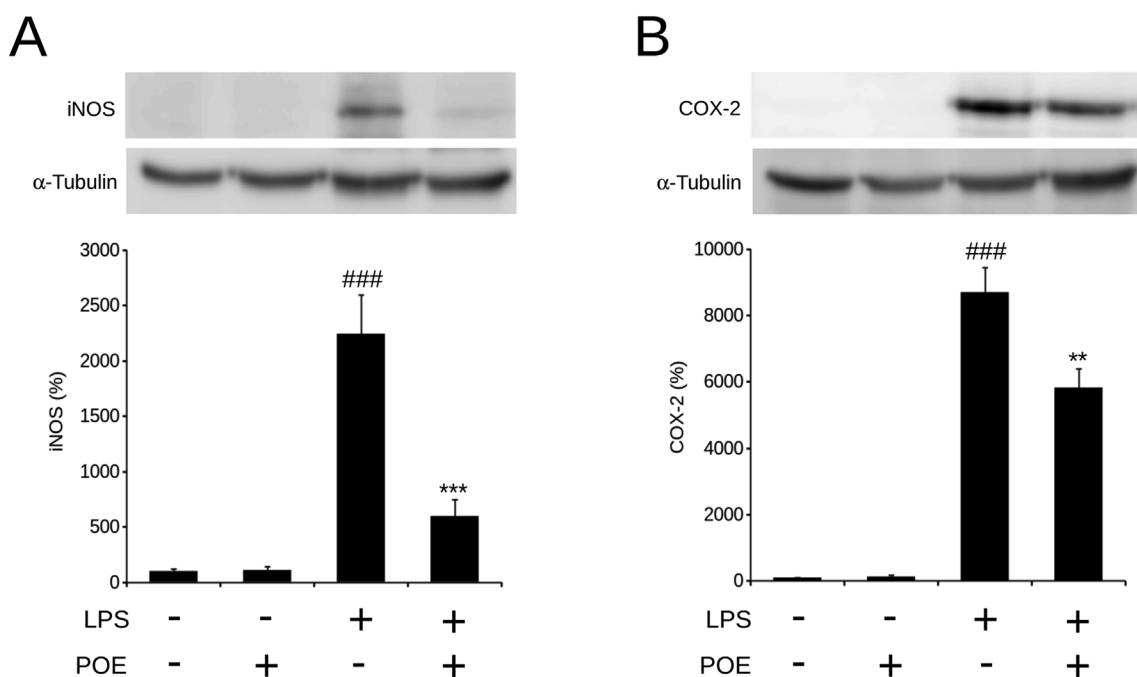


**Fig. 4.** Effect of POE on LPS-induced iNOS and COX-2 protein expression in RAW264.7 macrophages. Cells were untreated (-) or treated (+) with POE (1:500 dilution) or with LPS (1 µg/mL) for 18 h. The protein expression of iNOS (A) and COX-2 (B) was detected by Western blot analysis. Quantification of signals was determined by densitometry analysis. Error bars represent standard errors. ###: p-value < 0.001 vs. the untreated cells; \*\*: p-value < 0.01, \*\*\*: p-value < 0.001 vs. the LPS-stimulated cells. Tukey's test, (n = 3).

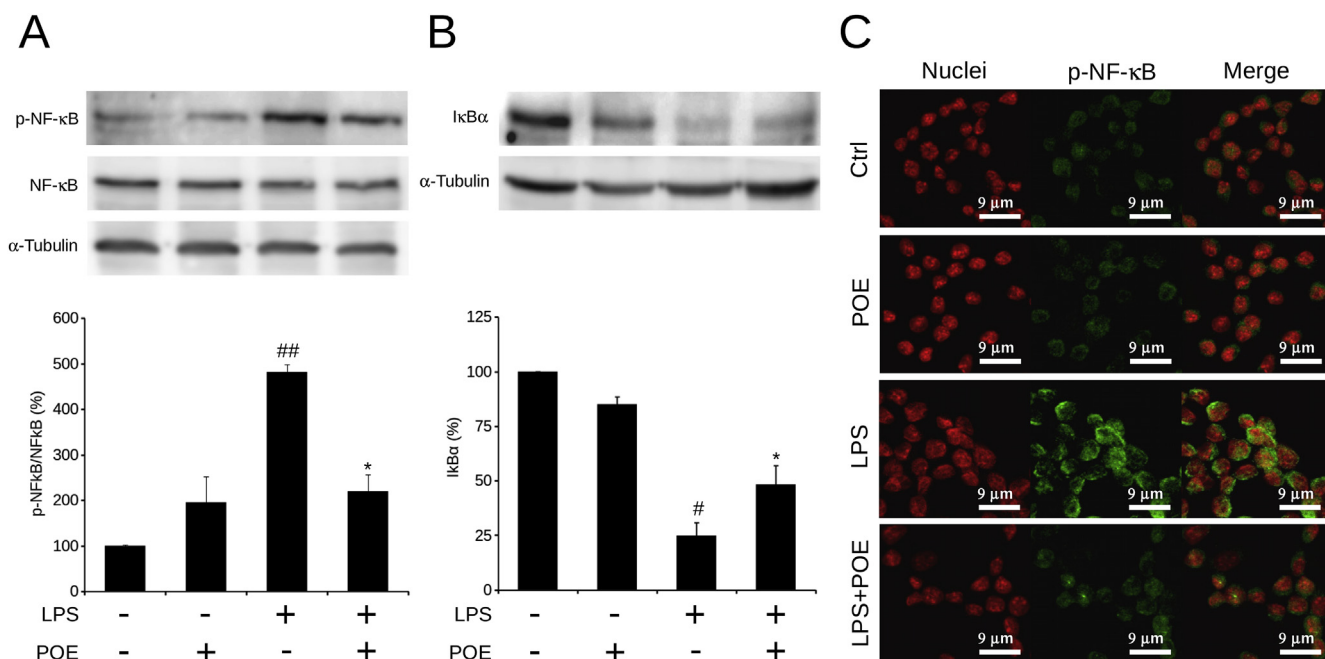


**Fig. 5.** Effect of POE on LPS-induced NF- $\kappa$ B signaling pathway activation in RAW264.7 macrophages. Cells were untreated (-) or treated (+) with POE (1:500 dilution) or with LPS (1  $\mu$ g/mL) for 45 min. The protein expression of p-NF- $\kappa$ B (A) and I $\kappa$ B $\alpha$  (B) was determined by Western blot analysis. Quantification of signals was measured by densitometry analysis. Error bars represent standard errors. #: p-value < 0.05, ##: p-value < 0.01 vs. the untreated cells; \*: p-value < 0.05 vs. the LPS-stimulated cells. Tukey's test, (n = 3). (C) Representative images of immunofluorescence staining of p-NF- $\kappa$ B (green) translocation into the nuclei (red). Scale bar = 9  $\mu$ m. (For interpretation of the references to color in this figure legend, the reader is referred to the Web version of this article.)

target the NF- $\kappa$ B signaling pathway further confirms its anti-inflammatory activity.

### 3.6. POE acts on NF- $\kappa$ B activation through modulation of ERK1/2 and Akt signaling pathways

In order to investigate upstream signaling cascades involved in the progression of inflammation, we examined the phosphorylation of ERK1/2 (p-ERK1/2) and Akt (p-Akt) after 45 min treatments, both implicated in the release of pro-inflammatory mediators through regulation of NF- $\kappa$ B pathway (Ngabire et al., 2018; Abekura et al., 2019).

As represented in Fig. 6, POE had no effect on ERK1/2 and Akt phosphorylation in the absence of LPS stimulus on macrophages. When cells were stimulated by LPS, p-ERK1/2 and p-Akt levels were increased by approximately 10 and 4 times, respectively, compared to untreated cells. On the contrary, the concurrent use of POE and LPS determined a decrease in both p-ERK1/2 and p-Akt of about 3 and 2 times respectively, compared to LPS-stimulated cells (Fig. 6).

Together with previously described results on the activation of NF- $\kappa$ B pathway, these data demonstrate the ability of POE to regulate the inflammation process through modulation of ERK1/2 and Akt signaling pathways.

## 4. Discussion

Inflammation is a complex biological response to certain harmful stimuli. The failure of a rapid resolution can evolve into a prolonged and chronic inflammation that could determine the onset of various diseases, from inflammatory diseases to cancer development (Chen et al., 2018).

Despite the use of NSAIDs is widespread due to their efficacy in reducing pain and inflammation, adverse effects, especially associated to a prolonged use, should not be underestimated. The inhibition of COX isoforms by NSAIDs is the main cause of complications in treated patients (Warner et al., 1999). Therefore, the modern challenge for human health is to develop novel therapeutic approaches based on

beneficial natural bioactive compounds working against inflammation with molecular mechanisms alternative to NSAIDs.

Our previous works focused on the bioactivities of *P. oceanica*, a marine plant to date poorly investigated in terms of its human health benefits (Barletta et al., 2015; Leri et al., 2018). In the current study, we explored the anti-inflammatory activity of *P. oceanica* extract on RAW264.7 macrophage cells stimulated with LPS. From the previously performed UPLC analysis, *P. oceanica* phytocomplex contained a large quantity of polyphenols, however a minor amount of compounds remained unknown and/or uncharacterized (Fig. 1). In this study, the total polyphenolic content in *P. oceanica* extract was further quantified as well as its total carbohydrate content. As known, polyphenols are secondary metabolites of plants involved in several biological activities and cellular protection against damaging agents (Shahidi and Yeo, 2018). Furthermore, some biological activities have been attributed to polysaccharides (Ben Salem et al., 2017).

Once activated by inflammatory stimulus, macrophages produce a considerable amount of mediators for the defense against damage agents and for the healing process. However, a not-controlled production of these molecules is involved in the so-called histotoxicity, representing the "dark" side of inflammation associated with suffering cells and tissues. Consequently, recent therapeutic strategies focused on the regulation of inflammatory mediators have been proposed (Li et al., 2019; Liu et al., 2017).

In this study, we highlighted the non-toxic efficacy of POE on macrophages, previously demonstrated in the fibrosarcoma cell line (Barletta et al., 2015; Leri et al., 2018). It is well-known that LPS stimulation decreases the viability of macrophages by releasing inflammatory molecules, which may act as cytotoxic agents (Zhuang and Wogan, 1997). The ability of the POE to inhibit the LPS-induced cell toxicity may be attributed to polyphenols of the extract that protect cells from damage by preventing synthesis and release of these molecules. Various investigations have recognized the anti-inflammatory and antioxidative properties of polyphenols (Hussain et al., 2016), however also carbohydrates, in particular polysaccharides, have shown to exert biological activities, including anti-oxidative (Ben Salem et al.,

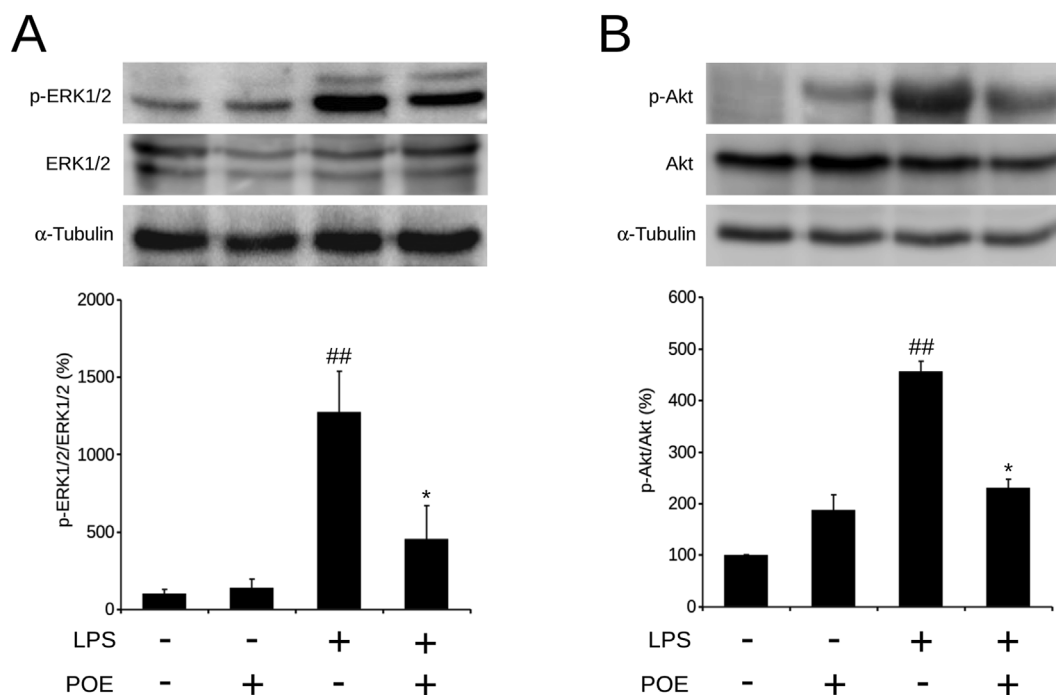


**Fig. 6.** Effect of POE on LPS-induced ERK1/2 and Akt activation in RAW264.7 macrophages. Cells were untreated (–) or treated with POE (1:500 dilution) or with LPS (1 µg/ml) for 45 min. Representative Western blots for p-ERK1/2 (A) and p-Akt (B) are shown. Quantification of signals was determined by densitometry analysis. Error bars represent standard errors. #: p-value < 0.05, ##: p-value < 0.01 vs. the untreated cells; \*: p-value < 0.05 vs. the LPS-stimulated cells. Tukey's test, (n = 3).

2017). Therefore, the ability of POE to impair ROS-mediated oxidative stress may be ascribed to both polyphenolic and carbohydrate compounds. In addition, considering data obtained from antioxidant assays, we may assume that POE acts as antioxidant phytocomplex by scavenging a wide range of ROS. Moreover, it is well-known that polyphenols may act against inflammation exploiting several molecular mechanisms, including the modulation of pivotal inflammation-associated enzymes expression – i.e. iNOS and COX-2 – (Upadhyay and Dixit, 2015), thus compromising the synthesis of metabolites noxious for cells and tissues. As this regards, POE affected NO production through the inhibition of iNOS expression, contributing to the oxidative stress reduction. Similarly, POE decreased the LPS-induced high levels of COX-2, thus exhibiting an anti-inflammatory role associated with antioxidant effects. Both iNOS and COX-2 expression and the production of many other inflammatory mediators depend on the activation of the nuclear transcription factor NF-κB (Jeong and Lee, 2018; Hwang et al., 2019). In this study, POE showed a regulatory role on the NF-κB signaling pathway. Our results notably evidenced that POE anti-inflammatory activity occurs through the retention of NF-κB in the cytoplasm, bound in its inactive form by IκBα. Therefore, this results confirmed that POE prevents NF-κB activation by interfering with NF-κB p65 phosphorylation and by reverting the LPS-induced reduction of IκBα levels. Many different molecular mechanisms on the anti-inflammatory role of polyphenols have been reported, including their interaction with ERK1/2 and Akt signaling pathways (Yahfoufi et al., 2018) known as upstream activators of NF-κB (Ngabire et al., 2018). In this study, POE clearly inhibited the phosphorylation - i.e. activation - of ERK1/2 and Akt during LPS stimulation. This event is closely correlated with the reduction of NF-κB activation and thus with the down-regulation of pro-inflammatory mediators gene expression. Consequently, we believed that POE might regulate inflammation by preventing NF-κB activation through the modulation of ERK1/2 and Akt signaling pathways. Our insights on *P. oceanica* molecular mechanism of action suggest its potential use as a safe and effective phytocomplex working upstream in the inflammatory process up to affect pro-

inflammatory gene expression. Therefore, we support the importance of *P. oceanica* for studying alternative strategies in tackling inflammation in order to reduce the usage of conventional drugs and, accordingly, their side effects.

In conclusion, this work encourages further investigations aimed at confirming the anti-inflammatory activity of POE in peripheral blood mononuclear cells and, more importantly, to establish its anti-inflammatory effect *in vivo*. These results provide important data on the potential use of *P. oceanica* for the development of novel health-promoting products in the co-treatment of inflammation especially in relation to chronic diseases. Nevertheless, our knowledge of POE ability to both compromise tumor cell migration and regulate inflammation will be exploited to study new approaches against malignancies, since inflammation is an important tumor microenvironment factor involved in cancer development and progression.

#### Author contributions

Marzia Vasarri and Manuela Leri performed experiments and wrote manuscript; Emanuela Barletta and Matteo Ramazzotti supervised and reviewed the manuscript; Riccardo Marzocchini contributed in data analysis; Donatella Degl'Innocenti contribute in study design, supervision and revising the manuscript. All authors approved the final manuscript.

#### Declaration of competing interest

The authors declare no conflict of interest.

#### Acknowledgments

This work was fully supported by grant of University of Florence [Fondi di Ateneo 2018 to DD].



## References

- Abekura, F., Park, J., Kwak, C.H., Ha, S.H., Cho, S.H., Chang, Y.C., Ha, K.T., Chang, H.W., Lee, Y.C., Chung, T.W., Kim, C.H., 2019. Esculentoside B inhibits inflammatory response through JNK and downstream NF- $\kappa$ B signaling pathway in LPS-triggered murine macrophage RAW 264.7 cells. *Int. Immunopharmacol.* 68, 156–163. <https://doi.org/10.1016/j.intimp.2019.01.003>.
- Barletta, E., Ramazzotti, M., Fratianni, F., Pessani, D., Degl'Innocenti, D., 2015. Hydrophilic extract from *Posidonia oceanica* inhibits activity and expression of gelatinases and prevents HT1080 human fibrosarcoma cell line invasion. *Cell Adhes. Migrat.* 9, 422–431. <https://doi.org/10.1080/19336918.2015.1008330>.
- Ben Salem, Y., Abdelhamid, A., Mkadmini Hammi, K., Le Cerf, D., Bouraoui, A., Majdoub, H., 2017. Microwave-assisted extraction and pharmacological evaluation of polysaccharides from *Posidonia oceanica*. *Biosci. Biotechnol. Biochem.* 81 (10), 1917–1925. <https://doi.org/10.1080/09168451.2017.1361808>.
- Chen, L., Deng, H., Cui, H., Fang, J., Zuo, Z., Deng, J., Li, Y., Wang, X., Zhao, L., 2018. Inflammatory responses and inflammation-associated diseases in organs. *Oncotarget* 9, 7204–7218. <https://doi.org/10.18632/oncotarget.23208>.
- Dorrington, M.G., Fraser, I.D.C., 2019. NF- $\kappa$ B signaling in macrophages: dynamics, crosstalk, and signal integration. *Front. Immunol.* 10, 705. <https://doi.org/10.3389/fimmu.2019.00705>.
- Gokce, G., Haznedaroglu, M.Z., 2008. Evaluation of antidiabetic, antioxidant and vasoprotective effects of *Posidonia oceanica* extract. *J. Ethnopharmacol.* 115, 122–130. <https://doi.org/10.1016/j.jep.2007.09.016>.
- Hobbs, S., Reynoso, M., Geddis, A.V., Mitrophanov, A.Y., Matheny Jr., R.W., 2018. LPS-stimulated NF- $\kappa$ B p65 dynamic response marks the initiation of TNF expression and transition to IL-10 expression in RAW 264.7 macrophages. *Phys. Rep.* 6, e13914. <https://doi.org/10.14814/phy2.13914>.
- Hussain, T., Tan, B., Yin, Y., Blachier, F., Tossou, M.C., Rahu, N., 2016. Oxidative stress and inflammation: what polyphenols can do for us? *Oxid. Med. Cell Longev.* 2016, 7432797. <https://doi.org/10.1155/2016/7432797>.
- Hwang, D., Kang, M., Jo, M.J., Seo, Y.B., Park, N.G., Kim, G.D., 2019. Anti-inflammatory activity of  $\beta$ -thymosin peptide derived from pacific oyster (*Crassostrea gigas*) on NO and PGE2 production by down-regulating NF- $\kappa$ B in LPS-induced RAW264.7 macrophage cells. *Mar. Drugs* 17, 129. <https://doi.org/10.3390/md17020129>.
- Jeong, Y.E., Lee, M.Y., 2018. Anti-inflammatory activity of *populus deltoides* leaf extract via modulating NF- $\kappa$ B and p38/JNK pathways. *Int. J. Mol. Sci.* 19, E3746. <https://doi.org/10.3390/ijms19123746>.
- Leri, M., Ramazzotti, M., Vasarri, M., Peri, S., Barletta, E., Pretti, C., Degl'Innocenti, D., 2018. Bioactive compounds from *Posidonia oceanica* (L.) delile impair malignant cell migration through autophagy modulation. *Mar. Drugs* 16, 137. <https://doi.org/10.3390/md16040137>.
- Li, M., Li, B., Hou, Y., Tian, Y., Chen, L., Liu, S., Zhang, N., Dong, J., 2019. Anti-inflammatory effects of chemical components from *Ginkgo biloba* L. male flowers on lipopolysaccharide-stimulated RAW264.7 macrophages. *Phytother. Res.* 33, 989–997. <https://doi.org/10.1002/ptr.6292>.
- Liu, F., Zhang, X., Li, Y., Chen, Q., Liu, F., Zhu, X., Mei, L., Song, X., Liu, X., Song, Z., Zhang, J., Zhang, W., Ling, P., Wang, F., 2017. Anti-inflammatory effects of a *Mytilus coruscus*  $\alpha$ -d-Glucan (MP-A) in activated macrophage cells via TLR4/NF- $\kappa$ B/MAPK pathway inhibition. *Mar. Drugs* 15, E294. <https://doi.org/10.3390/md15090294>.
- Mittal, M., Siddiqui, M.R., Tran, K., Reddy, S.P., Malik, A.B., 2014. Reactive oxygen species in inflammation and tissue injury. *Antioxidants Redox Signal.* 20, 1126–1167. <https://doi.org/10.1089/ars.2012.5149>.
- Ngabire, D., Seong, Y.A., Patil, M.P., Niyonizigiye, I., Seo, Y.B., Kim, G.D., 2018. Anti-inflammatory effects of *aster incisus* through the inhibition of NF- $\kappa$ B, MAPK, and Akt pathways in LPS-stimulated RAW 264.7 macrophages. *Mediat. Inflamm.* 2018, 4675204. <https://doi.org/10.1155/2018/4675204>.
- Pouvreau, C., Dayre, A., Butkowski, E.G., de Jong, B., Jelinek, H.F., 2018. Inflammation and oxidative stress markers in diabetes and hypertension. *J. Inflamm. Res.* 11, 61–68. <https://doi.org/10.2147/JIR.S148911>.
- Ricciotti, E., FitzGerald, G.A., 2011. Prostaglandins and inflammation. *Arterioscler. Thromb. Vasc. Biol.* 31, 986–1000. <https://doi.org/10.1161/ATVBAHA.110.207449>.
- Shahidi, F., Yeo, J., 2018. Bioactivities of phenolics by focusing on suppression of chronic diseases: a review. *Int. J. Mol. Sci.* 19, E1573. <https://doi.org/10.3390/ijms19061573>.
- Sharma, J.N., Al-Omran, A., Parvathy, S.S., 2007. Role of nitric oxide in inflammatory diseases. *Inflammopharmacology* 15, 252–259. <https://doi.org/10.1007/s10787-007-0013-x>.
- Upadhyay, S., Dixit, M., 2015. Role of polyphenols and other phytochemicals on molecular signaling. *Oxid. Med. Cell Longev.* 2015, 504253. <https://doi.org/10.1155/2015/504253>.
- Vacchi, M., De Falco, G., Simeone, S., Montefalcone, M., Morri, C., Ferrari, M., Bianchi, C.N., 2017. Biogeomorphology of the Mediterranean *Posidonia oceanica* seagrass meadows. *Earth Surf. Process. Landforms* 42, 42–54. <https://doi.org/10.1002/esp.3932>.
- Warner, T.D., Giuliano, F., Vojnovic, I., Bukasa, A., Mitchell, J.A., Vane, J.R., 1999. Nonsteroid drug selectivities for cyclo-oxygenase-1 rather than cyclo-oxygenase-2 are associated with human gastrointestinal toxicity: a full in vitro analysis. *Proc. Natl. Acad. Sci. U.S.A.* 96, 7563–7568. <https://doi.org/10.1073/pnas.96.13.7563>.
- Wink, M., 2015. Modes of action of herbal medicines and plant secondary metabolites. *Medicines (Basel)* 2, 251–286. <https://doi.org/10.3390/medicines2030251>.
- Wongrakpanich, S., Wongrakpanich, A., Melhado, K., Rangaswami, J., 2018. A comprehensive review of non-steroidal anti-inflammatory drug use in the elderly. *Aging Dis.* 9, 143–150. <https://doi.org/10.14336/AD.2017.0306>.
- Xu, J., Zhao, Y., Aisa, H.A., 2017. Anti-inflammatory effect of pomegranate flower in lipopolysaccharide (LPS)-stimulated RAW264.7 macrophages. *Pharm. Biol.* 55, 2095–2101. <https://doi.org/10.1080/13880209.2017.1357737>.
- Yahfoufi, N., Alsadi, N., Jambi, M., Matar, C., 2018. The immunomodulatory and anti-inflammatory role of polyphenols. *Nutrients* 10, 1618. <https://doi.org/10.3390/nu10111618>.
- Zhuang, J.C., Wogan, G.N., 1997. Growth and viability of macrophages continuously stimulated to produce nitric oxide. *Proc. Natl. Acad. Sci. U.S.A.* 94, 11875–11880. <https://doi.org/10.1073/pnas.94.22.11875>.

### 3.3.2.1. Efficacy of *P. oceanica* extract against inflammatory pain *in vivo*

The substantial efficacy of the *in vitro* anti-inflammatory role of POE encouraged further investigations to explore the POE effects against inflammatory pain *in vivo*.

In collaboration with Prof. Carla Ghelardini and Dr. Lorenzo Di Cesare Mannelli (Department of Neuroscience, Psychology, Drug Research and Child Health - NEUROFARBA -, University of Florence, Italy), some experimental tests were performed in different models of acute inflammatory pain *in vivo* in CD-1 mice (Figure 24). POE was administered acutely per os (oral administration) in a dose range from 10 mg kg<sup>-1</sup> to 100 mg kg<sup>-1</sup>.

It was obtained that POE was able to counteract inflammation-induced hypersensitivity following intraplantar injection of carrageenan, increasing pain threshold and reducing paw oedema in a dose-dependent manner. At the major doses (30 and 100 mg kg<sup>-1</sup>) POE was also able to reduce inflammatory pain induced by the direct intraplantar injection into the paw of IL-1 $\beta$ . Pain threshold was measured by the von Frey test and paw pressure test over time; at the same time, oedema was assessed by measuring joint diameter.

Other evidence revealed that POE had control over the nocifensive response evoked by intraplantar injection of formalin. Nocifensive behaviour was recorded as time taken to lift, favour, lick, shake, and jerk the injected paw.

POE was also found to alleviate inflammatory pain even in naïve animals characterized by a physiological pain threshold; in particular, in animals orally administered with POE, an increase in physiological pain threshold, assessed as a response to a hot stimulus by the hot plate test, was observed.

The protective profile of POE was also analysed *ex vivo* in the soft tissue of the paw of carrageenan-treated animals, collected after POE administration concurrently with the peak of pain-relieving efficacy. Specifically, it was observed that oral administration of POE resulted in a reduction in tissue inflammatory and oxidative mediators.

In particular, the tissue activity of myeloperoxidase (MPO), a primary marker of inflammatory responses and neutrophil recruitment, and the tissue concentration of proinflammatory cytokines, such as IL-1 $\beta$  and TNF- $\alpha$ , were examined. Indeed, these soluble factors are able to initiate peripheral sensitization, together ROS and free radicals activate their receptors and nociceptor terminals to decrease the pain threshold, causing hyperalgesia and inflammatory pain [120,121]. It was observed that in tissues from

animals orally administered with POE the activity of MPO and tissue concentrations of IL-1 $\beta$  and TNF- $\alpha$ , was markedly reduced.

Oxidative and nitrosative stress in tissues is a key parameter in carrageenan-induced paw inflammation, and contributes to the progression of oedema and increased hyperalgesia [122,123]. Tissue levels of NO were then measured, and it was found that POE dramatically inhibited NO production, suggesting that POE also had an effect against carrageenan-induced redox imbalance. These early data were consistent with those obtained from the *in vitro* experiments described above regarding the inhibitory role of POE on iNOS expression levels, and thus on NO production and release.

Because macrophages and neutrophils are the potential origins of NO during inflammation, POE-induced attenuation on neutrophil recruitment to paw tissue, indicated by reduced MPO activity, could be responsible for suppressing the carrageenan-induced increase in NO. According to the literature [124], carrageenan is responsible for lipid peroxidation. However, it had emerged that POE was ineffective against carrageenan-induced lipid change, probably because acute treatment was not ideal for reducing tissue damage.

Overall, these findings represent the first attempt to provide pharmacological evidence for the role of POE in relieving inflammatory pain in *in vivo* animal models alongside with a decrease in inflammatory and oxidative markers.

The detailed analysis of the achieved results can be found in the published paper [125] attached below.

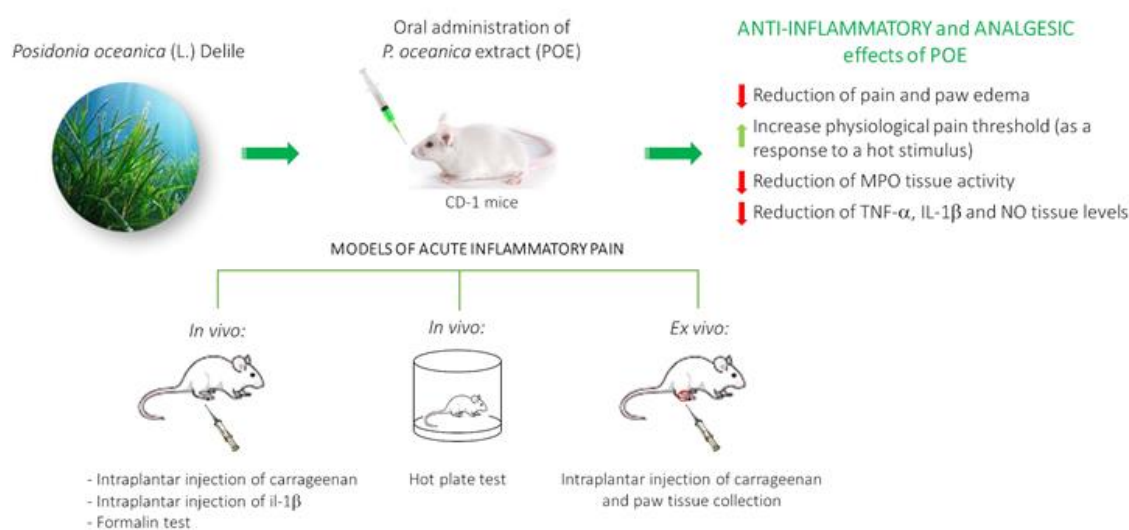


**Figure 24.** Graphic abstract summarizing the results obtained on the *P. oceanica* role against inflammatory pain *in vivo*. These results have already been published in 2021 in the international peer-reviewed scientific *Marine Drugs* [125].

## Article

# Efficacy of *Posidonia oceanica* Extract against Inflammatory Pain: In Vivo Studies in Mice

Laura Micheli <sup>1,†</sup>, Marzia Vasarri <sup>2,†</sup> , Emanuela Barletta <sup>2</sup>, Elena Lucarini <sup>1</sup> , Carla Ghelardini <sup>1</sup>, Donatella Degl'Innocenti <sup>2,3</sup>  and Lorenzo Di Cesare Mannelli <sup>1,\*</sup> 

<sup>1</sup> Department of Neuroscience, Psychology, Drug Research and Child Health (NEUROFARBA)-Pharmacology and Toxicology Section, University of Florence, Viale Gaetano Pieraccini, 6, 50139 Florence, Italy; laura.micheli@unifi.it (L.M.); elena.lucarini@unifi.it (E.L.); carla.ghelardini@unifi.it (C.G.)

<sup>2</sup> Department of Experimental and Clinical Biomedical Sciences, University of Florence, Viale Morgagni 50, 50134 Florence, Italy; marzia.vasarri@unifi.it (M.V.); emanuela.barletta@unifi.it (E.B.); donatella.deglinnocenti@unifi.it (D.D.)

<sup>3</sup> Interuniversity Center of Marine Biology and Applied Ecology "G. Bacci" (CIBM), Viale N. Sauro 4, 57128 Livorno, Italy

\* Correspondence: lorenzo.mannelli@unifi.it

† These authors contribute equally to this work.

**Abstract:** *Posidonia oceanica* (L.) Delile is traditionally used for its beneficial properties. Recently, promising antioxidant and anti-inflammatory biological properties emerged through studying the in vitro activity of the ethanolic leaves extract (POE). The present study aims to investigate the anti-inflammatory and analgesic role of POE in mice. Inflammatory pain was modeled in CD-1 mice by the intraplantar injection of carrageenan, interleukin IL-1 $\beta$  and formalin. Pain threshold was measured by von Frey and paw pressure tests. Nociceptive pain was studied by the hot-plate test. POE (10–100 mg kg<sup>-1</sup>) was administered per os. The paw soft tissue of carrageenan-treated animals was analyzed to measure anti-inflammatory and antioxidant effects. POE exerted a dose-dependent, acute anti-inflammatory effect able to counteract carrageenan-induced pain and paw oedema. Similar anti-hyperalgesic and anti-allodynic results were obtained when inflammation was induced by IL-1 $\beta$ . In the formalin test, the pre-treatment with POE significantly reduced the nocifensive behavior. Moreover, POE was able to evoke an analgesic effect in naïve animals. Ex vivo, POE reduced the myeloperoxidase activity as well as TNF- $\alpha$  and IL-1 $\beta$  levels; further antioxidant properties were highlighted as a reduction in NO concentration. POE is the candidate for a new valid strategy against inflammation and pain.

**Keywords:** *P. oceanica*; inflammation; pain; CD-1 mice



**Citation:** Micheli, L.; Vasarri, M.; Barletta, E.; Lucarini, E.; Ghelardini, C.; Degl'Innocenti, D.; Di Cesare Mannelli, L. Efficacy of *Posidonia oceanica* Extract against Inflammatory Pain: In Vivo Studies in Mice. *Mar. Drugs* **2021**, *19*, 48. <https://doi.org/10.3390/md19020048>

Received: 29 December 2020

Accepted: 19 January 2021

Published: 21 January 2021

**Publisher's Note:** MDPI stays neutral with regard to jurisdictional claims in published maps and institutional affiliations.



**Copyright:** © 2021 by the authors. Licensee MDPI, Basel, Switzerland. This article is an open access article distributed under the terms and conditions of the Creative Commons Attribution (CC BY) license (<https://creativecommons.org/licenses/by/4.0/>).

## 1. Introduction

*Posidonia oceanica* (L.) Delile is a marine vascular plant belonging to the Posidoniaceae family and the only endemic species of the Mediterranean Sea. It is a seagrass that blooms underwater forming vast meadows of tens of thousands of square kilometers of great ecological importance and is essential for the entire marine ecosystem [1].

According to tradition, *P. oceanica* provided benefits for human health. The first information on the *P. oceanica* healing properties comes from ancient Egypt, where it was assumed to be effective against sore throats and skin problems [2]. Other documents describe its traditional use to treat inflammation and irritation, but also acne, lower limbs pain and colitis [3].

A more recent tradition of the villagers of the west Anatolian coast concerns the use of *P. oceanica* leaves decoction as a natural remedy for diabetes and hypertension [4]. An in vivo preclinical study claimed that oral administration of an ethanolic extract from *P. oceanica* leaves in alloxan-induced diabetic rats lowered blood sugar, restored antioxidant

enzyme activity and reduced the lipid peroxidation process, supporting the antidiabetic and vasoprotective roles of *P. oceanica* [4].

Recently, the hydroalcoholic extract from *P. oceanica* leaves, called POE, has been the focus of a series of bioactivity studies. A first UPLC characterization analysis, conducted by some of our authors [5], showed that the hydrophilic fraction of POE consisted of 88% phenolic compounds. The polyphenolic profile was specifically represented by about 85% (+) catechins, while the remaining 5% by a mixture of gallic acid (0.4%), ferulic acid (1.7%), epicatechin (1.4%) and chlorogenic acid (0.6%). The small remaining fraction (11%) was represented by minor peaks, indicating the presence of further compounds, which, although detectable as phenols, are un-known/uncharacterized (Figure 1) [5].

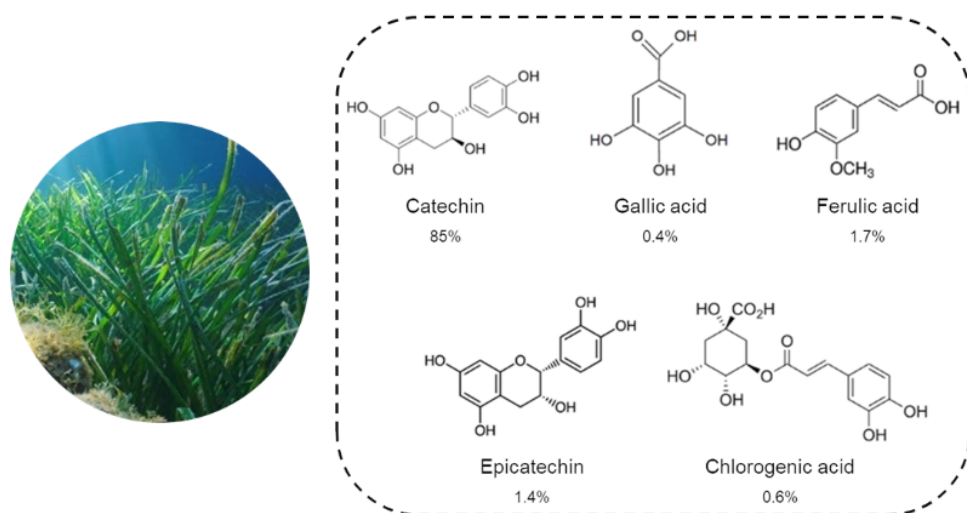


**Figure 1.** Phenolic profile of *P. oceanica* leaves extract (POE) obtained by UPLC analysis [5]. The percentage composition of each phenolic compound in POE is reported below each chemical structure. An additional 11% of POE composition remains unknown and/or uncharacterized.

Although the individual phenolic compounds identified have been tested in some experimental models of *in vitro* bioactivity [5], POE has been shown to be particularly effective as a phytocomplex. Indeed, POE has proved to be capable of inhibiting the migration of cancer cells, such as human fibrosarcoma HT1080 cells [5,6] and human neuroblastoma SH-SY5Y cells [7]. The total absence of cellular toxicity in POE activities has been attributed to its ability to modulate the activation of the autophagic process [6].

In relation to the traditional and recognized antidiabetic role of *P. oceanica*, POE has also proven to be an effective *in vitro* inhibitor of the protein glycation process, strengthening its potential use in the management of diabetic pathophysiology and associated complications [8].

In addition, some authors of this work have previously provided the first experimental support for the potential therapeutic application of POE against various inflammatory-associated disorders [9]. Indeed, POE was found to be able to effectively inhibit the LPS-induced inflammatory process in RAW264.7 murine macrophages, blocking the signaling cascades upstream of NF- $\kappa$ B, the crucial transcription factor for pro-inflammatory mediators' production.

Inflammation is a pathophysiological condition characteristic of many of the most life-threatening diseases in humans, encompassing pain as a main symptom.

Conventional non-steroidal anti-inflammatory drugs (NSAIDs) are commonly prescribed to relieve pain and reduce inflammation. However, prolonged clinical use of NSAIDs is strongly discouraged due to their common, even serious, side effects [10]. Novel, safe, pharmacological approaches are necessary for treating, in particular, chronic inflammatory diseases. The use of herbal medicines is still today one effective strategy

in the management of diseases and in relieving pain, as they are an important source of natural compounds with different bioactive properties [11].

The anti-inflammatory role of POE described above could be recognized as an innovative strategic weapon to fight the progression of these pathologies. Furthermore, the cell-safe POE profile [5–7,9] makes this phytocomplex an excellent candidate for the study of alternative natural strategies against inflammation in order to reduce the use of conventional drugs and, consequently, their side effects.

In light of these considerations, this work aims to investigate the effect of oral administration of POE on pain and inflammation in different models of acute inflammatory pain in CD-1 mice.

## 2. Results and Discussion

### 2.1. Biochemical Characterization and Antioxidant Activity of POE

The hydroalcoholic extraction method was able to recover polyphenols and carbohydrates from minced *P. oceanica* dried leaves.

Here, POE was found to contain  $0.7 \pm 0.02$  mg/mL gallic acid equivalents of polyphenols and  $10 \pm 2.3$  mg/mL glucose equivalents of carbohydrates. The antioxidant activity of POE was further evaluated by DPPH and FRAP assays. Particularly, POE exhibited radical scavenging and antioxidant activities of  $1.2 \pm 0.04$  and  $0.24 \pm 0.05$  mg/mL ascorbic acid equivalents, respectively.

The data were in agreement with those previously obtained [5].

### 2.2. The Effect of POE Against Inflammatory Pain

Inflammation is a physiological response to various stimuli (physical, chemical and biological or a combination) characterized by the recruitment and activation of immune cells, which rapidly manage the resolution and healing of damaged tissues [12].

Inflammation leads to the alteration of the pain threshold, inducing a pathological hypersensitivity, which represents the first passage from physiological nociception to persistent pain [13]. An uncontrolled immune response can make inflammation a pathological condition, so it is not surprising that inflammation and pain are key features of most human ailments.

In light of the recent discovery on the relevant *in vitro* anti-inflammatory effects of POE [9], the potential of POE to relieve pain in different models of acute inflammatory pain *in vivo* was investigated for the first time in this study.

Inflammatory pain was induced in mice by local injection of pro-inflammatory agents. The carrageenan model has been extensively used to study acute pain and inflammation [14,15]; in this work, carrageenan was intraplantarly administered to evoke a dramatic acute reaction characterized by pain and edema in mice.

In Figure 2a, pain threshold measurement by von Frey test is reported. Non-noxious mechanical paw stimulation (allodynia-like measure) allowed us to observe a decreased withdrawal response in carrageenan-treated animals that maintained a plateau between 2 and 3 h after treatment. Administration of POE ( $10$ – $100$  mg kg<sup>-1</sup>) in a dose-dependent manner increased the pain threshold; the higher dose was significantly effective between 15 and 45 min after treatment, completely blocking carrageenan-induced hypersensitivity.

POE efficacy was confirmed by paw pressure test, the extract was able to counteract carrageenan-dependent pain even when evoked by a noxious mechanical stimulus (hyperalgesia-like response), as illustrated in Figure 2b. POE 30 and 100 mg kg<sup>-1</sup> also reduced the joint's diameter made edematous by carrageenan (Figure 2c); POE 100 mg kg<sup>-1</sup> was fully effective even 60 min after administration.

The carrageenan-induced acute and local inflammation consists of two phases. The early phase (0–1 h) is related to the production of histamine, serotonin and bradykinin, as first mediators, while the second phase has been linked to the production of prostaglandins and various cytokines such as IL-1 $\beta$ , IL-6, IL-10 and TNF- $\alpha$  [16].



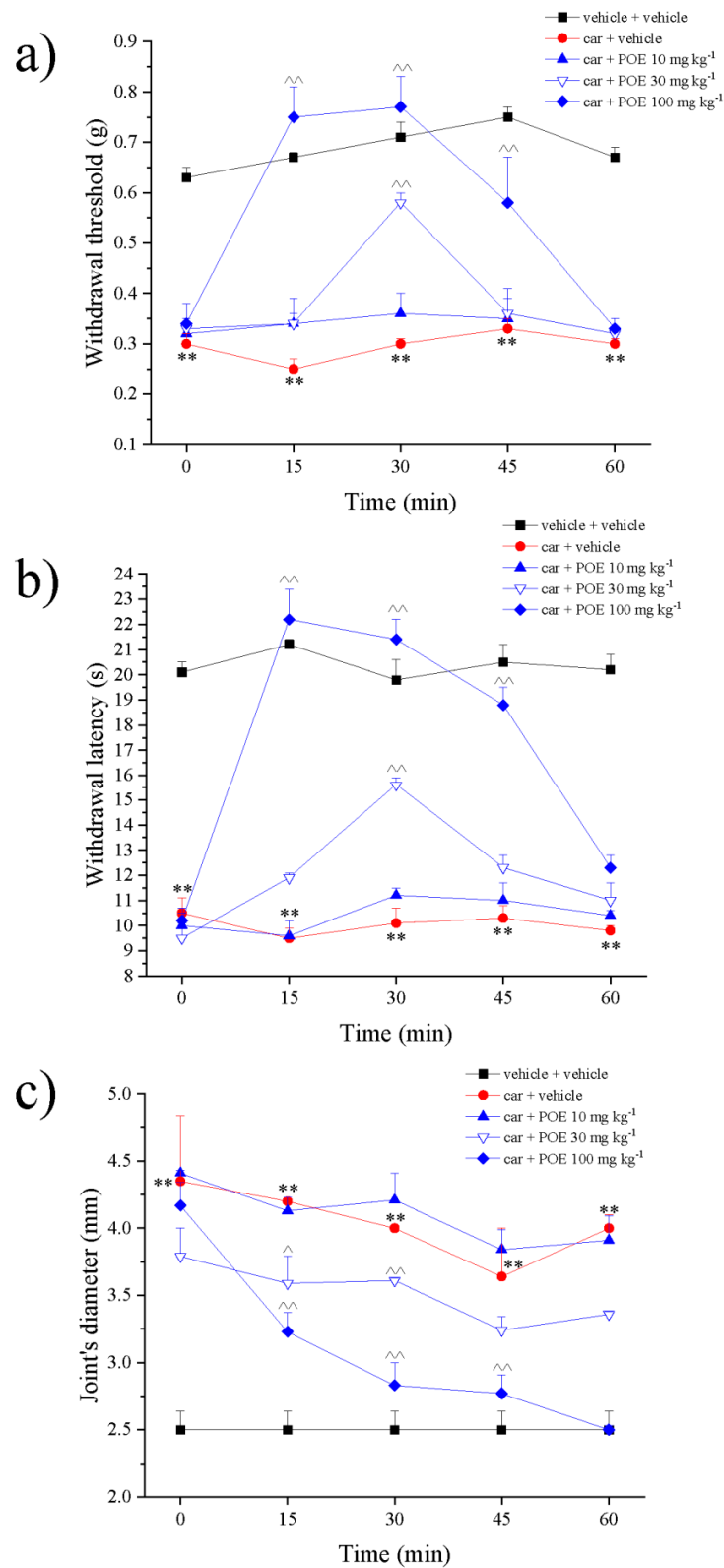


**Figure 2.** POE effects against carrageenan-induced pain and paw oedema. Two hours after the intraplantar injection of carrageenan (car), POE was per os administered. Pain threshold was measured by (a) von Frey test and (b) paw pressure test over time; (c) at the same time points, oedema was evaluated by measuring the joint's diameter. Results are reported as mean  $\pm$  S.E.M. of 10 mice analyzed in 2 different experimental sessions. \*\*  $p < 0.01$  vs. vehicle + vehicle; ^^  $p < 0.01$  vs. car + vehicle.



Accordingly, POE (30 and 100 mg kg<sup>-1</sup>) was also effective in decreasing pain induced by the direct injection into the paw of IL-1 $\beta$ ; efficacy was measured by both von Frey (Figure 3a) and paw pressure (Figure 3b) tests.

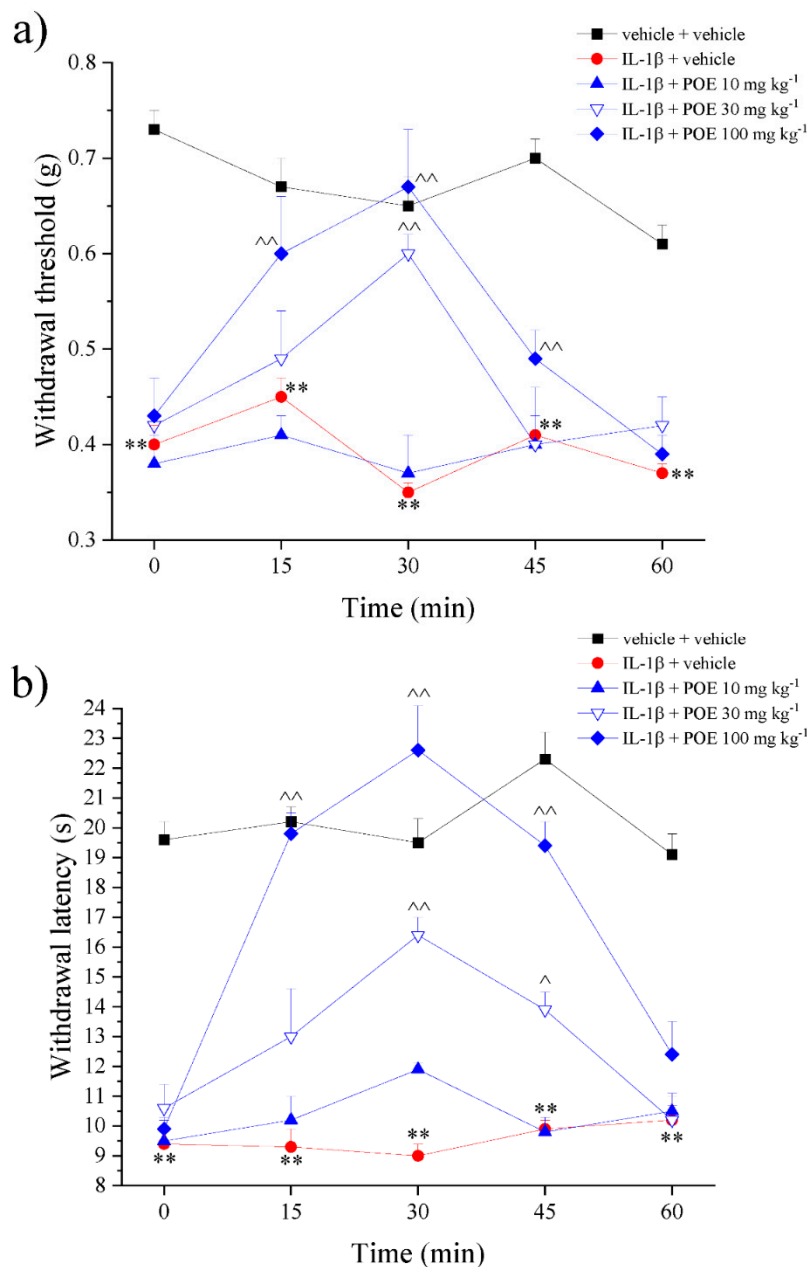


**Figure 3.** POE effects against IL-1 $\beta$ -induced pain. IL-1 $\beta$  was intraplantarly injected; 2 h later, POE was per os administered. Pain threshold was measured by (a) von Frey test and (b) paw pressure test over time. Results are reported as mean  $\pm$  S.E.M. of 10 mice analyzed in 2 different experimental sessions. \*\*  $p < 0.01$  vs. vehicle + vehicle; ^  $p < 0.05$  and ^^  $p < 0.01$  vs. IL-1 $\beta$  + vehicle.

Finally, the pain-relieving properties of POE were investigated in the formalin-induced sensitization model. Formalin shows a biphasic pain-related behavior, with an early, short-lasting first phase (0–7 min) caused by a primary afferent discharge produced by the stimulus, followed by a quiescent period and then a second, prolonged phase (15–60 min) of tonic pain related to inflammation and sensitization [17,18]. The nociceptive response was measured as the time spent in lifting, favoring, licking, shaking and flinching of the

injected paw. POE 100 mg kg<sup>-1</sup> was effective in both phases, the lower 30 mg kg<sup>-1</sup> dose was able to significantly counteract the second prolonged phase (Figure 4).

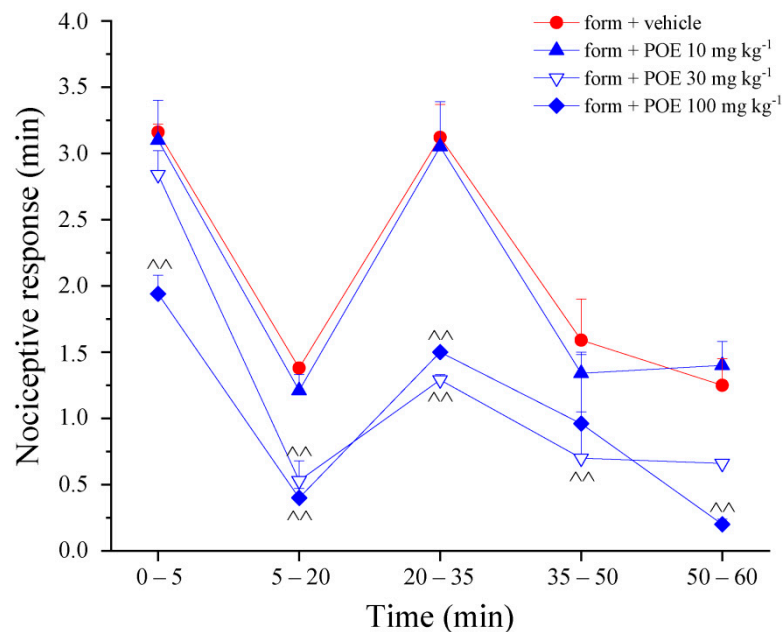


**Figure 4.** POE effects against formalin-induced pain. Formalin (form) was intraplantarly injected on time 0; in the following 60 min, the time spent lifting, favoring, licking, shaking and flinching the injected paw was recorded as nocifensive behavior. POE was p.o. administered 20 min before formalin. Control animals (vehicle + vehicle) showed 0 min as nociceptive response. Results are reported as mean  $\pm$  S.E.M. of 10 mice analyzed in 2 different experimental sessions.  $\wedge p < 0.01$  vs. form + vehicle.

In the writhing test, a model of visceral irritation [19] induced by the intraperitoneal injection of acetic acid able to stimulate nociceptive neurons by the release of several mediators in the peritoneal fluid [20], POE was not able to reduce the abdominal constrictions induced by the acetic acid intraperitoneal injection (Supplementary Table S1), revealing the lack of activity against irritative stimuli.

Based on the interesting findings collected in the hypersensitivity models mentioned above, the analgesic properties of POE were also explored in naïve animals characterized by a physiological pain threshold. Through the hot-plate test (Figure 5), it was found that POE (30 and 100 mg kg<sup>-1</sup>) was able to increase the physiological pain threshold evaluated as a response to a hot stimulus.

Overall, these results showed that POE had the dual characteristic of counteracting inflammation-induced hypersensitivity (hyperalgesia and allodynia) as well as enhancing the normal pain threshold by analgesic effects. To note the potency and efficacy of POE both in relieving pain and reducing paw edema is comparable to those of the widely clinically employed NSAID ibuprofen [21,22]. As discussed in a previous work as well [5], POE effectively exerts its bioactivities in the form of a phytocomplex. Thus, it is possible that its beneficial property against inflammatory pain, shown here, is due to the synergistic action of its constituents rather than that of individual bioactive compounds.

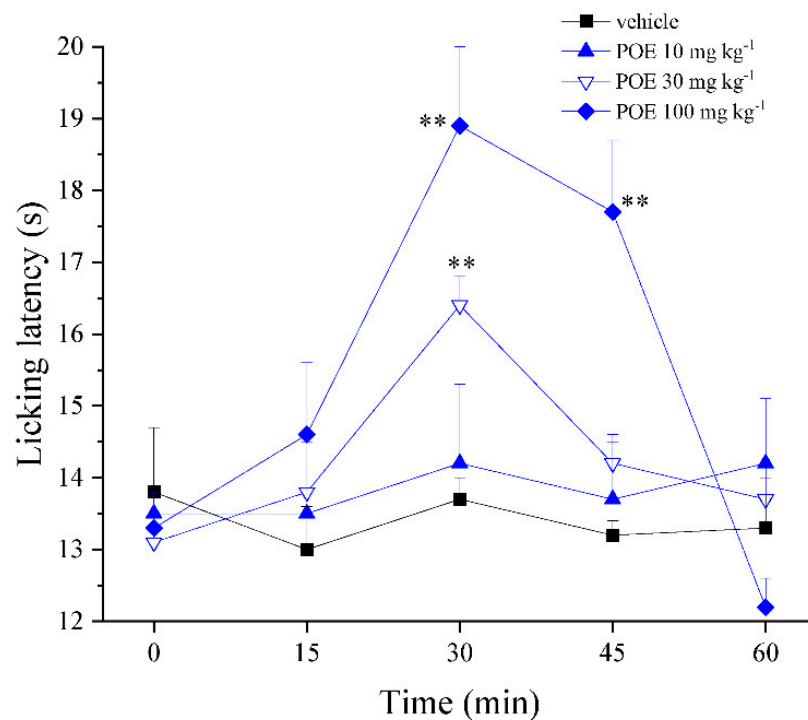


**Figure 5.** Analgesic effect of POE in naïve animals. The property to enhance the physiological pain threshold was evaluated in naïve mice by the hot-plate test. POE was p.o. administered; the time spent on a hot surface before showing nocifensive responses was recorded. Results are reported as mean  $\pm$  S.E.M. of 10 mice analyzed in 2 different experimental sessions. \*\*  $p < 0.01$  vs. vehicle + vehicle.

### 2.3. Effect of POE on the Inflammatory and Oxidative Mediators

The protective profile of POE was analyzed *ex vivo* in the paw soft tissue of carrageenan-treated animals by collecting the tissue 30 min after POE administration concurrent with the peak of pain-relieving efficacy.

The effect of POE in the tissue activity of myeloperoxidase (MPO), a primary indicator of inflammatory responses and neutrophil recruitment [23], and the tissue concentration of proinflammatory cytokines, i.e., IL-1 $\beta$  and TNF- $\alpha$ , were then evaluated. These soluble factors are able to initiate peripheral sensitization; together with reactive oxygen species (ROS) and free radicals, they activate their receptors and nociceptors terminals to decrease the pain threshold, causing hyperalgesia and inflammatory pain [24,25].

As illustrated in Figure 6a, carrageenan induced an increase in the tissue MPO activity at  $80.3 \pm 10.7 \mu\text{U}/\text{mg}$  compared to  $23 \pm 2.9 \mu\text{U}/\text{mg}$  of the vehicle; POE showed a significant inhibitory effect on the MPO activity by 50%. This result showed that POE was able to control pain in parallel with a significant decrease in tissue damage parameters.

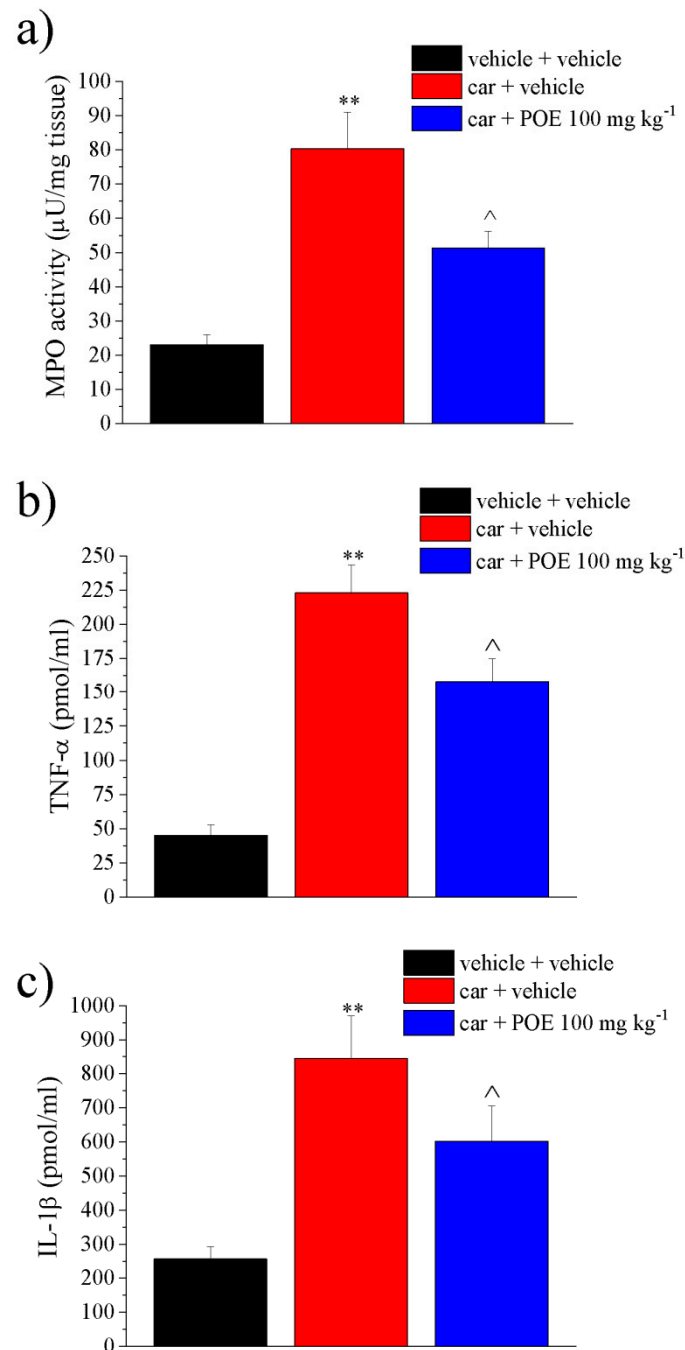
The TNF- $\alpha$  concentration also increased sharply from  $45.1 \pm 7.8 \text{ pmol}/\text{mL}$  of vehicle treated to  $223.2 \pm 20.5 \text{ pmol}/\text{mL}$  of the carrageenan group; this increase was inhibited by 37% after POE injection (Figure 6b); similarly, POE reduced the increase in IL-1 $\beta$  that occurred in the control group ( $256.3 \pm 36.1 \text{ pmol}/\text{mL}$ ) by 42% compared to the carrageenan-treated group ( $845.4 \pm 125.1 \text{ pmol}/\text{mL}$ ), as shown in Figure 6c.

Figure 7 shows the effects of POE against carrageenan-induced redox imbalance. The inflammatory stimulus doubled the NO levels compared to the control and tripled the lipid peroxidation. As shown in Figure 7a, POE completely reduced NO levels. Contrarily, POE was found to be ineffective against lipid changes (Figure 7b).

This finding was perfectly consistent with the POE *in vitro* ability to suppress the expression of major inflammation-associated enzymes, including inducible nitric oxide

synthase (iNOS), compromising the production of metabolites harmful to cells and tissues, such as NO, and in general the production of ROS [9].

Oxidative and nitrosative stress in tissue is a key parameter in carrageenan paw inflammation [26]. NO is a crucial mediator in the first and second phase of carrageenan-induced rat paw inflammation, which contributes to edema progression and hyperalgesia augmentation [27,28].



**Figure 6.** Ex vivo analysis of anti-inflammatory POE effects. Paw damage was induced by carrageenan (car, i.pl.); 2 h after car injection, POE was p.o. administered against carrageenan-induced pain and paw oedema. Two hours after the intraplantar injection of carrageenan (car), POE was p.o. administered. Thirty min later, paw tissue was collected for dosing (a) myeloperoxidase activity, (b) TNF- $\alpha$  and (c) IL-1 $\beta$  concentrations. Results are reported as mean  $\pm$  S.E.M. of 10 mice analyzed in 2 different experimental sessions. \*\*  $p < 0.01$  vs. vehicle + vehicle; ^  $p < 0.05$  vs. car + vehicle.

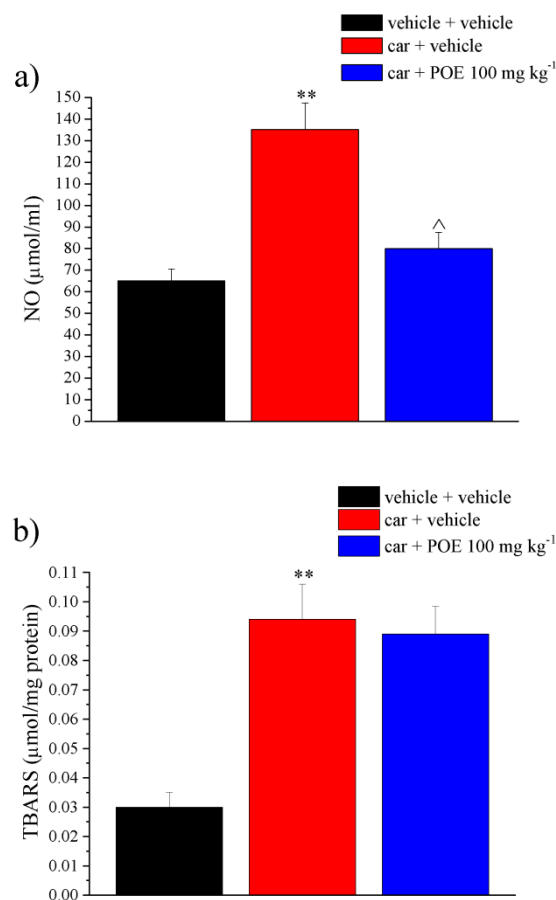


**Figure 7.** Ex vivo analysis of antioxidant POE effects. Paw damage was induced by carrageenan (car, i.pl.); 2 h after car injection, POE was p.o. administered against carrageenan-induced pain and paw oedema. Two hours after the intraplantar injection of carrageenan (car), POE was per os administered. Thirty min later, paw tissue was collected for dosing (a) NO levels were evaluated via nitrite and nitrate measurement according to the Griess reaction; (b) the peroxidation of lipids was quantified by the thiobarbituric-acid-reactive substances (TBARS) assay. Results are reported as mean  $\pm$  S.E.M. of 10 mice analyzed in 2 different experimental sessions. \*\*  $p < 0.01$  vs. vehicle + vehicle; <sup>^</sup>  $p < 0.05$  vs. car + vehicle.

Macrophages and neutrophils are the potential origins of NO during inflammation, so the attenuation in the recruitment of neutrophils into the paw tissue (as assessed by myeloperoxidase activity measurements) may be responsible for POE suppression of NO increase induced by carrageenan. According to the literature [29], carrageenan also induced an increase in lipid peroxidation that could not be modified by POE probably because acute treatment was not ideal for reducing tissue damage.

### 3. Materials and Methods

#### 3.1. Animals

CD-1 mice (Envigo, Varese, Italy) weighing 20–25 g at the beginning of the experimental procedure were used. Animals were housed in the Centro Stabulazione Animali da Laboratorio (University of Florence) and used at least 1 week after their arrival.

Ten mice were housed per cage (size 26  $\times$  41 cm); animals were fed a standard laboratory diet and tap water ad libitum and kept at  $23 \pm 1$  °C with a 12 h light/dark cycle (light at 7 a.m.).

All animal manipulations were carried out according to the Directive 2010/63/EU of the European Parliament and of the European Union Council (22 September 2010) on the protection of animals used for scientific purposes.

The ethical policy of the University of Florence complies with the Guide for the Care and Use of Laboratory Animals of the US National Institutes of Health (NIH Publication No. 85-23, revised 1996; University of Florence assurance number: A5278-01).

Formal approval to conduct the experiments described was obtained from the Italian Ministry of Health (No. 498/2017) and from the Animal Subjects Review Board of the University of Florence. Experiments involving animals have been reported according to ARRIVE guidelines [30].

All efforts were made to minimize animal suffering and to reduce the number of animals used.

### 3.2. *P. oceanica* Extract (POE) Preparation

The leaves of *P. oceanica* were extracted as previously described [5]. Briefly, 1 g of *P. oceanica* dried leaves were minced and suspended overnight in 10 mL of EtOH/H<sub>2</sub>O (70:30 *v/v*) at 37 °C under stirring and subsequently at 65 °C for 3 h.

Hydrophobic compounds were removed from the hydroalcoholic extraction by repeated shaking in n-hexane (1:1), whereas the recovered hydrophilic fraction was dispensed in 1 mL aliquots and then dried. A single batch of *P. oceanica* extract was dissolved in 0.5 mL of EtOH/H<sub>2</sub>O (70:30 *v/v*) before use and is hereafter referred to as POE.

Freshly dissolved POE was characterized for its total polyphenol (TP) and carbohydrate (TC) content and for its antioxidant and free-radical scavenging activities. Briefly, the Folin-Ciocalteu's and phenol/sulfuric acid methods were used to determine the TP and TC values of POE, respectively [5,6]. Gallic acid (0.5 mg/mL) and D-glucose (1 mg/mL) were used as reference to determine TP and TC values, respectively.

The antioxidant and free-radical scavenging activities of POE were established using ferric reducing/antioxidant power assays (FRAP) and DPPH, respectively [5,6]. Ascorbic acid (0.1 mg/mL) was used as a reference to evaluate both activities.

### 3.3. POE Administration

POE extract was suspended in 1% carboxymethylcellulose sodium salt (CMC; Sigma-Aldrich, Milan, Italy) and acutely administered per os (p.o.) in a dose ranging from 10 to 100 mg kg<sup>-1</sup>. Control animals were treated with vehicle.

### 3.4. Carrageenan-Induced Pain and Paw Oedema in Mice

The acute inflammatory response was induced by an intraplantar injection of carrageenan (Sigma-Aldrich, Milan, Italy) in the right hind paw (car: 300 µg/80 µL, i.pl.) or vehicle (V: sterile 0.9% saline, 80 µL, i.pl.) [31]. Two hours later, POE extract was suspended in 1% carboxymethylcellulose sodium salt (CMC) and orally administered.

Pain threshold was measured before (time 0) and after (15, 30, 45 and 60 min) POE treatment. Concomitantly, to evaluate the oedema, the paw thickness was measured using a digital caliper and expressed as mm [32]. In a separate experimental setting, animals were sacrificed 30 min after POE administration, the soft tissue of the paw was collected and frozen for evaluating anti-inflammatory and antioxidant properties.

### 3.5. Formalin-Induced Pain

Mice received formalin (1.25% in saline, 30 µL) in the dorsal surface of one side of the hind paw. Each mouse, randomly assigned to one of the experimental groups, was placed in a plexiglass cage and allowed to move freely. A mirror was placed at a 45° angle under the cage to allow full view of the hind limbs. Lifting, favoring, licking, shaking and flinching of the injected paw were recorded as nocifensive behavior [33]. The total time of the nociceptive response was measured up to 60 min after formalin injection and expressed in minutes (mean ± S.E.M.). Mice received vehicle (1% CMC) or different doses of POE 20 min before formalin injection.



### 3.6. IL-1 $\beta$ -Induced Pain

Interleukin-1 $\beta$  (IL-1 $\beta$ ) (R&D Systems Inc., Minneapolis, MN, USA) was i.pl. injected in the right hind paw (IL-1 $\beta$  0.05 U/80  $\mu$ L); control animals received sterile 0.9% saline, 80  $\mu$ L, i.pl.) [34]. Two hours later, POE extract was suspended in 1% carboxymethylcellulose sodium salt (CMC) and orally administered. The mechanical allodynia and hyperalgesia was measured before (time 0) and after (15, 30, 45 and 60 min) POE treatment by the von Frey test and paw pressure test, respectively.

### 3.7. Von Frey Test

The animals were placed in 20  $\times$  20 cm Plexiglas boxes equipped with a metallic meshy floor, 20 cm above the bench. A habituation of 15 min was allowed before the test. An electronic von Frey hair unit (Ugo Basile, Varese, Italy) was used: the withdrawal threshold was evaluated by applying force ranging from 0 to 5 g with a 0.2 g accuracy. Punctuate stimulus was delivered to the mid-plantar area of each anterior paw from below the meshy floor through a plastic tip and the withdrawal threshold was automatically displayed on the screen.

The paw sensitivity threshold was defined as the minimum pressure required to elicit a robust and immediate withdrawal reflex of the paw. Voluntary movements associated with locomotion were not taken as a withdrawal response. Stimuli were applied on each anterior paw with an interval of 5 s. The measure was repeated 5 times, and the final value was obtained by averaging the 5 measures [35,36].

### 3.8. Paw Pressure Test

Mechanical hyperalgesia was determined by measuring the latency in seconds to withdraw the paw away from a constant mechanical pressure exerted onto the dorsal surface [37]. A 15 g calibrated glass cylindrical rod (diameter = 10 mm) chamfered to a conical point (diameter = 3 mm) was used to exert the mechanical force. The weight was suspended vertically between two rings attached to a stand and was free to move vertically. A single measure was made per animal. A cutoff time of 40 s was used.

### 3.9. Hot-Plate Test

Analgesia was assessed using the hot plate test. With minimal animal–handler interaction, mice were taken from home-cages and placed onto the surface of the hot plate (Ugo Basile, Varese, Italy) maintained at a constant temperature of 49  $^{\circ}$ C  $\pm$  1  $^{\circ}$ C. Ambulation was restricted by a cylindrical Plexiglas chamber (diameter, 10 cm; height, 15 cm), with open top. A timer controlled by a foot peddle began timing response latency from the moment the mouse was placed onto the hot plate. Pain-related behavior (licking of the hind paw) was observed, and the time (seconds) of the first sign was recorded. The cutoff time of the latency of paw lifting or licking was set at 40 s [38].

### 3.10. Abdominal Constriction Test

Mice were injected i.p. with a 0.6% solution of acetic acid (10 mL kg<sup>-1</sup>), according to Koster et al. [39]. The number of stretching movements was counted for 10 min, starting 5 min after acetic acid injection. POE was injected 20 min before acetic acid.

### 3.11. Myeloperoxidase (MPO) Activity Assay

Tissue samples were homogenized in a solution containing 0.5% hexa-decyl-trimethyl-ammonium for 1 min. After three freeze-thawing cycles, samples were sonicated for 30 s, centrifuged for 30 min at 10,000  $\times$  g. One hundred microliter of supernatant with 2.9 mL of solution containing O-dianisidine, buffer phosphate (pH 6) and H<sub>2</sub>O<sub>2</sub> were mixed and after 5 min, 100 mL of chloridric acid solution (1.2 M) was added. Samples' absorbance was read spectrophotometrically at a 400 nm wavelength [40].

### 3.12. Tumor Necrosis Factor (TNF)- $\alpha$ and Interleukin (IL)-1 $\beta$ Assessment

The hind paw tissue levels of IL-1 $\beta$ , IL-6 and TNF- $\alpha$  were measured using the ELISA kits (Rat IL-1 $\beta$ , IL-6 and TNF- $\alpha$ , Biolegend, CA, USA) based on the manufacturer's guideline. In summary, the frozen hind paw tissue samples were homogenated in RIPA buffer. After centrifugation, the supernatants were incubated in the wells and after washing, diluted streptavidin-HRP-conjugated anti-rat IL-1 $\beta$ , IL-6 or TNF- $\alpha$  were added. Finally, after adding stop solution, the absorbance was read at 450 nm using an ELISA reader. The concentration of the cytokines was expressed as pg/mL of tissue.

### 3.13. Nitric Oxide (NO) Assay

NO swiftly oxidized to nitrite and nitrate subsequent to its creation. The level of total NO was evaluated via nitrite and nitrate measurement according to the Griess reaction [40]. In this colorimetric method, the final product absorbance can be determined at a wavelength of 540 nm in a microplate reader.

### 3.14. Lipid Peroxidation (Thiobarbituric Acid-Reactive Substances (TBARS) Assay)

The TBARS determination was carried out in paw tissue homogenate in PBS at the final concentration of 10% *w/v*. Then, FeCl<sub>3</sub> (20  $\mu$ M, Sigma-Aldrich, St. Louis, MO, USA) and ascorbic acid (100  $\mu$ M, Sigma-Aldrich) were added to obtain the Fenton reaction.

At the end of incubation, the mixture was added to 4 mL reaction mixture consisting of 36 mM thiobarbituric acid (Sigma-Aldrich) solubilized in 10% CH<sub>3</sub>COOH, 0.2% SDS, and pH was adjusted to 4.0 with NaOH. The mixture was heated for 60 min at 100 °C, and the reaction was stopped by placing the vials in an ice bath for 10 min. After centrifugation (at 1600  $\times$  *g* at 4 °C for 10 min) the absorbance of the supernatant was measured at 532 nm and 550 nm (PerkinElmer spectrometer, Milan, Italy), and TBARS were quantified in  $\mu$ mol/mg of total proteins using 1,1,3,3-tetramethoxypropane as the standard [41].

### 3.15. Statistical Analysis

Behavioral measurements were performed on 10 mice for each treatment carried out in 2 different experimental sets. All assessments were made by researchers blinded to animal treatments. Results were expressed as mean  $\pm$  (S.E.M.) with one-way analysis of variance. A Bonferroni's significant difference procedure was used as a post hoc comparison. *p*-values < 0.05 or < 0.01 were considered significant. Data were analyzed using the Origin 9 software (OriginLab, Northampton, MA, USA).

## 4. Conclusions

Recent evidence has revealed that POE works as a mixture of compounds capable of synergistically evoking an effective and totally safe *in vitro* response for cells against inflammation.

This study represents the first attempt to provide pharmacological evidence for POE ability to relieve inflammatory pain in *in vivo* animal models alongside with a decrease in inflammatory and oxidative markers. In particular, POE was found to be effective in a dose-dependent manner after a single oral administration in different models of acute inflammatory pain.

Faced with the relentless demand for new alternative natural analgesic and anti-inflammatory agents, the cell-safe POE profile, described in numerous *in vitro* studies, together with its analgesic and anti-inflammatory properties, makes this phytocomplex an excellent candidate for continuing the investigation of the potential use of POE in the management of painful inflammatory disease in order to reduce the use of conventional drugs and, consequently, their side effects.

**Supplementary Materials:** The following are available online at <https://www.mdpi.com/1660-3397/19/2/48/s1>, Table S1: Effect of acute administration of POE on acetic-acid-induced abdominal constrictions in mice: writhing test.

**Author Contributions:** Conceptualization, D.D. and L.D.C.M.; methodology, L.M., M.V. and E.B.; software, E.L.; formal analysis, E.L. and E.B.; investigation, L.M.; resources, C.G. and D.D.; data curation, L.M. and L.D.C.M.; writing—original draft preparation, L.D.C.M. and D.D.; writing—review and editing, C.G. and M.V.; supervision, C.G.; project administration, L.D.C.M.; funding acquisition, C.G. and D.D. All authors have read and agreed to the published version of the manuscript.

**Funding:** This research was funded by the Italian Minister of University and Research (MIUR) and by the University of Florence.

**Institutional Review Board Statement:** This study was carried out according to the Directive 2010/63/EU of the European parliament and of the European Union council (22 September 2010) on the protection of animals used for scientific purposes. The ethical policy of the University of Florence complies with the Guide for the Care and Use of Laboratory Animals of the US National Institutes of Health (NIH Publication No. 85-23, revised 1996; University of Florence assurance number: A5278-01). Formal approval to conduct the experiments described was obtained from the Italian Ministry of Health (No. 498/2017) and from the Animal Subjects Review Board of the University of Florence.

**Data Availability Statement:** The data presented in this study are available on request from the corresponding author.

**Conflicts of Interest:** The authors declare no conflict of interest.

## References

1. Vacchi, M.; De Falco, G.; Simeone, S.; Montefalcone, M.; Morri, C.; Ferrari, M.; Bianchi, C.N. Biogeomorphology of the Mediterranean *Posidonia oceanica* seagrass meadows. *Earth Surf. Process. Landf.* **2016**, *42*, 42–54. [[CrossRef](#)]
2. Batanouny, K.H. Wild Medicinal Plants in Egypt. *Entrep. Sustain. Issues* **2015**, *3*, 47.
3. El-Mokasabi, F.M. Floristic composition and traditional uses of plant species at Wadi Alkuf, Al-Jabal Al-Akhder, Libya. *Am.-Eurasian J. Sustain. Agric.* **2014**, *14*, 685–697. [[CrossRef](#)]
4. Gokce, G.; Haznedaroglu, M.Z. Evaluation of antidiabetic, antioxidant and vasoprotective effects of *Posidonia oceanica* extract. *J. Ethnopharmacol.* **2008**, *115*, 122–130. [[CrossRef](#)]
5. Barletta, E.; Ramazzotti, M.; Fratianni, F.; Pessani, D.; Degl’Innocenti, D. Hydrophilic extract from *Posidonia oceanica* inhibits activity and expression of gelatinases and prevents HT1080 human fibrosarcoma cell line invasion. *Cell Adhes. Migr.* **2015**, *9*, 422–431. [[CrossRef](#)]
6. Leri, M.; Ramazzotti, M.; Vasarri, M.; Peri, S.; Barletta, E.; Pretti, C.; Degl’Innocenti, D. Bioactive compounds from *Posidonia oceanica* (L.) Delile impair malignant cell migration through autophagy modulation. *Mar. Drugs* **2018**, *16*, 137. [[CrossRef](#)]
7. Piazzini, V.; Vasarri, M.; Degl’Innocenti, D.; Guastini, A.; Barletta, E.; Salvatici, M.C.; Bergonzi, M.C. Comparison of Chitosan Nanoparticles and Soluplus Micelles to optimize the bioactivity of *Posidonia oceanica* extract on human neuroblastoma cell migration. *Pharmaceutics* **2019**, *11*, 655. [[CrossRef](#)]
8. Vasarri, M.; Barletta, E.; Ramazzotti, M.; Degl’Innocenti, D. In vitro anti-glycation activity of the marine plant *Posidonia oceanica* (L.) Delile. *J. Ethnopharmacol.* **2020**, *259*, 112960. [[CrossRef](#)]
9. Vasarri, M.; Leri, M.; Barletta, E.; Ramazzotti, M.; Marzocchini, R.; Degl’Innocenti, D. Anti-inflammatory properties of the marine plant *Posidonia oceanica* (L.) Delile. *J. Ethnopharmacol.* **2020**, *247*, 112252. [[CrossRef](#)]
10. Wongrakpanich, S.; Wongrakpanich, A.; Melhado, K.; Ranganaswami, J. A comprehensive review of non-steroidal anti-inflammatory drug use in the elderly. *Aging Dis.* **2018**, *9*, 143–150. [[CrossRef](#)]
11. Rauf, A.; Jehan, N.; Ahmad, Z.; Mubarak, M.S. Analgesic potential of extracts and derived natural products from medicinal plants. In *Pain Relief-From Analgesics to Alternative Therapies*; Maldonado, C., Ed.; IntechOpen: Rijeka, Croatia, 2017. [[CrossRef](#)]
12. Chen, L.; Deng, H.; Cui, H.; Fang, J.; Zuo, Z.; Deng, J.; Li, Y.; Wang, X.; Zhao, L. Inflammatory responses and inflammation-associated diseases in organs. *Oncotarget* **2017**, *9*, 7204–7218. [[CrossRef](#)] [[PubMed](#)]
13. Xu, Q.; Yaksh, T.L. A brief comparison of the pathophysiology of inflammatory versus neuropathic pain. *Curr. Opin. Anesthesiol.* **2011**, *24*, 400–407. [[CrossRef](#)]
14. Iannitti, T.; Graham, A.; Dolan, S. Adiponectin-mediated analgesia and anti-inflammatory effects in rat. *PLoS ONE* **2015**, *10*, e0136819. [[CrossRef](#)] [[PubMed](#)]
15. Morales-Medina, J.C.; Flores, G.; Vallelunga, A.; Griffiths, N.H.; Iannitti, T. Cerebrolysin improves peripheral inflammatory pain: Sex differences in two models of acute and chronic mechanical hypersensitivity. *Drug Dev. Res.* **2019**, *80*, 513–518. [[CrossRef](#)]
16. Crunkhorn, P.; Meacock, S.C. Mediators of the inflammation induced in the rat paw by carrageenin. *Br. J. Pharmacol.* **1971**, *42*, 392–402. [[CrossRef](#)] [[PubMed](#)]
17. Fischer, M.; Carli, G.; Raboisson, P.; Reeh, P. The interphase of the formalin test. *Pain* **2014**, *155*, 511–521. [[CrossRef](#)] [[PubMed](#)]

18. Moriello, A.S.; Luongo, L.; Guida, F.; Christodoulou, M.S.; Perdicchia, D.; Maione, S.; Passarella, D.; Marzo, V.D.; Petrocellis, L. Chalcone derivatives activate and desensitize the transient receptor potential Ankyrin 1 cation channel, subfamily A, member 1 TRPA1 Ion channel: Structure-activity relationships in vitro and anti-nociceptive and anti-inflammatory activity in vivo. *CNS Neurol. Disord. Drug Targets* **2016**, *15*, 987–994. [[CrossRef](#)]
19. Nakamura, H.; Imazu, C.; Ishii, K.; Yokoyama, Y.; Kadokawa, T.; Shimizu, M. Site of analgesic action of zomepirac sodium, a potent non-narcotic analgesic in experimental animals. *Jpn. J. Pharmacol.* **1983**, *33*, 875–883. [[CrossRef](#)]
20. Boonyarikpunchai, W.; Sukrong, S.; Towiwat, P. Antinociceptive and anti-inflammatory effects of rosmarinic acid isolated from *thunbergia laurifolia* Lindl. *Pharmacol. Biochem. Behav.* **2014**, *124*, 67–73. [[CrossRef](#)]
21. Di Cesare Mannelli, L.; Tenci, B.; Zanardelli, M.; Maidecchi, A.; Lugli, A.; Mattoli, L.; Ghelardini, C. Widespread pain reliever profile of a flower extract of *Tanacetum parthenium*. *Phytomedicine* **2015**, *22*, 7–8. [[CrossRef](#)]
22. Moilanen, L.J.; Laavola, M.; Kukkonen, M.; Korhonen, R.; Leppänen, T.; Högestätt, E.D.; Zygmunt, P.M.; Nieminen, R.M.; Moilanen, E. TRPA1 contributes to the acute inflammatory response and mediates carrageenan-induced paw edema in the mouse. *Sci. Rep.* **2012**, *2*, 380. [[CrossRef](#)] [[PubMed](#)]
23. Strzepa, A.; Pritchard, K.A.; Dittel, B.N. Myeloperoxidase: A new player in autoimmunity. *Cell. Immunol.* **2017**, *317*, 1–8. [[CrossRef](#)] [[PubMed](#)]
24. Kadetoff, D.; Lampa, J.; Westman, M.; Andersson, M.; Kosek, E. Evidence of central inflammation in fibromyalgia-increased cerebrospinal fluid interleukin-8 levels. *J. Neuroimmunol.* **2012**, *242*, 33–38. [[CrossRef](#)] [[PubMed](#)]
25. Stejskal, V.; Ockert, K.; Bjørklund, G. Metal-induced inflammation triggers fibromyalgia in metal-allergic patients. *Neuroendocrinol. Lett.* **2013**, *34*, 559–565. [[PubMed](#)]
26. Mizokami, S.S.; Hohmann, M.S.; Staurengo-Ferrari, L.; Carvalho, T.T.; Zarpelon, A.C.; Possebon, M.I.; de Souza, A.R.; Veneziani, R.C.; Arakawa, N.S.; Casagrande, R.; et al. Pimaradienoic acid inhibits Carrageenan-induced inflammatory leukocyte recruitment and edema in mice: Inhibition of oxidative stress, nitric oxide and cytokine production. *PLoS ONE* **2016**, *11*, e0149656. [[CrossRef](#)]
27. Namgyal, D.; Sarwat, M. Saffron as a neuroprotective agent. In *Saffron*, 1st ed.; Sarwat, M., Sumaiya, S., Eds.; Elsevier: Amsterdam, The Netherlands, 2020; pp. 93–102. [[CrossRef](#)]
28. Sharma, B.; Kumar, H.; Kaushik, P.; Mirza, R.; Awasthi, R.; Kulkarni, G. Therapeutic benefits of Saffron in brain diseases: New lights on possible pharmacological mechanisms. In *Saffron*, 1st ed.; Sarwat, M., Sumaiya, S., Eds.; Elsevier: Amsterdam, The Netherlands, 2020; pp. 117–130. [[CrossRef](#)]
29. Haddadi, R.; Rashtiani, R. Anti-inflammatory and anti-hyperalgesic effects of milnacipran in inflamed rats: Involvement of myeloperoxidase activity, cytokines and oxidative/nitrosative stress. *Inflammopharmacology* **2020**, *28*, 903–913. [[CrossRef](#)]
30. McGrath, J.C.; Lilley, E. Implementing guidelines on reporting research using animals (ARRIVE etc.): New requirements for publication in *BJP. Br. J. Pharmacol.* **2015**, *172*, 3189–3193. [[CrossRef](#)]
31. Dallazen, J.L.; Maria-Ferreira, D.; da Luz, B.B.; Nascimento, A.M.; Cipriani, T.R.; de Souza, L.M.; Felipe, L.; Silva, B.; Nassini, R.; de Paula Werner, M.F. Pharmacological potential of alkylamides from *acmella oleracea* flowers and synthetic isobutylalkyl amide to treat inflammatory pain. *Inflammopharmacology* **2020**, *28*, 175–186. [[CrossRef](#)]
32. Micheli, L.; Ghelardini, C.; Lucarini, E.; Parisio, C.; Trallori, E.; Cinci, L.; Di Cesare Mannelli, L. Intra-articular mucilages: Behavioural and histological evaluations for a new model of articular pain. *J. Pharm. Pharmacol.* **2019**, *71*, 971–981. [[CrossRef](#)]
33. Abbott, F.V.; Guy, E.R. Effects of morphine, pentobarbital and amphetamine on formalin-induced behaviours in infant rats: Sedation versus specific suppression of pain. *Pain* **1995**, *62*, 303–312. [[CrossRef](#)]
34. Ferreira, S.H.; Lorenzetti, B.B.; Bristow, A.F.; Poole, S. Interleukin-1 beta as a potent hyperalgesic agent antagonized by a tripeptide analogue. *Nature* **1998**, *334*, 698–700. [[CrossRef](#)]
35. Sakurai, M.; Egashira, N.; Kawashiri, T.; Yano, T.; Ikesue, H.; Oishi, R. Oxaliplatin-induced neuropathy in the rat: Involvement of oxalate in cold hyperalgesia but not mechanical allodynia. *Pain* **2009**, *147*, 165–174. [[CrossRef](#)] [[PubMed](#)]
36. Di Cesare Mannelli, L.; Micheli, L.; Maresca, M.; Cravotto, G.; Bellumori, M.; Innocenti, M.; Mulinacci, N.; Ghelardini, C. Anti-neuropathic effects of *rosmarinus officinalis* L. terpenoid fraction: Relevance of nicotinic receptors. *Sci. Rep.* **2016**, *6*, 34832. [[CrossRef](#)] [[PubMed](#)]
37. Micheli, L.; Di Cesare Mannelli, L.; Del Bello, F.; Giannella, M.; Piergentili, A.; Quaglia, W.; Carrino, D.; Pacini, A.; Ghelardini, C. The use of the selective imidazoline I 1 receptor agonist carbophenylene as a strategy for neuropathic pain relief: Preclinical evaluation in a mouse model of oxaliplatin-induced neurotoxicity. *Neurotherapeutics* **2020**, *17*, 1005–1015. [[CrossRef](#)] [[PubMed](#)]
38. Micheli, L.; Di Cesare Mannelli, L.; Lucarini, E.; Parisio, C.; Toti, A.; Fiorentino, B.; Rigamonti, M.A.; Calosi, L.; Ghelardini, C. Intranasal low-dose naltrexone against opioid side effects: A preclinical study. *Front. Pharmacol.* **2020**, *11*, 576624. [[CrossRef](#)]
39. Koster, R.; Anderson, M.; De Beer, E.J. Acetic acid for analgesic screening. *Fed. Proc.* **1959**, *18*, 412–417.
40. Haddadi, R.; Poursina, M.; Zeraati, F.; Nadi, F. Gastrodin microinjection suppresses 6-OHDA-induced motor impairments in parkinsonian rats: Insights into oxidative balance and microglial activation in SNc. *Inflammopharmacology* **2018**, *26*, 1305–1316. [[CrossRef](#)]
41. Micheli, L.; Lucarini, E.; Trallori, E.; Avagliano, C.; De Caro, C.; Russo, R.; Calignano, A.; Ghelardini, C.; Pacini, A.; Di Cesare Mannelli, L. *Phaseolus vulgaris* L. Extract: Alpha-amylase inhibition against metabolic syndrome in mice. *Nutrients* **2019**, *11*, 1778. [[CrossRef](#)]

### **3.4. From tradition to science: the antidiabetic role of *P. oceanica***

Healing with herbal remedies is as old as humanity itself. The main source of knowledge on the medicinal use of plants is the result of decades of fighting diseases that have led humans to search for drugs in nature [126]. Contemporary science has recognized the active principle of medicinal plants and has included in modern pharmacotherapy a wide range of plant-derived drugs, known by ancient civilizations and used over the millennia [127].

Currently, research on marine ethno-medicine is relatively small compared to observations on terrestrial ethnobotany. However, traditional uses of marine organisms are documented in the literature.

The use of the *P. oceanica* seagrass as a medicinal plant dates back to Mediterranean civilizations that exploited its medicinal values to treat various human health ailments, as described in §1.5.

In particular, according to a more recent tradition, the villagers of the western Anatolian coast used the decoction of *P. oceanica* leaves as a natural remedy for diabetes and hypertension and also as a vitalizer.

Parallel to its use in traditional medicine, in 2008 Gokce et al. conducted an *in vivo* study to investigate the antidiabetic and vasoprotective effects of *P. oceanica* leaves extract. The continuous oral administration of POE to alloxan-induced diabetic rats was found to reduce blood sugar, restore the function of antioxidant enzymes, and reduce the process of lipid peroxidation. However, POE caused no change in antioxidant status while possessing hypoglycemic and vasoprotective activities, thus reinforcing the hypothesis that the verified antidiabetic role of POE may be independent of its antioxidant effects [55].

Diabetes is an extremely common and growing disease worldwide with great impact on human health. To date, managing diabetes with minimized side effects is still a complicated medical challenge. Patients often require the use of natural products with antidiabetic activity due to their safety and non-toxicity profile in the face of the unwanted side effects of both insulin and other hypoglycemic drugs [128].

Persistent hyperglycemia or uncontrolled diabetes has the potential to cause serious complications. An inevitable consequence of a long-lasting hyperglycemic state is an increased accumulation of advanced glycation end products (AGEs), a heterogeneous

group of products obtained from the non-enzymatic Maillard reaction between circulating macromolecules and free-reducing sugars. In addition to being a key indicator of diabetic complications onset, AGEs are also the main cause of almost all diabetes-related problems (Figure 24) [129].

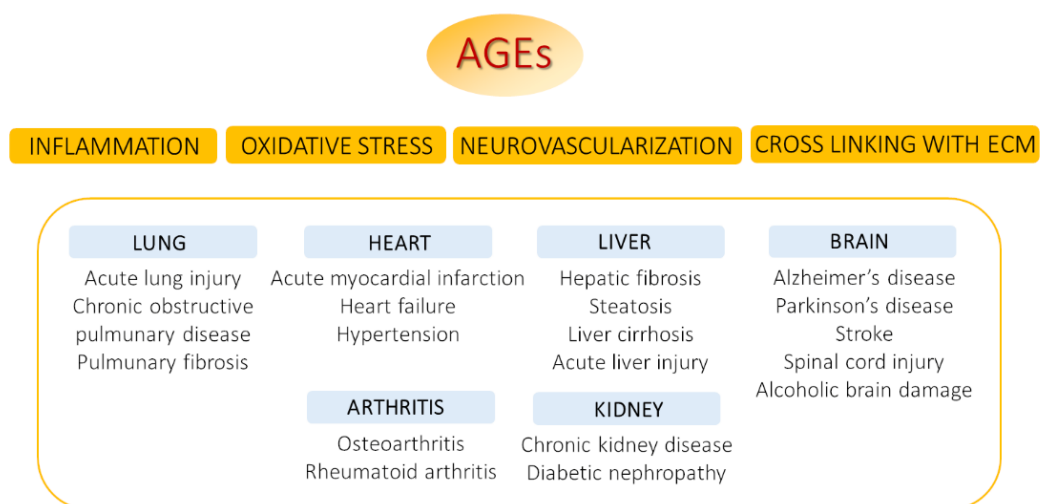


**Figure 24.** Relationship between advanced glycation end products (AGEs) and human diseases. AGEs commonly act through mechanisms of oxidative stress, neovascularization, inflammation or cross-linking with the extracellular matrix (ECM).

The use of AGE inhibitors is an essential strategy to prevent and/or alleviate pathophysiological conditions related to diabetes. Several glycation inhibitors have been studied over the years. Aminoguanidine is an excellent anti-glycation agent which however has never been approved for clinical use due to its cytotoxicity. Other safe drugs that have been approved by the FDA (USA) are however not effective enough in inhibiting the formation of AGEs under chronic hyperglycemia [130].

Hence, taking into account the importance of glycation in diabetes pathophysiology, research is continuously aimed at identifying new anti-glycation agents.

Considering the antidiabetic role of *P. oceanica* in traditional medicine, supported by preclinical *in vivo* studies described above, my research focused on investigating the hydroalcoholic extract of *P. oceanica* leaves (POE) as a potential agent against the protein glycation process (Figure 25).

In this study the advanced glycation end products from HSA and glucose, named aAGEs, were obtained through a thermal glycation process over time (§4.13.1). Since the glycation products have their own intrinsic fluorescence, by measuring this fluorescence (§4.13.2) it was found that the aAGEs were produced in a time-dependent manner.



In addition, the glycation of protein determined a net decrease of the positive charges in the AGEs, reasonably attributable to the involvement of positively charged residues (arginine and lysine) in the condensation with carbohydrates [131]. Since the loss of positive charges is the main factor affecting electrophoretic migration towards the anode, the formation of aAGEs was verified by native polyacrylamide gel electrophoresis (N-PAGE) under native conditions (§4.13.2).

Specifically, it was found that aAGEs obtained in a longer time migrate faster than those obtained in shorter times. These results were in perfect agreement with those obtained from the intrinsic fluorescence measurement of AGEs.

The ability of POE to inhibit protein glycation was then verified by adding POE during the *in vitro* thermal glycation process (§4.13.3).

The glycation products obtained in the presence of POE (aAGE+POE) exhibited both a marked reduction in intrinsic fluorescence emission and a reduced electrophoretic migration towards the anode, suggesting that POE exerted an effective anti-glycation effect *in vitro*. The results for aAGE+POE were comparable to those of aAGEs obtained in the presence of aminoguanidine (aAGE+AG), which further supported the efficacy of POE in inhibiting protein glycation.

However, to rule out that the anti-glycation activity of POE was attributable to its known antioxidant activity, aAGEs were also prepared in the presence of ascorbic acid (ASC) equivalents of POE. The difference in the intrinsic fluorescent signal between aAGE+POE and aAGE+ASC, and the different behaviour of the two samples in the electrophoretic migration confirmed that POE exerted its anti-glycation role apart from its antioxidant activity. However, the antioxidant role of POE is essential for effective action against protein glycation. Since the formation of AGEs is favoured by oxidative reactions, antioxidants play a key role in the mechanisms of glycation inhibition.

Overall, this first investigation into the inhibitory role of POE on protein glycation, together with its recognized antidiabetic role, has led to new insights into the potential of POE in the management of diabetes and associated complications. The detailed analysis of the achieved results can be found in the published paper [132] attached below.

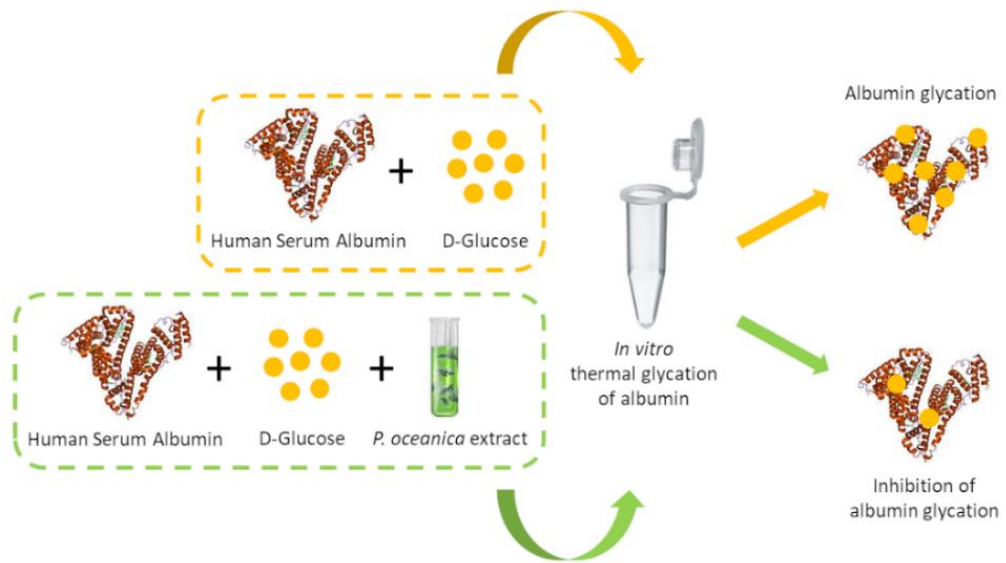


**Figure 25.** Graphic abstract summarizing the results obtained from my research activity on the *P. oceanica* anti-glycation role. These results have already been published in 2020 in the international peer-reviewed scientific *Journal of Ethnopharmacology* [132].



## *In vitro* anti-glycation activity of the marine plant *Posidonia oceanica* (L.) *Delile*



Marzia Vasarri<sup>a</sup>, Emanuela Barletta<sup>a</sup>, Matteo Ramazzotti<sup>a</sup>, Donatella Degl'Innocenti<sup>a,b,\*</sup>

<sup>a</sup> Department of Experimental and Clinical Biomedical Sciences, University of Florence, Viale Morgagni 50, 50134, Florence, Italy

<sup>b</sup> Italy Interuniversity Center of Marine Biology and Applied Ecology "G. Bacchi" (CIBM), Viale N. Sauro 4, 57128, Leghorn, Italy

### ARTICLE INFO

#### Keywords:

*Posidonia oceanica*  
AGEs  
Albumin glycation  
Anti-glycation  
Antioxidant

### ABSTRACT

**Ethnopharmacological relevance:** The marine plant *Posidonia oceanica* (L.) *Delile* is traditionally used by villagers of the west coast of Anatolia as a remedy for diabetes and hypertension.

**Aim of the study:** The aim of this study was to explore the role of the *P. oceanica* hydroalcoholic leaves extract (POE) against human serum albumin glycation.

**Material and methods:** Advanced glycation end products (AGEs) were obtained with the albumin-glucose *in vitro* assay. The AGEs intrinsic fluorescence intensity and the electrophoretic migration under native conditions allowed us to verify the effective glycation of albumin. The presence of POE during glycation process was intended to evaluate its anti-glycation role.

**Results:** POE exhibited a strong *in vitro* anti-glycation ability which occurred independently from its known antioxidant property.

**Conclusions:** Overall, the antidiabetic, antioxidant, anti-inflammatory and anti-glycation properties of POE could be exploited as an effective tool against diabetes and related complications.

### 1. Introduction

Diabetes and its complications are the most significant cause of mortality in the world and the number of diabetic patients is continuously growing. During hyperglycemia, advanced glycation end products (AGEs), an heterogeneous non-enzymatic products of Maillard reaction between circulating proteins and free reducing sugars, accelerate the risk of developing diabetes-related complications. In fact, protein glycation causes aberrant molecular conformation, impaired enzymatic activity, reduced degradation capacity and interference in receptor recognition (Singh et al., 2014). Human serum and membrane basal proteins are subjected to non-enzymatic glycation *in vivo*. Human serum albumin (HSA; pI = 4.7, MW 66.4 kDa) is highly susceptible to non-enzymatic glycation due to its high concentration (about 35–50 g/L) and a long half-life of about 20 days (Rondeau and Bourdon, 2011). In addition to being a fundamental marker of diabetic complications onset, endogenously formed AGEs are also identified as the core reason for almost all diabetes-related problems (Singh et al., 2014). Discovery

of AGE inhibitors is an essential strategy for preventing and/or alleviating diabetes-related pathophysiological conditions.

Over the years, several glycation inhibitors have been studied with generally disappointing results. Indeed, aminoguanidine is an excellent anti-glycation agent, but it has not been approved for clinical use due to its cytotoxicity. Some safe drugs have been approved by the FDA (USA), however, they are not efficient enough in inhibiting the AGEs formation under chronic hyperglycemia (Rasheed et al., 2018).

Hence, taking into account the importance of glycation in the diabetes pathophysiology, it is necessary to identify novel agents against protein glycation to prevent and/or treat diabetic complications. In this regard, the almost endless and unique chemical diversity of marine organisms has encouraged researchers to explore the marine environment as an excellent source of novel and powerful natural anti-glycation agents (Lauritano and Ianora, 2016).

The marine vascular plant *Posidonia oceanica* (L.) *Delile* is the only endemic species of the Mediterranean Sea belonging to Posidoniaceae family. It is a marine angiosperm that flowers underwater forming vast

**Abbreviations:** POE, *Posidonia oceanica* extract; HSA, Human Serum Albumin; GLC, D-Glucose; ASC, Ascorbic acid; AG, Aminoguanidine; aAGE, Advanced end product glycation from HSA and Glucose; aAGE + POE, Albumin glycated in the presence of POE; aAGE + AG, Albumin glycated in the presence of Aminoguanidine; aAGE + ASC, Albumin glycated in the presence of Ascorbic acid

\* Corresponding author. . Department of Experimental and Clinical Biomedical Sciences, University of Florence, Viale Morgagni 50, 50134, Florence, Italy.

E-mail addresses: [marzia.vasarri@unifi.it](mailto:marzia.vasarri@unifi.it) (M. Vasarri), [emanuela.barletta@unifi.it](mailto:emanuela.barletta@unifi.it) (E. Barletta), [matteo.ramazzotti@unifi.it](mailto:matteo.ramazzotti@unifi.it) (M. Ramazzotti), [donatella.deglinnocenti@unifi.it](mailto:donatella.deglinnocenti@unifi.it) (D. Degl'Innocenti).

<https://doi.org/10.1016/j.jep.2020.112960>

Received 23 March 2020; Received in revised form 30 April 2020; Accepted 7 May 2020

Available online 11 May 2020

0378-8741/ © 2020 Elsevier B.V. All rights reserved.

meadows covering tens of thousands of square kilometers considered an important marine habitat. The decoction of the leaves has been cited to be used as a remedy for diabetes and hypertension by villagers living by the sea coast of Western Anatolia. The antidiabetic and vasoprotective effects of *P. oceanica* extract have been supported also by *in vivo* pre-clinical studies on alloxan-induced diabetic rats (Gokce and Haznedaroglu, 2008). Based on this knowledge and aiming to search for novel natural AGE inhibitors, we have undertaken a more in-depth study on the anti-glycation role of *P. oceanica* leaves hydroalcoholic extract (POE), previously investigated and characterized by our group (Vasarri et al., 2020). In this short communication we demonstrate for the first time the interesting *in vitro* POE anti-glycation activity.

## 2. Material and methods

### 2.1. Materials and reagents

Human Serum Albumin (HSA), D-glucose (GLC), aminoguanidine (AG), ascorbic acid (ASC) and all other chemicals were purchased from Sigma Aldrich-Merck. Electrophoresis reagents and Coomassie Brilliant Blue G were provided by Bio-Rad (Hercules, CA, USA). Disposable plastics were from Sarstedt (Nümbrecht, Germany). *P. oceanica* leaves were collected in July by the authorized personnel of the Interuniversity Center of Marine Biology and Applied Ecology "G. Bacchi" in the protected marine area of Meloria at a depth of about 15 m at 43° 35' 13" N and 010° 10' 21" E geographical coordinates.

### 2.2. *P. oceanica* leaves extraction

The hydroalcoholic extract of *P. oceanica* leaves was obtained according to the previously described method (Barletta et al., 2015). The *P. oceanica* dry extract was dissolved in DMSO prior to use, and hereinafter named POE.

The total polyphenols and carbohydrates content and antioxidant and radical scavenging activities of POE were determined according to previously described methods (Vasarri et al., 2020).

### 2.3. Preparation of albumin-AGE

Albumin-AGE is obtained *in vitro* by incubating HSA (1 mg/mL) with GLC (500 mM) in phosphate-buffered saline (PBS: pH 7.4, 1.37 M NaCl, 27 mM KCl, 100 mM Na<sub>2</sub>HPO<sub>4</sub>, 18 mM KH<sub>2</sub>PO<sub>4</sub>) at 60 °C for 24h, 48h and 72h, under stirring (300 rpm) using Thermo-Shaker TS-100 (Biosan, Riga, LV), and hereafter named aAGE. HSA solution without GLC was prepared as control and incubated under the same conditions. The aAGE formation was verified by measuring typical AGEs fluorescence at  $\lambda_{ex}/\lambda_{em}$  335/385 nm (Séro et al., 2013) using a Biotek Synergy 1H plate reader.

### 2.4. Inhibition of aAGE formation

The anti-glycation effect was evaluated by incubating HSA with GLC in the presence of POE (0.2 mg of dry extract) for 72h. The positive control of inhibition of aAGE formation was also performed in the presence of AG (10 mM), a known synthetic anti-glycation agent. The contribution of POE antioxidant activity on the inhibition of glycation process was assessed in the presence of ASC equivalents. DMSO at concentrations resembling those derived from POE was used as negative control of inhibition of aAGE formation. The percentage of aAGE intrinsic fluorescence intensity was calculated as follows (1):

$$\text{aAGE (\%)} = \frac{(\text{HSA} + \text{GLC} + \text{inhibitor}^1) - (\text{HSA} + \text{inhibitor}^1)}{(\text{HSA} + \text{GLC}) - (\text{HSA})} \times 100$$

<sup>1</sup>Inhibitor: POE, AG or ASC

(1)

### 2.5. Native polyacrylamide gel electrophoresis (N-PAGE)

The aAGE formation was analyzed by 12% N-PAGE under native condition [Tris-glycine buffer: 25 mM Tris and 192 mM Glycine, pH 8.3]. The samples were diluted 1:1 with Sample Buffer [62.5 mM Tris-HCl pH 6.8, 25% (w/v) glycerol and 0.5% bromophenol blue] without reducing agents. AAGE samples (1.5 µg) were separated on N-PAGE for 100 min at 200V. Proteins bands were stained by colloidal Coomassie Brilliant Blue G dye, following manufacturer's instructions.

## 3. Results and discussion

Diabetes is an extremely common disease worldwide and its complications strongly impact on human health. Since endogenous formation of AGEs are crucial for the onset of almost all diabetic complications (Singh et al., 2014), scientific research has focused on the identification of novel effective and non-toxic agents with anti-glycation properties to prevent and/or alleviate diabetes-related pathophysiological conditions. Given the traditional antidiabetic usage of *P. oceanica*, supported by *in vivo* preclinical studies (Gokce and Haznedaroglu, 2008), here we investigated POE as a potential agent against HSA glycation. The polyphenolic profile of POE has been previously characterized by UPLC analysis, evidencing a large amount of catechins and a minor amount of other polyphenols (gallic acid, chlorogenic acid, epicatechin and ferulic acid) (Barletta et al., 2015). In addition, POE was found to contain 0.18 mg of polyphenols (gallic acid equivalents) and 0.35 mg of carbohydrates (glucose equivalents) per mg of dry extract, with an antioxidant and radical scavenging activity of 45 µg and 0.6 mg of ASC equivalents, respectively (Vasarri et al., 2020). DMSO vehicle did not interfere with all performed assays. These values perfectly agree with our previous reports (Barletta et al., 2015; Leri et al., 2018), confirming the robustness of our hydroalcoholic extraction method.

Albumin, which represents about 50% of plasma proteins, is highly exposed to glycation process especially under hyperglycemia (Rondeau and Bourdon, 2011). In this work, we performed the *in vitro* aAGE formation by incubating HSA (1 mg/mL) with GLC (500 mM) from 0h to 72 h at 60 °C. In order to evaluate the aAGE formation, its intrinsic fluorescence intensity was measured. As depicted in Fig. 1A, aAGE showed a marked incubation time-dependent fluorescence emission augmentation with 3, 10 and 16 times increase at 24h, 48h and 72h incubation, respectively, compared to non-glycated albumin (aAGE at 0h). These data suggest that an albumin conformational change occurred by means of glucose-induced glycation, confirming the effective production of aAGE. The aAGE formation was also assessed by incubating HSA with GLC at the same concentrations for 8 weeks at 37 °C with the aim of making the glycation process as physiological as possible. However, the HSA glycation at 37 °C for a longer time gave resulted almost identical to that performed at 60 °C for shorter times (data not shown). Therefore, for subsequent anti-glycation experiments, aAGE were prepared following the experimental conditions of thermal glycation at 60 °C.

During the glycation process, there is a clear decrease in cationic charges in AGEs, reasonably ascribable to the involvement of positively charged residues (arginine and lysine) in condensation with carbohydrates (Rondeau and Bourdon, 2011). Hence, the aAGE formation can also be verified through N-PAGE, since the loss of positive charges is the main factor influencing the electrophoretic migration toward the anode. As depicted in Fig. 1B, a faster migration of aAGE was observed compared to that of non-glycated albumin. Specifically, aAGE migration gradually increased from 24h-formed aAGE to 72h-formed ones. This result agrees perfectly with the increase in the fluorescence intensity emitted by aAGE obtained at the various time points and suggests that aAGE are extensively produced at 72h.

In order to investigate the POE anti-glycation role, HSA was incubated with GLC for 72h in the presence of POE (0.2 mg of dry

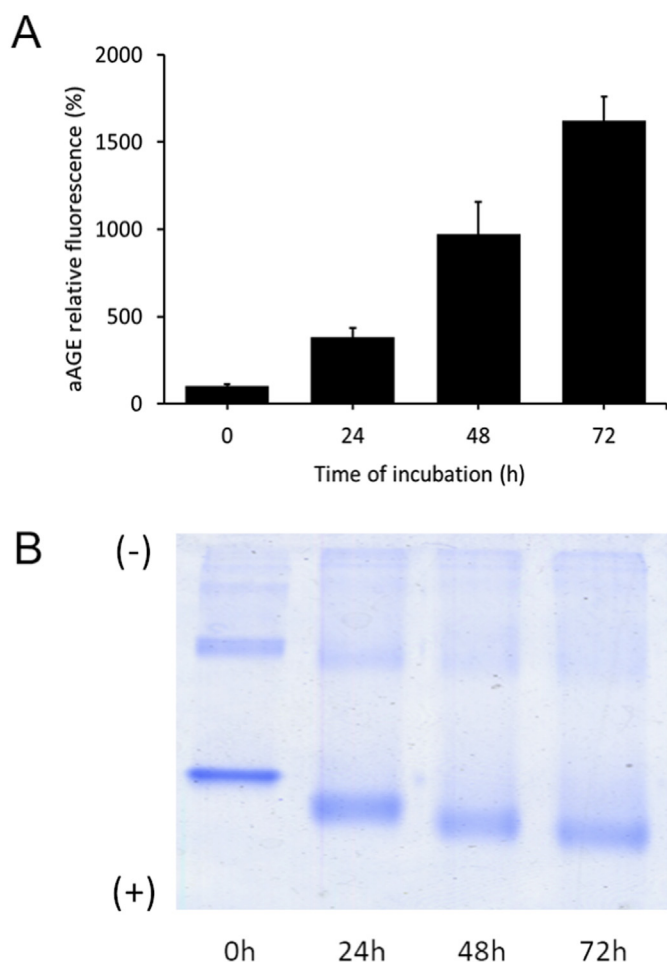


**Fig. 1. aAGE preparation with HSA-GLC reaction system model.** (A) Relative fluorescence intensity ( $\lambda_{\text{ex}}/\lambda_{\text{em}}$  335/385 nm) of aAGE obtained at different time points. Data are reported as percentage values compared to non-glycated albumin (aAGE at 0h). Data are the mean of at least three independent experiments. Error bars represent standard errors. (B) Representative image of N-PAGE on the electrophoretic migration of aAGE obtained at different times.

extract), corresponding to 0.2 mM of polyphenols (gallic acid equivalents) and to an antioxidant activity of ASC equivalents (50  $\mu\text{M}$ ).

Specifically, POE clearly reduced the aAGE production, as evidenced by the 60% decrease in the aAGE fluorescence intensity (Fig. 2A). Its anti-glycation role was further confirmed by the net reduction of the electrophoretic migration of aAGE + POE compared to aAGE in the N-PAGE (Fig. 2B). POE proved not to influence fluorescence determination and alone was unable to induce HSA glycation (data not shown). As an inhibition control, HSA glycation was performed in the presence of AG, causing an almost 90% reduction in aAGE fluorescence intensity (Fig. 2A) and a notably reduced electrophoretic migration of aAGE + AG compared to that of aAGE (Fig. 2B). The migration performance of aAGE + AG was extremely similar to that of non-glycated albumin, supporting the strong AG anti-glycation role. Furthermore, the similarity of the aAGE + POE and aAGE + AG migration profile suggests a noticeable role of POE in inhibiting the aAGE formation.

In order to exclude that the observed POE anti-glycation ability was due to its known antioxidant activity, the aAGE formation was examined in the presence of ASC equivalents (50  $\mu\text{M}$ ) of POE. The aAGE + ASC fluorescence intensity was only 15% lower than that of aAGE, while it was approximately 50% higher than that of aAGE + POE (Fig. 2A). Based on these findings, POE anti-glycation role cannot be attributed exclusively to its antioxidant activity. The higher

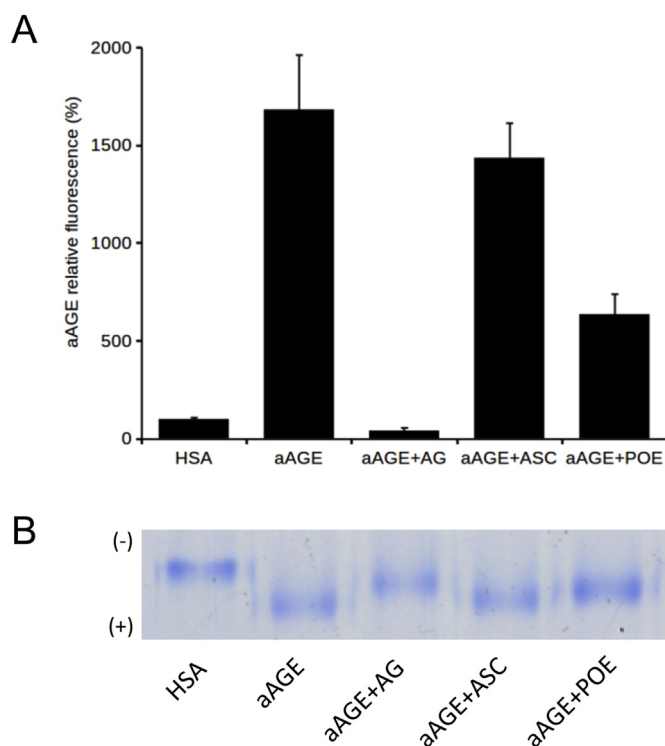


**Fig. 2. anti-glycation assay.** (A) Relative aAGE fluorescence intensity ( $\lambda_{\text{ex}}/\lambda_{\text{em}}$  335/385 nm) following 72h HSA-GLC glycation with POE. Non-glycated HSA was used as control. AG and ASC equivalents of POE were used as additional inhibition controls. Data are reported as percentage ratio compared to HSA. Data are the mean of at least three independent experiments. Error bars represent standard errors. (B) Representative image of N-PAGE on the anti-glycation assay.

electrophoretic migration capacity of aAGE + ASC compared to aAGE + POE confirms that the POE anti-glycation effect occurs apart from its antioxidant activity (Fig. 2B).

However, the POE antioxidant activity is essential for efficient action against albumin glycation. Since the formation of AGEs is favored by oxidative reactions (Nowotny et al., 2015), antioxidants play a key role in glycation inhibition mechanisms (Bonnefont-Rousselot, 2001). Moreover, under diabetic conditions, AGEs themselves are a critical source of ROS and oxidative stress. The possibility of acting both against the aAGE formation and the ROS-mediated oxidative stress (Vasarri et al., 2020) could make POE effective in preventing the onset of diabetes complications.

In conclusion, our preliminary results shed light on the anti-glycation role of POE, known to be free of toxicity for cells, with a similar efficacy as AG. In diabetic patients, AGEs cause both oxidative stress and inflammatory reactions implicated in the development of various diabetes-related complications. Therefore, the recognized traditional antidiabetic role of POE, together with its anti-glycation, antioxidant and anti-inflammatory properties could positively impact on the prevention and/or treatment of diabetes and related pathophysiological conditions. These promising *in vitro* results encourage us for further investigations aimed at exploring the mechanism of action through which POE acts against albumin and other several proteins glycation.

#### Author contributions

D.D.I. conceived and designed the experiments; M.V. performed the experiments; E.B and M.R analyzed the data; M.V and D.D.I. wrote the paper; D.D.I. provided materials for the experiments. All authors have read and approved the manuscript.

## Funding

This work was fully supported by grant of University of Florence (Fondi di Ateneo, 2018 to D.D.I).

## Declaration of competing interest

The authors declare no conflict of interest.

## References

- Barletta, E., Ramazzotti, M., Fratianni, F., Pessani, D., Degl'Innocenti, D., 2015. Hydrophilic extract from *Posidonia oceanica* inhibits activity and expression of gelatinases and prevents HT1080 human fibrosarcoma cell line invasion. *Cell Adhes. Migrat.* 9, 422–431. <https://doi.org/10.1080/19336918.2015.1008330>.
- Bonnefont-Rousselot, D., 2001. Antioxidant and anti-AGE therapeutics: evaluation and perspectives. *J. Soc. Biol.* 195, 391–398. <https://doi.org/10.1051/jbio/2001195040391>.
- Gokce, G., Haznedaroglu, M.Z., 2008. Evaluation of antidiabetic, antioxidant and vasoprotective effects of *Posidonia oceanica* extract. *J. Ethnopharmacol.* 115, 122–130. <https://doi.org/10.1016/j.jep.2007.09.016>.
- Lauritano, C., Ianora, A., 2016. Marine organisms with anti-diabetes properties. *Mar. Drugs* 14, 220. <https://doi.org/10.3390/md14120220>.
- Leri, M., Ramazzotti, M., Vasarri, M., Peri, S., Barletta, E., Pretti, C., Degl'Innocenti, D., 2018. Bioactive compounds from *Posidonia oceanica* (L.) delile impair malignant cell migration through autophagy modulation. *Mar. Drugs* 16, 137. <https://doi.org/10.3390/md16040137>.
- Nowotny, K., Jung, T., Höhn, A., Weber, D., Grune, T., 2015. Advanced glycation end products and oxidative stress in type 2 diabetes mellitus. *Biomolecules* 5, 194–222. <https://doi.org/10.3390/biom5010194>.
- Rasheed, S., Sánchez, S.S., Yousuf, S., Honoré, S.M., Choudhary, M.I., 2018. Drug repurposing: in-vitro anti-glycation properties of 18 common drugs. *PLoS One* 13, e0190509. <https://doi.org/10.1371/journal.pone.0190509>.
- Rondeau, P., Bourdon, E., 2011. The glycation of albumin: structural and functional impacts. *Biochimie* 93, 645–658. <https://doi.org/10.1016/j.biochi.2010.12.003>.
- Séro, L., Sanguinet, L., Blanchard, P., Dang, B.T., Morel, S., Richomme, P., Séraphin, D., Derbré, S., 2013. Tuning a 96-well microtiter plate fluorescence-based assay to identify AGE inhibitors in crude plant extracts. *Molecules* 18, 14320–14339. <https://doi.org/10.3390/molecules181114320>.
- Singh, V.P., Bali, A., Singh, N., Jaggi, A.S., 2014. Advanced glycation end products and diabetic complications. *Korean J. Physiol. Pharmacol.* 18, 1–14. <https://doi.org/10.4196/kjpp.2014.18.1.1>.
- Vasarri, M., Leri, M., Barletta, E., Ramazzotti, M., Marzocchini, R., Degl'Innocenti, D., 2020. Anti-inflammatory properties of the marine plant *Posidonia oceanica* (L.) Delile. 247, 112252. <https://doi.org/10.1016/j.jep.2019.112252>.



## 4. MATERIALS AND METHODS

### 4.1. Materials and reagents

3-(2-Pyridyl)-5,6-diphenyl-1,2,4-triazine-4,4''-disulfonic acid sodium salt (Ferrozine<sup>®</sup>),  $\alpha,\alpha$ -diphenyl- $\beta$ -picrylhydrazyl (DPPH), Folin-Ciocalteu's phenol reagent, gallic acid, ascorbic acid, D-glucose, aminoguanidine, gelatin, 1-(4,5-dimethylthiazol-2-yl)-3,5-diphenyl formazan (MTT), 2',7'-dichlorofluorescein diacetate (DCFH-DA), lipopolysaccharide (LPS), Griess reagent, Bovine Serum Albumin (BSA) and Human Serum Albumin (HSA), Dulbecco's Modified Eagle's Medium (DMEM), Ham's F-12 nutrient mixture, Fetal Bovine Serum (FBS), L-glutamine, penicillin and streptomycin and all other chemicals and solvents were all purchased from Sigma Aldrich-Merck (St. Louis, MO, USA). Electrophoresis reagents and Coomassie Brilliant Blue G were purchased from Bio-Rad (Hercules, CA, USA). Disposable plastics were from Sarstedt (Nümbrecht, Germany). All the primary antibodies used in Western blotting and immunofluorescence experiments are listed in Table 4.

Primary antibody	Target	Dilution	Host	Source
SQTSM1/p62	SQTSM1/p62 protein	1:1000	Rabbit	Abcam
LC3A/B	Microtubule-associated protein light chain 3 (A/B)	1:1000	Rabbit	Cell Signaling
P-AKT1	P-AKT1 serine/threonine kinase (Ser473)	1:5000	Rabbit	Abcam
AKT1/2	AKT1/2 serine/threonine kinase	1:5000	Rabbit	Abcam
p44/42 MAPK(ERK1/2)	Mitogen-activated protein kinases p44/42 (ERK 1/2)	1:2000	Mouse	Cell Signaling
P-p44/42 MAPK(ERK 1/2)	Mitogen-activated protein kinases p44/42 (ERK 1/2) (Thr202/Thr204)	1:1000	Rabbit	Cell Signaling
Beclin-1	Beclin-1 protein	1:1000	Rabbit	Cell Signaling
S6	Ribosomal protein S6	1:1000	Rabbit	Cell Signaling
P-S6	Ribosomal protein S6 (Ser235/236)	1:2000	Rabbit	Cell Signaling
IGF-IR	total IGF-I receptor $\beta$ protein	1:100	Mouse	Cell Signaling
$\alpha$ -Tubulin	$\alpha$ -Tubulin protein	1:1000	Mouse	Cell Signaling
$\beta$ -Actin	$\beta$ -Actin protein	1:1000	Mouse	Santa Cruz
iNOS	iNOS protein	1:1000	Rabbit	Cell Signaling
COX-2	total COX-2 protein	1:1000	Rabbit	Cell Signaling
p-NF- $\kappa$ B p65	NF- $\kappa$ B p65 phosphorylated at Ser536	1:1000	Rabbit	Cell Signaling
NF- $\kappa$ B p65	total NF- $\kappa$ B p65/RelA protein	1:1000	Rabbit	Cell Signaling
I $\kappa$ B $\alpha$	total I $\kappa$ B $\alpha$ protein	1:1000	Mouse	Cell Signaling

**Table 4.** Primary antibodies used in Western blotting experiments

Secondary antibodies as goat anti-rabbit IgG HRP-linked, goat anti-mouse IgG HRP-linked, Alexa 488-conjugated antirabbit IgG and Alexa 488-conjugated anti-mouse IgG were purchased from Molecular Probes<sup>™</sup> (Invitrogen, USA).

## 4.2. Preparation of *P. oceanica* leaves extract

The leaves of *P. oceanica* (L.) Delile were collected in the protected area of Meloria by authorized personnel of the CIBM (Livorno, Tuscany, Italy) at a depth of about 15 m at the following geographical coordinates: 43° 35' 13" N and 010° 10' 21" E (Figure 26).



**Figure 26.** *P. oceanica* leaves collected by CIBM personnel.

After the leaves were removed from the epiphytes and carefully washed with bi-distilled water, the extraction of hydrophilic compounds was performed according to the method developed in the laboratory of Prof. Degl'Innocenti and described by Barletta et al. (2015) [80]. Hence, 1 gram of *P. oceanica* dried leaves were minced and suspended overnight in 10 mL of EtOH/H<sub>2</sub>O (70:30 v/v) at 37 °C under stirring and subsequently at 65 °C for 3h. The hydroalcoholic extract was then separated from the debris by centrifugation at 2000xg and the recovered supernatant was mixed with *n*-hexane in a 1:1 ratio (Figure 27).

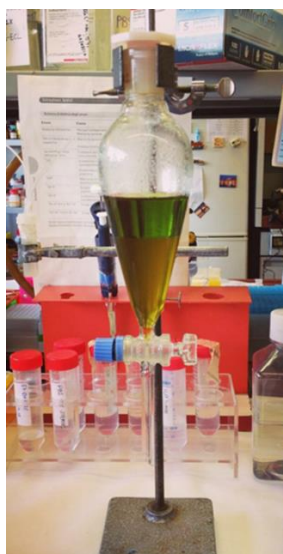


**Figure 27.** Mixing of hydroalcoholic extract of *P. oceanica* with *n*-hexane for the removal of hydrophobic compounds by means of the separating funnel.

After repeated shaking in the separating funnel, the hydrophobic phase of the extract was removed, while the hydrophilic phase of the extract was recovered and dispensed in 1 mL aliquots, then dried by a Univapo<sup>TM</sup> vacuum concentrator. Each aliquot of *P. oceanica* leaves extract was then dissolved in 0.5 mL of 70% ethanol or DMSO before use, and hereinafter referred to as POE.

### **4.3. Determination of total polyphenols and carbohydrates content in POE**

The total content of polyphenols (TP) and carbohydrate (TC) in POE was determined using the Folin-Ciocalteu's and phenol-sulfuric acid colorimetric methods, respectively [133,134]. Gallic acid (0.5 mg/mL) and D-glucose (1 mg/mL) were used as a reference in the range of 0-10 µg and 0-50 µg, respectively, to determine TP and TC values. Then, TP and TC were expressed as mg of gallic acid and D-glucose equivalents, respectively, per mL of extract after resuspension. The specific values of TP and TC referred to each hydroalcoholic extraction carried out are reported in Table 3.

### **4.4. Evaluation of antioxidant and radical scavenging activities of POE**

The antioxidant and radical scavenging activities of POE were investigated using the FRAP (ferric-reducing/antioxidant power) assay and DPPH ( $\alpha,\alpha$ -Diphenyl- $\beta$ -picrylhydrazyl) assay, respectively [135,136]. Ascorbic acid (0.1 mg/mL) was used as a reference in the range of 0-4 µg to evaluate both activities. The antioxidant and radical scavenging activities of POE were expressed as mg of ascorbic acid equivalents per mL of extract after resuspension. Specific values referred to each hydroalcoholic extraction carried out are reported in Table 3.

### **4.5. Cell lines and culture conditions**

Human fibrosarcoma HT1080 cells (ATCC<sup>®</sup> CCL-121<sup>TM</sup>), human neuroblastoma SH-SY5Y cells (ATCC<sup>®</sup> CRL-2266<sup>TM</sup>) and murine RAW264.7 macrophages (ATCC<sup>®</sup> TIB-71<sup>TM</sup>) were used to perform the cell-based *in vitro* experiments described in the following paragraphs. All cell lines were grown in complete culture media, i.e. DMEM for HT1080 cells and RAW264.7 macrophages, while a 1:1 mixture of Ham's F12 and DMEM for

SH-SY5Y cells, each supplemented with 2 mM L-glutamine, 100 µg/mL streptomycin, 100 U/mL penicillin and 10% FBS, at 37 °C in a 5% CO<sub>2</sub>-humidified atmosphere.

Once a confluence of 70-80% was reached, both HT1080 and SH-SY5Y cells were detached by trypsinization (0.025% trypsin - 0.5 mM EDTA) and propagated after suitable dilution. Instead, RAW264.7 macrophages were harvested by scraping with cell lifter and re-seeded at appropriate cell density.

The specific cell culture conditions are described in detail in the "Materials and methods" section of the articles attached to the thesis.

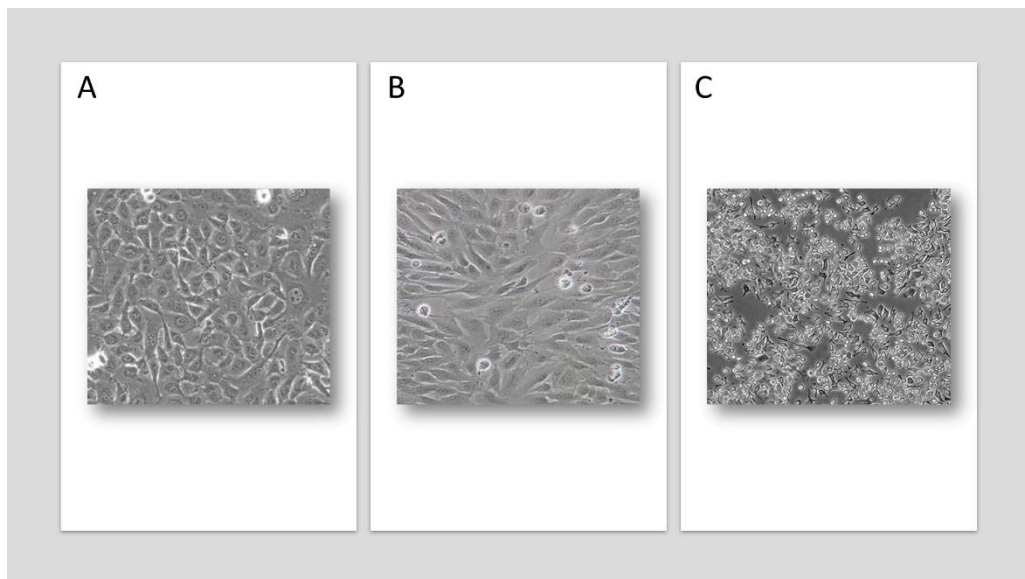


**Figure 28.** The different cell lines used. (A) Human fibrosarcoma HT1080 cells; (B) human neuroblastoma SH-SY5Y cells; (C) murine macrophages RAW264.7. The images were acquired by 10X magnification optical microscope.

#### 4.6. Cell viability assay

The viability of HT1080, SH-SY5Y cells and RAW264.7 macrophages was determined using the MTT activity colorimetric assay. Cells were seeded in 96- or 24-well plates at different densities, depending on cell line, and incubated in complete medium overnight. Then, cells were treated with different POE dilutions ranging from 1:100 to 1:1000 under different experimental conditions, described in detail in the specific section “Materials and Methods” of the articles attached to the thesis. Untreated cells and cells treated with vehicle solutions were used as controls. After appropriate cell treatment, culture media were removed and 100 µL/well of MTT solution (0.5 mg/mL) was added and incubated in the dark at 37 °C for 1h. After removing supernatant, the insoluble formazan product was dissolved in 80 µL/well of lysis buffer [20% (w/v) sodium dodecyl sulfate (SDS) in

50% (v/v) N, N-dimethylformamide] or in 200  $\mu$ L dimethyl sulfoxide (DMSO). The absorbance values were measured using the iMARK microplate reader (Bio-Rad, USA) at 595 nm. Data were expressed as a percentage of untreated control cells.

#### 4.7. Wound Healing Assay

Cell migration was analysed using the scratch wound healing assay. This analysis was performed on both HT1080 and SHSY5Y cells. Cells were seeded at different densities depending on the cell line and incubated in a complete medium until confluence. Subsequently, a vertical wound was performed through the cell monolayers using a sterile 200  $\mu$ L plastic tip (Figure 29). Each well was washed with PBS to remove cell debris. Then, cells were treated with POE at different dilutions from 1:500 to 1:1000 and under different experimental conditions, described in detail in the "Materials and methods" section of the specific documents attached to the thesis. Untreated cells were used as a control. The cell-free area was observed under a phase contrast microscope and images were acquired at time points between 0h and 24h using a Nikon TS-100 microscope equipped with a digital acquisition system (Nikon Digital Sight DS Fi -1, Nikon, Minato-ku, Tokyo).

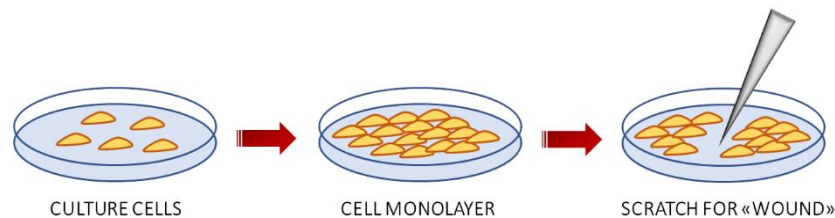


**Figure 29.** *In vitro* wound healing assay.

#### 4.8. Gelatin Zymography

Gelatin zymography was performed to detect matrix metalloproteinase-2/9 (MMP-2/MMP-9) activity in conditioned media. HT1080 cells suitably seeded in 24-well plates were incubated in complete medium overnight. Subsequently, the cells were treated with two different POE dilutions (1:500 and 1:1000) in thermally inactivated FBS medium (HI-FBS medium) for 16h. Untreated cells were used as a control. Then, the culture media were collected and centrifuged at 9,700 $\times$ g for 1 min at 4  $^{\circ}$ C to remove cell debris. Then, 2.5  $\mu$ L aliquots of conditioned medium from control cells or POE-treated cells were electrophoresed in 8% polyacrylamide gel containing 1 mg/mL gelatin under non-reducing conditions. After electrophoretic separation, gels were washed twice in 2.5%

Triton X-100 for 1h to remove SDS and then incubated at 37 °C for 24h in reaction buffer (50 mM Tris-HCl pH 7.4, 0.2 M NaCl, 5 mM CaCl<sub>2</sub>, 1 M ZnCl). Gels were stained with 0.05% Coomassie Brilliant G-250 dissolved in 1.6% phosphoric acid, 8% ammonium sulfate and 20% methanol and decoloured in 1% acetic acid. Gelatinase activities appeared as bands of light against a blue background. The zymography images were acquired with a digital scanner.

#### **4.9. Analysis of Autophagic Vacuoles**

Autophagy activation was investigated in HT1080 cells by fluorescence microscopy using the Cyto-ID<sup>®</sup> Autophagy Detection Kit (Enzo Life Sciences, Shanghai, China). Indeed, Cyto-ID<sup>®</sup> dye selectively labels autophagic vacuoles in living cells. Cells were adequately seeded in a 24-well plate for 24h containing sterilized coverslips, then treated at different times with different POE dilutions (1:500 and 1:1000). Next, cells were washed twice with PBS and then with 100 µL of an assay buffer supplied with the detection kit. Cells treated with rapamycin (0.5 M) and chloroquine (10 µM) were used as positive and negative controls, respectively. Then, cells were incubated for 30 min at 37 °C with 100 µL of Double Detection Reagent protected from light. Finally, cells were fixed with 2% paraformaldehyde for 20 min and washed three times with the assay buffer. Coverslips were placed on microscope slides using Fluoromount<sup>™</sup> aqueous mounting medium (Sigma Aldrich-Merck). The fluorescent signals were visualized using a Leica TCS SP5 confocal scanning microscope (Leica, Mannheim, Germany) equipped with a HeNe/Ar laser source to allow for fluorescence measurements at 488 nm. Cell observations were performed using a Leica Plan 7 Apo X63 oil immersion objective, suitable with optics for DIC acquisition. Cells from three independent experiments and three different fields (approximately 20 cells/field) per experiment were analysed. Fluorescence intensity was analysed with ImageJ software (Image version 1.51j8, National Institutes of Health Bethesda, Bethesda, MD, USA) and expressed as a percentage increase over untreated cells.

#### **4.10. SDS-PAGE and Western blot assay**

Western blot experiments were performed on total lysates of HT1080 cells and RAW264.7 macrophages suitably seeded and treated with POE under the different experimental conditions. After appropriate treatments, cells were washed with PBS and



lysed in 80  $\mu$ L of Laemmli buffer [62.5 mM Tris-HCl pH 6.8, 10% (w/v) SDS, 25% (w/v) glycerol] without bromophenol. Total cell lysates were collected and boiled at 95 °C for 5 min and then centrifuged at 12,000xg for 5 min at 4 °C. Total protein concentration of lysates was measured by the BCA Protein Assay Kit. An equal amount of protein from each sample, added with  $\beta$ -mercaptoethanol and bromophenol blue, was separated on 12% polyacrylamide SDS gel by electrophoresis and transferred to PVDF membranes (0.45  $\mu$ m). Subsequently, membranes were saturated using a blocking solution [5% (w/v) BSA in 0.1% (v/v) PBS-Tween<sup>®</sup>-20] and then incubated overnight at 4 °C with primary antibodies suitably diluted in blocking buffer. After washing three times in a 0.1% (v/v) PBS-Tween<sup>®</sup>-20 solution, membranes were incubated for 1h at room temperature with specific secondary antibodies in blocking buffer. Finally, membranes were washed three times in 0.5% (v/v) PBS-Tween<sup>®</sup>-20 and the protein bands were detected using the Clarity Western ECL solution and chemiluminescent signals were acquired using the imaging system Amersham<sup>™</sup> 600 Imager (GE Healthcare Life Science, Pittsburgh, PA, USA). Densitometric analysis was conducted using Quantity One software (version 4.6.6, Bio-Rad).

#### **4.11. Immunofluorescence assay**

Immunofluorescence experiments were performed on both HT1080 cells and RAW264.7 macrophages. Cells were seeded in 24-well plates containing sterilized slides for 24h and then treated appropriately. RAW264.7 cells were also incubated with Hoechst 33342 for 30 min at room temperature to label the nuclei. Both cell lines were then fixed with 2% paraformaldehyde for 5 min and permeabilized with a cold 1:1 acetone/ethanol solution for 4 min at room temperature. Then, cells were washed in PBS and blocked in a BSA (0.5%) and gelatin (2%) solution for 30 min at 37 °C. After 1h incubation at room temperature with specific primary antibodies, cells were washed with PBS for 30 min under stirring conditions. Subsequently, cells were incubated with the appropriate Alexa-488 conjugated secondary antibodies (diluted 1: 200 in PBS) for 1h at 37 °C in the dark. Non-specific antibodies were removed by washing twice in PBS and once in distilled water. Fluorescent signals were visualized using both a Leica TCS SP5 scanning confocal microscope (Leica, Mannheim, Germany) equipped with a HeNe/Ar laser source for fluorescence measurements and a Leica TCS SP8 AOBS scanning confocal microscope (Leica, Mannheim, Germany). In the first case the observations were performed using a

Leica Plan 7 Apo X63 oil immersion objective, suited with optics for DIC acquisition, while in the second case using a Leica HC PL Apo CS2  $\times$  63 oil immersion objective.

## **4.12. Detection of intracellular ROS and nitric oxide nitric oxide production**

### **4.12.1. Measurement of intracellular ROS levels**

High concentrations of reactive oxygen species (ROS) promote oxidative stress causing associated cell damage to the histolesivity of inflammation. In addition, activated macrophages release a considerable amount of nitric oxide (NO) as pro-inflammatory mediator largely produced by inducible nitric oxide synthase (iNOS). In the study of the antioxidant and anti-inflammatory role of *P. oceanica* extract, intracellular ROS levels and NO production were evaluated in RAW264.7 murine macrophages exposed to a pro-inflammatory stimulus and treated with POE. Therefore, to determine the intracellular ROS level, RAW264.7 cells were seeded in a 24-well plate ( $5 \times 10^5$  cells/well) for 24h and subsequently exposed to the pro-inflammatory stimulus of LPS (1 mg/mL) and treated with POE (1:500). Untreated cells or cells treated only with POE or cells exposed only to LPS were used as controls. After appropriate cell treatments, the ROS specific DCFH-DA fluorescence probe (10  $\mu$ M) was added to each well and left in the dark for 1.5h at 37  $^{\circ}$ C. Then, culture medium was removed and cells were lysed with 200  $\mu$ L/well of RIPA lysis buffer (50 mM Tris-HCl, 150 mM NaCl, 100 mM NaF, 2 mM EGTA, 1% Triton<sup>TM</sup> X-100; pH 7.5) and 100  $\mu$ L of each cell lysate was transferred to a 96-well black plate. DCF fluorescence intensity was recorded at excitation and emission wavelengths of 485/538 nm, respectively, using a fluorescence microplate reader (Fluoroskan Ascent<sup>TM</sup> FL Microplate Fluorometer, Thermo Fisher Scientific, USA). Data were normalized with respect to total cell proteins and expressed as a percentage with respect to untreated control cells.

### **4.12.2. Griess reaction assay**

Nitric oxide (NO) production was determined by measuring nitrite levels in culture media according to the Griess reaction. RAW264.7 murine macrophages were seeded at a density of  $4 \times 10^4$  cells/well in a 96-well plate for 24h. Briefly, 50  $\mu$ L of cell culture medium from each treatment was collected and mixed with equal volume of Griess reagent and then incubated at room temperature for 15 min. The absorbance of 540 nm was recorded with the iMARK microplate reader. The concentration of nitrite in the

sample was determined using sodium nitrite as a reference in the range 0-50  $\mu\text{M}$ . Data were normalized for cell viability and expressed as a percentage of untreated control cells.

### **4.13. Advanced glycation end products of albumin (aAGEs)**

#### **4.13.1. The *in vitro* formation of aAGEs**

In order to investigate the potential role of *P. oceanica* leaves extract as an anti-glycation agent, thermal albumin glycation was used as a method of choice for the *in vitro* formation of advanced glycation end products (AGEs). In this regard, the albumin-AGEs were obtained *in vitro* by incubating HSA (1 mg/mL) with D-glucose (GLC; 500 mM) in phosphate buffered saline (PBS: pH 7.4, 1.37 M NaCl, 27 mM KCl, 100 mM Na<sub>2</sub>HPO<sub>4</sub>, 18 mM KH<sub>2</sub>PO<sub>4</sub>) at 60 °C for 24h, 48h and 72h, under stirring (300 rpm) using Thermo-Shaker TS-100 (Biosan, Riga, LV), and hereinafter referred to as aAGEs. A GLC-free HSA solution was prepared as a control and incubated under the same conditions.

#### **4.13.2. Detection of aAGEs by means of fluorescent measurements and polyacrylamide gel electrophoresis under native conditions (N-PAGE)**

The formation of aAGEs was verified both by measuring the typical AGE fluorescence [137] at an excitation and emission wavelength of 335 and 385 nm, respectively, and by resolving aAGEs samples by polyacrylamide gel electrophoresis (12%) under native conditions (N-PAGE). In fact, the aAGE samples (1.5  $\mu\text{g}$ ), diluted 1:1 with sample buffer [62.5 mM Tris-HCl pH 6.8, 25% (w/v) glycerol and 0.5% bromophenol blue] without reducing agents, were separated on N-PAGE (Tris-glycine buffer: Tris 25 mM and glycine 192 mM, pH 8.3) for 100 min at 200 V. The protein bands were stained with Coomassie Brilliant Blue G-250 colloidal dye, following the manufacturer's instructions.

#### **4.13.3. Inhibition of aAGEs formation**

The anti-glycation effect of POE was evaluated by incubating HSA (1 mg/mL) with D-glucose (GLC; 500 mM) in the presence of POE (0.2 mg dry extract) for 72h. Aminoguanidine (AG; 10 mM), a known synthetic anti-glycation agent was added to the HSA and GLC solution as a positive control for the inhibition of aAGE formation.

The contribution of POE antioxidant activity on the inhibition of glycation process was also evaluated by adding the equivalents of ascorbic acid (ASC) to the HSA and GLC solution. DMSO at concentrations similar to those derived from POE was used as a negative control for the inhibition of aAGE formation.

The percentage of intrinsic fluorescence intensity of aAGE was calculated as follows (1):

$$\text{aAGE (\%)} = (\text{HSA} + \text{GLC} + \text{inhibitor}^1) - \frac{\text{HSA} + \text{inhibitor}^1}{\text{HSA} + \text{GLC}} - (\text{HSA}) \times 100$$

<sup>1</sup>: POE, AG or ASC

## 5. CONCLUSIONS AND FUTURE PERSPECTIVES

For a long time *P. oceanica* has attracted the attention of researchers for its importance in the ecological field, however the research group of Prof. Degl'Innocenti was one of the first to look at this plant from another perspective. The study of Barletta et al. (2015) shed light on the ability of *P. oceanica* crude extract (POE), rather than its individual constituents, to inhibit human fibrosarcoma HT1080 cell migration by reducing the expression and activity of MMP-2/9 without affecting cell viability. For the first time, the *P. oceanica* phytocomplex has been proposed to the entire scientific community as a reservoir of potentially exploitable molecules in the science of human health.

Over the years, marine environment has become the focus of drug discovery research on natural products due to its relatively unexplored biodiversity compared to terrestrial environments. The uncommon and unique structural and chemical characteristics of marine-derived compounds can be exploited for the molecular modelling and chemical synthesis of new drugs with greater efficacy and specificity for various therapies. Therefore, the possibility of working with a mixture of effective and cell-safe compounds of marine origin caught my attention and prompted me to explore more deeply the molecular mechanisms and targeted signalling pathways underlying their activity, thus opening up new research perspectives on the potential benefits of *P. oceanica* for human health.

One of the goal of my research was to explore the mechanism of action by which *P. oceanica* phytocomplex controlled the migratory behaviour of HT1080 cancer cells. Evaluating the contribution of autophagy on the POE-induced cell migration inhibition, it was found that POE bioactivity was highly correlated with the increase of an autophagic transient that had no detectable effects on cell viability. This was further proved also on SH-SY5Y human neuroblastoma cells.

To date, many malignancies lack resolving therapies and the only ones available do not spare the patient serious side effects. Very often the mechanism of action of anticancer drugs is based on the differential cellular toxicity and the sensitivity of actively growing cancer cells compared to normal cells. Therefore, the development of novel cancer therapeutics is the main challenge to improve patient survival by overcoming the high toxicity linked to anticancer drugs. In this regard, the use of a mixture of non-toxic

compounds as alternative anticancer strategies could prove to be an exceptional approach both to have greater bioactive effectiveness, exploiting the synergistic action of several compounds, and to limit the adverse effects associated with toxicity of anticancer drugs. The proven inhibitory role of POE on cancer cell migration thus suggests that *P. oceanica* phytocomplex could be a source of potent and cell-safe molecules useful in the management of malignancies, but also of other chronic pathophysiological conditions in which gelatinolytic progression is the hallmark. However, further experimental *in vivo* investigations are needed to verify the efficacy of POE as an antimetastatic agent in animal models.

In the context of innovative strategies, the use of nano-delivery systems has already brought great benefits to cancer therapeutics, as it can increase drug efficacy and reduce systemic toxicity during cancer treatment compared to use of "free" drugs.

My research examined the antimigratory role of POE on SH-SY5Y neuroblastoma cells, once loaded into chitosan nanoparticles or Soluplus polymeric micelles. Both nanoformulations proved to be good candidates for increasing the aqueous solubility of POE, and nanomicelles in particular for the bio-enhancement of POE activity. Overall, this study shows that the development of nanomicelles suitable for the administration of natural compounds offers an advanced approach to improve the bioavailability and/or optimize the solubility and stability of single natural compounds or phytocomplexes, and to enhance the traditional application of *P. oceanica* in cancer and other chronic disease. In light of a tradition handed down in Anatolia on the antidiabetic role of *P. oceanica*, confirmed by an *in vivo* study in animal models, my research also investigated POE as an antioxidant, anti-inflammatory and inhibitor of protein glycation. Oxidative stress and inflammation are characterizing factors of diabetic pathophysiology, just as protein glycation is a crucial event responsible for the onset of diabetes-related complications under chronic hyperglycemia.

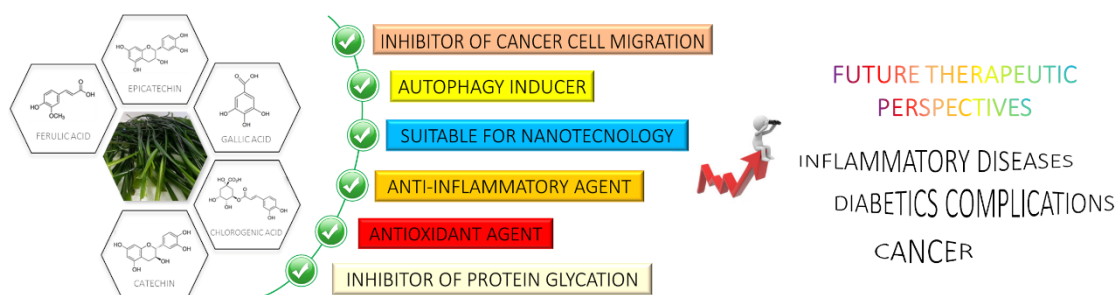
For the first time, my research established the ability of POE to inhibit inflammation in LPS-induced RAW264.7 cells, related to its antioxidant power. In this regard, *in vivo* studies on animal models are already underway to strengthen my research on the anti-inflammatory role of POE. The importance of these findings reflects the goal of one of the modern challenges for human well-being, i.e. the development of new natural health-promoting strategies based on alternative mechanisms of action against inflammation to those of non-steroidal anti-inflammatory drugs (NSAIDs), in order to overcome the toxicity problems associated with the prolonged use of these conventional drugs.



My research also showed that POE was capable of inhibiting the formation of advanced glycation end products (AGEs) *in vitro*. However, this first investigation on the anti-glycation role of POE needs to be deepened to understand the molecular mechanism or interactions underlying the POE-induced inhibition of the protein glycation process, and above all to establish this role also in *in vivo* animal models.

Overall, my research greatly contributes to providing a more complete picture of POE mechanisms of action potentially exploitable in the management of diabetes and associated complications, and other inflammatory chronic diseases, including cancer. Inflammation is a relevant factor in the tumor microenvironment and is involved in cancer progression; the anti-inflammatory role of POE, together with its proven ability to impair cancer cell migration, could also prove to be an effective and innovative weapon against cancer progression.

In conclusion, the research carried out in the three years of the PhD has certainly contributed to spreading in the scientific community a new awareness on the importance of *P. oceanica* as a reservoir of effective and cell-safe molecules potentially useful in the science of human health, opening up new perspectives of experimental investigation.



***Posidonia oceanica* in a new eco-sustainable perspective linking environment and human health: a final note**

*“P. oceanica tells a story of 120 million years of authoritarian presence in the entire marine ecosystem, but also of close relationships with humans.*

*Unfortunately, persistent pollution and incessant climate change, as well as anthropogenic pressures, cause the progressive regression of the P. oceanica meadows, threatening the well-being of the entire marine ecosystem.*

*However, the ongoing global change has made it known that current economic development and over-exploitation of resources do not necessarily imply an increase in human well-being and that the value of natural capital cannot be further neglected in environmental management decisions.*

*Awareness of the complex interactions between humans and the marine environment is an essential challenge to fully understand that humans can enjoy important benefits from environmental protection and to spread a culture of prevention to protect human and environmental wellness.*

*In this regard, the novelties brought by my scientific research on the potential benefits of P. oceanica for human health should be the key argument to encourage even further studies on the ecological macro-roles of P. oceanica from new eco-innovative perspectives.*

*Finding the right balance between protecting P. oceanica in the seas and exploiting it for the human well-being undoubtedly represents a global challenge”.*



## REFERENCES

1. Papenbrock J. Highlights in Seagrasses' Phylogeny, Physiology, and Metabolism: What Makes Them Special? *ISRN Bot.* 2012;2012:1-15. doi: 10.5402/2012/103892.
2. Duarte CM. Seagrass depth limits. *Aquat Bot.* 1991;40:363-377. [https://doi.org/10.1016/0304-3770\(91\)90081-F](https://doi.org/10.1016/0304-3770(91)90081-F).
3. Ogden J. Seagrasses: Biology, Ecology and Conservation. *Marine Ecology.* 2006;27:431-432. <https://doi.org/10.1111/j.1439-0485.2006.00138.x>
4. Hartog C, Kuo J. Taxonomy and Biogeography in Seagrasses. In: Larkum AW, Orth RJ, Duarte C (eds.) *Seagrasses: Biology, Ecology and Conservation*. Springer, Dordrecht, The Netherlands. [https://doi.org/10.1007/978-1-4020-2983-7\\_1](https://doi.org/10.1007/978-1-4020-2983-7_1).
5. Procaccini G, Buia MC, Gambi M, Perez M, Pergent G, Pergent-Martini C, Romer J. The Seagrasses of Western Mediterranean. In: Green EP, Short FT (eds.) *World Atlas of Seagrasses*. University of California Press, Berkeley, CA, USA. 2003;48-58.
6. Buia MC, Gambi MC, Dappiano M. I sistemi a fanerogame marine. Manuale di metodologie di campionamento e studio del benthos marino mediterraneo. *Biol Mar Mediterr.* 2003;10:145-198.
7. Gobert S, Cambridge MT, Velimirov B, Pergent G, Lepoint G, Bouquegneau JM, Dauby P, Pergent-Martini C, Walker DI. Biology of Posidonia. In: Larkum AW, Orth RJ, Duarte C (eds.) *Seagrasses: Biology, Ecology and Conservation*. Springer, Dordrecht, The Netherlands. 2006;387-408.
8. Vacchi M, De Falco G, Simeone S, Montefalcone M, Morri C, Ferrari M, Bianchi CN. Biogeomorphology of the mediterranean posidonia oceanica seagrass meadows. *Earth Surf Process.* 2017;42:42-54. DOI: 10.1002/esp.3932.
9. Boudouresque CF, Bernard G, Bonhomme P, Charbonnel E, Diviacco G, Meinesz A, Pergent G, Pergent-Martini C, Ruitton S, Tunesi L. Protection and conservation of Posidonia oceanica meadows. *RAMOGE and RAC/SPA publisher*, Tunis. 2012;1-202.
10. Bonhomme D, Boudouresque CF, Astruch P, Bonhomme J, Bonhomme P, Goujard A, Thibaut T. Typology of the reef formations of the Mediterranean seagrass Posidonia oceanica, and the discovery of extensive reefs in the Gulf of Hyères (Provence, Mediterranean). *Sci Rep Port-Cros Natl Park.* 2015;29:41-73.
11. Borum J, Duarte CM, Krause-Jensen D, Greve TM (eds.). European seagrasses: an introduction to monitoring and management (p. 2006). M&MS project. 2004.
12. Ceccherelli G, Piazzoli L, Cinelli F. Response of the non-indigenous Caulerpa racemosa (Forsskål) J. Agardh to the native seagrass Posidonia oceanica (L.) Delile: effect of density of shoots and orientation of edges of meadows. *J Exp Mar Biol Ecol.* 2000;243:227-240. DOI: 10.1016/S0022-0981(99)00122-7
13. Telesca L, Belluscio A, Criscoli A, Ardizzone G, Apostolaki ET, Fraschetti S, Gristina M, Knittweis L, Martin CS, Pergent G, Alagna A, Badalamenti F, Garofalo G, Gerakaris V, Pace ML, Pergent-Martini C, Salomidi M. Seagrass meadows (Posidonia oceanica) distribution and trajectories of change. *Sci Rep.* 2015;5:12505. DOI: 10.1038/srep12505
14. Platini F. La protection des habitats aux herbiers en Méditerranée. Report. PNUE, PAM, CAR/ASP. 2000.
15. Boudouresque CF. Marine biodiversity in the Mediterranean: state of species, populations and communities. *Sci Rep Port-Cros Natl Park.* 2004;20:97-146
16. Pergent G. The legal protection of Posidonie en France: an effective outil. Nécessité de son extension a d'autres pays méditerranéens in Les Espèces Marines a Protéger en Méditerranée: Rencontres scientifiques de la Cote Bleue (eds Boudouresque, CF, Avon, M. & Gravez, V.) 29-34 (GIS Posidonie, 1991).
17. Montefalcone M. Ecosystem health assessment using the Mediterranean seagrass posidonia oceanica: a review. *Ecol Indic.* 2009;9:595-604.

18. European Commission. Directive 2008/56/EC of the European Parliament and of the Council of 17 June 2008 establishing a framework for Community actions in the field of marine environmental policy (Marine Strategy Framework Directive). *O J Eur Communities*. 2008;164:19-40.
19. Luque A, Templado J (eds.) Praderas y bosques marinos de Andalucía: Las praderas de Posidonia. In: *Praderas y bosques marinos de Andalucía*. Andalucía. Junta de Andalucía. Consejería de Medio Ambiente. 2004.
20. De Falco G, Baroli M, Cucco A, Simeone S. Intrabasinal conditions promoting the development of a biogenic carbonate sedimentary facies associated with the seagrass *Posidonia oceanica*. *Cont Shelf Res*. 2008;28:797-812. <https://doi.org/10.1016/j.csr.2007.12.014>.
21. Di Carlo G, Badalamenti F, Jensen AC, Koch EW. Colonization process of vegetative fragments of *Posidonia oceanica* (L.) Delile on rubble mounds. *Mar Biol*. 2005;147:1261-1270.
22. Di Carlo G, Badalamenti F, Terlizzi A. Recruitment of *Posidonia oceanica* on rubble mounds: substratum effects on biomass partitioning and leaf morphology. *Aquat Bot*. 2007;87:97-103.
23. Marbà N, Duarte CM. Interannual changes in seagrass (*Posidonia oceanica*) growth and environmental change in the Spanish Mediterranean littoral zone. *Limnol Oceanogr*. 1997;42:800-810.
24. Boudouresque CF, Ponel P, Astruch P, Barcelo A, Blanfuné A, Geoffroy D, Thibaut T. The high heritage value of the Mediterranean sandy beaches, with a particular focus on the *Posidonia oceanica* “banquettes”: a review. *Sci Rep Port-Cros Natl Park*. 2017;31:23-70.
25. Buia MC, Mazzella L. Reproductive phenology of the Mediterranean seagrasses *Posidonia oceanica* (L.) Delile, *Cymodocea nodosa* (Ucria) Aschers., and *Zostera noltii* Hornem. *Aquat Bot*. 1991;40:343-362.
26. Orsini L, Acunto S, Piazzini L, Procaccini G. Sexual Reproduction and Recruitment in *Posidonia Oceanica* (L.) Delile, a Genetic Diversity Study. In: Faranda FM, Guglielmo L, Spezie G. (eds) *Mediterranean Ecosystems*. Springer, Milano. 2001. [https://doi.org/10.1007/978-88-470-2105-1\\_50](https://doi.org/10.1007/978-88-470-2105-1_50).
27. Ruiz JM, Bernardeau J, García Muñoz R, Ramos Segura A. Red de seguimiento de las praderas de *Posidonia oceanica* y cambio climático en la Región de Murcia: periodo 2004-2015. Grupo de Ecología de Angiospermas Marinas, Instituto Español de Oceanografía, Centro Oceanográfico de Murcia, Murcia, 2015;152.
28. Micheli C, D'Esposito D, Belmonte A, Peirano A, Valiante LM, Procaccini G. Genetic diversity and structure in two protected *Posidonia oceanica* meadows. *Mar Environ Res*. 2015;109:124-31. doi: 10.1016/j.marenvres.2015.06.016.
29. Lepoint G, Havelange S, Gobert S, Bouqueneau JM. Fauna vs flora contribution to the biomass of leaf epiphytes in a bed of oceanic *Posidonia* (Revellata bay, Corsica). *Hydrobiologia*. 1999;394:63-67.
30. Bellisario B, Camisa F, Abbattista C, Cimmaruta R. A network approach to identify bioregions in the distribution of Mediterranean amphipods associated with *Posidonia oceanica* meadows. *PeerJ*. 2019;7:e6786. <https://doi.org/10.7717/peerj.6786>.
31. Velimirov B. Grazing of *Sarpa salpa* L. on *Posidonia oceanica* and utilization of soluble compounds. In: Boudouresque CF (ed), *II International Workshop on Posidonia Beds*. GIS Posidonie Publ., Marseille. 1984;381-387.
32. Pergent G, Romero J, Pergent-Martini C, Mateo MA, Boudouresque C. Primary production, stocks and fluxes in the mediterranean seagrass *Posidonia oceanica*. *Mar Ecol Progr*. 1994;106:139-146.
33. Buia MC, Zupo V, Mazzella L. Primary production and growth dynamics in *Posidonia oceanica*. *P.S.Z.N.I: Marine Ecology*. 1992;13:2-16.
34. Vassallo P, Paoli C, Rovere A, Montefalcone M, Morri C, Nike Bianchi C. The value of the seagrass *Posidonia oceanica*: A natural capital assessment. *Mar Pollut Bull*. 2013;75:157-167.
35. Campagne CS, Salles JM, Boissery P, Deter J. The seagrass *Posidonia oceanica*: Ecosystem services identification and economic evaluation of goods and benefits. *Mar Pollut Bull*. 2015;97:391-400. doi: 10.1016/j.marpolbul.2015.05.061.

36. Personnic S, Boudouresque CF, Astruch P, Ballesteros E, Blouet S, Bellan-Santini D, Bonhomme P, Thibault-Botha D, Feunteun E, Harmelin-Vivien M, Pergent G, Pergent-Martini C, Pastor J, Poggiale JC, Renaud F, Thibaut T, Ruitton S. An ecosystem-based approach to assess the status of a Mediterranean ecosystem, the *Posidonia oceanica* seagrass meadow. *PLoS One*. 2014;9:e98994. doi: 10.1371/journal.pone.0098994.
37. Hemminga MA, Duarte CM. *Seagrass Ecology*. Cambridge University Press. 2000.
38. Boudouresque CF, Bernard G, Bonhomme P, Charbonnel E, Diviacco G, Meinesz A, Pergent G, Pergent-Martini C, Ruitton S, Tunesi L. Préservation et Conservation des herbiers à *Posidonia oceanica*. *RAMOGE pub*. Monaco. 2006;1-202.
39. Mcleod E, Chmura GL, Bouillon S, Salm R, Björk M, Duarte CM, Lovelock CE, Schlesinger WH, Silliman BR. A blueprint for blue carbon: toward an improved understanding of the role of vegetated coastal habitats in sequestering CO<sub>2</sub>. *Front Ecol Environ*. 2011;9:552-560. <https://doi.org/10.1890/110004>.
40. Dauby P, Bale AJ, Bloomer N, Canon C, Ling RD, Norro A, Robertson JE, Simon A, Théate JM, Watson AJ, Frankignoulle M. Particle fluxes over a Mediterranean seagrass bed: a one-year sediment trap experiment. *Mar Ecol Prog Ser*. 1995;126:233-246.
41. Fonseca MS, Koehl MAR, Kopp BS. Biomechanical factors contributing to self-organization in seagrass landscapes. *J Exp Mar Biol Ecol*. 2007;340:227-246. <https://doi.org/10.1016/j.jembe.2006.09.015>
42. Mateo MA, Sanchez-Lizaso JL, Romero J. *Posidonia oceanica* 'banquettes': a preliminary assessment of the relevance for meadow carbon and nutrients budget. *Estuar Coast Shelf Sci*. 2003;56:85-90. [https://doi.org/10.1016/S0272-7714\(02\)00123-3](https://doi.org/10.1016/S0272-7714(02)00123-3)
43. Weddel. Note sur les aegagropiles de mer. *Actes Congr Internation Bot Amsterdam*: 1877;58-62.
44. Tackolom V, Drar M. Flora of Egypt: Angiospermae, Part Monocotyledones: LiliaceaeMusaceae. *Bull Fac Sci*. Egypte. 1954;30:1-648.
45. Boudouresque CF, Meinesz A. Découverte de l'herbier de posidonie. *Parc national de Port-Cros*. Cahier. 1982;4:1-79.
46. Le Floch E. Contribution à une étude ethnobotanique de la flore tunisienne. *Ministère de l'Education Nationale et de la Recherche Scientifique* publ., Tunis, 1983;1-402.
47. Germain De Sain-Pierre E. Sur la germination et le mode de développement de *Posidonia caulini*. *Bull Soc bot Fr*. 1857;4:575-577.
48. Knoche H. Flora balearica. Etude phytogéographique sur les îles baléares. III. Partie générale. *Roumegous and Dehan* publ. Montpellier. 1923;1-411.
49. Braun-Blanquet J, Roussine N, Negre R. Les groupements végétaux de la France méditerranéenne. *Macabet Frères* publ. Vaison-la-Romaine. 1952:1-297.
50. Sauvageau C. Observations sur la structure des feuilles des plantes aquatiques (suite). *J Bot Paris*. 1890;4:181-192.
51. Lami R. L'utilisation des végétaux marins des côtes de France. *Rev Bot appl Agric tropic*. 1941;21:653-670.
52. Batanouny KH. *Wild Medicinal Plants in Egypt*. Academy of Scientific Research and Technology: Cairo, Egypt, 1999.
53. Cazzuola F. Le piante utili e nocive agli uomini e agli animali che crescono spontanee e coltivate in Italia con brevi cenni sopra la coltura, sopra i prodotti e sugli usi che se ne fanno Loescher ed. Torino: 1880;1-217.
54. El-Mokasabi FM. Floristic composition and traditional uses of plant species at Wadi Alkuf, Al-Jabal Al-Akhder, Libya. *Am Eur J Agric Environ Sci*. 2014;14:685-697. DOI: 10.5829/idosi.aejaes.2014.14.08.12375.
55. Gokce G, Haznedaroglu MZ. Evaluation of antidiabetic, antioxidant and vasoprotective effects of *Posidonia oceanica* extract. *J Ethnopharmacol*. 2008;115:122-30. doi: 10.1016/j.jep.2007.09.016.

56. Bernard P, Pesando D. Antibacterial and Antifungal Activity of Extracts from the Rhizomes of the Mediterranean Seagrass *Posidonia oceanica* (L.) Delile. *Bot. Mar.* 1989;32:85–88. <https://doi.org/10.1515/botm.1989.32.2.85>
57. Cornara L, Pastorino G, Borghesi B, Salis A, Clericuzio M, Marchetti C, Damonte G, Burlando B. *Posidonia oceanica* (L.) Delile Ethanolic Extract Modulates Cell Activities with Skin Health Applications. *Mar Drugs.* 2018;16:21. doi: 10.3390/md16010021.
58. Dias DA, Urban S, Roessner U. A Historical Overview of Natural Products in Drug Discovery. *Metabolites.* 2012;2:303-336. <https://doi.org/10.3390/metabo2020303>.
59. Hu Y, Chen J, Hu G, Yu J, Zhu X, Lin Y, Chen S, Yuan J. Statistical Research on the Bioactivity of New Marine Natural Products Discovered during the 28 Years from 1985 to 2012. *Mar Drugs.* 2015;13:202-221. <https://doi.org/10.3390/md13010202>.
60. Bergmann W, Feeney R. Contribution on the Study of Marine Sponges, XXXII. The Nucleosides of Sponges. *J Org Chem.* 1951;16:981-987. <https://doi.org/10.1021/jo01146a023>.
61. Dyshlovoy SA, Honecker F. Marine Compounds and Cancer: The First Two Decades of XXI Century. *Mar Drugs.* 2020;18:20. <https://doi.org/10.3390/md18010020>.
62. Carroll AR, Copp BR, Davis RA, Keyzers RA, Prinsep MR. Marine natural products. *Nat Prod Rep.* 2019;36:122-173. DOI: 10.1039/C8NP00092A.
63. Lindequist U. Marine-Derived Pharmaceuticals? Challenges and Opportunities. *Biomol Ther.* 2016;24:561-571. <https://doi.org/10.4062/biomolther.2016.181>
64. Desbois AP, Mearns-Spragg A, Smith VJ. A fatty acid from the diatom *Phaeodactylum tricornutum* is antibacterial against diverse bacteria including multi-resistant *Staphylococcus aureus* (MRSA). *Mar Biotechnol (NY).* 2009;11:45-52. doi: 10.1007/s10126-008-9118-5.
65. Cheung RCF, Ng TB, Wong JH, Chen Y, Chan WY. Marine natural products with anti-inflammatory activity. *Appl Microbiol Biotechnol.* 2016;100:1645-1666. doi: 10.1007/s00253-015-7244-3.
66. Skov MJ, Beck JC, de Kater AW, Shopp GM. Nonclinical safety of ziconotide: an intrathecal analgesic of a new pharmaceutical class. *Int J Toxicol.* 2007;26:411-421. DOI: 10.1080/10915810701582970.
67. Mayer AM, Glaser KB, Cuevas C, Jacobs RS, Kem W, Little RD, McIntosh JM, Newman DJ, Potts BC, Shuster DE. The odyssey of marine pharmaceuticals: a current pipeline perspective. *Trends Pharmacol Sci.* 2010;31:255-65. doi: 10.1016/j.tips.2010.02.005.
68. Stonik VA. Marine natural products: a way to new drugs. *Acta Naturae.* 2009;1:15-25.
69. Agostini S, Desjobert JM, Pergenta G. Distribution of phenolic compounds in the seagrass *Posidonia oceanica*. *Phytochemistry.* 1998;48:611-617. [https://doi.org/10.1016/S0031-9422\(97\)01118-7](https://doi.org/10.1016/S0031-9422(97)01118-7).
70. Mannino AM, Micheli C. Ecological Function of Phenolic Compounds from Mediterranean Furoid Algae and Seagrasses: An Overview on the Genus *Cystoseira* sensu lato and *Posidonia oceanica* (L.) Delile. *J Mar Sci Eng.* 2020;8:19. doi:10.3390/jmse8010019.
71. Dumay O, Costa J, Desjobert JM, Pergent G. Variations in the concentration of phenolic compounds in the seagrass *Posidonia oceanica* under conditions of competition. *Phytochemistry.* 2004;65:3211-3220. <https://doi.org/10.1016/j.phytochem.2004.09.003>.
72. Cuny P, Serve L, Jupin H, Boudouresque CF. Water soluble phenolic compounds of the marine phanerogam *Posidonia oceanica* in a Mediterranean area colonised by the introduced chlorophyte *Caulerpa taxifolia*. *Aquat Bot.* 1995;52:237-242,
73. Haznedaroglu MZ, Zeybek U. HPLC Determination of Chicoric Acid in Leaves of *Posidonia oceanica*. *Pharm Biol.* 2007;45:745-748. DOI: 10.1080/13880200701585717
74. Cariello L, Zanetti L. Distribution of Chicoric Acid during Leaf Development of *Posidonia oceanica*. *Bot Mar.* 1979;22:359-360. <https://doi.org/10.1515/botm.1979.22.6.359>
75. Grignon-Dubois M, Rezzonico B. Phenolic fingerprint of the seagrass *Posidonia oceanica* from four locations in the Mediterranean Sea: first evidence for the large predominance of chicoric acid. *Bot Mar.* 2015;58:379–391. <https://doi.org/10.1515/bot-2014-0098>.

76. Heglmeier A, Zidorn C. Secondary metabolites of *Posidonia oceanica* (Posidoniaceae). *Biochem Syst Ecol.* 2010;38:964-970. <https://doi.org/10.1016/j.bse.2010.07.001>.
77. Cannac M, Ferrat L, Pergent-Martini C, Pergent G, Pasqualini V. Effects of fish farming on flavonoids in *Posidonia oceanica*. *Sci Total Environ.* 2006;370:91-8. doi: 10.1016/j.scitotenv.2006.07.016.
78. Viso AC, Pesando D, Bernard P, Marty JC. Lipid components of the mediterranean seagrass *Posidonia Oceanica*. *Phytochemistry.* 1993;34:381-387. [https://doi.org/10.1016/0031-9422\(93\)80012-H](https://doi.org/10.1016/0031-9422(93)80012-H).
79. Hammami S, Salem AB, Ashour ML, Cheriaa J, Graziano G, Mighri Z. A novel methylated sesquiterpene from seagrass *Posidonia oceanica* (L.) Delile. *Nat Prod Res.* 2013;27:1265-70. doi: 10.1080/14786419.2012.725401.
80. Barletta E, Ramazzotti M, Fratianni F, Pessani D, Degl'Innocenti D. Hydrophilic extract from *Posidonia oceanica* inhibits activity and expression of gelatinases and prevents HT1080 human fibrosarcoma cell line invasion. *Cell Adh Migr.* 2015;9:422-31. doi: 10.1080/19336918.2015.1008330.
81. Bray F, Ferlay J, Soerjomataram I, Siegel RL, Torre LA, Jemal A. Global cancer statistics 2018: GLOBOCAN estimates of incidence and mortality worldwide for 36 cancers in 185 countries. *CA Cancer J Clin.* 2018;68:394-424. Erratum in: *CA Cancer J Clin.* 2020;70:313. DOI: 10.3322/caac.21492
82. Pucci C, Martinelli C, Ciofani G. Innovative approaches for cancer treatment: current perspectives and new challenges. *Ecancermedicalscience.* 2019;13:961. doi: 10.3332/ecancer.2019.961.
83. Liu W, Li Q, Hu J, Wang H, Xu F, Bian Q. Application of natural products derivatization method in the design of targeted anticancer agents from 2000 to 2018. *Bioorg Med Chem.* 2019;27:115150. <https://doi.org/10.1016/j.bmc.2019.115150>.
84. Newman DJ, Cragg GM. Natural Products as Sources of New Drugs over the Nearly Four Decades from 01/1981 to 09/2019. *Nat Prod.* 2020;83:770–803. <https://doi.org/10.1021/acs.jnatprod.9b01285>.
85. Khalifa SAM, Elias N, Farag MA, Chen L, Saeed A, Hegazy MEF, Moustafa MS, Abd El-Wahed A, Al-Mousawi SM, Musharraf SG, Chang FR, Iwasaki A, Suenaga K, Alajlani M, Göransson U, El-Seedi HR. Marine Natural Products: A Source of Novel Anticancer Drugs. *Mar Drugs.* 2019;17:491. <https://doi.org/10.3390/md17090491>.
86. Ruiz-Torres V, Encinar JA, Herranz-López M, Pérez-Sánchez A, Galiano V, Barrajon-Catalán E, Micol V. An Updated Review on Marine Anticancer Compounds: The Use of Virtual Screening for the Discovery of Small-Molecule Cancer Drugs. *Molecules.* 2017;22:1037. <https://doi.org/10.3390/molecules22071037>
87. Nigel MH, Yoshifumi I, Hideaki N. Matrix metalloproteinases in cancer. *Essays Biochem.* 2002;21-36. doi: <https://doi.org/10.1042/bse0380021>.
88. Li F, Guo H, Yang Y, Feng M, Liu B, Ren X, Zhou H. Autophagy modulation in bladder cancer development and treatment (Review). *Oncol Rep.* 2019;42:1647-1655. doi: 10.3892/or.2019.7286.
89. Gugnoni M, Sancisi V, Manzotti G, Gandolfi G, Ciarrocchi A. Autophagy and epithelial-mesenchymal transition: An intricate interplay in cancer. *Cell Death Dis.* 2016;7:e2520.
90. Mutschelknaus L, Azimzadeh O, Heider T, Winkler K, Vetter M, Kell R, Tapio S, Merl-Pham J, Huber SM, Edalat L, Radulović V, Anastasov N, Atkinson MJ, Moertl S. Radiation alters the cargo of exosomes released from squamous head and neck cancer cells to promote migration of recipient cells. *Sci Rep.* 2017;7:12423. doi: 10.1038/s41598-017-12403-6.
91. Leri M, Ramazzotti M, Vasarri M, Peri S, Barletta E, Pretti C, Degl'Innocenti D. Bioactive Compounds from *Posidonia oceanica* (L.) Delile Impair Malignant Cell Migration through Autophagy Modulation. *Mar Drugs.* 2018;16:137. doi: 10.3390/md16040137.
92. Steeg PS. Tumor metastases: mechanistic insights and clinical challenges. *Nat Med.* 2006;12:895-904. doi: 10.1038/nm1469.



93. Zage PE. New therapies for relapsed and refractory neuroblastoma. *Children*. 2018;5:148. doi: 10.3390/children5110148.
94. Mouhieddine TH, Nokkari A, Itani MM, Chamaa F, Bahmad H, Monzer A, El-Merahbi R, Daoud G, Eid A, Kobeissy FH, Abou-Kheir W. Metformin and Ara-a Effectively Suppress Brain Cancer by Targeting Cancer Stem/Progenitor Cells. *Front Neurosci*. 2015;9:442. doi: 10.3389/fnins.2015.00442.
95. Cruz FD, Matushansky I. Solid tumor differentiation therapy - is it possible? *Oncotarget*. 2012;3:559-67. doi: 10.18632/oncotarget.512.
96. Matthyay KK, Maris JM, Schleiermacher G, Nakagawara A, Mackall CL, Diller L, Weiss WA. Neuroblastoma. *Nat Rev Dis Primers*. 2016;2:16078. doi: 10.1038/nrdp.2016.78.
97. Falzone L, Salomone S, Libra M. Evolution of Cancer Pharmacological Treatments at the Turn of the Third Millennium. *Front. Pharmacol*. 2018;9:1300. doi: 10.3389/fphar.2018.01300.
98. Colone M, Calcabrini A, Stringaro A. Drug Delivery Systems of Natural Products in Oncology. *Molecules*. 2020;25:4560. doi: 10.3390/molecules25194560.
99. Kumari P, Ghosh B, Biswas S. Nanocarriers for cancer-targeted drug delivery. *J Drug Target*. 2016;24:179-91. doi: 10.3109/1061186X.2015.1051049.
100. Falagan-Lotsch P, Grzincic EM, Murphy C. New Advances in Nanotechnology-Based Diagnosis and Therapeutics for Breast Cancer: An Assessment of Active-Targeting Inorganic Nanoplatfoms. *Bioconjug Chem*. 2017;28:135-152. DOI:10.1021/acs.bioconjchem.6b00591.
101. Watkins R, Wu L, Zhang C, Davis RM, Xu B. Natural products-based nanomedicine: Recent advances and issues. *Int J Nanomed*. 2015;10:6055-6074.
102. Bilia AR, Piazzini V, Risaliti L, Vanti G, Casamonti M, Wang M, Bergonzi MC. Nanocarriers: A Successful Tool to Increase Solubility, Stability and Optimise Bioefficacy of Natural Constituents. *Curr Med Chem*. 2019;26:4631-4656. doi: 10.2174/0929867325666181101110050.
103. Yuan H, Lu LJ, Du YZ, Hu FQ. Stearic Acid-g-chitosan Polymeric Micelle for Oral Drug Delivery: In Vitro Transport and in Vivo Absorption. *Mol Pharm*. 2010;8:225-238. DOI: 10.1021/mp100289v.
104. Piazzini V, D'Ambrosio M, Luceri C, Cinci L, Landucci E, Bilia AR, Bergonzi MC. Formulation of Nanomicelles to Improve the Solubility and the Oral Absorption of Silymarin. *Molecules*. 2019;24:1688. doi: 10.3390/molecules24091688.
105. Piazzini V, Vasarri M, Degl'Innocenti D, Guastini A, Barletta E, Salvatici MC, Bergonzi MC. Comparison of Chitosan Nanoparticles and Soluplus Micelles to Optimize the Bioactivity of Posidonia oceanica Extract on Human Neuroblastoma Cell Migration. *Pharmaceutics*. 2019;11:655. doi: 10.3390/pharmaceutics11120655.
106. Castellano G, Tena J, Torrens F. Classification of polyphenolic compounds by chemical structural indicators and its relationship with the antioxidant properties of Posidonia oceanica (L.) Delile. *MATCH Commun Mathematics Comput Chem*. 2012;67:231-250.
107. Piva G, Fracassetti D, Tirelli A, Mascheroni E, Musatti A, Inglese P, Piergiovanni L, Rollini M. Evaluation of the antioxidant/antimicrobial performance of Posidonia oceanica in comparison with three commercial natural extracts and as a treatment on fresh-cut peaches (*Prunus persica* Batsch). *Postharvest Biol Tec*. 2017;124:54-61. <https://doi.org/10.1016/j.postharvbio.2016.10.001>.
108. Benito-González I, López-Rubio A, Martínez-Abad A, Ballester AR, Falcó I, González-Candelas L, Sánchez G, Lozano-Sánchez J, Borrás-Linares I, Segura-Carretero A, Martínez-Sanz M. In-Depth Characterization of Bioactive Extracts from Posidonia oceanica Waste Biomass. *Mar Drugs*. 2019;17:409. <https://doi.org/10.3390/md17070409>.
109. Sureda A, Box A, Terrados J, Deudero S, Pons A. Antioxidant response of the seagrass Posidonia oceanica when epiphytized by the invasive macroalgae Lophocladia lallemandii. *Mar Environ Res*. 2008;66:359-63. doi: 10.1016/j.marenvres.2008.05.009.
110. Kesraoui O, Marzouki MN, Maugard T, Limam F. In vitro evaluation of antioxidant activities of free and bound phenolic compounds from Posidonia oceanica (L.) Delile leaves. *Afr J Biotechnol*. 2011;10:3176-3185. DOI: 10.5897/AJB10.847.

111. Tutar O, Marín-Guirao L, Ruiz JM, Procaccini G. Antioxidant response to heat stress in seagrasses. A gene expression study. *Mar Environ Res.* 2017;132:94-102. doi: 10.1016/j.marenvres.2017.10.011.
112. Holmer M, Marbà N, Lamote M, Duarte CM. Deterioration of Sediment Quality in Seagrass Meadows (*Posidonia oceanica*) Invaded by Macroalgae (*Caulerpa* sp.). *Estuar Coast.* 2009;32:456-466. <https://doi.org/10.1007/s12237-009-9133-4>.
113. Sureda A, Box A, Terrados J, Deudero S, Pons A. Antioxidant response of the seagrass *Posidonia oceanica* when epiphytized by the invasive macroalgae *Lophocladia lallemandii*. *Mar Environ Res.* 2008;66:359-363. <https://doi.org/10.1016/j.marenvres.2008.05.009>.
114. Hsieh HL, Yang CM. Role of redox signaling in neuroinflammation and neurodegenerative diseases. *Biomed Res Int.* 2013;2013:484613. doi: 10.1155/2013/484613.
115. Vasarri M, Leri M, Barletta E, Ramazzotti M, Marzocchini R, Degl'Innocenti D. Anti-inflammatory properties of the marine plant *Posidonia oceanica* (L.) Delile. *J Ethnopharmacol.* 2020;247:112252. doi: 10.1016/j.jep.2019.112252.
116. Bondi M, Lauková A, de Niederhausern S, Messi P, Papadopoulou C. Natural Preservatives to Improve Food Quality and Safety. *J Food Qual.* 2017;2017:1090932. <https://doi.org/10.1155/2017/1090932>
117. Lorenzo JM, Munekata PE, Gomez B, Barba FJ, Mora L, Perez-Santaescolastica C, Toldra F. Bioactive Peptides as Natural Antioxidants in Food - A Review. *Trends Food Sci Technol.* 2018;79:136-147. DOI: 10.1016/j.tifs.2018.07.003.
118. Chen L, Deng H, Cui H, Fang J, Zuo Z, Deng J, Li Y, Wang X, Zhao L. Inflammatory responses and inflammation-associated diseases in organs. *Oncotarget.* 2018;9:7204-7218. <https://doi.org/10.18632/oncotarget.23208>.
119. Mittal M, Siddiqui MR, Tran K, Reddy SP, Malik AB. Reactive oxygen species in inflammation and tissue injury. *Antioxidants Redox Signal.* 2014;20:1126-1167. <https://doi.org/10.1089/ars.2012.5149>.
120. Kadetoff D, Lampa J, Westman M, Andersson M, Kosek E. Evidence of central inflammation in fibromyalgia-increased cerebrospinal fluid interleukin-8 levels. *J Neuroimmunol.* 2012;242:33-8. doi: 10.1016/j.jneuroim.2011.10.013.
121. Stejskal V, Ockert K, Bjørklund G. Metal-induced inflammation triggers fibromyalgia in metal-allergic patients. *Neuro Endocrinol Lett.* 2013;34:559-65.
122. Namgyal D, Sarwat M. Safron as a neuroprotective agent. Safron. Elsevier, Netherlands. 2020;93-102. <https://doi.org/10.1016/B978-0-12-818462-2.00008-5>.
123. Sharma B, Kumar H, Kaushik P, Mirza R, Awasthi R, Kulkarni G. Therapeutic benefits of Safron in brain diseases: new lights on possible pharmacological mechanisms. Safron. Elsevier, Netherlands. 2020;117-130.
124. Haddadi R, Rashtiani R. Anti-inflammatory and anti-hyperalgesic effects of milnacipran in inflamed rats: involvement of myeloperoxidase activity, cytokines and oxidative/nitrosative stress. *Inflammopharmacology.* 2020;28:903-913. doi: 10.1007/s10787-020-00726-2.
125. Micheli L, Vasarri M, Barletta E, Lucarini E, Ghelardini C, Degl'Innocenti D, Di Cesare Mannelli L. Efficacy of *Posidonia oceanica* Extract against Inflammatory Pain: In Vivo Studies in Mice. *Mar Drugs.* 2021;19:48. doi: 10.3390/md19020048.
126. Dias DA, Urban S, Roessner U. A historical overview of natural products in drug discovery. *Metabolites.* 2012;2:303-36. doi: 10.3390/metabo2020303.
127. Petrovska BB. Historical review of medicinal plants' usage. *Pharmacogn Rev.* 2012;6:1-5. doi: 10.4103/0973-7847.95849.
128. Choudhury H, Pandey M, Hua CK, Mun CS, Jing JK, Kong L, Ern LY, Ashraf NA, Kit SW, Yee TS, Pichika MR, Gorain B, Kesharwani P. An update on natural compounds in the remedy of diabetes mellitus: A systematic review. *J Tradit Complement Med.* 2017;8:361-376. doi: 10.1016/j.jtcme.2017.08.012.

129. Nowotny K, Jung T, Höhn A, Weber D, Grune T. Advanced glycation end products and oxidative stress in type 2 diabetes mellitus. *Biomolecules*. 2015;5:194-222. <https://doi.org/10.3390/biom5010194>.
130. Rasheed S, Sánchez SS, Yousuf S, Honoré SM, Choudhary MI. Drug repurposing: in-vitro anti-glycation properties of 18 common drugs. *PLoS One*. 2018;13:e0190509. <https://doi.org/10.1371/journal.pone.0190509>.
131. Rondeau P, Bourdon E. The glycation of albumin: structural and functional impacts. *Biochimie*. 2011;93:645–658. <https://doi.org/10.1016/j.biochi.2010.12.003>.
132. Vasarri M, Barletta E, Ramazzotti M, Degl'Innocenti D. In vitro anti-glycation activity of the marine plant *Posidonia oceanica* (L.) Delile. *J Ethnopharmacol*. 2020;259:112960. doi: 10.1016/j.jep.2020.112960.
133. Oeste CL, Seco E, Patton WF, Boya P, Pérez-Sala D. Interactions between autophagic and endo-lysosomal markers in endothelial cells. *Histochem Cell Biol*. 2012;139:659–670.
134. Masuko T, Minami A, Iwasaki N, Majima T, Nishimura S, Lee YC. Carbohydrate analysis by a phenol-sulfuric acid method in microplate format. *Anal Biochem*. 2005;339:69-72.
135. Pulido R, Bravo L, Saura-Calixto F. Antioxidant activity of dietary polyphenols as determined by a modified ferric reducing/antioxidant power assay. *J Agric Food Chem*. 2000;48:3396-3402.
136. Fukumoto LR, Mazza G. Assessing antioxidant and prooxidant activities of phenolic compounds. *J Agric Food Chem*. 2000;48:3597-3604.
137. Séro L, Sanguinet L, Blanchard P, Dang BT, Morel S, Richomme P, Séraphin D, Derbré S. Tuning a 96-well microtiter plate fluorescence-based assay to identify AGE inhibitors in crude plant extracts. *Molecules*. 2013;18:14320–14339.